

MODELS OF DEFECTIVE INSULIN SECRETION IN HUMAN AND MOUSE PANCREATIC ISLETS: IMPACT OF GRANULE EXOCYTOSIS, MITOCHONDRIAL METABOLISM, AND AGEING

Hyun Woong Do

Department of Medicine
University of Oxford
St Cross College

Thesis submitted for the Degree of Doctor of Philosophy

Trinity Term, 2015

Abstract

Models of defective insulin secretion in human and mouse pancreatic islets: impact of granule exocytosis, mitochondrial metabolism, and ageing

A thesis submitted for the Degree of Doctor of Philosophy

HyunWoong Do **St. Cross College** **Trinity Term, 2015**

Type-2 diabetes (T2D), a multi-factorial disease characterised by chronic hyperglycaemia, is caused by a complex interaction between genetic and environmental factors. Genetic and phenotypic characterisations of diabetic patients suggest that a combination of β-cell failure, culminating in defective insulin secretion, as well as impairment of glucagon secretion in α-cells is central to the aetiology of the disease. Mouse models represent a valuable tool in such investigations.

With the advent of large-scale genetic tools, a myriad of novel susceptibility loci associated with T2D have been identified. For many of these genes, it is unclear how genetic variation is linked to increased disease susceptibility. Our first study elucidates the implication of a transcription factor, *SOX4*, which is believed to underlie a T2D susceptibility locus (*CDKAL1*) in human. Using an N-ethyl-N-nitrosourea (ENU) mouse model, we explored β-cell function in mice carrying a point mutation in *Sox4* (*Sox4*mt mice). This mouse strain displayed a significant reduction in glucose-stimulated insulin secretion (GSIS) that was associated with a 2-fold increase in wild-type *Sox4* expression. The exocytotic events in mutant β-cells, as measured by single-vesicle (on-cell) capacitance measurements, suggested the presence of a persistent fusion pore. Subsequent failure of fusion pore expansion beyond the initial 1–2 nm results in an incomplete insulin release due to steric hindrance (insulin diameter: 3–4 nm). The proportion of full fusion events diminished in favour of kiss-and-run events in mutant β-cells. *Stxbp6*, which encodes amisyn, was shown to be the target gene of *Sox4*. Increased expression of amisyn, a protein previously shown to be involved in the stabilisation of the fusion pore in chromaffin cells, was observed in islets isolated from *Sox4*mt mice. The possible involvement of amisyn is further suggested by the finding that overexpression of amisyn mimicked the effect of the *Sox4* mutation and resulted in reduced insulin secretion. Knockdown of amisyn expression restored the secretory defect in *Sox4*mt-overexpressing cells. Importantly, the effect of the *Sox4* mutation was recapitulated by the overexpression of *Sox4*. Similar effects were obtained in the human β-cell line EndoC-βH2. We also observed a negative correlation between *SOX4* expression and GSIS in a large collection of human islet preparations. There was also a positive correlation between *SOX4* expression and *STXBP6* (amisyn) expression and a tendency towards increased *SOX4* expression in islets from organ donors with T2D.

The second part of the thesis focuses on the role of the Krebs cycle enzyme fumarate hydratase (FH) in insulin release. Ablation of the *Fh1* gene (which is initially implicated as a tumour suppressor in hereditary leiomyomatosis and renal cell cancer) in pancreatic β-cells led to a complete loss of GSIS, as determined by *ex vivo* pancreatic perfusion studies, although this was not associated with any detectable abnormalities in $[Ca^{2+}]_i$ homeostasis, ATP production or glucose oxidation. The phenotype was rescued by the introduction of the human orthologue *FH* into the cytosol alone or in both the cytoplasm and mitochondria of *Fh1* knockout (*Fh1*KO) mice, confirming the role of *Fh1* in insulin secretion. Moreover, the addition of exogenous glutamate, previously implicated as a 2nd messenger between glucose metabolism and insulin secretion, corrected the insulin secretory defect in *Fh1*$^{-/-}$ β-cells. We hypothesise that the loss of GSIS in *Fh1*KO mice results from enhanced anaplerosis, which is necessary to replenish Krebs cycle reactants. Consequently, this is followed by the depletion of the intracellular amino acid pool (including glutamate). Thus, our study demonstrates that the pancreatic *Fh1*KO mouse is a novel model of severe hyperglycaemia that harbours dysregulated metabolic features at the interface between both cancer and diabetes.

The final study investigates the effect of ageing, a risk factor for T2D, on glucose-stimulated insulin and glucagon release. However, GSIS increased rather than decreased with ageing in both human and mouse islets (6 and 20 mmol/l glucose). Notably, ageing was not associated with reduced insulin content. Normal calcium homeostasis was observed in old (24-month-old) mice, demonstrating that the glucose sensing machinery was intact. In human islets, the inhibitory effect of glucose on glucagon secretion deteriorated with age. In the oldest group (>60 years of age), the inhibitory effect was completely abolished with 20 mmol/l glucose, while 6 mmol/l glucose only achieved less than 20% inhibition (which was not statistically significant). Our study reports the exciting possibility that hypersecretion of glucagon represents a link between senescence and increased diabetes risk.

Acknowledgements

Foremost, I would like to express my sincere gratitude to my supervisor Professor Patrik Rorsman for the continuous support of my DPhil study, for his patience, motivation, enthusiasm, and immense knowledge. His guidance helped me in all the time of research and writing of this thesis. What I learnt from him is not just how to do experiments or write a thesis, but how to develop a big picture of the project and a critical view on even the finest detail of the subject. Hence, I feel I have grown so much over the past five years as an independent thinker as well as a scientist.

I cannot express enough thanks to my co-supervisor Dr. Stephan Collins. I offer my sincere appreciation for his unreserved help and guidance which led me to finish my thesis step by step. It is truly unbelievable that I am actually writing an acknowledgement. He was the one who got me involved with this amazing *Sox4* project which I have thoroughly enjoyed. He was not just a good supervisor but also a good listener. Thus, I could discuss with him almost everything beyond just science. Once again, thank you so much.

My grateful thanks are extended to Rorsman laboratory members.

I would like to thank Dr. Quan Zhang who was here from the beginning of my DPhil study. He always provided me with useful advice on electrophysiology (never said 'I am busy') and inspired me with his insights and work ethics.

I would like to thank Dr. Benoit Hastoy for being a good friend as well as a good advisor. His knowledge on SNARE proteins and hGH secretion has allowed me to successfully deliver the key experiment in the *Sox4* chapter. You were a life-saver!

I would like to thank Dr. Makoto Shigeto for helping me clarify many questions on electrophysiology, islet isolation and tissue culture techniques. I also would like to thank him for being a good travel partner when we both went to Glasgow and Philadelphia for conferences. In addition, I was always astonished by his 'one-meal per day' policy.

I would like to thank Dr. Reshma Ramracheya for sharing her expertise on static incubation insulin secretion studies. I always enjoyed having a conversation with her while she was hand-picking a few hundred islets!

I would like to thank Dr. Juris Galvanovskis for introducing me to the world of confocal microscopy. His extreme depth of knowledge on microscopy in general gave me a clear direction whenever I was challenged with many obstacles.

I would like to thank Dave Wiggins for giving me useful tips on RIA and islet isolations. He also had been helpful in setting up new software and fixing technical problems of the computer. I remember the time when I spilled sulforhodamine B on the floor and thought I might get killed because the red stuff was all over the floor. His patience as a lab manger was really appreciated!

I would like to thank Dr. Eduardo Rebelato for being such a good colleague. He was always open for a scientific discussion even the project was not directly related to him. Thank you for your insights and, also your support when I had to deal with personal issues.

I would like to thank Dr. Andrei Tarasov for demonstrating a living example of a hard-working scientist and also for his guidance for the ZIMIR experiments. He was always in the lab, and it did not matter to him whether it was 1 or 2 am.

I would like to thank Nils Rorsman for showing me how to do the perfusion studies. I remember the time when he managed to do the surgery less than 9 minutes with his sophiscated touch!

I would like to thank Dr. ChaeYoung Cha for being a good colleague. It was good to have a fellow Korean on the same team. Her in-depth knowledge on materials and methods helped me prepare for viva.

I would like to thank Dr. William Sones for being a good colleague. Over numerous lunches that we had, I thoroughly enjoyed having discussions with him on a variety of topics. I still remember few of his British jokes! ☺

I would like to thank Elisa Vergari for being a good friend as well as a good colleague. She brought a happy vibe into the lab and, I enjoyed her presence, particularly when she talks to Dave Wiggins ☺.

I would like to thank Dr. Margarita Chibalina for showing me what the molecular biology is about. Her attitude towards science taught me the importance of paying attention to small details in every step of gene cloning.

I would like to thank Nancy Lee for her kind assistance to all the trips and numerous social and academic events.

Also, thanks to Dr. Elizabeth Jones and Dr. Orit Braha for providing guidance and advices on electrophysiology, and helping me settle down into the lab.

Special thanks to all my collaborators of *Sox4* project: Professor Roger Cox, Dr. Michelle Goldsworthy and Dr. Alison Hough. I really want to thank them all for providing *Sox4* mutant mice and sharing important previous findings which provided basis for the current project. This should also be extended to the collaborators of *Fh1* project: I would like to thank Patrick and Julie for getting me involved in the *Fh1* project, and encouraged me to give the presentation on this topic during the OCDEM seminars. I also would like to thank Anne for introducing me into the EM world.

I would like to express my deepest gratitude to my family for their support and encouragement. Your prayer for me was what sustained me thus far. Without them this work would not have been possible. Particularly, a very special thanks goes out to my brother HyunSung, who accompanied me over 14 years in the UK, always patiently listened to all my concerns and never lost faith in me. We laughed together, and cried together. Thank you so much brother.

Finally, I am deeply grateful to my caring and loving Inji. Words cannot express how thankful I am for your emotional support during the past 18 months. Your encouragement when the times got really rough sustained me. Thank you for instilling in me confidence and a drive for completing my thesis. I am now totally excited about the next chapter of our lives in the UK and Korea.정말 고맙고 너무 너무 사랑한다 인지야. 변치 않을께.

Declaration of originality

This thesis is an account of work carried out by the author in the OCDEM (Oxford Centre for Diabetes, Endocrinology and Metabolism), University of Oxford under the supervision of Professor Patrik Rorsman and Dr Stephan Collins. The work of collaborators has been drawn upon and this is duly acknowledged in the text, in which all of them are put into supplementary figures and tables, and a list of references is presented at the end of the thesis. No part of this thesis has been submitted towards the completion of another degree at the University of Oxford or elsewhere.

Table of Contents

CHAPTER 1 INTRODUCTION 1

1.1 The importance of homeostasis 2

1.2 A history of diabetes 3

1.3 The aetiology of diabetes and a role for the β-cell 4

1.3.1 From normal insulin signalling to insulin resistance 6

1.4 Pancreas organisation and function in controlling energy homeostasis 9

1.4.1 Exocrine component of the pancreas 9

1.4.2 The endocrine component of pancreas 10

1.4.3 Innervation of pancreas 13

1.5 Glucose regulation of biphasic insulin secretion 14

1.5.1 Triggering pathway of insulin secretion 15

1.5.2 Amplifying pathway 19

1.6 Glucagon action in glucose homeostasis 22

1.6.1 Glucagon secretion in pancreatic α-cells 23

1.6.2 Paracrine regulation of glucagon secretion 26

1.7 Molecular steps involved in granule fusion and exocytosis 28

1.7.1 SNARE classification 28

1.7.2 SNARE structure 31

1.7.3 SNARE in membrane fusion 32

1.7.4 SNARE in pancreatic β-cell 33

1.8 Fusion pore and two forms of granule fusion 36

1.8.1 Full fusion 36

1.8.2 Kiss-and-run exocytosis 37

1.9 Advancement of T2D mouse models 41

1.9.1 KO strategy 41
1.9.2 ENU mutagenesis 42
1.10 Aims of the thesis 44

CHAPTER 2 MATERIALS AND METHODS 45

2.1 Animals 46
2.1.1 Generation of *Sox4* mutant mice 46
2.1.2 *Fh1*KO and FH rescue mice 46
2.2 Islet isolation 47
2.3 Glucose tolerance test (IPGTT) 48
2.4 ATP measurements 48
2.5 Intracellular calcium measurements 48
2.6 Electrophysiology 49
2.6.1 General 49
2.6.2 Whole-cell capacitance and Ca^{2+} currents 50
2.6.3 On-cell single-granule exocytosis measurements 50
2.6.4 $P2X_2$ receptor analysis 51
2.7 Culture of INS-1 832/13 cell line 51
2.8 Culture of EndoC-βH2 cell line 52
2.9 Human islet secretion and microarray studies 52
2.9.1 Human islets 53
2.10 Insulin and glucagon secretion assays 54
2.10.1 Static incubation 54
2.10.2 Hormone measurements in human islets 54
2.10.3 Pancreatic perfusion studies 55
2.10.4 Islet perifusion studies 55

2.10.5 Growth hormone secretion assays 56

2.11 ZIMIR Imaging by confocal fluorescence microscopy 58

2.12 Two-photon and confocal imaging of exocytosis 59

2.13 qRT PCR 60

2.14 Western blot 61

2.15 Electron microscopy for mitochondrial quantitation 62

CHAPTER 3 *SOX4* MODULATES INSULIN SECRETION BY INCREASING KISS-AND-RUN EXOCYTOSIS AT THE EXPENSE OF FULL FUSION 64

3.1 Introduction 65

3.2 Results 68

3.2.1 Glucose- and sulphonylurea-stimulated insulin secretions are reduced in *Sox4*mt islets 68

3.2.2 The *Sox4* mutation has no effect on Ca^{2+} homeostasis 71

3.2.3 Normal granule fusion in *Sox4*mt mice 74

3.2.4 The *Sox4* mutation increases the stability of the fusion pore 76

3.2.5 SRB uptake correlates with the exocytotic marker ZIMIR 79

3.2.6 VAMP-pHluorin reveals an increase in kiss-and-run exocytosis in *Sox4m*t β-cells 82

3.2.7 Release of ATP is hindered by the presence of the fusion pore in *Sox4m*t β-cells 86

3.3 Discussion 88

CHAPTER 4 MOLECULAR MECHANISM OF *SOX4* IN DEFECTIVE EXOCYTOSIS 93

4.1 Introduction 94

4.2 Results 96

4.2.1 Identification of a candidate gene(s) mediating the effect of *Sox4* 96

4.2.2 Optimisation of the triple-transfection to assess the effect of *Stxbp6* (amisyn) 97

4.2.3 *Sox4* mutation impairs insulin secretion via increased *Stxbp6* 101

4.3 Discussion 106

CHAPTER 5 ROLE OF *SOX4* IN HUMAN T2D 116

5.1 Introduction 117

5.2 Results 120

5.2.1 Increased *SOX4* expression reduces GSIS in a human β-cell line 120

5.2.2 Increased *SOX4* expression shows diabetic-like phenotypes in humans 124

5.3 Discussion 126

CHAPTER 6 *FH1* PLAYS A KEY ROLE IN INSULIN SECRETION BY A DISTAL EFFECT ON EXOCYTOSIS: EVIDENCE FOR A MITOCHONDRIAL SIGNAL? 130

6.1 Introduction 131

6.2 Results 134

6.2.1 *Fh1* mediates an active role in GSIS 134

6.2.2 Both control and *Fh1*$^{-/-}$ islets show normal increases in ATP content upon glucose exposure 136

6.2.3 *Fh1*-induced secretory defects is not due to either impaired $[Ca^{2+}]_i$ or reduced exocytosis 138

6.2.4 Electron microscopy (EM) reveals morphological defects in mitochondria 142

6.2.5 GSIS in *Fh1*$^{-/-}$ islets is rescued by re-expression of *FH* 144

6.2.6 Exogenous glutamate improves insulin secretion in *Fh1*$^{-/-}$ islets 146

6.3 Discussion 148

CHAPTER 7 AGE-DEPENDENT ALTERATIONS OF INSULIN AND GLUCAGON SECRETION IN MOUSE AND HUMAN PANCREATIC ISLETS 154

7.1 Introduction 155

7.2 Results 158

7.2.1 No effect of ageing on GSIS in mouse islets 158

7.2.2 Normal calcium homeostasis in old mice 160

7.2.3 GSIS increases with age in human islets 162

7.2.4 Age-dependent decrease in the inhibitory effect of glucose on glucagon secretion in human islets 165

7.3 Discussion 169

CHAPTER 8 CONCLUSION 173

8.1 Concluding remarks 174

8.2 Future work 180

8.3 Summary 182

REFERENCES 184

List of figures

Figure 1. Disruption of insulin signalling pathway when insulin resistance (highlighted in red) develops..... 8
Figure 2. Regulation of blood glucose levels by reciprocal release of insulin and glucagon..... 12
Figure 3. Consensus model for GSIS (triggering pathway)..... 18
Figure 4. Glucagon secretion in pancreatic α-cells..... 25
Figure 5. A skeleton diagram of the four-helix bundle structure..... 30
Figure 6. Domain structure of the SNARE proteins..... 31
Figure 7. Mechanisms of exocytosis involving SNARE proteins..... 35
Figure 8. Schematic representation of the two modes of granule fusion steps leading to secretory granule exocytosis..... 40
Figure 9. HMG (High Mobility Group) box mutation in *Sox4*mt mouse in comparison to the normal genes..... 67
Figure 10. Effects of *Sox4* mutation on GSIS..... 68
Figure 11. Impaired insulin secretion in *Sox4* islets is not due to impaired $[Ca^{2+}]_i$ signalling..... 72
Figure 12. Current (I)-voltage (V) relationship for the Ca^{2+} currents was recorded in β-cells isolated from WT and *Sox4*mt mice..... 73
Figure 13. *Sox4*mt β-cells show normal depolarisation-evoked exocytosis..... 75
Figure 14. On-cell measurement allows detection of kiss-and-run exocytosis..... 78
Figure 15. Optical imaging of exocytosis using SRB and ZIMIR in intact islets..... 80
Figure 16. Confocal fluorescence microscopy studies reveal a higher proportion of kiss-and-run in *Sox4*mt mice..... 84
Figure 17. Slow expansion of fusion pore in *Sox4*mt β-cells hinders ATP release..... 87
Figure 18. The narrow fusion pore that is formed during kiss-and-run exocytosis hinders the release of insulin, but not ATP..... 89
Figure 19. Optimal post-transfection time for maximum *Stxbp6* siRNA efficiency..... 99
Figure 20. Timeline for triple-transfection for INS-1 832/13 cells..... 100
Figure 21. Mutant *Sox4* mediates its effects on insulin secretion via *Stxbp6*..... 104
Figure 22. Western blot analysis of GFP expression level..... 105

Figure 23. Alignment of human SOX4 (A) and STXBP6 (B) with respective orthologues of mouse 119
Figure 24. Increased *SOX4* mediates its effects on insulin secretion via *STXBP6* 122
Figure 25. Effects of *SOX4* and *STXBP6* on human β-cell function 125
Figure 26. Overview of the Krebs cycle 132
Figure 27. Potential mechanism of the dual targeting of mammalian fumarate hydratase (FH) 133
Figure 28. Representative traces of intracellular $[Ca^{2+}]_i$ in control (A) and *Fh1*$^{-/-}$ islets (B) 139
Figure 29. Current (I) - Voltage (V) relationship for Ca^{2+} currents recorded from dispersed β-cells isolated from control (black squares) and *Fh1*KO mice (grey circles) 140
Figure 30. Standard whole-cell capacitance measurements in control and *Fh1*$^{-/-}$ β-cells 141
Figure 31. Ablation of *Fh1* alters the size distribution of mitochondria.. 143
Figure 32. No difference in intracellular β-cell $[Ca^{2+}]_i$ between control (black; left) and rescue (blue; right) islets 145
Figure 33. Glutamate involvements in both anaplerosis and cataplerosis during the Krebs cycle 151
Figure 34. Prevalence of T2D in the UK 155
Figure 35. Impact of age on GSIS in mouse pancreatic islets 159
Figure 36. Impact of age on glucose-stimulated increases in cytoplasmic $[Ca^{2+}]_i$ in mouse β-cells 161
Figure 37. Impact of age on GSIS in human pancreatic islets 163
Figure 38. Impact of age on glucose-induced suppression of glucagon secretion in human pancreatic islets 167

List of supplementary figures

Figure S1. Insulin secretory responses of WT and *Sox4*mt 70
Figure S2. Insulin release measured by *in situ* pancreatic perfusion 135
Figure S3. Ablation of *Fh1* does not interfere with ATP production 137
Figure S4. Rescue of *Fh1*KO by human *FH* 144
Figure S5. Improvement of impaired GSIS in *Fh1*$^{-/-}$ islets by membrane-permeable L-glutamate 147

List of supplementary table

Table S1. GCRMA (Guanine Cytosine Robust Multi-Array Analysis) normalised differentially expressed genes with p≤0.05 and a fold change increase between WT and *Sox4*mt of ≥1.5 110

List of abbreviations

$[Ca^{2+}]_i$: Intracellular calcium concentration

ADP: Adenosine diphosphate

AMP: Adenosine monophosphate

ANOVA: Analysis of variance

AP: Action potential

ATP: Adenosine triphosphate

BSA: Bovine serum albumin

cAMP: cyclic AMP

CoA: Coenzyme A

DsRed: *Discosoma* red fluorescent protein

ELISA: Enzyme-linked immunosorbent assay

EM: Electron microscopy

ENU: N-ethyl-N-nitrosourea

Epac2: Guanidine nucleotide exchange factor, type 2

FCS: Foetal calf serum

FH: Fumarate hydratase

GDH: Glutamate dehydrogenase

GFP: Green fluorescent protein

GLP-1: Glucagon-like peptide-1

GLUT: Glucose transporter type

GSIS: Glucose stimulated insulin secretion.

GWAS: Genome wide association studies

HBSS: Hank's Balanced Salt Solution

HEPES: 4-(2-hydroxyethyl)-1-piperazineethanesulfonic acid

hGH: Human growth hormone

HLA: Human leukocyte antigen

HLRCC: Hereditary leiomyomatosis and renal cancer

HMG: High mobility group

K_{ATP}: ATP-sensitive potassium channel

KO: Knockout

KRB: Krebs-Ringer buffer

mTOR: mammalian target of rapamycin

mROS: mitochondrial reactive oxygen species

MW: Molecular weight

NEFA: Non-esterified fatty acids

NEM: N-ethylmaleimide

NSF: N-ethylmaleimide sensitive factor

PBS: Phosphate buffered saline

qRT PCR: quantitative reverse transcription polymerase chain reaction

RIA: Radioimmunoassay

RRP: Readily releasable pool

Slc25a10: Solute carrier family 25 member 10

SNAP-25: Cytoplasmic synaptosomal-associated protein of 25kD

SNARE: Soluble N-ethylmaleimide-sensitive factor attachment protein receptor

SNP: Single nucleotide polymorphism

Sox4: SRY-related HMG-box

*Sox4*mt: *Sox4* mutant

SRB: Sulforhodamine B

SRY: Sex-determining region Y

T2D: Type-2 diabetes

VAMP: Vesicle-associated membrane protein

VGCC: Voltage-gated Ca^{2+} channels

WT: Wild-type

ZIMIR: Zinc indicator for monitoring induced exocytotic release

CHAPTER 1

Introduction

1.1 The importance of homeostasis

Many quantitative traits or physiological variables in our body are maintained within a specific (narrow) range. Our body operates complex negative feedback systems to reduce the discrepancies between the actual/detected and desired/normal physiological values. This requires 'receptors' to detect the changes and 'effectors' to reduce those discrepancies to support normal biological function. Claude Bernard clarified this concept after key historical experimental discoveries such as the glycogenic function of the liver and the regulation of temperature by vasomotor nerves (Bernard, 1876). He then developed the underlying principle of '*milieu interieur*', where he explained that 'the highest organism' (a warm-blooded animal) has the ability to maintain an almost uniform condition of its internal environment despite great variation of the external milieu. This concept was later elaborated by Walter Bradford Cannon who coined the word 'homeostasis' (Cannon, 1932).

Blood glucose homeostasis results from a complex balance of hormone secretion and actions, several of which are secreted by the islets of Langerhans in the pancreas. Insulin and glucagon are secreted during hyperglycaemia or hypoglycaemia, respectively, and play a central role in systemic glucose homeostasis. Disruptions in the balance between these hormones may result in severe metabolic effects. The most widely known example of such metabolic defect is diabetes mellitus.

1.2 A history of diabetes

The term ‘diabetes’, meaning ‘siphon’, is assumed to have been coined by the Egyptian physician Apollonius of Memphis around 250 BC. ‘Mellitus’, meaning ‘sweet’, was added to the word diabetes by Thomas Willis in 1675. In 1776, Matthew Dobson confirmed the sweet taste of diabetic urine, due to the presence of a brown sugar-like substance. He also observed that some diabetic patients became acutely ill within 5 weeks, with others more or less in a chronic state (Dobson, 1776). This was the first time it was recognised that the diagnosis diabetes mellitus actually refers to two distinct diseases (now referred to as ‘type-1’ and ‘type-2’ diabetes) with rather different symptoms and progression.

Diabetes mellitus (or diabetes for short) is a multi-factorial disorder characterised by chronic hyperglycaemia. The disease affects all cells of the body, which may account for the wide spectrum of complications. They typically include cardiovascular diseases such as coronary heart disease, stroke, and/or diabetic nephropathy. These injuries are classified as macrovascular (stroke, peripheral arterial disease and coronary artery disease), or microvascular complications (diabetic retinopathy and neuropathy), both resulting in thicker but more fragile blood vessels. In general, the micro- and macro-vascular complications share similar underlying causes, such as hyperglycaemia and insulin resistance (Brownlee, 2001, DeFronzo, 2010). In addition, those vascular diseases lead to amputation of the feet and lower limbs.

1.3 The aetiology of diabetes and a role for the β-cell

It is generally accepted that in type-1 diabetes (T1D), the insulin-producing pancreatic β-cells are destroyed in an autoimmune attack, and the complete lack of insulin leads to severe hyperglycaemia, which is further exacerbated by over-secretion of glucagon (Brown et al., 2008, Walker et al., 2011a). In addition to the deleterious effect, partially reversible dysfunction of β-cells in T1D patients were observed, which results in the diabetic milieu (Krogvold et al., 2015b). Furthermore, enteroviral infection have demonstrated a link to the development of T1D patients (Krogvold et al., 2015a). These patients require life-long insulin injections. Type-1 diabetes accounts for 5-10% of all diabetes. It is known to exhibit a polygenic nature, and a number of susceptible loci that predispose individuals to the disease have been identified. Human leukocyte antigen (HLA) region on chromosome 6p21 was the first locus to be reported (Singal and Blajchman, 1973, Cudworth and Woodrow, 1974) and it remains the strongest susceptibility locus (Erlich et al., 2008). Briefly, HLA is believed to modify the immune response to direct an attack against pancreatic β-cell autoantigens (Nepom, 1990). Amongst other identified risk loci, three more loci account for a significant proportion of familial clustering (with OR (odd ratio) >1.5): the insulin gene (*INS*) region at chromosome 11p15 (*IDDM2*); the protein tyrosine phosphatase-22 (*PTPN22*) on 1p13; and the interleukin-2 receptor alpha (*IL2RA*) on 10p15 (Pociot et al., 2010). However, it is important to remember that environmental factors also contribute to the pathogenesis of the disease (Maclaren and Atkinson, 1992).

Type-2 diabetes is a completely different disease. In pre-diabetic states, a predisposed or acquired resistance to the biological action of insulin may initially be compensated for by increased insulin secretion and/or β-cell proliferation (Ashcroft and Rorsman, 2012).

However, as the insulin resistance increase (as a consequence of increasing age or body weight), the insulin needs eventually exceed those that can be provided by β-cells, causing overt T2D (Kahn et al., 2006, Samuel et al., 2010).

Since the discovery of insulin, there has been a dramatic increase in our understanding of the processes involved in glycaemic control. The structure of the insulin molecule was reported by Frederick Sanger in 1955 (Brown et al., 1955), and the three-dimensional structure of insulin by X-ray crystallography was established by the group of Dorothy Hodgkin in 1969 (Adams et al., 1969). The sequence of the rat insulin gene (*IDDM2*) (Ullrich et al., 1977) and subsequently the human insulin gene (Bell et al., 1980) provided basis for insulin becoming the first ever genetically engineered protein to be used in clinical practice (Thim et al., 1986). It is clear that many aspects of β-cell failure have been studied in diabetic models, but the exact pathophysiological mechanisms underlying defective insulin secretion upon increased demand in man. Importantly, their relative significance and interactions remain elusive.

Through the advancement of genomic tools, a number of susceptibility loci (and genes) underlying T2D were recently detected. The genome-wide association studies (GWAS) have discovered ~90 loci that predispose individuals to T2D risk (Bonnefond and Froguel, 2015). Interestingly, the majority of these common variants, including *HHEX* (Pascoe et al., 2007, Staiger et al., 2008), *CDKAL1* (Pascoe et al., 2007, Groenewoud et al., 2008) and *KCNQ1*(Yasuda et al., 2008, Mussig et al., 2009), are believed to affect the process of insulin release (McCarthy, 2010). This constitutes a compelling justification for detailed studies of the pancreatic islets.

1.3.1 From normal insulin signalling to insulin resistance

The insulin receptor is a transmembrane receptor that belongs to a large class of tyrosine kinase receptors which consists of two α- and two β-subunits linked by disulphide bridges (Menting et al., 2013). Insulin binds to the α-subunits that in turn phosphorylate the β-subunits, which then recruit insulin receptor substrates (IRS)-1 and -2. Both of the IRS undergo tyrosine kinase phosphorylation. This allows docking of a subset of downstream signalling molecules (Figure 1). In insulin-sensitive tissues, the PI3K (phosphatidylinositol-3-kinase) pathway has a central role in glucose regulation. Once it becomes activated, mTOR is stimulated via AKT activation (Jewell et al., 2013). Through this pathway, insulin exerts three main effects: (1) stimulation of glucose uptake in the liver (Nigro et al., 2006); (2) inhibition of apoptosis in vascular smooth muscle and inflammatory cells which suppresses atherogenesis (Rask-Madsen and King, 2007); and (3) vasodilation by increasing the eNOS (endothelial nitric oxide synthase) expression to produce powerful vasodilator NO (nitric oxide) (Nigro et al., 2006).

Insulin resistance is a common characteristic amongst T2D patients. It is a condition where the body is not able to respond to insulin, and triggers inadequate metabolic responses. This leads to hyperglycaemia (when it cannot be compensated for by stimulation of insulin secretion) and eventually, results in clinically overt T2D (Kahn et al., 2006). Obesity is a common trait amongst patients with metabolic syndrome. Increased levels of circulating NEFA (non-esterified fatty acids), due to impaired suppression of lipolysis (Kovacs and Stumvoll, 2005), has been postulated to be associated with insulin resistance, and/or obesity (Montague and O'Rahilly, 2000, Kahn et al., 2006), which may also affect β-cell function (Weir and Bonner-Weir, 2004, Cerf, 2013). Indeed, tyrosine kinase phosphorylation of IRS-1/2 is reduced by fatty acids

metabolites via the activation of protein kinase C (PKC), thereby inhibiting downstream insulin signalling pathways (Figure 1). This affects three sites in the body which may explain some features of the pathogenesis of T2D. First, accumulation of triacylglycerol in muscle significantly reduces glucose uptake via an impairment of AKT activation (Kim et al., 2002). Second, abnormal control of hepatic glucose metabolism increases gluconeogenesis as a consequence of impaired activation of IRS-1/2, thereby increasing hepatic glucose production which in turn exacerbates the metabolic imbalance (Samuel et al., 2004). Third, insulin is no longer able to trigger an anti-lipolytic action on adipose tissues, thus provoking excessive NEFAs production, leading to further increase in insulin resistance (Kovacs and Stumvoll, 2005). It should be noted however that some evidence suggests that excessive NEFAs production might not be related to insulin resistance (Karpe et al., 2011). Indeed, some observations suggest that increasing the level of NEFA per se does not cause insulin resistance. For example, women have higher NEFA levels than men and yet are more insulin-sensitive (Magkos et al., 2007, Stefan et al., 2010).

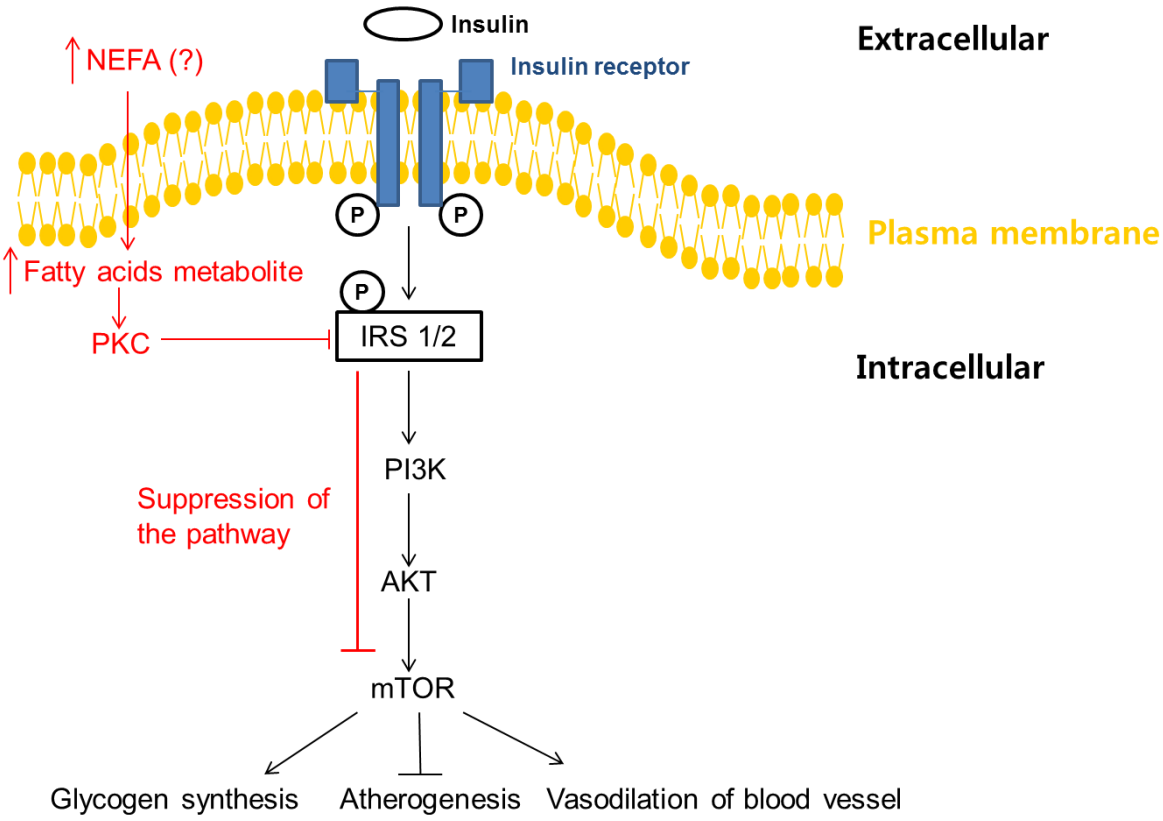


Figure 1. Disruption of insulin signalling pathway when insulin resistance (highlighted in red) develops. Cellular elevation of NEFAs triggers the activation of atypical PKC isoforms. Instead of the usual tyrosine kinase phosphorylation of IRS, the increased level of PKC leads to serine/threonine residue phosphorylation. Consequently PI3K/mTOR signalling pathways are inhibited. The arrowheads and the flat lines implicate stimulation and suppression, respectively. Normally, the activation of insulin signalling pathway leads to glycogenesis in the liver, suppression of atherogenesis and vasodilation of blood vessels in smooth muscle cells.

1.4 Pancreas organisation and function in controlling energy homeostasis

The direct role of the pancreas in carbohydrate metabolism was first observed in 1889 by Oskar Minkowski and Joseph von Mering when they demonstrated how the removal of the pancreas in dogs produced diabetes (von Mering, 1890). The hypothetical hormone 'insulin' was then named by De Meyer in 1909 (De Meyer, 1909), and in the early 1920s, Banting, Best, Collip and Macleod at the University of Toronto discovered and isolated insulin from the pancreatic islets (Banting et al., 1922). From October 1923, isolated insulin became available for the treatment of diabetics in North America and Europe.

The word pancreas derives from the Greek 'pan', meaning 'all', and 'kreas', meaning 'flesh', alluding to the organ's fleshy consistency, first described by the Greek anatomist Rufus of Ephesus around 100 AD. The organ consists of three physical parts: the head (caput) is situated near the curvature of the duodenum; the body (corpus) is attached to the stomach and the tail (cauda) of the organ lies in contact with the spleen. The pancreas develops from two buds which are formed from the gut endoderm at around the 5^{th} week of gestation (in man). The dorsal bud eventually forms the body, tail and part of the head of the pancreas. The ventral bud forms the rest of the head, and the two buds fuse together at approximately the 7^{th} week of gestation. In terms of its function, the pancreas can be divided into the exocrine and the endocrine gland.

1.4.1 Exocrine component of the pancreas

A major part (98-99%) of the pancreas is the exocrine gland. It consists of a number of lobules supported by connective tissue. Each lobule comprises of secretory cells surrounding a central branch of the pancreatic duct. This structure is called an 'acinus',

meaning ‘berry’, and the secretory cells are therefore referred to as acinar cells. The acinar cells secrete the digestive enzymes amylase, chymotrypsin, trypsin and pancreatic lipase. These enzymes are then transported down the pancreatic duct into the common bile duct and finally reach the duodenum via the common pancreatic duct (Wirsung’s duct). Additionally, a bicarbonate rich solution (up to 140 mmol/l of HCO_3^- (Steward et al., 2005)) is produced by the centroacinar cells lining the pancreatic ducts, which are enriched with carbonic anhydrase (Nishimori et al., 1999, Nishimori and Onishi, 2001). This enzyme catalyses the formation of the solution from CO_2 and H_2O, which neutralises the acidity (gastric acid) that is produced by parietal cells lining the stomach. Gastric acid is required for the initial digestion of proteins into polypeptides by pepsin with a pH optimum of ~2, and that is completed by trypsin (optimum pH of ~8) in the duodenum by hydrolysis of peptide bonds.

1.4.2 The endocrine component of pancreas

The endocrine part of the pancreas which aims to maintain glucose homeostasis is composed of the islets of Langerhans, so named after Paul Langerhans who first described them in 1869. In man, the normal adult pancreas contains ~1 million islets, or approximately 1-2% of the pancreas mass/volume. The islets of Langerhans (or pancreatic islets) in adult mice are composed of β-cells (70%) and α-cells (20%) with the remainder consisting of the somatostatin-releasing δ-cells (<10%) and the rare pancreatic polypeptide (PP)-cells (<5%) (Cabrera et al., 2006). Human pancreatic islets have a rather different composition: β-cells (50%), α-cells (35–40%), δ-cells (10–15%) and a negligible proportion of PP-cells (Cabrera et al., 2006). Furthermore, the architecture of the islets varies amongst different species. Rodent islets (both mouse and rat) have a central aggregation of β-cells which are surrounded by the other types, but human

pancreatic islets show a less well-defined architecture. Notably, the size of islets in rodents are highly variable; some islets are very small (~50 x 10^3 μm^3 in volume) while others are as big as ~500 x 10^3 μm^3 (Alanentalo et al., 2007, Kim et al., 2009).

The two major cell types, β- and α-cells, regulate plasma glucose concentration through the secretion of insulin and glucagon, respectively. They collectively form a negative feedback loop maintaining blood glucose level within a specific narrow range. The normal blood glucose concentration in man ranges between 4 and 5 mmol/l, and insulin release is triggered in a concentration-dependent manner when the blood concentration exceeds above 3 mmol/l (Henquin et al., 2006a, Saberi et al., 2008, Braun et al., 2010) as compared to the threshold of ~6 mmol/l in mice (Hedeskov, 1980). As a consequence of insulin release, uptake of glucose increases in tissues such as muscle and glycogen storage is enhanced. Furthermore, gluconeogenesis and lipolysis are suppressed (Figure 2). In contrast, the release of glucagon is triggered by hypoglycaemia (<5 mmol/l), and increases plasma glucose levels by the mobilisation of hepatic glycogen.

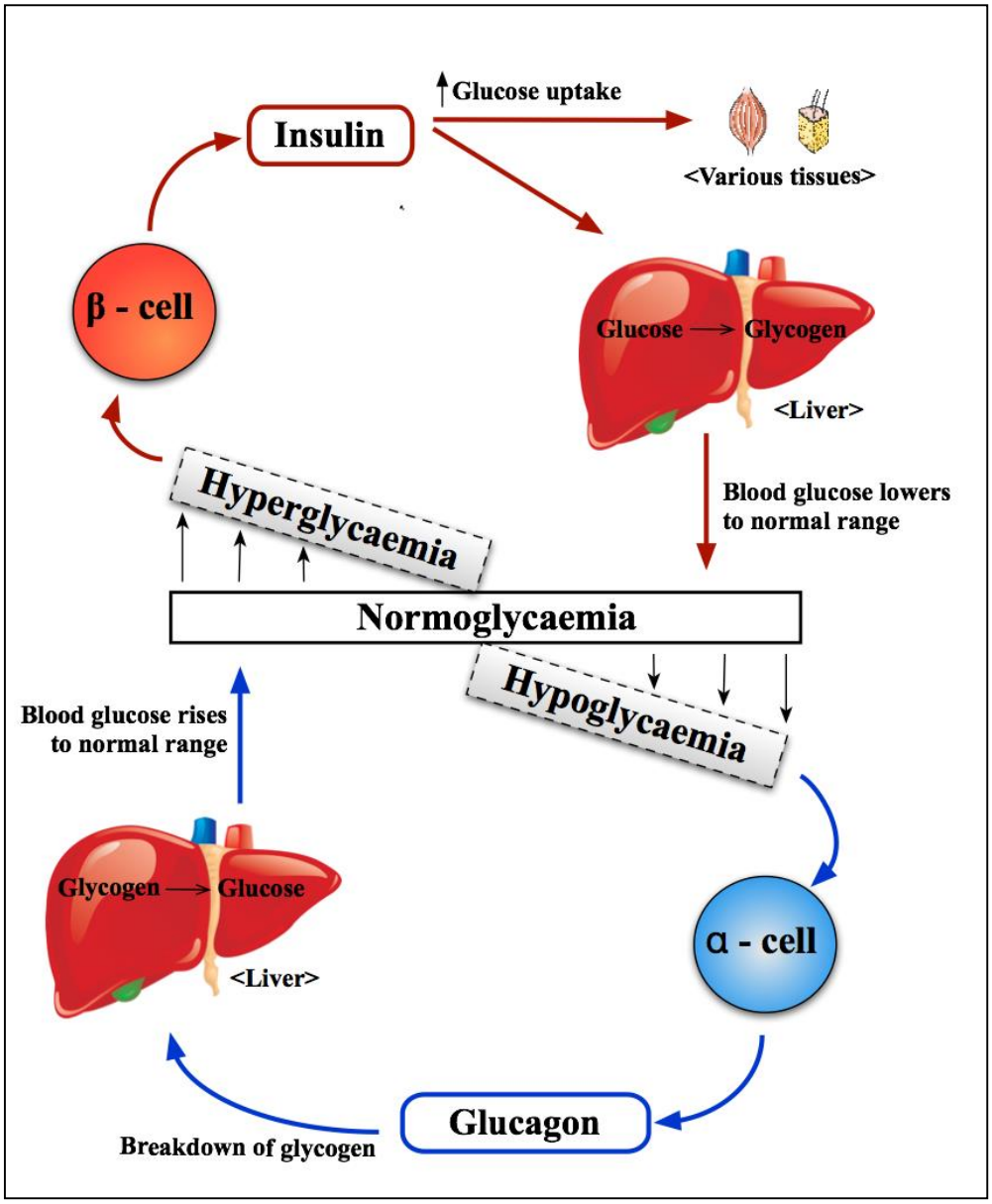


Figure 2. Regulation of blood glucose levels by reciprocal release of insulin and glucagon. When blood glucose level is high (highlighted by red), insulin is released from β-cell which stimulates glucose uptake and glycogen formation so that blood glucose level is lowered. When the blood glucose level is low (highlighted by blue), release of glucagon from α-cell stimulates glycogen breakdown, thereby increasing the amount of blood glucose (Modified from (Marieb, 2005)).

1.4.3 Innervation of pancreas

The pancreatic islets are densely innervated by a fine network of sympathetic and parasympathetic nerve endings (Radke and Stach, 1986, Barreto et al., 2010). These nerve fibres release various neurotransmitters upon stimulation such as acetylcholine and neuropeptide Y, which bind to their respective receptors on β– and/or α–cells to regulate hormone secretions. The sympathetic and parasympathetic innervations are derived from the splanchnic and vagus nerves, respectively (Salvioli et al., 2002). Insulin secretion is regulated by the counter-regulatory actions of both the parasympathetic and sympathetic nervous systems (Bloom and Edwards, 1980, Berthoud and Powley, 1990). Thus, vagal acetylcholine (ACh) stimulates insulin secretion whereas adrenaline/noradrenaline (sympathetic) inhibit it. Sympathetic innervation plays a very important stimulatory role in the regulation of glucagon release (Marliss et al., 1973, Ahren, 2000, Gautam et al., 2010). The neuronal regulation of pancreatic hormone secretion is mainly triggered by glucose-sensing in the hypothalamus, specifically in the arcuate and paraventricular nuclei (Guillod-Maximin et al., 2004).

1.5 Glucose regulation of biphasic insulin secretion

Glucose-stimulated insulin secretion (GSIS) exhibits a biphasic pattern (Henquin et al., 2006b). An initial and transient stimulation of insulin secretion (GSIS) is observed shortly after inducing hyperglycaemia, which is known as 1st phase insulin secretion. This is followed by a slowly developing but sustained component of insulin release that may last for several hours until normoglycaemia is restored, which is referred to as 2nd phase insulin release (Lacy et al., 1972). It has been proposed that both 1st and 2nd phases involve the exocytosis of geographically or functionally distinctive pools of insulin granules (Daniel et al., 1999). To elaborate further, insulin granules are considered to be located in 3 major functional pools below the plasma membrane: an intracellular reserve pool (~90%), morphologically/ultra-structurally docked pool (<10%), and a readily releasable pool (RRP) (~1%) which is a subset of the docked pool or near-membrane of granules (Rorsman et al., 2000). The RRP granules attain fusion competence by 'priming', a process that involves a series of ATP- and Ca^{2+}-dependent reactions (Parsons et al., 1995), and the formation of SNARE complexes (to be discussed further below) (Rettig and Neher, 2002). Accordingly, 1st phase insulin secretion has been proposed to reflect the fusion of docked granules (RRP) with the plasma membrane upon elevation of $[Ca^{2+}]_i$. After the depletion of the RRP, the 1st phase is terminated, and new granules are recruited for release from the reserve pool (Olofsson et al., 2002, Straub and Sharp, 2004). As a result, insulin is continuously released but at a lower rate (still higher than pre-stimulatory state) as long as increased glucose levels stimulate the β-cell.

Interestingly, 2nd phase insulin release can only be trigged by glucose and certain other nutrient stimuli, but not by non-nutrient stimuli such as tolbutamide (Gembal et al., 1992, Wang and Thurmond, 2009). In part, this reflects the ATP-requirement of granule

priming: in the absence of glucose, the cytoplasmic ATP concentration ($[ATP]_c$) is not high enough to sustain priming. It has also been proposed that it reflects the re-organisation of filamentous actin (F-actin) that acts as a physical barrier preventing the numerous granules of the reserve pool from reaching fusion competence. This re-organisation allows reserve granules to move closer to the plasma membrane to replenish the loss of the RRP resulting from 1st phase of insulin secretion (Thurmond et al., 2003, Jewell et al., 2008, Olofsson et al., 2009). Actin re-organisation is also influenced by Rho-family GTPases such as Rac1 and Cdc42. These co-localise with the insulin secretory granule (Regazzi et al., 1992, Kowluru et al., 1996, Veluthakal et al., 2009). The significance of these mechanisms for insulin secretion is illustrated by the disruption of 2nd phase insulin secretion following *Cdc42* deletion (via loss of *Pak1* and inactivation of *Rac1*) (Wang et al., 2007) and by the fact that *Rac1*KO mice exhibit reduced GSIS (Asahara et al., 2013). Notably, in addition to the conventional pools, another subset of granules originating from the reserve pool operates differently to the RRP. These granules are released at a lower $[Ca^{2+}]_i$ than the RRPs which are tethered to L-type Ca^{2+} channels and undergo exocytosis at $[Ca^{2+}]_i$ of 10-20 μmol/l (Barg et al., 2001). These are accordingly referred to as the highly calcium-sensitive pool of granules (HCSP) (Yang and Gillis, 2004). However, the contribution of the different granule pools, identified in isolated β-cells (that are maintained in tissue culture), to biphasic insulin secretion *in vivo* remains poorly understood.

1.5.1 Triggering pathway of insulin secretion

Glucose uptake into the β-cells is mediated by glucose transporters. In mice, this process mainly depends on glucose transporter 2 (Glut2) (Johnson et al., 1990) whereas in humans, GLUT1 is the main transporter (McCulloch et al., 2011). Glucose, taken up by

the β-cell, is phosphorylated to glucose-6-phosphate by glucokinase. The enzyme is a member of the hexokinase family (hexokinase IV), and exhibits two important characteristics making it particularly useful as a 'glucose sensor'. First, it has a lower affinity for glucose with a dissociation constant (K_m) of ~6 mmol/l glucose (close to the normal plasma glucose concentration), whereas other hexokinases (I, II, III) operate with their full capacity at this concentration (Xu et al., 1995). Second, it is not affected by the concentration of its product, glucose-6-phosphate (Meglasson and Matschinsky, 1984). Additionally, the expression of the other hexokinases is strongly suppressed in β-cells (Schuit et al., 1999). Glucose-6-phosphate is then further metabolised by aerobic glycolysis that results in the production of NADH and pyruvate in the cytoplasm. Cytoplasmic pyruvate enters the mitochondrial matrix, where it is converted into acetyl coenzyme A (acetyl CoA). Acetyl CoA then undergoes a series of oxidation reactions through the Krebs cycle (or tricarboxylic acid cycle; TCA). Reduced mitochondrial NADH, H^+ and $FADH_2$ generated in the Krebs cycle finally, via oxidative phosphorylation in the electron transport chain, produce ATP while decreasing cytosolic Mg-ADP concentration (Van Schaftingen, 1994). The coupled exchange of ATP and ADP across the inner mitochondrial membrane is mediated by ATP-ADP translocase (Brandolin et al., 1985).

In β-cells, the increase of cytosolic ATP serves as an intracellular second messenger which closes the ATP-sensitive potassium (K_{ATP}) channels in the plasma membrane (Tarasov et al., 2004). The K_{ATP} channel is an octameric complex consisting of four inward rectifier K^+-channel (Kir6.2) subunits, each associated to a single sulphonylurea receptor (SUR1) (Inagaki et al., 1995, Sakura et al., 1995). ATP binds to Kir6.2, while SUR1 mediates an activating effect of ADP on channel activity, thus allowing the K_{ATP}

channel to function as a sensor of the cytosolic ATP/ADP ratio (Nichols, 2006). Closure of the K_{ATP} channel causes membrane depolarisation, which in turn opens voltage-gated Ca^{2+} channels (VGCC), allowing Ca^{2+} ions to enter. The L-type Ca^{2+} channel, specifically Cav1.2, is responsible for ~50% of the total Ca^{2+} currents in mice (Schulla et al., 2003), and notably 1st phase insulin secretion is coupled with the activation of the L-type Ca^{2+} channels (Barg et al., 2002a). By contrast, in human β-cells, Ca^{2+} influx is mediated mainly through P/Q-type (Braun et al., 2008). The elevation of $[Ca^{2+}]_i$ triggers exocytosis of the insulin-containing secretory granules (Ammala et al., 1993, Bokvist et al., 1995) (Figure 3). In addition, Ca^{2+} influx through R-type Ca^{2+} channels (Cav2.3) has shown to contribute to 2nd phase of insulin secretion in mouse β-cells by triggering granule mobilisation and RRP replenishment (Jing et al., 2005, Pedersen and Sherman, 2009), but these channels are not at all present in human β-cells (Rorsman and Braun, 2013), illustrating the potential pitfalls of extrapolating observations in rodents to man.

The key role of K_{ATP} channels is demonstrated by the fact that GSIS is completely suppressed in the presence of the K_{ATP} channel opener diazoxide. Conversely, the K_{ATP} channel inhibitor tolbutamide triggers electrical activity, an increase in $[Ca^{2+}]_i$ and stimulates insulin secretion, even in the complete absence of nutrients (Trube et al., 1986, Henquin, 2000). The stimulation of insulin secretion that occurs via glucose- or tolbutamide-induced closure of the K_{ATP} channels is often referred to as the 'triggering pathway'.

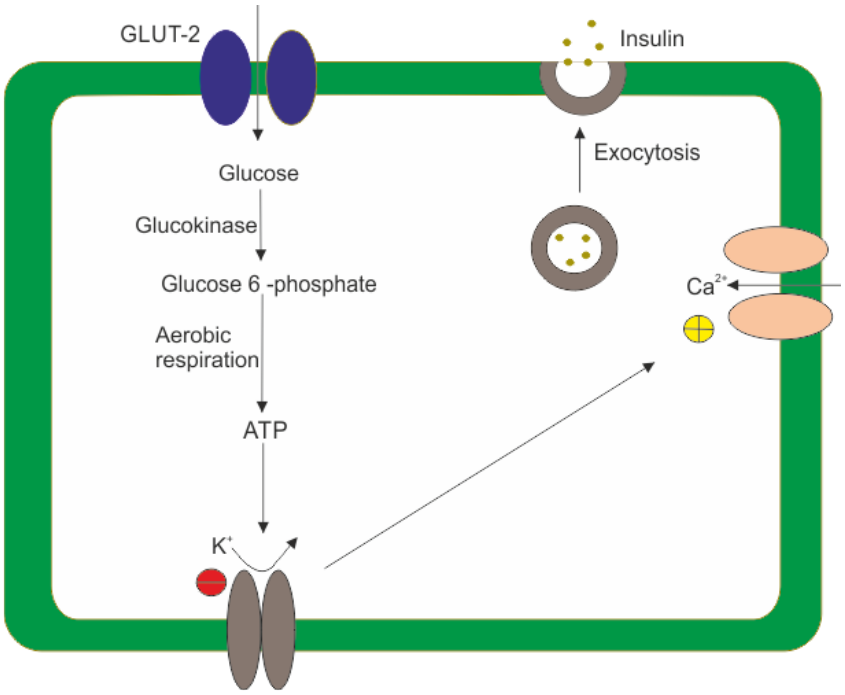


Figure 3. Consensus model for GSIS (triggering pathway). Glucose entry is mediated by Glut2 which then followed by cytosolic glycolysis and mitochondrial oxidative phosphorylation. Hence, cytoplasmic ATP concentration increases at the expense of $[ADP]_c$, leading to closure of the K_{ATP} channel. This results in membrane depolarisation and activation of voltage-dependent Ca^{2+} channels. The resulting submembrane elevation of $[Ca^{2+}]_i$ triggers exocytosis of insulin-containing granules, many of which are situated in the immediate vicinity of the Ca^{2+} channels.

1.5.2 Amplifying pathway

Accumulating evidence suggests that glucose, in addition to the 'triggering effect' described above, also exerts an amplifying mechanism. The existence of this mechanism was first documented in experiments in which β-cells were depolarised by high K^+ extracellular solution in the presence of diazoxide. Using this experimental paradigm, where $[Ca^{2+}]_i$ is maximally elevated, the application of glucose enhanced insulin secretion without any further elevation of $[Ca^{2+}]_i$ (Henquin et al., 1982, Henquin et al., 2009). Glucose also increases insulin secretion when K_{ATP} channels are completely blocked by a maximally effective sulphonylurea concentration (Best et al., 1992, Sato et al., 1999). These experiments illustrate that glucose increases insulin in a concentration-dependent manner even when the effects of glucose on K_{ATP} channel activity have been bypassed. Accordingly, the amplifying effect is sometimes referred to as the 'K_{ATP}-channel-independent mechanism', but this is a misnomer that can easily be misinterpreted. Physiologically, the amplifying pathway cannot operate independently from the triggering mechanism. This is because it acts via enhancing the secretory response to a given increase in $[Ca^{2+}]_i$, but it does not stimulate insulin secretion in the absence of such an increase. In this way, the amplifying pathway may augment the efficacy of a secretory response induced by the triggering signals (Gembal et al., 1993). Hence, the amplifying pathway may be described as an 'indirect' K_{ATP}-channel-dependent mechanism.

A number of second messengers resulting from glucose metabolism have been implicated as the 'amplification signal'.

ATP is a permissive factor that mediates the priming process of exocytosis (Eliasson et al., 1997). This mechanism is dependent on the reacidification of granules that is

facilitated by an intracellular chloride channel called ClC-3 (chloride channel-3) that favours the entry of chloride ions into the granules (Renstrom et al., 2002).

Glutamate is implicated as a potentiating factor. It is produced in β-cell mitochondria during glucose metabolism from the Krebs cycle intermediate α-ketoglutarate. Glutamate has shown to stimulate insulin exocytosis during GSIS in pancreatic β-cells without affecting $[Ca^{2+}]_i$, although the precise mechanism remains elusive (Maechler and Wollheim, 1999, Gheni et al., 2014). Furthermore, the β-cell specific glutamate dehydrogenase (GDH) (which catalyses the production of glutamate from α-ketoglutarate) KO mice exhibit impaired glutamate synthesis which resulted in reduced GSIS (Vetterli et al., 2012). However, others have failed to observe any amplifying effect of glutamate on GSIS (Bertrand et al., 2002, Jitrapakdee et al., 2010). This discrepancy might have arisen because the latter authors used glutamine (instead of glutamate), which has to go through several steps of metabolism to produce glutamate. Thus, further elucidation on the role of the metabolite is necessary.

Incretins have long been recognised to potentiate GSIS and their action relies on another important second messenger: cyclic AMP (cAMP). In particular, gastric inhibitory peptide (GIP) (also known as the glucose-dependent insulinotropic peptide) and glucagon-like peptide-1 (GLP-1) that are respectively secreted from enteroendocrine K and L cells, enhance GSIS by increasing intracellular cAMP via PKA-dependent and PKA-independent pathways (Hatakeyama et al., 2007). The activation of PKA leads to an enhancement of β-cell electrical activity thus facilitating Ca^{2+} influx through VGCC (Henquin and Meissner, 1983), and direct stimulation of exocytosis by triggering the release of granules from RRP while mediating the subsequent replenishment of the pool

(Renstrom et al., 1997). On the other hand, PKA-independent pathway involves a cAMP sensor, guanidine nucleotide exchange factor, type 2 (Epac2) (Holz, 2004). Its activation regulates calcium release from the intracellular stores (Kang et al., 2003), the granule acidity for the priming (Eliasson et al., 2003), and recruitment of insulin granules to the vicinity of the plasma membrane (Shibasaki et al., 2007).

1.6 Glucagon action in glucose homeostasis

A normal range of blood glucose (3.5–5.5 and <8 mmol/l for pre- and post-prandial level, respectively in humans) (Diabetes UK, 2015) is maintained by the reciprocal action of insulin secreting β-cells and glucagon-secreting α-cells in the pancreas (Unger and Orci, 1977).

Glucagon first came to Banting and Best's attention in 1921. They observed an initial increase in the glucose level when they injected insulin-enriched pancreatic extracts into pancreatectomised dogs (Best, 1972). However, they viewed it as an unwanted effect of the extracts due to the release of adrenaline. Murlin and colleagues confirmed the hyperglycaemic effect of pancreatic extracts independent of insulin in 1923. They regarded it as a hyperglycaemic contaminant and thus named it glucagon, meaning '**gluc**ose **agon**ist' (Murlin et al., 1923). In 1948, Sutherland and de Duve reported that α-cells of the islets of Langerhans secrete glucagon. Furthermore, they found that glucagon is required for hypoglycaemia, which triggers both glycogenolysis and lipolysis in the liver and adipose tissue, respectively (Sutherland and De Duve, 1948). In the 1970s, glucagon was finally recognised as a hormone (Unger, 1976). Unger and colleagues developed a radioimmunoassay specific for glucagon detection. This enabled physiological studies to confirm its role in glycaemic homeostasis during fasting (Unger et al., 1959, Unger et al., 1961, Unger et al., 1962).

More recently, there has been renewed interests in α-cells and glucagon secretion. It has been shown that diabetic patients secrete increased amounts of glucagon (Shah et al., 2000), and that in the absence of glucagon receptors, even the complete destruction of β-cells does not lead to hyperglycaemia (Lee et al., 2011).

1.6.1 Glucagon secretion in pancreatic α-cells

Pancreatic α-cells are electrically active, and they secrete dense core granules containing glucagon via Ca^{2+}-dependent exocytosis (Gromada et al., 1997). They are equipped with various ion channels that are responsible for action potential firing, which will be discussed later. The precise mechanism mediating the suppressor effect of elevated glucose on glucagon secretion remains obscure.

In a hypoglycaemic state (<3 mmol/l glucose), the secretory activity of pancreatic α-cells is maximised (Gromada et al., 1997, Zhang et al., 2013) (Figure 4A). A low concentration of glucose is transported into α-cells, presumably via Glut1 (Heimberg et al., 1995), which leads to a basal rate of glucose metabolism. Importantly, the ATP/ADP ratio at 1 mmol/l glucose in α-cells is comparable to that observed at 6 mmol/l glucose in β-cells (Detimary et al., 1998). This is high enough to close almost every K_{ATP}-channel (99%) in a metabolically intact α-cell (Gopel et al., 2000, Rorsman and Hellman, 1988), which leads to membrane depolarisation and AP firing. Pancreatic α-cells possess large-amplitude Na^+ currents that (unlike those found in β-cells) remain activated at physiological membrane potentials. The activation of the Na^+ channels contributes to the AP upstroke in mouse α-cells (Barg et al., 2000). The significance of the Na^+ channels is underscored by the effects on glucagon secretion that is observed upon application of tetrodotoxin (TTX). TTX leads to a complete inhibition of the Na^+ channels (but it does not suppress AP firing) which decreases the amplitude of the AP by 20 mV. In effect, it inhibits glucagon secretion as strongly as a maximally inhibitory glucose concentration (6 mmol/l) (Zhang et al., 2013, Rorsman et al., 2014).

Several types of voltage-gated calcium channel have been identified in α-cells. Human and mouse α-cells are equipped with low-voltage activated T-type calcium channels.

They are activated near the physiological membrane potential of α-cells (-60 mV) and they play a pace-making role in the initiation of APs (Leung et al., 2006, Vignali et al., 2006). Furthermore, despite the low density of P/Q-type calcium channels (~20%) as compared with L-type channels (~70%), the P/Q-type calcium channels are mainly responsible for glucagon secretion at low glucose. The application of ω-agatoxin (a specific P/Q type calcium channel blocker) in the presence of 1 mmol/l glucose inhibited glucagon secretion to a similar extent as 6 mmo/l glucose (Zhang et al., 2013). Overall, AP firing at low glucose leads to Ca^{2+} entry through P/Q-type calcium channels, which triggers the exocytosis of secretory granules containing glucagon (Ashcroft and Rorsman, 2013) (Figure 4A).

Glucagon secretion is maximally inhibited at >6 mmol/l glucose (Rorsman et al., 2014) (Figure 4B). Elevated glucose metabolism increases the ATP/ADP ratio. High glucose is associated with two important effects in pancreatic α-cells. First, it increases the frequency of AP firing (which would be expected to stimulate secretion). Second, the AP amplitude is reduced. This is due to voltage-dependent inactivation of voltage-gated Na^{+} channels. Thus, increasing the glucose concentration leads to a reduced Ca^{2+} influx through P/Q-type channels which are supposedly activated at the peak of APs (Rorsman et al., 2014). Notably, the inhibitory effect of the reduced AP amplitude is stronger than the stimulation by the increased AP frequency. Therefore, the net response to glucose is an inhibition rather than a stimulation (Zhang et al., 2013) (Figure 4B).

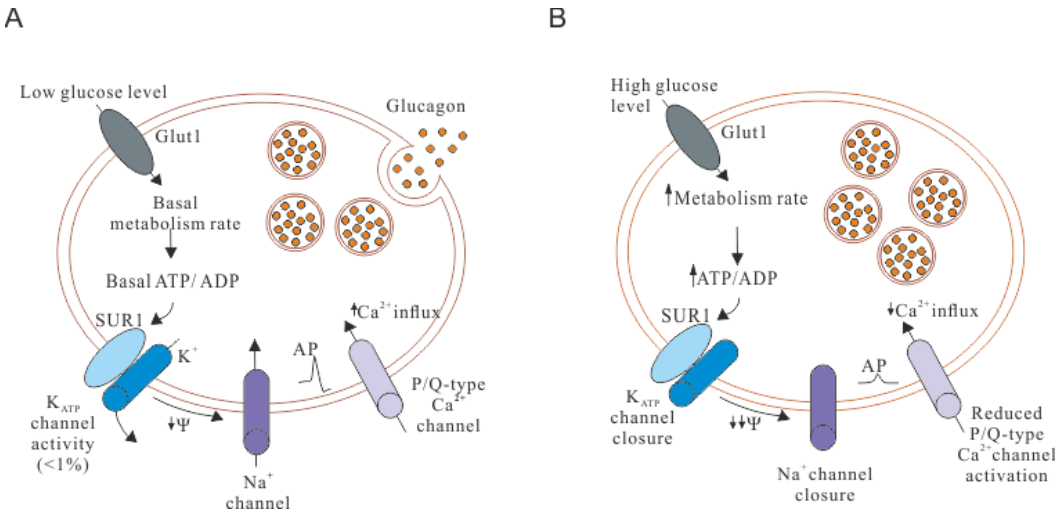


Figure 4. Glucagon secretion in pancreatic α-cells. (A) Glucagon is released at low glucose level. Glucose enters α-cells via Glut1 which leads to a basal glucose metabolism. This in turn produces a low level of ATP, but the ATP/ADP ratio is high enough to close almost all K_{ATP} channels (99%). Thus, the membrane potential of the cells becomes sufficiently depolarised to trigger AP firings. Both Na^+ and Ca^{2+} channels open, thereby triggering glucagon secretion. (B) A high level of glucose increases the ATP/ADP ratio which leads to a complete closure of K_{ATP} channels. This increases the frequency of AP firings, but also inactivates the Na^+ channels. In effect, Ca^{2+} influx is reduced which inhibits glucagon release (Modified from (Ashcroft and Rorsman, 2013)).

K_{ATP}-independent mechanism has been also suggested. Rorsman and colleagues (Rorsman et al., 2014) observed a glucose-dependent increase of glucagon secretion in the islets isolated from Kir6.2 mutant mice (with no functional K_{ATP} channels).

Furthermore, glucose increase may prevent glucagon secretion by a store-operating mechanism (Liu et al., 2004). Endoplasmic reticulum (ER) in pancreatic β-cells sequesters the increasing cytosolic Ca^{2+} concentration ($[Ca^{2+}]_i$) at high glucose concertation. Once the capacity of the ER is filled up by the extracellular calcium, it turns off the store-operated current, thereby repolarising the α-cell. Thus, glucagon secretion is inhibited.

1.6.2 Paracrine regulation of glucagon secretion

Paracrine factors, especially insulin and somatostatin, have been suggested to affect glucagon secretion. Both hormones are attractive candidates because of the close proximity of α- and δ-cells to β-cells, especially in human islets (Cabrera et al., 2006).

A regulatory role of insulin signalling on glucagon secretion has been observed (Kawamori et al., 2009). The α-cell-specific insulin receptor KO mice secreted more glucagon than WT mice upon L-arginine stimulation (which triggers both insulin and glucagon secretion). This is consistent with insulin acting as a paracrine suppressor of glucagon secretion but it was noted that the effect of ablating the insulin receptors in α-cells was fairly mild (Gromada et al., 2009). In human studies, an infusion of insulin reduced the glucagon secretion elicited by hypoglycaemia (Banarer et al., 2002). *In vitro*, exogenous insulin inhibits glucagon secretion, but only at a low glucose (Ramracheya et al., 2010). The inhibitory effect of insulin has been attributed to increased K_{ATP} channel activity (Franklin et al., 2005) that, via membrane repolarisation, may explain the reported lowering of $[Ca^{2+}]_i$ (Ravier and Rutter, 2005).

Somatostatin also represents a plausible candidate for a glucose-dependent extrinsic regulator of glucagon release. It is released from pancreatic δ-cells in response to an elevated glucose. Islets isolated from *Sst*$^{-/-}$ mice showed an elevated glucagon secretion in the presence of 1 mmol/l glucose. Furthermore, in the presence of 7 mmol/l glucose, the duration of the glucose-induced suppression of glucagon secretion was much shorter in *Sst*$^{-/-}$ islets than in WT islets (Cheng-Xue et al., 2013). A tonic inhibitory effect was similarly observed in another strain of *Sst*$^{-/-}$ mice (Hauge-Evans et al., 2009). It was also

reported that incubation of *Sst*$^{-/-}$ islets with exogenous somatostatin reduced glucagon secretion to a level that is comparable to that observed in WT mice.

1.7 Molecular steps involved in granule fusion and exocytosis

Eukaryotic cells communicate each other by releasing membrane-impermeable cargo through regulated secretion. This involves the fusion of secretory vesicles with the plasma membrane. Many physiological processes including neurotransmission (Sudhof, 2004) and hormonal secretion in homeostasis involve such regulated secretion. Indeed, the release of insulin into the blood stream proceeds in tightly regulated sequential steps of exocytosis: docking, priming, and fusion (Figure 7). These processes are assisted by a series of proteins in which membrane-associated SNARE (soluble N-ethylmaleimide-sensitive factor attachment protein receptor) proteins play a central role. The term SNARE came after the discovery of NSF (N-ethylmaleimide sensitive factor) and SNAP. Rothman and colleagues observed an inhibitory effect of the toxin NEM (N-ethylmaleimide) on Golgi trafficking (Balch et al., 1984). It was found to target the mammalian homologue of *SEC18* (Wilson et al., 1989), and the protein was named NSF (NEM-sensitive factor) (Block et al., 1988). With its adaptor molecule SNAP, the two soluble proteins are shown to be involved in intracellular trafficking pathways (Clary et al., 1990). It became apparent that 3 proteins (see below) universally mediate the membrane fusion in mammalian cells. These proteins are collectively referred to as SNARE proteins (Sollner et al., 1993b, Weber et al., 1998). Subsequent discovery of a large group of SNARE protein superfamily has established that they are similarly involved in the molecular machinery of all cellular vesicle trafficking steps (Chen and Scheller, 2001, Jahn et al., 2003).

1.7.1 SNARE classification

The first glimpse of the molecular basis behind ‘vesicle exocytosis’ was revealed in 1993 after the discovery of the SNARE proteins in neuronal cell types (Sollner et al., 1993a,

Sollner et al., 1993b) and the finding that they are the targets of tetanus and botulinum toxins (Schiavo et al., 1992, Blasi et al., 1993). The fundamental aspect of vesicle exocytosis is the formation of the SNARE complex, which involves association of three key SNARE proteins in opposing membranes (Sollner et al., 1993a): VAMP (vesicle-associated membrane protein) that is classified as a v-SNARE (vesicle-membrane SNARE), syntaxin and SNAP-25 (synaptosomal-associated protein of 25kD) both of which reside on the plasma membrane, referred to as t-SNAREs (target-membrane SNAREs) (Sollner et al., 1993b). Notably, specific isoforms of SNARE proteins, SNAP-23/SNAP-25 (Regazzi et al., 1996, Sadoul et al., 1997), syntaxin-1A and VAMP-2/VAMP-3 (Regazzi et al., 1995, Wheeler et al., 1996) are identified in pancreatic β-cell and they are involved in insulin secretion.

The formation of the SNARE complex during exocytosis is mediated by four conserved SNARE motifs that assemble into parallel α-helices (four-helix bundle) in a reversible manner. The bundle consists of 16 layers of interacting side chains in which the interface between the layers is mainly hydrophobic except for a central '0' layer. It contains four residues; three glutamines (Q) (one from syntaxin and two from the two SNAP-25s) and one arginine (R) (from VAMP). These residues combine to form an ionic interaction (Figure 5) (Fasshauer et al., 1998). Therefore, another way of classifying the SNAREs is based on which of these residues they contain: R– (VAMP), Qa – (syntaxin) and Qbc – (SNAP25) SNAREs (Fasshauer et al., 1998).

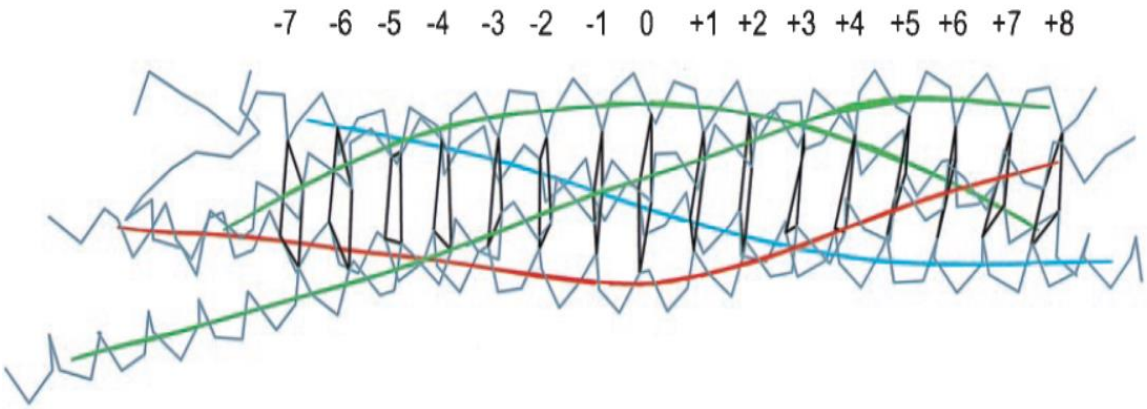


Figure 5. A skeleton diagram of the four-helix bundle structure. 16 layers of interacting side chains are indicated by the numbers above the trace. Cα traces are shown in grey, and four helices are presented as green, red and blue lines that respectively indicate for SNAP-25b, syntaxin-1A and VAMP-2 (Adopted from (Fasshauer et al., 1998)**)**.

1.7.2 SNARE structure

The SNARE proteins share a highly conserved SNARE motif consisting of 60-70 amino acids that are arranged in heptad repeats (Sutton et al., 1998). For VAMP-2 and syntaxin 1A, each SNARE domain is connected to the transmembrane domain (C-terminal end) by a linker (Figure 6). SNAP-25 contains one N-terminal and one C-terminal SNARE motifs that are connected by a linker domain. Although SNAP-25 lacks the transmembrane domain, it still can connect to the plasma membrane by its linker domain through palmitoylation (Figure 6) (Hess et al., 1992). It is generally accepted that at least one SNARE with a transmembrane domain must reside in each membrane for fusion to occur (Parlati et al., 2000, Shi et al., 2012). However, the role of the transmembrane domain still remains contradictory, as recently the replacement of the transmembrane domain of syntaxin 1A and/or VAMP-2 with a lipid anchor in embryonic neuronal cell did not prevent Ca^{2+}-induced exocytosis (Zhou et al., 2013).

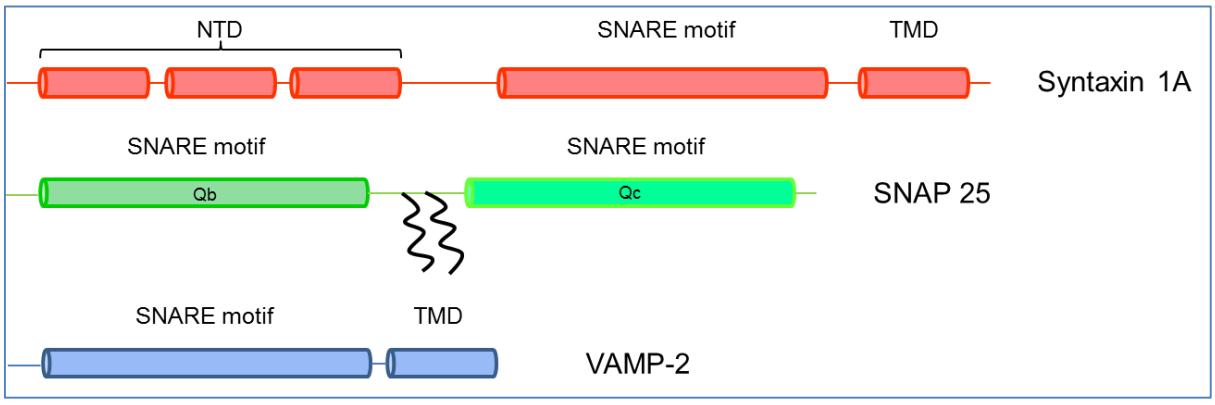


Figure 6. Domain structure of the SNARE proteins. Syntaxin 1A has antiparallel three-helix bundles at its N-terminus that are connected to SNARE motif and a single transmembrane domain at its C-terminus. SNAP-25 contains one Qb-SNARE motif and one Qc-SNARE motif that are connected by a palmitoylated linker (indicated by black zig-zag lines). VAMP-2 contains a C-terminal TMD and a conserved SNARE motif. Abbreviations used: NTD, N-terminal domain; TMD, transmembrane domain (Modified from (McNew, 2008)).

1.7.3 SNARE in membrane fusion

SNARE proteins undergo conformational changes that are hypothesised to promote the formation of the fusion pore during exocytosis (Sudhof, 2004, Jahn and Scheller, 2006). The initial observation of parallel alignment of syntaxin and VAMP in opposing membranes with their C-terminal transmembrane domains at one end provides basis for the zipper model during the SNARE complex assembly (Hanson et al., 1997, Lin and Scheller, 1997).

Free Q-SNAREs on target plasma membrane are first assembled into acceptor complexes (syntaxin and SNAP-25) (Fiebig et al., 1999, Fasshauer and Margittai, 2004), which are supposedly mediated by a number of proteins including members of the SM (Sec1/Munc-18) family. Notably, the association between syntaxin and SNAP-25 was observed *in vivo* using fluorescently tagged SNAP-25 which generated a FRET (fluorescence resonance energy transfer) signal when bound to syntaxin in PC12 cells (An and Almers, 2004). Munc-18 is considered to act before the SNARE complex formation (Yang et al., 2000, Dulubova et al., 2007), which stabilises the acceptor complex until VAMP-2 enters the complex. VAMP-2 displaces Munc-18 from the N-terminal of syntaxin 1 in the presence of SNAP-25, which triggers the conformational change of syntaxin from closed to open state, facilitating the SNARE complex formation. It proceeds in a zipper-like fashion from the N-terminus to the C-terminus, thereby overcoming the energy barrier created from electrostatic repulsion of opposing membranes and hydration repulsion between the hydrophilic surfaces of the phospholipid bilayers (Helm et al., 1989, Helm et al., 1992), and draws the secretory vesicle closer to the target membrane (Sutton et al., 1998). The assembled SNARE complexes linking the two membranes are called *trans*-SNARE complexes. Certain proteins regulate the full zippering of the *trans*-SNARE proteins

required for membrane fusion. Complexin binds to the assembled SNARE complex to clamp the fusion process to prevent exocytosis (Schaub et al., 2006). Its central helix has shown to associate with the VAMP and syntaxin, potentially blocking the full zippering of the SNARE complex (Chen et al., 2002). Upon Ca^{2+} stimulation, synaptotagmin (a calcium sensor protein) interacts with the already-assembled SNARE complex and displaces complexin to reduce the intensity of the clamp in a Ca^{2+}-dependent manner so that exocytosis can be triggered. This allows the full zipper to the tight conformation of the SNARE complex (Chapman and Jahn, 1994, Tang et al., 2006). This conformational change would bend the membranes by pulling the transmembrane domains which subsequently induces the fusion of the lipid bilayers of the membranes (Hanson et al., 1997, Lin and Scheller, 1997). During fusion, *trans*-SNARE complex is changed to *cis*-complex in which all the SNAREs are located in a single membrane.

Following granule exocytosis, the ATPase NSF dismantles the *cis*-complex using energy from ATP hydrolysis to restore SNARE proteins back to their original (pre-stimulatory) state (Block et al., 1988, Morgan et al., 1994). It is important to note that NSF interacts with the SNARE complex through the cofactor α/β-SNAPs which bind to the central zero layer of the complex (Clary et al., 1990, Marz et al., 2003).

1.7.4 SNARE in pancreatic β-cell

Initially, most exocytosis studies in relation to the SNARE complex have been carried out in neurones or chromaffin cells (Sudhof and Rizo, 2011, Jahn and Fasshauer, 2012) but the mechanisms involved extend to all cells exhibiting regulated release, including insulin-producing pancreatic β-cells (Wheeler et al., 1996, Torrejon-Escribano et al., 2011, Zhu et al., 2012).

The SNARE core complex has been shown to play a major role in GSIS from pancreatic β-cells (Regazzi et al., 1995, Sadoul et al., 1995, Dubois et al., 2007, Lam et al., 2013). Around 400 complexes of syntaxin 1 and SNAP-25 aggregate along the plasma membrane in a mouse β-cell (Vikman et al., 2006). This number is in reasonable agreement with the number of morphologically docked granules in the β-cell (Olofsson et al., 2002). The role of granule docking and the formation of the SNARE complex is also highlighted by the fact that 1st phase insulin secretion is greatly reduced in syntaxin 1 KO mice (Ohara-Imaizumi et al., 2007). The importance of the SNARE proteins in insulin secretion is further explained by their close proximity to the Ca^{2+} channels (Figure 7). The Ca^{2+} channels bind directly to the SNARE proteins through a synaptic protein interaction (synprint) site in the large intracellular loop connecting their domains II and III (L_{II-III}) of their α-1 subunits. Syntaxin, SNAP-25 and synaptotagmin bind to a L-type Ca^{2+} channel in a way that tethers the secretory granules, and the Ca^{2+} channel within a 10 nm range (Barg et al., 2002a). Therefore, the RRP is exposed to a high local concentration upon activation of the Ca^{2+} channels. This feature ensures high-speed exocytosis in β-cells despite the Ca^{2+}-channel density of only 5-10% of that seen in, for example, chromaffin cells (Barg et al., 2001). Moreover, a number of β-cell specific isoforms of the synaptotagmin have been identified; synaptotagmin 1,2 (Lang et al., 1997), 7 and 9 are postulated to mediate Ca^{2+}-dependent exocytosis in insulin-secreting cells (Gao et al., 2000, Iezzi et al., 2004, Grise et al., 2007). Notably, synaptotagmin 7 has a number of spliced variants and α- and β-isoforms are found to be specifically involved in GSIS. Both of them are co-localised in insulin granules and their expression was detected in INS1-E and rat β-cells (Gauthier et al., 2008, Sugita et al., 2001). Complexin, initially implicated as a regulator of neurotransmitter release, has been shown to play a regulatory role in GSIS in pancreatic β-cells (c cAbderrahmani et al., 2004).

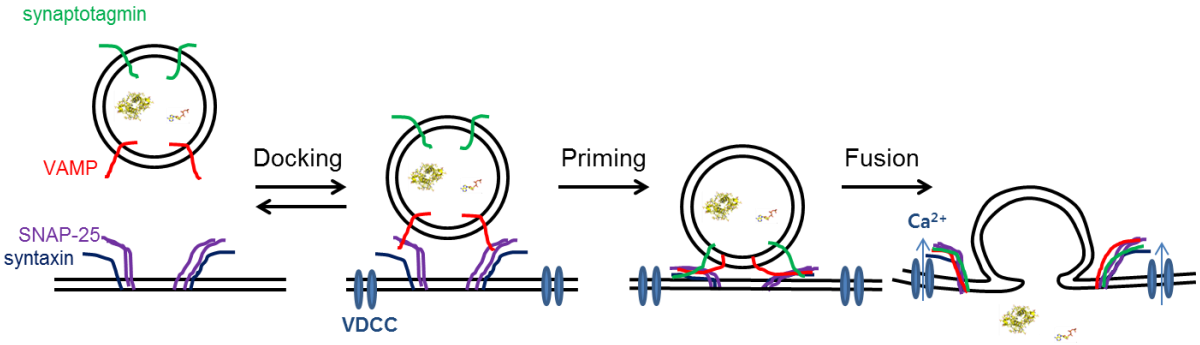


Figure 7. Mechanisms of exocytosis involving SNARE proteins. The secretory granule containing insulin (larger molecule) and small transmitters (ATP) moves close to the plasma membrane. During the docking process, the vesicular protein VAMP-2 (red) associates with the t-SNARE syntaxin (blue) and SNAP-25 (purple). After docking, the secretory granule may be tethered to the voltage-dependent L-type Ca^{2+} channel (VDCC). During priming, the SNARE complex pulls the vesicle closer to the plasma membrane and the vesicle becomes fusion-competent. The opening of Ca^{2+} channels leads to a localised elevation of $[Ca^{2+}]_i$, thereby enabling the fusion of the granule and release of insulin and ATP. Close physical association of the Ca^{2+} channels with the secretory granules ensures high-speed of exocytosis (Modified from (Rorsman and Renstrom, 2003)).

1.8 Fusion pore and two forms of granule fusion

Ca^{2+}-dependent exocytosis begins with the fusion of the lipid bilayers of the granule and the plasmalemma. The reorganisation of the resulting single lipid bilayer, by processes that are assisted by the SNARE proteins, leads to the formation of the fusion pore. The fusion pore is a (presumably) lipidic pore that connects the vesicle lumen and the extracellular space. Electrophysiological measurements of membrane conductance have confirmed that the fusion pore, following its formation, usually quickly expands until the granule collapses into the cell membrane, a process known as 'full fusion' (Neher, 1998). Alternatively, the fusion pore may remain stable for some time, leaving the granule intact, and the granule may be recycled back into the cytosol, a process known as 'kiss-and-run' exocytosis (Lollike et al., 1998).

1.8.1 Full fusion

Heuser and Reese first observed full fusion exocytosis in frog neuromuscular junction which was accompanied by clathrin-mediated retrieval of vesicles (Heuser and Reese, 1973). This concept was underpinned by the observation that the area of plasma membrane remained constant following synaptic fusion even after the intense electrical stimulation (Bittner and Kennedy, 1970). Based on these observations, the concept of full fusion became established, and was further identified in the CNS (central nervous system) (Sankaranarayanan and Ryan, 2000, Li and Murthy, 2001, Harata et al., 2006) and pancreatic β-cells (Orci et al., 1973, Taraska et al., 2003, Obermuller et al., 2005).

Full fusion allows efficient delivery of large molecules, including insulin stored in secretory granules. Since the granule's membrane is completely incorporated into the plasma membrane, the added granule membrane must subsequently be recaptured by

clathrin-dependent endocytosis to maintain constant volume of the membrane. Clathrin initiates an inward curvature of the membrane that is followed by the formation of a ring structure mediating the scission of the vesicle from the plasma membrane (Artalejo et al., 2002, Holroyd et al., 2002). The formation of the ring structure is catalysed by the GTPase dynamin (Roux et al., 2006). This mechanism is also implicated in restoring fusion-competent vesicles: Upon stimulation, a vesicle collapses into the membrane via full fusion, and soon after the SNARE protein is retrieved back into an empty vesicle (Sankaranarayanan and Ryan, 2000, Harata et al., 2006). At some neuronal synapses, retrieved granules are reacidified by a vesicular H^+ pump (Nishi and Forgac, 2002), allowing the reuptake of neurotransmitters (Granseth et al., 2006, Zhu et al., 2009). In addition, a change in lipid composition during fusion in chromaffin (Chasserot-Golaz et al., 2005) and mast cells (Puri and Roche, 2006) was suggested to create a microdomain in which some of SNARE proteins are protected from the granule/plasmalemma mix during exocytosis, facilitating their retrieval as a 'functional complex'. In chromaffin cells, stimulation results in changes in lipid composition which creates separate lipid domains near the primed granules (Umbrecht-Jenck et al., 2010). However, unlike neuronal cells, pancreatic β-cells are not equipped with such mechanisms. Thus, insulin-containing granules are destined for lysosomal degradation and cannot be refilled with insulin once the peptide hormone has been released (MacDonald and Rorsman, 2007).

1.8.2 Kiss-and-run exocytosis

Alternatively, in kiss-and-run exocytosis, the full expansion of the fusion pore may be interrupted, resulting in a semi-stable and relatively long-lived fusion pore, which will close. The granule is left structurally intact and the process can be reversed simply by the closure of the fusion pore. In stimulated β-cells, the majority of granule fusion is via full

fusion (~80%), and only 20% occurs via kiss-and-run (MacDonald et al., 2006). A series of classical experiments using frog neuromuscular junction have shown vesicular recovery after electrical stimulation without the collapse of the granule into the plasma membrane (Ceccarelli et al., 1972, Ceccarelli et al., 1973, Ceccarelli et al., 1979). In β-cells, kiss-and-run fusion pores are estimated to be only 1-2 nm in diameter (MacDonald et al., 2006). Whilst this is sufficient to allow the exit of small molecules (like ATP or GABA), it is too narrow to accommodate larger molecules including insulin itself (dimension: 3.2 x 3 x 2.5 nm) (Barg et al., 2002b). Hence, it has been hypothesised that full fusion is the only mode of exocytosis allowing the release of insulin (Obermuller et al., 2005, MacDonald et al., 2006) (Figure 8).

Importantly, there are factors which influence the prevalence of kiss-and-run exocytosis. A negative correlation between $[Ca^{2+}]_i$ and kiss-and-run has been demonstrated in rat hippocampal neurons. At a basal level of ~1 mmol/l extracellular Ca^{2+}, synaptic vesicles collapse and decay by ~1.9 s, which typically represents kiss-and-run. In contrast, once the extracellular Ca^{2+} was increased to 8 mmol/l, the duration of vesicle retrieval and reacidification was shortened by almost 7-fold (Leitz and Kavalali, 2011). Furthermore, the intensity of stimulation influences the rate of kiss-and-run exocytosis. Thus, when the frequency of stimulus (action potential train) was increased from 5 to 10 Hz, a gradual decrease of kiss-and-run from 75 to 0% was observed in hippocampal neurons (Harata et al., 2006, Richards, 2010). These observations suggest that high $[Ca^{2+}]_i$ favours full fusion at the expense of kiss-and-run exocytosis, and that kiss-and-run represents an economical way of vesicle exocytosis allowing recapture at low stimulatory intensities.

The importance of kiss-and-run exocytosis has been demonstrated in several types of cells. In adrenal chromaffin cells, dense core vesicles (DCVs) undergo kiss-and-run exocytosis (Lollike et al., 1998, Dernick et al., 2003). During kiss-and-run exocytosis, catecholamines are released into the intercellular space via the fusion pore (Albillos et al., 1997, Dernick et al., 2005). Interestingly, a new type of kiss-and-run exocytosis, called 'extended' kiss-and-run, has recently been documented in PC12 cells where the fusion pore expands to much greater width than in conventional kiss-and-run, allowing effective neurotransmitter release (Mellander et al., 2012). These vesicles, which remain largely structurally intact, may subsequently be refilled with the neurotransmitter (Toll et al., 1977). Analogously, synaptic vesicles in dopaminergic neurones primarily undergo kiss-and-run exocytosis to regulate release of neurotransmitters (Staal et al., 2004). Thus, the amount neurotransmitter/hormone (and even the molecular species) may be regulated by switching between different modes of kiss-and-run exocytosis. In either case, this allows for the economical use of the synaptic vesicles. However, it is important to note that physiological significance of kiss-and-run as a major form of exocytosis even in the synapse remains controversial. Ultrastructural morphological studies showing the formation of an omega-shaped structure during fusion have been regarded to constitute of kiss-and-run exocytosis, but such electron microscopy (EM) snapshots cannot tell whether the granule was ultimately destined for full fusion or kiss-and-run exocytosis (Heuser, 1989). More recently, evidence that kiss-and-run represents a major form of fusion (~60%) in hippocampal neurones was provided by use of pH-dependent quenching of quantum dots (Zhang et al., 2009), which detects pH changes inside the lumen during membrane fusion (Miesenbock et al., 1998). This notion was subsequently reinforced by using a pH-dependent fluorescent dye (synaptophysin-pHluorin) (Granseth et al., 2009). However, it was also reported that the proportion of kiss-and-run exocytosis may be over-

estimated depending on the analysis methods and experimental conditions. The observation that synaptic vesicles are principally retrieved by clathrin-mediated endocytosis (Granseth et al., 2006, Zhu et al., 2009), not a feature expected for kiss-and-run exocytosis, contributes to the uncertainty pertaining to the functional significance of kiss-and-run exocytosis. Thus, the occurrence of kiss-and-run exocytosis must be carefully validated before any firm conclusions can be drawn. Finally, the functional role (if any) of kiss-and-run in β-cells (which will be discussed in chapter 3) still remains controversial.

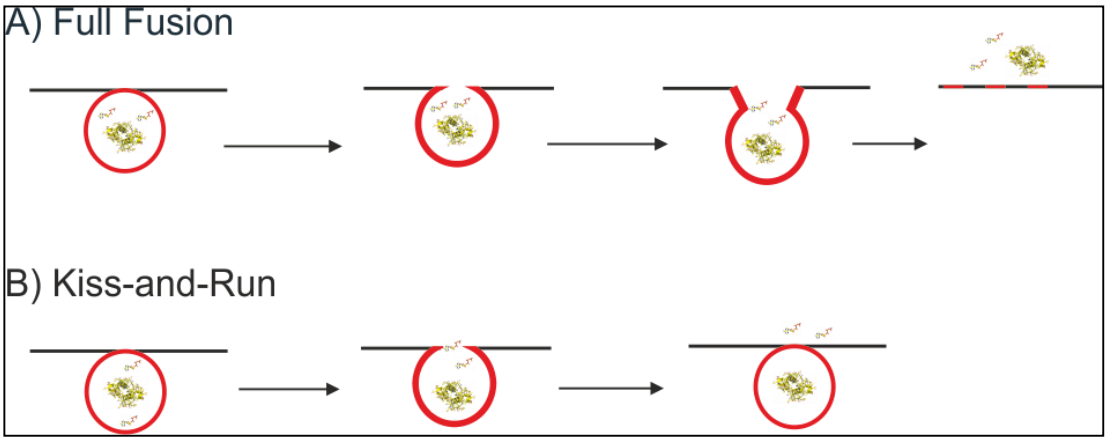


Figure 8. Schematic representation of the two modes of granule fusion steps leading to secretory granule exocytosis. (A) The membrane of the granule fuses with the plasmalemma and the granule then collapses into the plasma membrane, thereby releasing all of its content. (B) In kiss-and-run, the fusion pore remains stable and the granule may subsequently be recaptured by fusion pore re-sealing. In this case, only small molecules such as ATP are released, but not insulin (larger molecule) (Modified from (Hanna et al., 2009)).

1.9 Advancement of T2D mouse models

The GWAS have led to the identification of a number of genes increasing the risk of T2D by affecting β-cell function. Many of these genes were not previously implicated in the control of insulin secretion and precisely how they increase diabetes risk is therefore not immediately evident.

Studying the function of a gene of interest in mouse models allows us to gain insight into the function of corresponding orthologous human genes. To assess the role of a gene, a common way is to create a mouse model without the gene of interest (knock-out), or by introducing a gene mutation that changes the amino acid sequence of the protein.

1.9.1 KO strategy

A series of knockout (KO) models have been developed, which greatly enhanced our understanding of T2D. Notably, an international KO consortia initiated in 2006 aims to decode the function of all genes (International Mouse Knockout et al., 2007). So far, 40% of the mouse genes have been deleted in single gene KOs but their function have only partially been characterised (Skarnes et al., 2011).

Homozygous *Insr* KO mice exhibit severe hyperglycaemia and diabetic ketoacidosis (Accili et al., 1996, Joshi et al., 1996). Heterozygous *Insr* KO mice are insulin resistant but exhibit normal glucose tolerance (Accili et al., 1996). As most T2D patients tend to develop dysfunctional insulin receptor as the disease progresses (Olefsky et al., 1982), the milder heterozygous *Insr* KO mice were often chosen to investigate the consequence of genetic predisposition because this would facilitate the identification of novel diabetes genes which on their own have a fairly subtle effect.

Tissue-specific deletion became possible by use of the Cre-loxP system. The Cre-loxP recombination system is widely used for conditional KO models (Lakso et al., 1992, Akagi et al., 1997). The system consists of a single enzyme, site-specific Cre recombinase that recombines a pair of loxP flanking the target sequences (floxed). It is important to note that the orientation and location of flanking loxP sites mediate different kinds of recombination. To specifically delete the gene of interest, two loxP sites should be arranged in the same direction on the chromosome. If loxP sites face towards each other, it will result in an inversion of the target sequence (Nagy, 2000). Prior to the tissue-specific deletion of the target gene, the floxed strain is first crossed with a Cre-transgenic mouse that is equipped with a tissue-specific promoter controlling the expression of the recombinase Cre to produce a Cre-loxP mouse. In the presence of an active Cre recombinase, the enzyme excises the floxed gene of interest by joining the loxP sites, thereby generating a null allele in the target cell. In the mouse lacking Cre recombinase expression, the target gene remains intact. By utilising the Cre-loxP system, pancreatic β-cell – (Kulkarni et al., 1999), liver – (Michael et al., 2000), neuronal – (Bruning et al., 2000), and muscle – (Bruning et al., 1998) specific *Insr* KO models were created. The β-cell specific *Insr* KO model displays a reduction in the 1st phase of GSIS and progressively develops glucose intolerance, resembling a T2D phenotype (Kulkarni et al., 1999).

1.9.2 ENU mutagenesis

The injection of N-ethyl-N-nitrosourea (ENU), an alkylating agent, into male mice induces random point mutations in spermatogonial stem cells with a specific locus mutation rate generally of $>10^{-3}$ (i.e. a functional mutation at a single locus in 1000 mice (Noveroske et al., 2000)). Point mutations can lead to several types of adverse effects in

genes such as loss- or gain-of-function, which resembles the underlying cause of most human diseases. Although ENU mutants have an advantage of maintaining the intact genome and the gene of interest is not completely destroyed (which only results in severe phenotype) (Justice et al., 1999), ENU-triggered mutations are random, so the specific function of the gene of interest can be better investigated in a KO model. Furthermore, once a functional mutation is identified, the ENU-treated mouse still has to go through a number of back-crossing steps to ensure the specificity of the mutation, and also the fertility of the offspring.

The ENU resource facilitates two main screens: phenotype-driven (forward) or genotype-driven (backward) approaches (Lee and Cox, 2011). The phenotype-driven approach seeks for desired characteristics in ENU-treated mice, and subsequently the causative mutation is mapped by genotyping to locate the site of mutation precisely. Conversely, in genotype-driven strategies, ENU mutation is screened first in a gene of interest, specifically in DNA or frozen sperm samples. Then the mouse is generated from the chosen frozen sperm for functional characterisation. Gene-driven strategies using this mutagen have been developed to provide new disease models for the study of a mammalian gene function (Brown and Balling, 2001).

As alluded to above, the advent of GWAS has resulted in the identification of several common gene variants conferring small increments in T2D risk. This information may eventually pave the way for the elucidation of molecular causes of the β-cell defect(s) that cause T2D. This is critically needed in translational endeavours. ENU mouse models thus provide a valuable means in this context, but less so for phenotype-driven approaches since genes are not directly associated in human samples.

1.10 Aims of the thesis

The main aim of the thesis is to characterise three novel T2D mouse models. Each of them carries distinct diabetes-associated phenotype. We were also interested why senescence is associated with increased diabetes risk. The specific aims were therefore to:

1) determine the pathophysiological mechanism on how an insulin secretion defect provokes overt diabetes through investigating a mouse model harbouring an ENU-induced *Sox4* mutation;
2) elucidate the precise role of β-cell specific *Fh1* (which is known as a tumour suppressor gene) in GSIS;
3) investigate the effects of age on GSIS, insulin content and glucagon secretion

CHAPTER 2

Materials and Methods

2.1 Animals

All experiments were conducted in accordance with the UK Animals Scientific Procedures Act (1986) and ethical guidelines of the University of Oxford. Mice were maintained on a 12 h light/dark cycle with free access to water and a standard diet.

2.1.1 Generation of *Sox4* mutant mice

Male mice (heterozygous for the insulin receptor knockout mutation) obtained from the Jackson lab (Accili et al., 1996) were treated with 2 x 100 mg/kg doses of ENU at 7-day intervals (Coghill et al., 2002). ENU-treated mice were checked for their fertility by crossing with C3H female mice. F1 male offspring that exhibit heterozygous insulin receptor KO were then assessed for glucose tolerance. Identified glucose intolerant mice were further tested for their ability to pass on the phenotype by backcrossing to female C3H. A mutation in the *Sox4* gene was identified through genetic screening (Goldsworthy et al., 2008). The original male identified in the screen carried the heterozygous *Sox4* mutant allele in the presence of a heterozygous insulin receptor KO allele. In our study, this mouse was further mated with C3H female mice to select the mouse which only carries the heterozygous *Sox4* mutant allele. Therefore, mice used for our investigations were heterozygous for the *Sox4* mutation and were $Insr^{+/+}$. These procedures were carried out at the MRC Harwell by our collaborator Roger Cox.

2.1.2 *Fh1*KO and FH rescue mice

Pancreatic β-cell specific *Fh1*KO mice were provided by our collaborator Patrick J. Pollard (WTCHG, Oxford). This line was generated by crossing a floxed *Fh1* mouse and a mouse expressing the Cre recombinase under the control of the rat insulin promoter 2

(Rip2) as previously reported (Postic et al., 1999, Pollard et al., 2007). Sex- and age-matched littermates clear of the Rip2-Cre transgene were used as controls.

The CAG-FH/Cre transgenic mice were generated by integration of full length (human) *FH* cDNA under the control of the ubiquitous CAG promoter (chicken-beta actin promoter/CMV immediate early promoter enhancer) into C57BL/6 females (Adam et al., 2013). These mice were then crossed with *Fh1*KO to generate FH rescue mice. In addition, FH transgenic mice (which serve as a rescue control) were created by mating with C57BL/6 males instead of *Fh1*KO mice to validate any side-effect of *FH* cDNA insertion.

Effective deletion of *Fh1* in β-cells of the pancreatic islets and correct integration of the FH construct were confirmed in sections of pancreases from *Fh1*KO, FH rescue and FH transgenic mice, respectively by both immunohistochemistry and PCR. These procedures were carried out by Dr J Adams.

2.2 Islet isolation

Mice were killed by cervical dislocation, and the pancreas was quickly removed. Isolation of pancreatic islets was carried out by injecting collagenase (1.9 units/ml) through the common bile duct. Islets were hand-picked from the digest, washed and maintained for up to 72 h in RPMI 1640 medium (Gibco, Paisley, UK) supplemented with 5 mmol/l glucose, 10% FCS, 100 µg/ml streptomycin and 100 i.u./ml penicillin at 37°C in a humidified atmosphere of 5% CO_2 in air.

2.3 Glucose tolerance test (IPGTT)

Mice were weighed and fasted overnight (~16 h). Weights and basal glucose levels were measured prior to a 2g/kg intraperitoneal glucose injection. Glycaemia was then measured at 15, 30, 60, 90, 120 and 180 min using an Accuchek Aviva meter (Roche, Hertfordshire, UK). This was carried out by Dr J Adams.

2.4 ATP measurements

Isolated islets were allowed to recover for 3 h before the ATP measurements. Batches of 10 similar-sized islets were washed and then pre-incubated for 1 h at 37^{o}C in 300 µl Krebs-Ringer buffer (KRB) solution which contained (in mmol/l) 140 NaCl, 3.6 KCl, 2.6 $CaCl_2$, 0.5 $MgSO_4.7H_2O$, 0.5 NaH_2PO_4, 2 $NaHCO_3$, 2 glucose and 5 HEPES (pH adjusted to 7.4 using NaOH) and was supplemented with 2 mg/ml BSA. The supernatant was discarded and the islets were further incubated for 1 h in 300 µl of KRB supplemented with test conditions as indicated. Each glucose concentration was tested in 12 separate replicates across 3 mice per condition. The supernatant was replaced by 100 µl of detergent (Lonza Group Ltd, Basel, Switzerland). ATP was measured from 50 µl aliquots using a luciferin-luciferase bioluminescent assay (Lonza Group Ltd, Basel, Switzerland) and a luminometer (Turner Designs, Sunnyvale, California). This was carried out by Dr K Shimomura.

2.5 Intracellular calcium measurements

The intracellular calcium concentration ($[Ca^{2+}]_i$) was assessed in freshly isolated intact islets using a dual wavelength PTI system (PTI, Monmouth, USA) fitted on an inverted Zeiss microscope allowing ratiometric measurements using the calcium probe, fura-2

AM (Invitrogen, Paisley, UK). Islets were loaded with 3 µmol/l fura-2 AM in the presence of 0.007% w/v pluronic acid (Invitrogen, Paisley, UK) for 20 min at 37°C. Islets were held in place in the experimental chamber using a wide-bore fire polished borosilicate glass pipette. The chamber was superfused with a pre-heated solution (37ºC) composed of (in mmol/l: 140 NaCl, 2.6 $CaCl_2$, 3.6 KCl, 2 $NaHCO_3$, 0.5 NaH_2PO_4, 0.5 $MgSO_4$ and 5 HEPES (pH 7.4 adjusted with NaOH). Glucose and tolbutamide were included in the extracellular medium as indicated. The fluorochrome was excited at 340 and 380 nm. Emitted light was collected at 510 nm. The F_{340}/F_{380}-ratio was determined at a frequency of 25 Hz.

2.6 Electrophysiology

2.6.1 General

Patch electrodes (2-3 or 5-7 MΩ resistance when filled with the pipette solution for on-cell and whole-cell recordings, respectively) were pulled from borosilicate glass capillaries (Hilgenberg, Malsfeld, Germany). The electrodes were coated with Sylgard close to the tips and fire-polished. The electrophysiological measurements were made using an EPC-10 patch clamp amplifier and Pulse 8.51 software (Heka Elektronik, Lambrecht/Pfalz, Germany) for whole-cell measurements and using Patchmaster 2.20 software for on-cell capacitance measurements.

β-cells were plated on cover slips to allow for the cells to attach during tissue culture, and maintained at 32°C during perfusion. They were identified based on their typical larger size (>5.5pF) or complete inactivation of the Na^+ current at -70mV. In rodents, immunohistochemical experiments indicate that almost all cells fulfilling these criteria are β-cells (Rorsman et al., 2014).

2.6.2 Whole-cell capacitance and Ca^{2+} currents

Exocytosis and whole-cell Ca^{2+} currents were recorded on isolated β-cells using the standard whole-cell configuration. Cells were superfused with a solution (EC1) containing (in mmol/l: 118 NaCl, 20 TEA-Cl_2, 5.6 KCl, 2.6 $CaCl_2$, 1.2 $MgCl_2$, 5 glucose and 5 HEPES (pH 7.4 at 32°C adjusted with NaOH). The membrane capacitance that reflects exocytosis was monitored using the software lock-in (which adds a 500 Hz sine wave to the holding potential). The stimulus consisted of a train of ten 50-ms or ten 500-ms depolarisations from -70 to 0 mV. The pipette solution contained (in mmol/l) 125 Cs-glutamate, 10 CsCl, 10 NaCl, 1 $MgCl_2$, 0.05 EGTA, 3 Mg-ATP, 0.1 cAMP and 5 HEPES (pH adjusted to 7.35 with CsOH at 32°C). Access and seal resistance were <15 MΩ and >1 GΩ, respectively.

2.6.3 On-cell single-granule exocytosis measurements

Exocytosis and fusion pore were detected in the cell-attached configuration, which allows the simultaneous recording of the membrane capacitance and the fusion pore conductance. The extracellular solution (EC1, see above) was also used to fill the pipette. The PATCHMASTER software (Heka Electronics, Lamprecht/Pfalz, Germany) together with the EPC10 implements an 'internal calibration'. They automatically correct for phase-shifts and frequency-dependent attenuation when a sinusoidal voltage command of 25 kHz is generated (Neef et al., 2007). To stimulate the cells, 20 mmol/l glucose was perfused. The scaled apparent capacitance (Im/ω) and conductance (Re) are then calculated online by the software. Pore diameters were calculated by assuming a cylindrical pore length of 15 nm (i.e. 2 x 7.5 nm; 7.5 nm being the thickness of a single membrane layer) and a solution resistivity of 66.7 Ω.cm (equation 11.1 in (Hille, 2001)).

2.6.4 $P2X_2$ receptor analysis

Ad$P2X_2$R-GFP was made using an Adeno-X™ Expression system (BD Biosciences Clontech, Erembodegem, Belgium). The cDNA encoding the rat $P2X_2R$ linked to GFP (kindly provided by B.S. Khakh, Cambridge, UK) was subcloned into a pShuttle vector. The expression cassette was then excised using PI-Sce and I-Ceu I, and ligated into pAdeno-X. Adenoviral particles were amplified into HEK293 cells. Primary β-cells were in culture for 12 h and they were infected with the adenoviral construct. The culture medium was replaced after 4 h. Experiments were carried out 24 h after infection. Whole-cell currents were measured in identified β-cells that were superfused with EC1 dialysed with Ca^{2+} using an intracellular solution containing (mmol/l) 125 $CsCl_2$, 10 NaCl, 1 $MgCl_2$, 10 EGTA, 9 $CaCl_2$, 3 Mg-ATP, 0.1 cAMP, 5 HEPES (pH 7.4 at 32^{o}C adjusted with NaOH). The current spikes (reflecting ATP release) were analysed using the Mini Analysis Program 6.0.3 (Synaptosoft, Decatur, USA) to determine the charge (integrated current; Q) and rise times ($t_{0.5}$) of the individual events.

2.7 Culture of INS-1 832/13 cell line

INS-1 832/13 cells (Hohmeier et al., 2000) were cultured in RPMI 1640 containing 11 mmol/l glucose, 10% foetal calf serum (Sigma, Dorset ,UK), 100 µg/ml streptomycin, 100 µg/ml penicillin, 50 µmol/l 2-mercaptoethanol, 1 mmol/l sodium pyruvate, 10 mmol/l HEPES, and 2 mmol/l GlutaMAX (L-alanyl-L-glutamine) at 37°C in an atmosphere of humidified air (95%) and CO_2 (5%). All the reagents were purchased from Invitrogen (Paisley, UK) with the exception of foetal calf serum (as indicated above).

2.8 Culture of EndoC-βH2 cell line

EndoC-βH2 cells (Scharfmann et al., 2014) were cultured in low glucose (5.6 mmol/l) Dulbecco's modified Eagle's medium (DMEM) (Sigma, Dorset, UK) with 2% BSA fraction V (Roche Diagnostics, West Sussex, UK), 50 mmol/l 2-mercaptoethanol, 10 mmol/l nicotinamide (Calbiochem Nottingham, UK), 5.5 mg/ml transferrin (Sigma, Dorset, UK), 6.7 ng/ml selenite (Sigma, Dorset, UK), 100 mg/ml penicillin (Invitrogen, Paisely, UK), 100 mg/ml streptomycin (Invitrogen, Paisely, UK), and 2 mmol/l GlutaMAX (L-alanyl-L-glutamine) (Invitrogen, Paisely, UK). Cells were seeded at a density of 5 * 10^4 cells/cm^2 on Matrigel (1%)/2 mg/ml fibronectin (Sigma, Dorset, UK) - coated plates and cultured at 37 ^oC and 5% CO_2.

2.9 Human islet secretion and microarray studies

Islets from 62 cadaveric donors of European ancestry were provided by the Nordic Islet Transplantation Programme (http://www.nordicislets.org). Islets were isolated at Lund University Diabetes Centre. All procedures were approved by the ethics committee at Lund University. There islets were from non-diabetic donors with median age of 57 (27-73 range) and median BMI (kg/m^2) of 25 (18-34 range). Purity of islets was assessed by dithizone staining, while measurement of DNA content and estimate of the contribution of exocrine and endocrine tissue. The islets were cultured in CMRL 1066 (ICN Biomedicals) supplemented with 10 mmol/l HEPES, 2 mmol/l L-glutamine, 50 µg/ml gentamicin, 0.25 µg/ml Fungizone (GIBCO), 20 µg/ml ciprofloxacin (Bayer Healthcare), and 10 mmol/l nicotinamide at 37 °C (5% CO_2) for 1–9 days prior to RNA preparation. Total RNA was isolated with the AllPrep DNA/RNA Mini Kit following the manufacturer's instructions (Qiagen). RNA quality and concentration were measured

using an Agilent 2100 bioanalyzer (Bio-Rad) and Nanodrop ND-1000 (NanoDrop Technologies).

The Affymetrix GeneChip® Human Gene 1.0 ST microarray chip was used for gene expression analysis in accordance with the standard protocol. Briefly, total RNA was converted into biotin-targeted cRNA following the manufacturer's specifications, and the biotin-labeled cRNA was fragmented into strands with 35 to 200 nucleotides. This was hybridized onto the chip overnight in a GeneChip® Hybridization 6400 oven using standard procedures. The arrays were washed and stained in a GeneChip® Fluidics Station 450. Scanning was carried out with the GeneChip® Scanner 3000 and image analysis was done with the GeneChip® Operating Software. Data normalisation was performed using Robust Multi-array Analysis (RMA). This was carried out by Dr A Rosengren and associates at the Lund University Diabetes Centre.

2.9.1 Human islets

For studies in chapter 7, independent of the human islets that are described above, human pancreases were provided by the Oxford DRWF Human Islet Isolation Facility within OCDEM with ethical approval and clinical consent from donors without a known clinical history of diabetes. Islets were isolated in the Diabetes Research & Wellness Foundation. Human Islet Isolation Facility by collagenase digestion (Serva, Heidelberg, Germany), using modified versions of published procedures (Ricordi et al., 1988, Lake et al., 1989).

2.10 Insulin and glucagon secretion assays

2.10.1 Static incubation

For studies in chapter 3, isolated islets were cultured for 2-4 h. Insulin secretion was measured from batches of 10 islets per group. The islets were washed twice in glucose-free RPMI-1640. The islets were pre-incubated for 1 h in humidified 5% CO_2, 95% air at 37°C in the presence of 300 µl of KRB supplemented with 1 mmol/l glucose. The pre-incubation buffer was discarded and the islets were further stimulated for 1 h with test conditions as indicated. 250 µl of the supernatant was collected and stored at -20^{o}C for further insulin measurement using a commercially available radioimmunoassay (RIA) kit (Linco, Watford, UK). The islets were lysed in 100 µl of ice-cold acid ethanol mixture (containing ethanol, H_2O and HCl at a ratio of 52:17:1) to release intracellularly stored insulin. The lysates were immediately frozen at -20^{o}C.

2.10.2 Hormone measurements in human islets

For studies in Oxford (data presented in chapter 7), either freshly isolated mouse islets were used, whereas human islets were cultured overnight in CMRL medium containing 5.5 mmol/l glucose and 2 mmol/l l-glutamine. Briefly, groups of 10–20 size-matched islets were preincubated in 0.3ml of a modified Krebs-Ringer buffer containing 3 mmol/l glucose and 2 mg/ml BSA for 1 h at 37°C, followed by 1 h test incubation in 0.3 ml of the same medium supplemented with 1, 6 and 20 mmol/l glucose as indicated. Islet hormone content was determined after extraction with acidic ethanol. Insulin and glucagon were assayed using Millipore RI-3K (Billerica, MA, USA) and Eurodiagnostica RB 306 (Malmo, Sweden) radioimmunoassay, respectively. This was carried out by Dr R Ramracheya.

2.10.3 Pancreatic perfusion studies

For studies in chapter 6, mice were killed by cervical dislocation, and placed on a modified heated rodent operating table (Harvard Apparatus, Kent, UK). The abdomen was surgically opened and ligatures were placed on the following vessels: the renal arteries, the gastric and hepatic artery and veins, the abdominal aorta (below and above the coeliac and supermesenteric artery) and the hepatic portal vein. Catheters (Fisher Instruments, Loughborough, UK) were inserted into the hepatic portal vein above the pancreatic vein and the abdominal aorta. After the surgery, mice were covered with an aluminium foil to minimise the drying of the internal organs. The mice were pre-perfused at a rate of ~0.4 ml/min with KRB supplemented with 1 mmol/l glucose for 20 min through the abdominal aorta, and the perfusate was collected via the hepatic portal vein as previously described (Qader et al., 2003). A steady flow was maintained using a peristaltic pump (Reglo Digital MS-2/8) (Ismatec, Wertheim, UK). Following the pre-stimulation period, the normal vascular supply of the pancreas was further stimulated up to 1 h with test conditions as indicated. The perfusate was collected and stored at -20^{o}C for further insulin measurement by RIA. This was carried out by Mr NJG Rorsman.

2.10.4 Islet perifusion studies

For studies in chapter 3, islets isolated from wild-type and *Sox4* mutant mice were immediately placed into perifusion chambers. Fifty size-matched islets of each genotype were first pre-incubated for 30 minutes in pre-warmed KRB supplemented with 2 mmol/l glucose. The islets were then perifused with KRB at a flow rate of 1 ml/min for 40 minutes in the presence of 20 mmol/l glucose or 20 mmol/l glucose + 200 μmol/l tolbutamide. The perfusate was collected every minute and insulin secretion was

determined by RIA. Values were normalised to total insulin content and calculated as a percentage of islet content. This was carried out by Ms A Hough.

2.10.5 Growth hormone secretion assays

2.10.5.1 Rat INS-1 832/13 cells

Cells were plated at a density of 150,000 – 200,000 cells/well in a 24-well plate. After 9 h of incubation at 37°C in a humidified atmosphere of 5% CO_2 in air, the cells were transfected with a siRNA (50 nmol/l) using Lipofectamine RNAiMAX (Life Technologies, Paisley, UK) following the manufacturer's instructions with minor modifications. For RNA interference, the following siRNAs were used: ON-TARGETplus siRNA SMARTpool for the rat *Stxbp6* gene (5′-ACACAGGCAUCUAUCACGA-3', 5′-GGUCAAGGCGAAUAUUUAA-3', 5′- CCGCCAAGUUAAUGGUAUU-3', and 5′-UAGUGUGACCAGUGCGGUA-3') and ON-TARGETplus Non-Targeting Control siRNA (5′-UGGUUUACAUGUCGACUAA-3') (Thermo Scientific, Hemel Hempstead, UK).

After 24 h, the medium in each well was replaced with fresh culture medium, and INS-1 832/13 cells were immediately co-transfected with human growth hormone (hGH) and a gene of interest using GeneJuice (Millipore, Nottingham, UK) according to the manufacturer's instruction. The cells were then incubated under the same conditions for 24 h, and the medium in each well was replaced with fresh culture medium. An additional 24-h incubation was conducted at 37°C in a humidified atmosphere of 5% CO_2 in air. The culture medium was then replaced with 50% less glucose containing culture medium, and the cells were incubated for another 12 h. After the incubation, the transfection

efficiency was determined under a fluorescence microscope (genes of interests were tagged with a fluorescent probe). The cells were pre-incubated for 2 h at 37°C in glucose-free Hanks' balanced salt solution (HBSS) buffer consisting of (mmol/l) 114 NaCl, 4.7 KCl, 25.5 $NaHCO_3$, 1.2 KH_2PO_4, 1.16 $MgSO_4$, 2.5 $CaCl_2$ and 20 HEPES (pH adjusted to 7.4 at 37°C with NaOH). Additionally, the solution was supplemented with 0.1% bovine serum albumin (BSA) (weight/volume).

Following pre-incubation, cells were stimulated for 25 min in the presence of HBSS buffer supplemented with 1 mmol/l, 20 mmol/l, or 20 mmol/l glucose with 70 mmol/l $[K^+]_o$ at 37°C in a humidified atmosphere of 5% CO_2 in air. The supernatant was collected to analyse hormone release, and the pellets were resuspended in 10 mmol/l EDTA in phosphate-buffered saline (PBS). The amount of growth hormone in the supernatants and cell extracts was measured by ELISA using the hGH ELISA kit (Roche Diagnostics, West Sussex, UK) according to the manufacturer's instructions. Growth hormone secretion was expressed as a percentage of the total growth hormone content of the cells.

Commercially available GFP-tagged *Sox4* and *Stxbp6* plasmids were used for transfection (OriGene Technologies, Rockville MD, USA). Based on the quick-change site-directed mutagenesis method, the Y123C mutation was introduced using the WT *Sox4* plasmid as a template in order to create the *Sox4*mt plasmid. This part was carried out by Dr M Chibalina.

2.10.5.2 EndoC-βH2 cells

Approaches similar to those employed for INS-1 832/13 cells were used for transfection of EndoC-βH2 cells but with the following modifications. For the co-transfection of hGH and a gene of interest, Lipofectamine 2000 (Invitrogen, Paisley, UK) was used according

to the manufacturer's instruction as GeneJuice was not designed for EndoC-βH2 cells. Furthermore, pre-incubation in glucose-free HBSS only lasted for 1 h instead of 2 h to minimise cell deaths.

For the siRNA-based gene knockdown, ON-TARGETplus siRNA SMARTpool for human *STXBP6* gene was used (5′-GGUUAAUGGUAUCGAUCCU-3', 5′-GAAUGAGCGUGGAGAGCGA-3', 5′-AACUGGAGGUCAAGGCGAA-3', and 5′-CGGCAGAGUUUGAUUUGUU-3'). Commercially available human specific *SOX4* and *STXBP6* plasmids were used for transfection (OriGene Technologies, Rockville MD, USA).

2.11 ZIMIR Imaging by confocal fluorescence microscopy

Isolated islets were pre-incubated in DMSO solution of ZIMIR (1 μmol/l) dissolved in KRB buffer at room temperature and in the dark for 120 min. The islets were then washed twice with fresh KRB buffer and placed in a perifusion chamber. Imaging was conducted by confocal fluorescence microscopy on the upright Zeiss Axioskop 2F microscope (Carl Zeiss, Jena, Germany) using a C-Apochromat 40x/1.2 water immersion objective that is controlled by ZEN 2009 software. The islets were maintained at 37 °C throughout recordings using a heating stage which was further insulated by a chamber system.

To image Zn^{2+} secretion and SRB (see below) uptake concurrently, we continuously perifused the islets (pre-loaded with ZIMIR) with KRB buffer containing 20 mmol/l glucose and 0.7 mmol/l SRB at a rate of 60 μl/min. The extracellular solution was supplemented with 10 μmol/l EDTA to chelate the residual Zn^{2+}. Images were acquired

at 0.03 Hz. For the ZIMIR recordings, a laser with 488 nm excitation wavelength was used and the emission signals were detected at 505 nm.

After image acquisitions, ZIMIR fluorescence intensity was measured by drawing regions of interest (ROI) along the plasma membrane. The imaging data were presented as F/F_0. Analysis were carried out by Image J.

2.12 Two-photon and confocal imaging of exocytosis

SRB imaging of full fusion: Mouse pancreatic islets were superfused with extracellular medium containing the fluorescent polar tracer sulforhodamine B (SRB), which consisted of (in mmol/l): 73.6 NaCl, 2.6 $CaCl_2$, 70 KCl, 2 $NaHCO_3$, 0.5 $MgSO_4.7H_2O$, 0.5 NaH_2PO_4, 5 HEPES and 0.7 SRB (pH adjusted to 7.4 with NaOH). SRB was excited in the two-photon mode at 830 nm using a Chameleon laser (Coherent, Santa Clara, CA, USA). Emitted light (580 nm) was collected through an oil apochromatic objective ×63/1.4 (Carl Zeiss, Jena, Germany) between 570 and 650 nm.

VAMP-pHluorin imaging of fusion pore opening: Mouse islets in culture for 12 h were infected with an adenovirus expressing the pH-sensitive GFP-tagged reporter VAMP-pHluorin. The culture medium was replaced after 4 h. Cells were used for experimental analysis after 24 h of the infection. VAMP-pHluorin fluorescence was excited by an argon laser set at 488 nm and emitted light was collected through an oil apochromatic objective ×63/1.4 (Carl Zeiss, Jena, Germany) between 510 and 540 nm. The islets were stimulated with the 70 mmol/l KCl solution specified above (but without SRB).

Data analysis was carried out using MetaMorph version 7.53 (Universal Imaging, Downingtown, USA). An automatic MetaMorph routine recognised all 'spots' with an inclusive low pass threshold ranging from 42-255 pixels for SRB measurements, and 38-255 pixels for VAMP-pHluorin measurements, empirically defined when manually identifying exocytotic events. The spots were chosen based on their brightness that was above the local background of surrounding pixels. Metamorph data was further processed with Microsoft Excel 2010. Only events with an area of 0.06 - 0.6 μm² were taken to represent insulin granule exocytosis and included from further analysis.

2.13 qRT PCR

Total RNA was isolated from INS-1 832/13 or EndoC-βH2 cells using the TRIzol RNA extraction kit (Invitrogen, Paisley, UK) according to the manufacturer's instruction. 300ng of total RNA was converted to cDNA using a High Capacity cDNA Reverse Transcription kit (life technologies, Paisley, UK).

Quantitative real-time PCR was performed using a standard curve method on a 7900HT instrument (Applied Biosystems, Paisley, UK). Each PCR reaction contains 4μl of 2x QuantiFast SYBR Green PCR Master Mix (Qiagen, Manchester, UK), 0.8μl of QuantiTect primers (Qiagen, Manchester, UK), 2μl of cDNA and 1.2μl of RNase-free water. Primer efficiencies were determined using a series of four cDNA dilution points (1/4, 1/16, 1/64 and 1/256). Triplicates were tested for each dilution point, and a triplicate negative control that contained sterile water instead of cDNA was tested for any contamination of the reagents. PCR conditions were as follows: initial activation step of 95 °C for 15 min and followed by 40 cycles of 95 °C for 15s, 60 °C for 1 min and 72°C for 30s. Primer specificity was checked every set of run by analysing melting curves. The

relative expression ratio of a target gene in qRT PCR was calculated according to the mathematical equation (Pfaffl, 2001):

Relative expression (R) = ($E_{\text{gene of interest}}^{-\text{Ct gene of interest}}$) / ($E_{\text{housekeeping gene}}^{-\text{Ct housekeeping gene}}$)

All the data were normalised against a housekeeping gene (*Gapdh*/*GAPDH*). A list of primers follows which were all purchased from Qiagen: rat Sox4 (QT00386078), rat Stxbp6 (QT01567769), rat Gapdh (QT00199633), human SOX4 (QT00220605), human STXBP6 (QT00073647), and human GAPDH (QT00079247).

2.14 Western blot

INS-1 832/13 cells were washed with ice-cold PBS and homogenised by regular vortexing and sonication in lysis buffer (25 mmol/l Tris-HCL adjusted to pH 7.4, 50 mmol/l NaF, 100 mmol/l NaCl, 5 mmol/l EGTA, 1 mmol/l EDTA, 20 mmol/l NaPyPi, 1% Triton X-100, 0.27 mol/l sucrose, 1 mmol/l Na_3VO_4, 0.1% 2-mercaptoethanol, and EDTA-free protease inhibitor tablet (Roche Diagnostics, West Sussex, UK)) on ice. Samples were put on a centrifuge for 20 min at 13,000g in a pre-cooled 4 °C condition. Protein concentrations of the whole cell lysates were determined using the Bradford reagent.

Lysates (25µg) were mixed with Laemmli buffer (Biorad, Hertfordshire, UK) in a 1:1 ratio and heated to 95°C for 5 min and then centrifuged for 1 min at 16,000g. Supernatants were carefully collected. Total cellular protein was separated by 10% SDS-PAGE (Biorad, Hertfordshire, UK) for the initial 10 min at 70V and then 120V for 1 h. The gel was then assembled with a nitrocellulose membrane in a Bio-Rad transfer module and

transferred for 1 h at 100V in the presence of an ice block. Transfer efficiency was checked with Ponceau solution. The stain was removed by washing with a combination of water and TBST (Tris-buffered saline with Tween 20; 20 mmol/l Tris adjusted to pH 7.5, 150 mmol/l NaCl, and 0.1% Tween 20). The blot was then blocked in 5% Marvel TBST for 1 h on a rocking platform. Primary antibody incubation was carried out at 4 °C overnight on a shaking platform. The antibodies that we used as follows: Sox4 (Santa Cruz, sc-17326; Abcam, ab90696; Millipore, AB5803), Stxbp6 (Santa Cruz, sc-271959 & sc-68400; Abcam, ab85039; Novus Biologicals, NBP2-15376), tGFP (Origene, TA150061). A rabbit polyclonal antibody against calnexin (Millipore, 208880) was used as a loading control. Membranes were washed with TBST and then incubated in a secondary antibody according to the species of the first antibody for 1 h on a shaking platform at room temperature. A list of secondary antibodies that we used as follows: Polyclonal porcine anti-rabbit immunoglobulins/HRP (Dako, P0399), polyclonal goat anti-mouse immunoglobulins/HRP (Dako, P0447), donkey anti-goat IgG-HRP (Santa Cruz, sc-2020). Signals were visualised using the SuperSignal West Pico Chemiluminescent Substrate kit (life technologies, Paisley, UK).

2.15 Electron microscopy for mitochondrial quantitation

Islets isolated from control and *Fh1*KO mice were fixed in 2.5% glutaraldehyde (Sigma, Dorset, UK) in 0.1 mmol/l phosphate buffer for 1 h. Islets were post-fixed for 2 h in 1% osmium tetroxide. They were then block stained in 2% uranyl acetate and embedded in Spurr's resin (Agar Scientific, UK) for 36 h at 50°C. Ultrathin sections (~50 nm) were cut onto nickel grids and images were viewed under a Joel 1010 microscope. The ratio of the mitochondrial area relative the cytoplasm (excluding the nucleus) was calculated for each image. Statistical analyses were performed using Origin 8 (OriginLab, Bucks,

UK), and significance was evaluated by Kolmogorov-Smirnov test and two-tailed Student's *t*-test.

2.16 Statistical analysis

Data are presented as mean values ± SEM. Statistical significance measurements were performed by Student's *t*-test unless stated otherwise in the figure legends.

CHAPTER 3

Sox4 modulates insulin secretion by increasing kiss-and-run exocytosis at the expense of full fusion

3.1 Introduction

The genetics of T2D is complicated by its polygenic nature. Historically, much work has initially been done in animal models in order to pinpoint the genes controlling glucose homeostasis (Terauchi et al., 1997, Rosengren et al., 2010, Atanur et al., 2013), and to evaluate their role in human populations (Florez, 2008, Voight et al., 2010). The advent of the genomic era, facilitated by the collection of large and well-characterised human data sets, and the development of ultra-high throughput genotyping and sequencing techniques have led to ground-breaking studies in human populations bearing sufficient mapping resolution to identify disease-causing variants and genes. Through the advancement of GWAS, the number of novel T2D susceptibility loci keeps increasing; 3 were identified until 2007, followed by 50 more loci from 2007 including *CDKAL1*, *CDKN2A/CDKN2B, IGF2BP2, HHEX-IDE,* and *SLC30A8* (McCarthy, 2010, Visscher et al., 2012). The majority of these loci are believed to affect (directly or indirectly) insulin secretion, which supports the notion that abnormal β-cell function underlies T2D (Florez, 2008, Voight et al., 2010). Currently, there are more than 90 T2D susceptibility loci (Bonnefond and Froguel, 2015).

Most of the discovered SNPs (single nucleotide polymorphisms) fall into non-coding introns that are associated with linkage disequilibrium blocks. It is therefore possible that these SNPs can influence the expression of nearby genes or further away ones. One such example is the disease-susceptibility locus, *CDKAL1* which contains highly conserved synteny blocks that may control the expression of the SRY-related high mobility group (HMG)-box 4 (*SOX4*) rather than *CDKAL1* itself (Ragvin et al., 2010). *Sox4* has been implicated in pancreatic development and insulin secretion in mice (Wilson et al., 2005, Goldsworthy et al., 2008). The findings that *Cdkal1* knockout (KO) mice have normal

glucose tolerance *in vivo* and display no effect on GSIS *in vitro* (Ohara-Imaizumi et al., 2010) provides additional arguments for exploring the functional effects of genetic manipulation of *Sox4.*

SOX4 is a transcriptional regulator that belongs to one of 20 isoforms of SOX proteins that exist among both human and mouse genomes (Schepers et al., 2002). In general, SOX proteins are characterised by the presence of a highly conserved HMG box (DNA binding domain) that is located near the transactivation domain (Bernard and Harley, 2010). Functional disruption of SOX proteins causes developmental and congenital diseases in humans (Wegner, 1999). Specifically, *SOX4* is implicated in a number of developmental processes including the development of the endocrine pancreas (Wilson et al., 2005). It is expressed in adult pancreatic islets (Wilson et al., 2005), and disruption of *SOX4* leads to abnormal pancreatic islet development characterised by a lack of endocrine cells. The role of *Sox4* in insulin secretion has previously been shown by the use of N-ethyl-N-nitrosourea (ENU) mutant mice exhibiting defective insulin secretion. In this model, the ENU mutation resides in the highly conserved HMG box of the *Sox4* (Figure 9). Additionally, the elimination of the *Sox4* transcript in rat INS-1 and mouse MIN6 clonal β-cells resulted in the reduction of GSIS (Goldsworthy et al., 2008). The underlying mechanism is believed to involve defect(s) downstream of the K_{ATP} channel closure but the precise mechanism remains unknown**.**

In the studies described below, we evaluated the exocytotic function of *Sox4* mutant (*Sox4*mt) mice. These mice bear a point mutation in their DNA binding domain of *Sox4* that wrongly translates cysteine instead of the usual tyrosine (Figure 9) and they are referred to as *Sox4*mt mice.

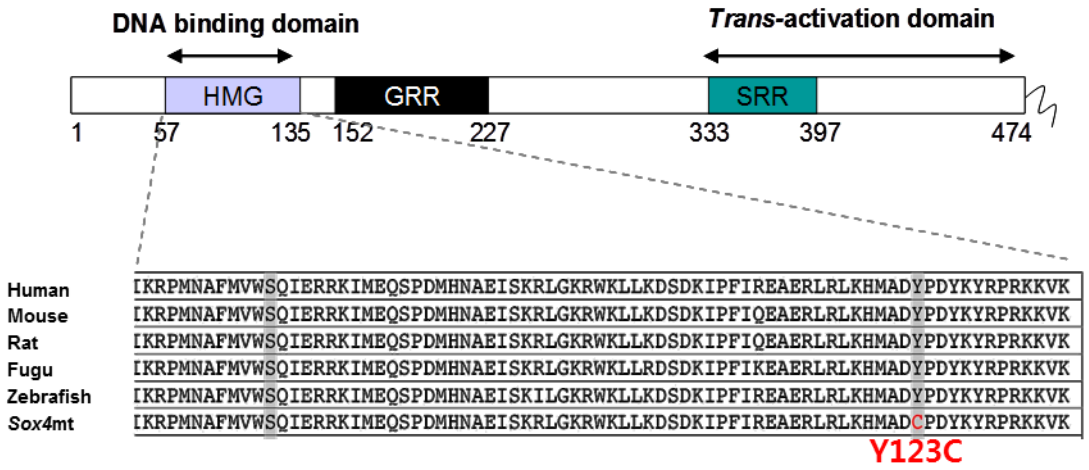


Figure 9. HMG (High Mobility Group) box mutation in *Sox4*mt mouse in comparison to the normal genes. *Sox4* mutation changes a tyrosine to a cysteine at amino acid 123 (Modified from (Goldsworthy et al., 2008)**)**.

3.2 Results

3.2.1 Glucose- and sulphonylurea-stimulated insulin secretions are reduced in *Sox4*mt islets

Isolated *Sox4*mt islets were incubated for an hour at 1 and 20 mmol/l glucose to determine the effect of the Y123C *Sox4* mutation on glucose-stimulated insulin secretion (GSIS). GSIS in islets from *Sox4*mt was reduced by 50% relative to that observed in wild-type (WT) islets (1.98 ± 0.17 and 0.96 ± 0.15 % of total insulin content for WT and *Sox4*mt, respectively; $p<0.005$) (Figure 10). Thus, the Y123C mutation leads to suppression of GSIS, in agreement with the previous results (Goldsworthy et al., 2008).

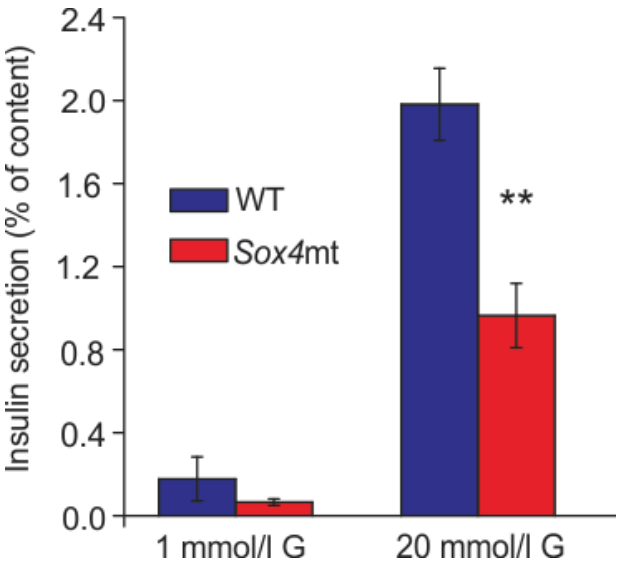


Figure 10. Effects of *Sox4* mutation on GSIS. Insulin secretory responses of isolated islets from WT (blue) and *Sox4*mt (red) mice were measured in the presence of 1 and 20 mmol/l glucose (G). Insulin release has been normalised to insulin content. Data are mean values ± SEM of 8 experiments using n=2 mice per genotype; $^{**}P < 0.005$.

The kinetics of insulin secretion was further validated by islet perifusion studies. The amplitude of 1st phase GSIS was diminished in *Sox4*mt islets (Figure S1). The peak value for the WT and *Sox4*mt mice was reduced by ~50% ($P<0.01$). The 2nd phase insulin secretion was also reduced in *Sox4*mt islets. Over the course of the entire stimulation period, the total amount of insulin secreted in response to 20 mmol/l glucose in *Sox4*mt islets was reduced by 55% compared to WT islets. Hence, the ablation of *Sox4* has diminished ~50% of GSIS encompassing both 1st and 2nd phase in islets isolated from the ENU mutant.

In addition, there was a tendency of insulin reduction (~50%; an effect without significance) evoked by the combination of high glucose and the sulphonylurea in the mutant islets (Figure S1). This argues that the secretory defect must reside downstream of the K_{ATP} channel closure.

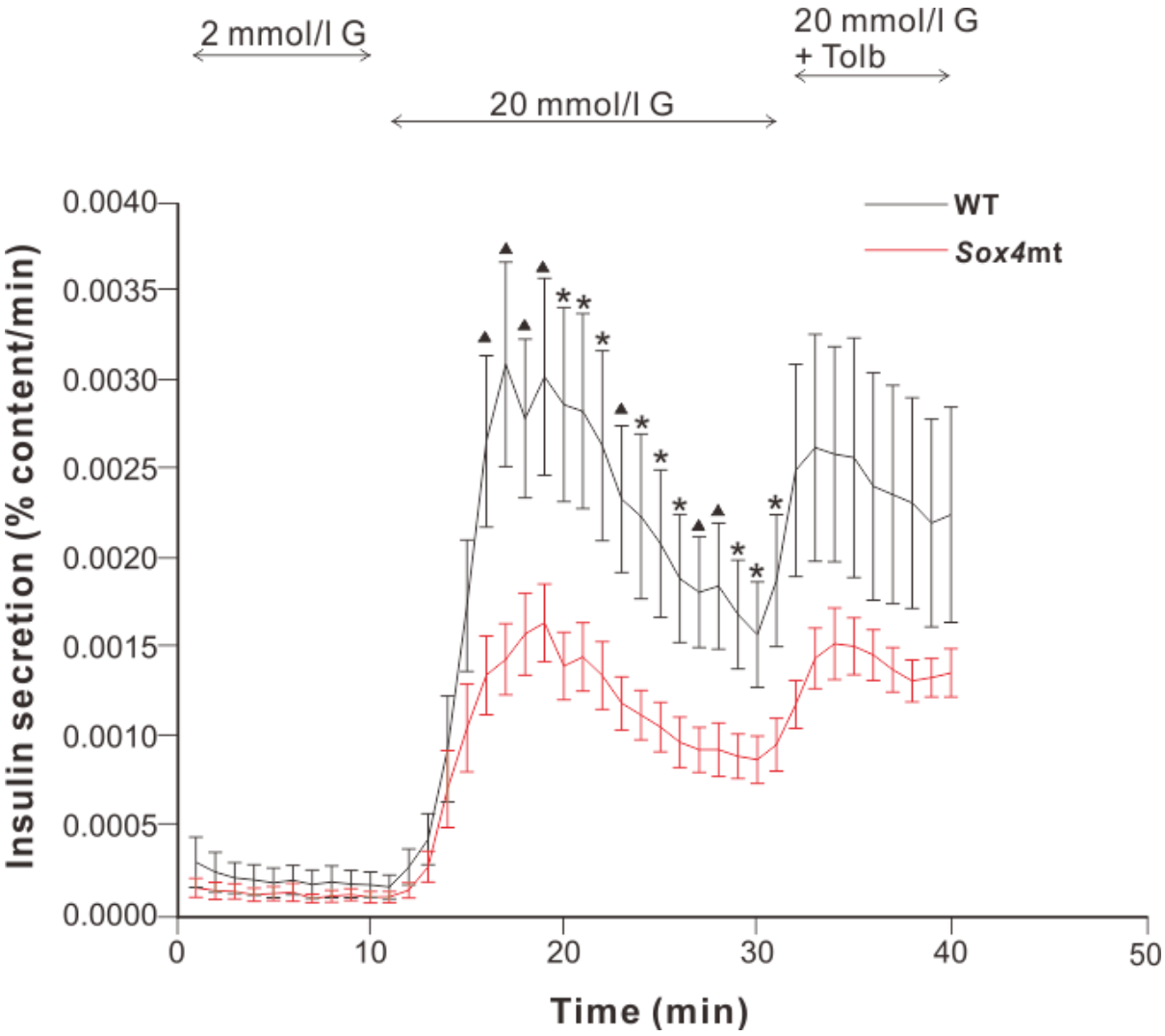


Figure S1. Insulin secretory responses of WT and *Sox4*mt. Isolated islets in batches of 50 were simultaneously incubated in the presence of 20 mmol/l glucose (G) alone followed by 20 mmol/l glucose and 200 µmol/l tolbutamide (Tolb). Data are presented as mean values ± SEM (*P<0.05, ▲<0.01; Student's *t*-test), and experiments were repeated with 50 islets isolated per batch from n=6 mice per genotype. Experiments performed by Dr A Hough.

3.2.2 The *Sox4* mutation has no effect on Ca^{2+} homeostasis

The measurements of insulin secretion and, especially, the failure of tolbutamide to correct the insulin secretion defect, highlight the involvement of the processes taking place downstream of the K_{ATP} channel closure. In β-cells, K_{ATP} channel closure results in membrane depolarisation, and activation of L-type Ca^{2+} channels (in mouse), which subsequently increases $[Ca^{2+}]_i$ and triggers insulin exocytosis. We thus monitored $[Ca^{2+}]_i$ (reported as the F_{340}/F_{380} fluorescence ratio) in WT and *Sox4*mt islets to check the potential defects in $[Ca^{2+}]_i$ homeostasis that may have been caused by the *Sox4* mutation (Figure 11). At basal glucose level, $[Ca^{2+}]_i$ levels were not different between the genotypes. Upon 20 mmol/l glucose exposure, an initial lowering of $[Ca^{2+}]_i$ was followed by a sharp increase in $[Ca^{2+}]_{i,}$ and eventually settled at a somewhat lower steady-state plateau. Addition of tolbutamide had similar effects on $[Ca^{2+}]_i$ in WT and *Sox4*mt islets.

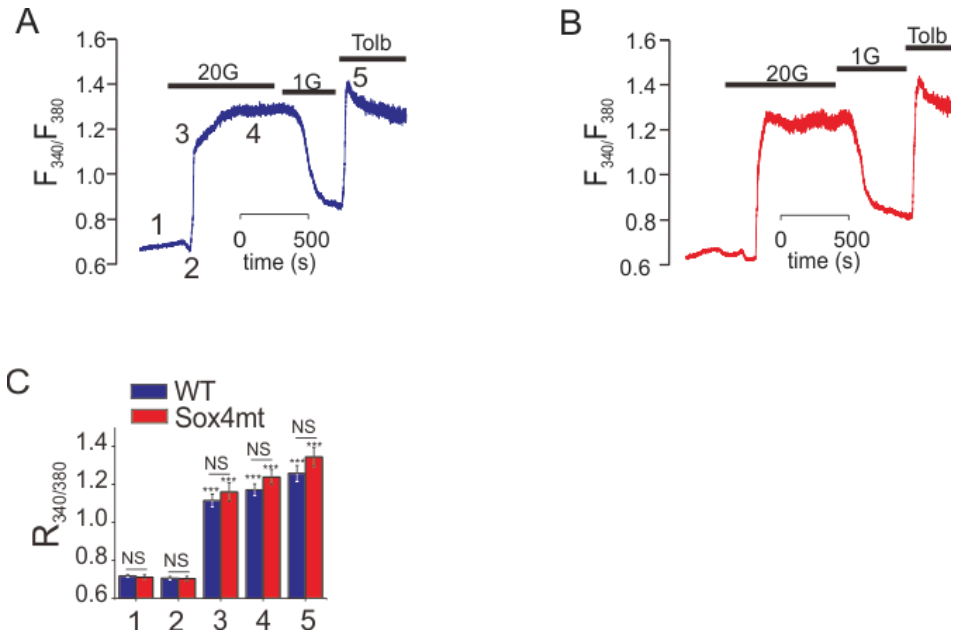


Figure 11. Impaired insulin secretion in *Sox4* islets is not due to impaired $[Ca^{2+}]_i$ signalling. (A-B) Representative traces of glucose (G)- and tolbutamide (Tolb)-evoked changes in $[Ca^{2+}]_i$ in WT (blue) or *Sox4*mt islets (red). (C) Histogram summarises $[Ca^{2+}]_i$ (quoted as the fura-2 AM F_{340}/F_{380}-ratio) into 5 different stages as indicated by numbers on the traces: basal conditions (1 mmol/l glucose; 1), initial nadir (2), peak after elevation of glucose to 20 mmol/l (3), plateau phase in the presence of 20 mmol/l (4) and in the presence of 1 mmol/l glucose and 0.2 mmol/l tolbutamide (5). ***p<0.001 for comparisons to the respective basal ratio (Student's *t*-test). NS implies no significance for the indicated comparisons. Data are mean values ± SEM of 9 islets from n=3 animals for each genotype.

We also determined whole-cell Ca^{2+} currents in WT and *Sox4*mt β-cells (Figure 12). Both the magnitude and voltage dependence of the currents overlap in the two types of β-cells, suggesting that the gating and Ca^{2+} channel density is unperturbed by the *Sox4* mutation.

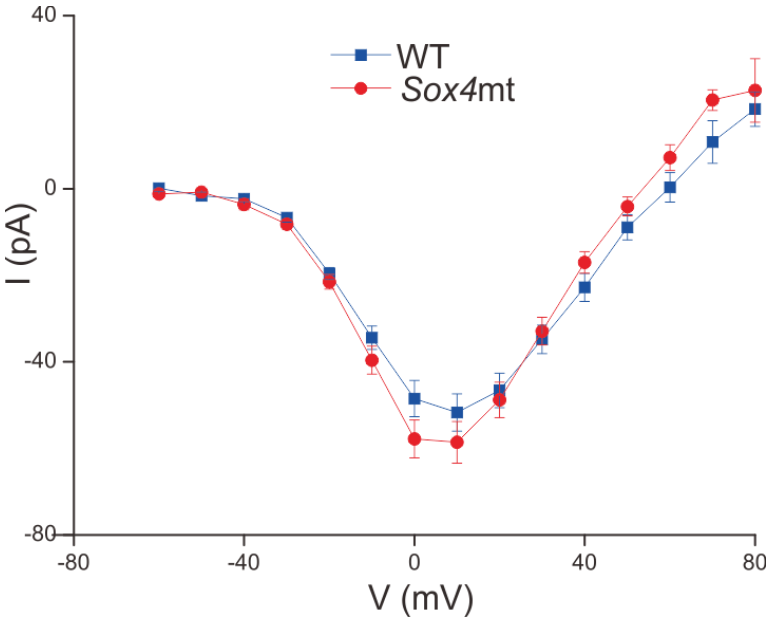


Figure 12. Current (I)-voltage (V) relationship for the Ca^{2+} currents was recorded in β-cells isolated from WT and *Sox4*mt mice. Data are presented as mean values ± SEM (42 and 38 cells in WT and *Sox4*mt from n=5 mice per genotype).

3.2.3 Normal granule fusion in *Sox4*mt mice

Measurements of membrane capacitance have been widely used to study exocytosis at the single-cell level with high temporal resolution (Neher, 1998). The capacitance of a cell is proportionally related to the cell surface area. Capacitance measurements of exocytosis detect the minute increases of cell surface area that result when secretory granules fuse with the plasma membrane. A particular advantage of this technique is that it is performed under voltage-clamp conditions and exocytosis can therefore be evoked in a very precise way by the application of depolarising voltage-clamp pulses (Rorsman et al., 2000). This has allowed the kinetics and voltage dependence of exocytosis to be characterised in great detail. A large body of data suggests that the observed increases in cell capacitance principally (if not exclusively) reflect exocytosis during the fusion of the insulin-containing secretory granules and the plasma membrane (Braun et al., 2008, Karanauskaite et al., 2009).

In our study, exocytosis was evoked by a train of ten 50-ms depolarising pulses from -70 to 0 mV. The 50-ms train mimics closely the duration of action potentials generated by β-cells when exposed to glucose (Hoppa et al., 2009). Surprisingly, the exocytotic responses elicited by the train tended to be larger in *Sox4*mt than in WT β-cells (Figure 13A). In fact, the total exocytotic responses triggered by the train was 50% larger in *Sox4*mt than in WT β-cells (Figure 13B) but this effect did not reach statistical significance ($P<0.18$). Collectively, these data suggest that the exocytotic machinery remains intact in *Sox4*mt β-cells.

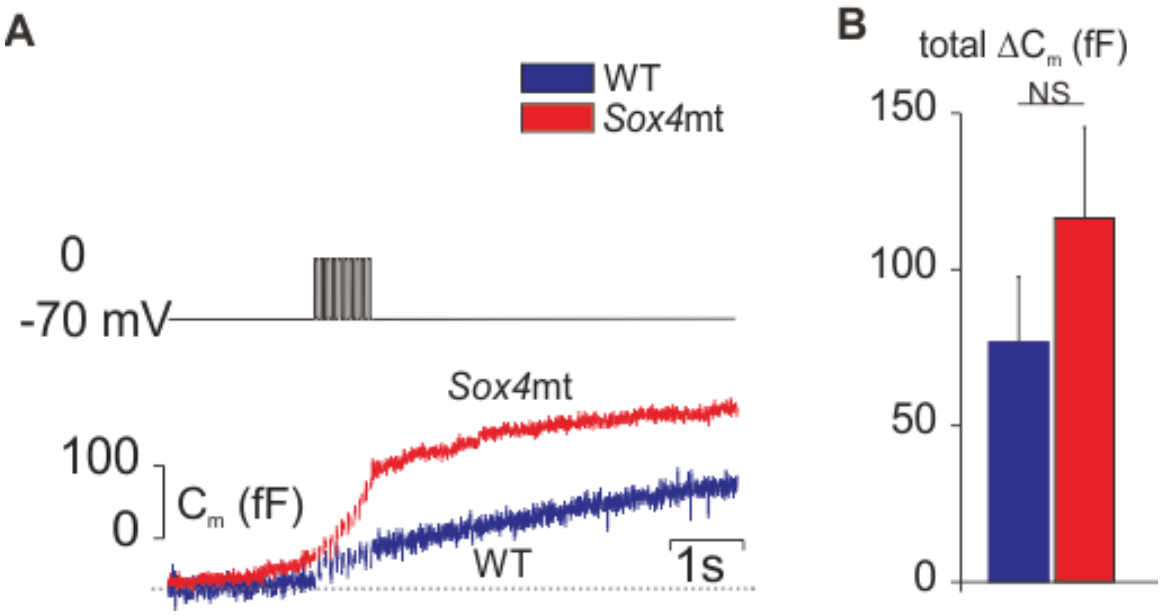


Figure 13. *Sox4*mt β-cells show normal depolarisation-evoked exocytosis. (A) Representative recordings of exocytosis during a train of ten 50-ms depolarisations (1 Hz) from -70 to 0 mV in WT (blue) and *Sox4*mt (red) β-cells. (B) Total capacitance following the train of ten 50-ms depolarisations. NS indicates no significant changes between the groups (Student's *t*-test). Data are shown as mean values ± SEM (42 and 38 cells in WT and *Sox4*mt from n=4 mice per genotype, respectively).

3.2.4 The *Sox4* mutation increases the stability of the fusion pore

On-cell capacitance measurement allows the recording of single-vesicle exocytosis. It detects changes in membrane area enclosed within the small piece of membrane enclosed by the recording electrode (Figure 14A). As a result, the relative importance of the area of a single vesicle fusing with the plasma membrane is greater, given the small surface of the area patched, compared to the whole-cell configuration. For this reason, the signal-to-noise ratio is significantly improved and it allows the detection of small changes in membrane capacitance (down to single small synaptic vesicles; (Lollike and Lindau, 1999)). The technique also allows the simultaneous measurement of the fusion pore conductance. This is made possible by the fact that a fusion pore is small enough to create an electrical resistance (conductance=1/resistance) to the passage of current from the pipette into the granule (Lollike et al., 1995, Neef et al., 2007). The conductance is proportionally related to the cross-sectional area of the fusion pore that in turn is related to the square of the radius. When the fusion pore is formed, the radius is initially small and the conductance is low. As the pore expands (and the radius increases), the conductance increases exponentially. Thus, the diameter of the fusion pore can be derived from its conductance using conservative estimates of membrane thickness (7.5 nm) and electrolyte mobility (66.7 Ω.cm) (Debus and Lindau, 2000).

Figure 14B show examples of parallel on-cell measurements of membrane capacitance (C_m) and conductance (G_m) in small patches of membrane on WT (Figure 14B (I)) and *Sox4*mt β-cells (Figure 14 (II)). In both WT and *Sox4*mt β-cells, stepwise increases in cell capacitance were observed. In WT β-cells, these capacitance steps were irreversible and associated with no detectable or transient increases in membrane conductance, indicating rapid and irreversible expansion of the fusion pore. However, in *Sox4*mt β-cells, the

capacitance step could flicker between baseline and an elevated level (often referred to as ‘kiss-and-run’ exocytosis). During these ‘flickery’ capacitance steps, persistent increases in membrane conductance were observed.

Our on-cell capacitance measurements indicate that only 20% of release events occurring in WT β-cells were of the kiss-and-run type, as compared with 50% in *Sox4*mt β-cells (Figure 14C). The fraction of full fusion events was thus reduced from 80% in WT cells to 50% in *Sox4*mt β-cells.

The fusion pore radius during kiss-and-run exocytosis in *Sox4*mt β-cells averaged 0.9±0.1 nm; similar to the values that are reported previously (Takahashi et al., 2002, MacDonald et al., 2006).

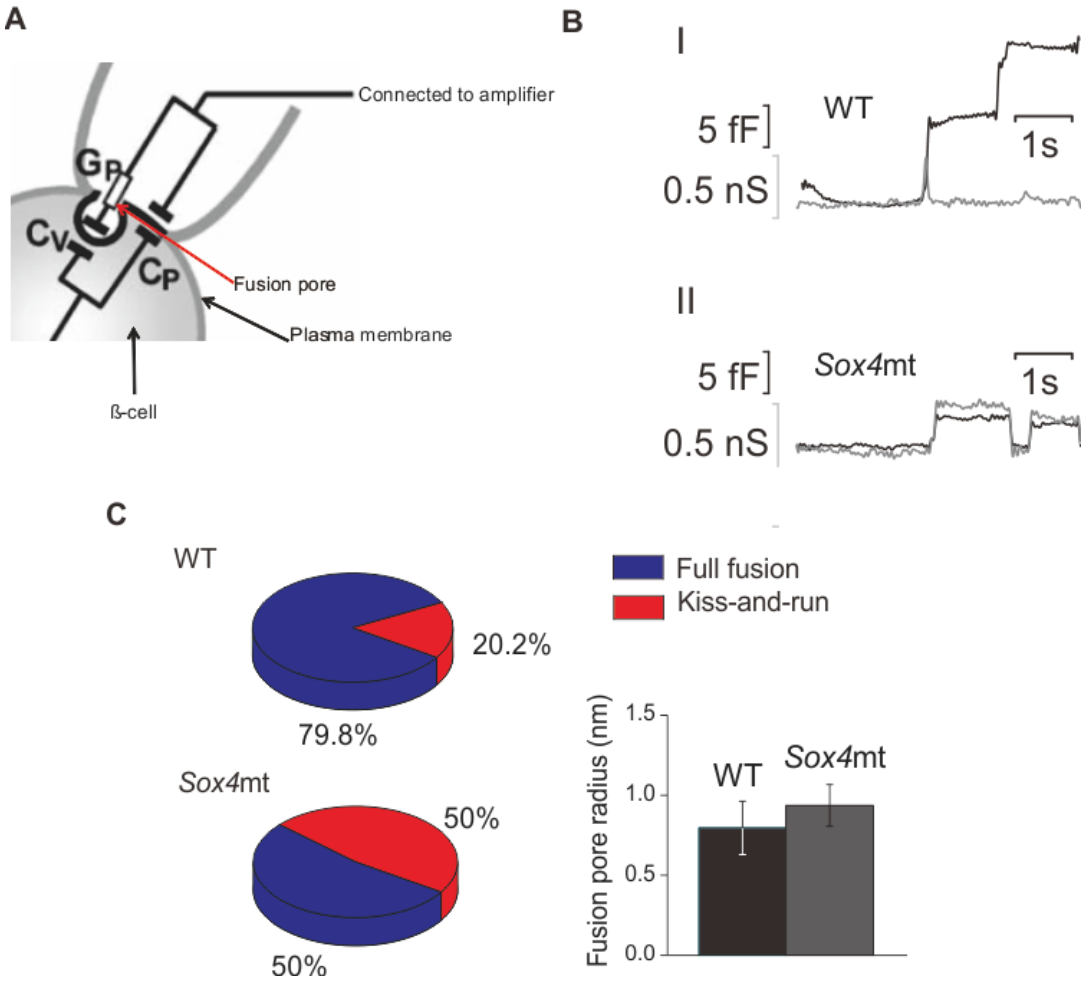


Figure 14. On-cell measurement allows detection of kiss-and-run exocytosis. (A) A schematic diagram of the on-cell configuration with the equivalent circuit. A fire-polished glass pipette creates a small patched area, and the capacitance measurements are specifically made from that area by the recording electrode. When kiss-and-run occurs, it establishes an electrical connection between the granule lumen and the extracellular environment via the fusion pore (as indicated in the diagram). Therefore, the conductance of the fusion pore can be determined. C_v, C_p, and G_p are capacitance of vesicle, capacitance of plasma membrane, and conductance of fusion pore, respectively (Lindau, 2012). (B) Membrane capacitance (C_m) and conductance (G_m) recordings show 2 distinct types of exocytotic events, a full fusion event from a WT β-cell (I), and a kiss-and-run event from a *Sox4*mt β-cell (II). (C) Mutation in *Sox4* increased the proportion of kiss-and-run exocytosis without a change in fusion pore radius (~1 nm). Values represent mean ± SEM (119 and 120 events in WT and *Sox4*mt, respectively recorded from 23 WT and 30 mutant β-cells from n=4 mice per genotype).

3.2.5 SRB uptake correlates with the exocytotic marker ZIMIR

A previous report demonstrated that SRB (a small, aqueous, polar, fluorescent tracer) detects individual exocytotic events in pancreatic β-cell (Takahashi et al., 2002). Therefore, we adopted the same approach to document insulin release to further support the observations that *Sox4*mt β-cells exhibit a disproportionate level of kiss-and-run exocytosis.

Although SRB is an established exocytotic marker, controversy remains as to whether SRB events are only exocytotic and not endocytotic. Therefore, we simultaneously correlated the rate of SRB uptake to the release of Zn^{2+} using the fluorescent Zn^{2+} dye ZIMIR (**z**inc **i**ndicator for **m**onitoring **i**nduced exocytotic **r**elease). ZIMIR anchors to the outer layer of the plasma membrane and detects Zn^{2+} ion when they are co-released with insulin upon stimulation (Michael et al., 2006, Li et al., 2011) (Figure 15A).

Insulin secretion in islets preloaded with ZIMIR was stimulated by exposure to 20 mmol/l glucose. The medium also contained 0.7 mmol/l SRB. SRB rapidly diffuses within interstitial spaces, and puncta appear when the dye flows into intra-vesicular cavities created by fusing vesicles (Figure 15 B-C). We also observed an increase ZIMIR fluorescence throughout the islet (Figure 15D). Importantly, SRB uptake and Zn^{2+} release proceeded with almost superimposable time courses (Figure 15E), confirming that SRB puncta do represent insulin granule exocytosis.

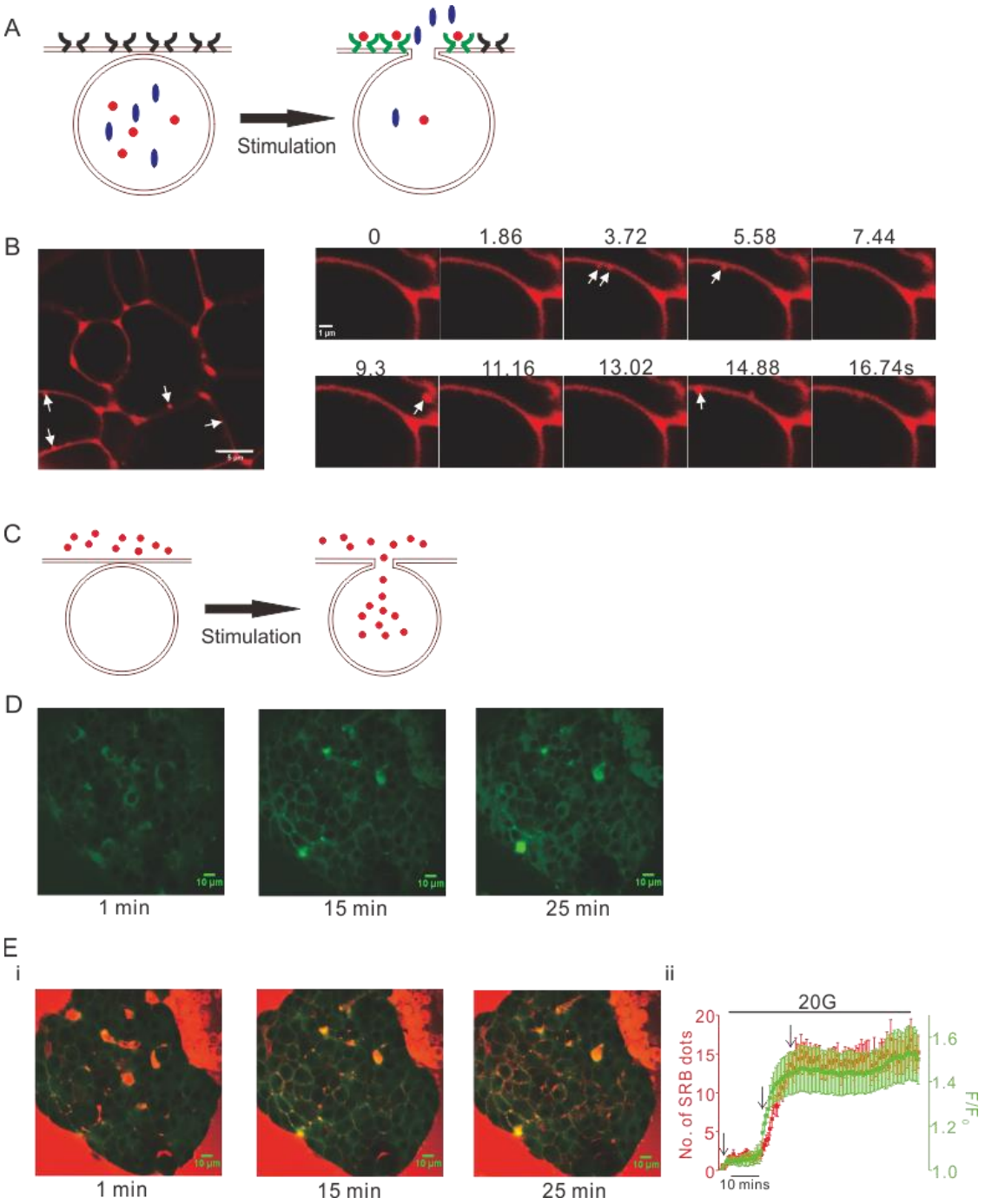


Figure 15. Optical imaging of exocytosis using SRB and ZIMIR in intact islets. (A) ZIMIR anchors to the outer membrane of lipid bilayer. Upon stimulation, secretory granules undergo exocytosis and release both zinc (red) and insulin (blue). Zinc binds to ZIMIR and gives a rise to green fluorescence. (B) SRB recordings: Upon stimulation, small dots (indicated by white arrows) appear at the plasma membrane indicating exocytotic events (scale bar: 5 μm). Example of typical single events (indicated by white arrows) in the presence of 20 mmol/l glucose (scale bar: 1 μm). Images were taken at the indicated times (relative to the leftmost image). (C) A schematic diagram shows that SRB

(which is contained in the extracellular solution) enters the vesicle by aqueous diffusion after stimulation. (D) Image stacks of events recorded with ZIMIR at three different times as indicated. 20 mmol/l glucose was added at 5 min (scale bar: 10 μm). (E) (i) Image stacks of events simultaneously recorded with both ZIMIR and SRB at three different times in the same islet as B. The appearance of SRB dots coincided with intensified ZIMIR response in the cells (scale bar: 10 μm). (ii) Kinetics of exocytosis simultaneously determined by both SRB uptake (indicated by number of dots; red y-axis) and ZIMIR response (ratio $F/F_{0,}$ fold increase of ZIMIR fluorescence above basal responses; green y-axis). '20G' indicates the time of adding 20 mmol/l glucose to the perfusion medium. Three arrows indicate the corresponding times of the image stacks (1, 5 and 25 min). Note that the two curves superimpose. Data are presented as mean values ± SEM of 14 events in 4 islets from n=2 mice).

3.2.6 VAMP-pHluorin reveals an increase in kiss-and-run exocytosis in *Sox4m*t β-cells

The SRB measurements of granule emptying were complemented by VAMP-pHluorin measurements to determine the total number of events associated with fusion pore opening with or without the release of the insulin cargo.

VAMP-pHluorin fluorescence is quenched in the acidic environment prevailing in the insulin granule (Figure 16A). Exocytosis results in pH neutralisation and a subsequent increase in VAMP-pHluorin fluorescence. Protons are very small (~0.1 nm) and can easily equilibrate via the narrow fusion pore during exocytosis (Figure 16A). Thus, opening of the fusion pore will be associated with increased pHluorin fluorescence regardless of whether kiss-and-run or full fusion exocytosis has occurred. This provides us with the means to determine the total number of release events.

Figure 16 (i-ii) show the cumulative exocytosis detected by SRB (i) or VAMP-pHluorin (ii) before and after membrane depolarisation induced by increasing the extracellular K^+ concentration ($[K^+]_o$) to 70 mmol/l. Under basal conditions (1 mmol/l glucose), the rate of exocytosis detected by SRB was very low but it increased dramatically upon the elevation of $[K^+]_o$. By contrast, increases in VAMP-pHluorin were detected also before membrane depolarisation. We estimated the relative contribution of full fusion and kiss-and-run exocytosis by subtracting the number of events detected by SRB by the number of events detected by VAMP-pHluorin (Figure 16C (iii)). In WT β-cells, 87±2% of the exocytotic events were of the full fusion type. The corresponding value in *Sox4*mt β-cells was 40±2%. Thus, the fraction of kiss-and-run openings increased from 13±2% in WT

β-cells to 60±2% in mutant β-cells (Figure 16D). These values are in good agreement with those suggested by the on-cell capacitance measurements (Figure 14C).

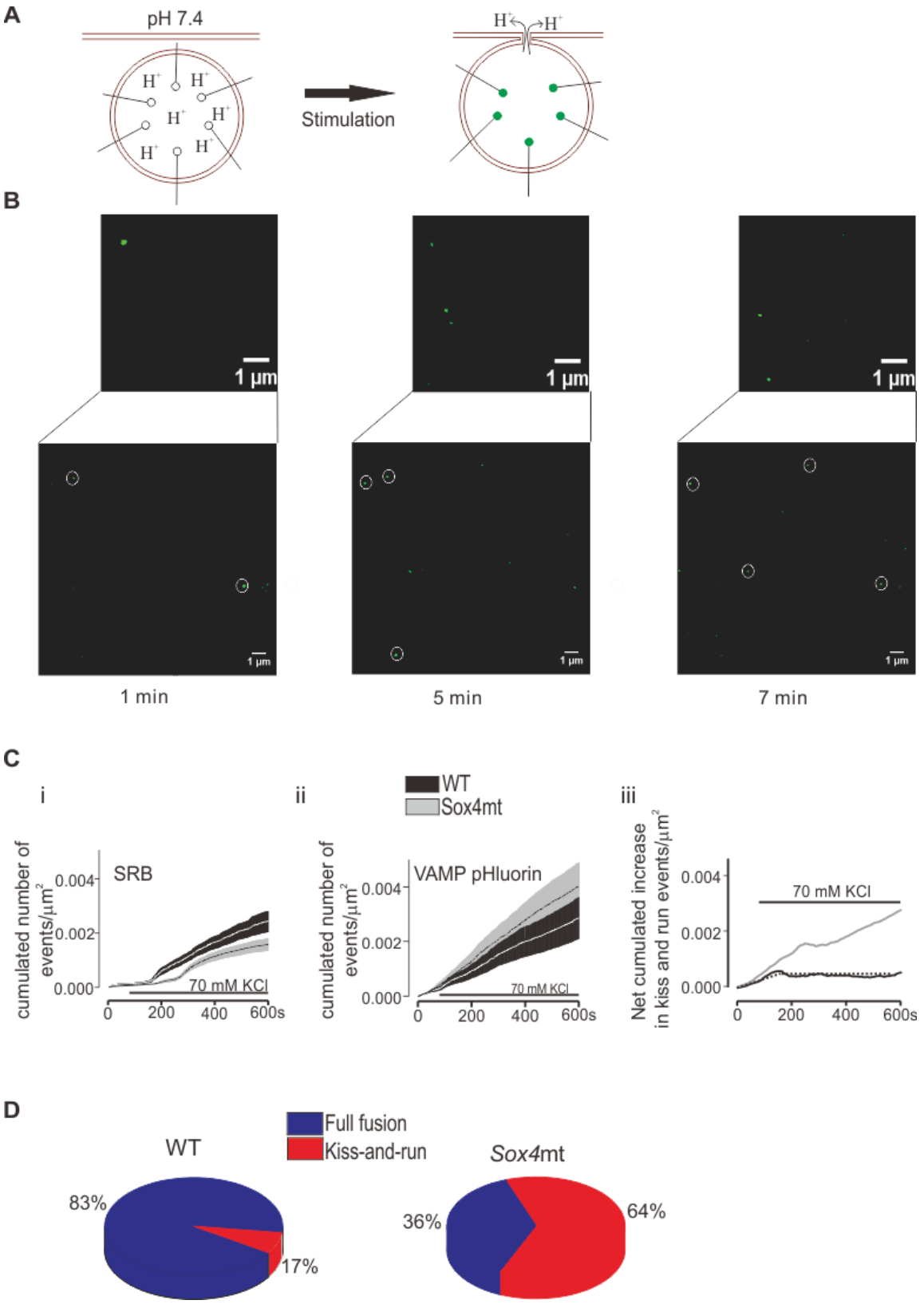


Figure 16. Confocal fluorescence microscopy studies reveal a higher proportion of kiss-and-run in *Sox4*mt mice. (A) Acidified secretory granule is fused with VAMP-pHluorin

where the fluorescence is quenched. Upon stimulation, the granule undergoes exocytosis thereby establishing the connection with the neutral extracellular environment. VAMP-pHluorin becomes excited and emits green fluorescence. (B) VAMP-pHluorin recordings at three different times as indicated: Real exocytotic events are indicated by white circles (scale bar: 1 μm). Insets show individual exocytotic events at an increased magnification (scale bar: 1 μm). High potassium was applied at ~80 seconds. (C) Cumulative exocytosis measured over 600 s using SRB (i) and VAMP-pHluorin (ii) under basal conditions (1 mmol/l glucose) and after in the presence of 70 mmol/l KCl (iso-osmotic replacement of NaCl); the data are presented as mean values (black lines) ± SEM (shaded areas). Net cumulated histogram of kiss-and-run events (iii) determined by subtracting (ii) to (i). (D) There is a significantly higher proportion of kiss-and-run in *Sox4*mt β-cells as compared to the WT ($p<0.005$; Student's *t*-test). In SRB recordings, for control, 19 islets from n=3 mice and, for *Sox4*mt, 15 islets from n=5 mice were investigated. In VAMP recordings, for control, 8 islets from n=3 mice and, for *Sox4*mt, 15 islets from n=3 mice were characterised.

3.2.7 Release of ATP is hindered by the presence of the fusion pore in *Sox4mt* β-cells

To investigate the effect of the fusion pore on the release of a small granule cargo, we infected *Sox4*mt β-cells with an adenovirus encoding the ATP-sensing purinergic ionotropic $P2X_2$ receptor ($P2X_2R$). When the insulin granule fuses, ATP is released (together with insulin), and this can be detected as transient inward whole-cell currents (Khakh et al., 1999, Braun et al., 2007).

Exocytosis in β-cells was triggered by dialysing the cytosol with 0.2 μmol/l Ca^{2+} through the patch pipette (whole-cell configuration) while the cell was being clamped at -70 mV. The kinetics of the current transients provides information on the opening of the fusion pore. Figure 17A-C show examples of events recorded in WT and *Sox4*mt β-cells. Majority of current transients detected in *Sox4*mt β-cells exhibit a slower kinetics than the WT counter parts. The size and kinetics of these currents respectively depend on the amount and speed of ATP release (Galvanovskis et al., 2011). Thus, we analysed the rise time (i.e. the time required for the event to increase from 10 to 90% of the maximum amplitude) of the events. It then became evident that the distribution of the rise times in *Sox4*mt β-cells was shifted to the right as compared to that observed in WT cells ($p<0.005$, Kolmogorov-Smirnov test) (Figure 17D). However, no significant difference in the total charge distribution was observed (5560 ± 340 and 5340 ± 408 pC for WT and *Sox4*mt, respectively) (Figure 17E). Taken together, these observations suggest that the total amount of ATP remains the same in WT and *Sox4*mt β-cells, but that the mean rate of release is 2.5-fold slower in the mutant β-cells. Such a shift can be expected to occur if many of the ATP release event in *Sox4*mt β-cells involve the slower exit of ATP via a narrower fusion pore.

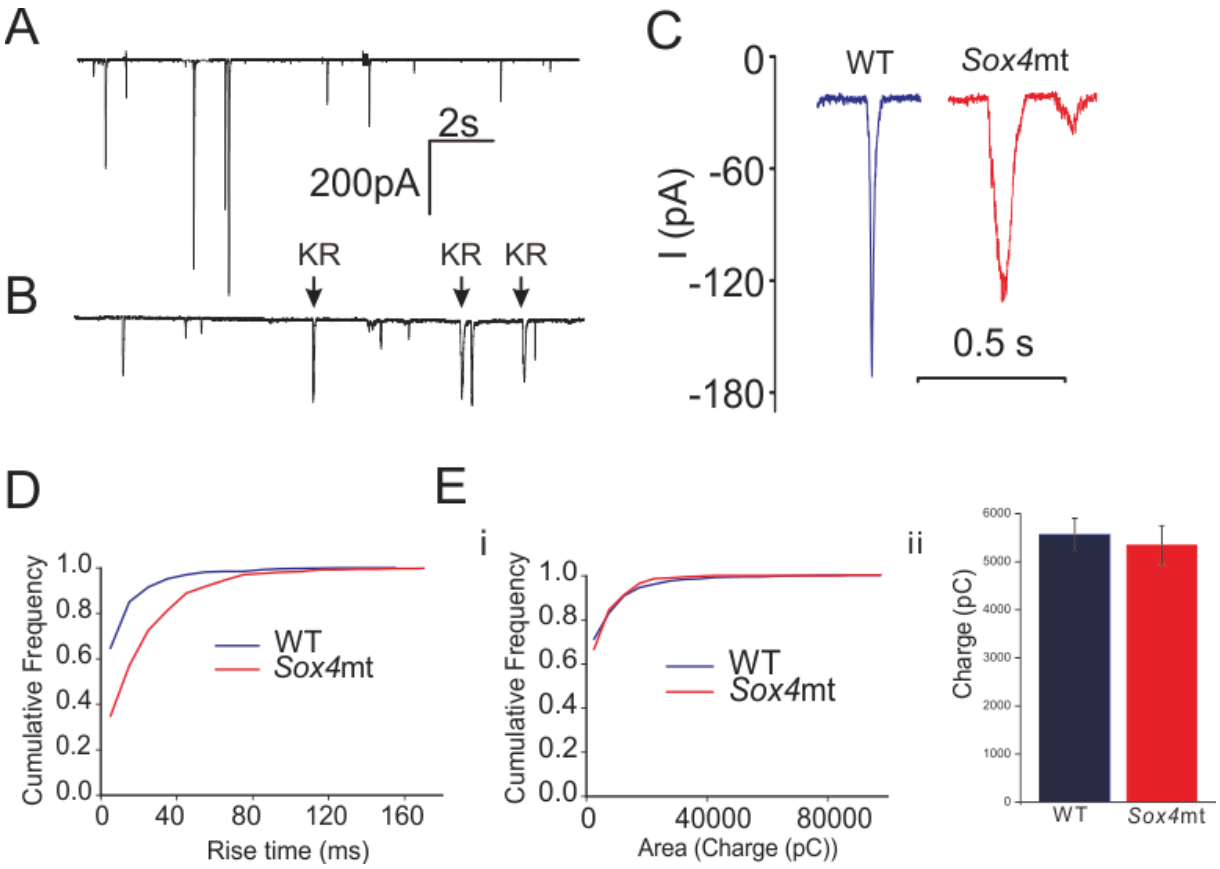


Figure 17. Slow expansion of fusion pore in *Sox4*mt β-cells hinders ATP release. (A) Release of ATP monitored in individual WT β-cells expressing ionotropic $P2X_2$ receptors infused with 0.2 µM free $[Ca^{2+}]_i$. (B) As in (A) but using mutant β-cells. Arrows indicate kiss-and-run (KR) events. (C) Superimposed examples of representative rapid event recorded in a WT β-cell (blue) and a slow event recorded in a *Sox4*mt β-cell (red). (D) Cumulative frequencies of $P2X_2$ rise time in WT (blue line; 771 events, 15 cells, n=4 mice) and *Sox4*mt β-cells (red line; 368 events, 10 cells, n=4 mice) ($P<0.005$, Kolmogorov-Smirnov test). (E) (i) As in A, but the cumulative frequencies of $P2X_2$ charge was compared. (ii) Mean area under the curve indicates the total charge. NS indicates no significant changes between the groups (Student's *t*-test). Values are presented as mean ± SEM.

3.3 Discussion

Our *Sox4*mt mice displayed a GSIS defect by a mechanism that cannot be corrected by the sulphonylurea tolbutamide (Goldsworthy et al., 2008). Since the secretory defect was not simply attributable to reduced insulin content and/or β-cell area, it was proposed that *Sox4* mutation interferes with a mechanism downstream of the elevation of $[Ca^{2+}]_i$. However, some of these earlier findings were made in INS-1 insulinoma cells, which may not be representative of primary β-cells.

We now confirm that *Sox4*mt β-cells are normal with regard to glucose sensing and metabolism as suggested by the similarity in glucose-stimulated $[Ca^{2+}]_i$ responses in WT and *Sox4*mt β-cells (Figure 11). Exocytosis measured as whole-cell depolarisation-evoked capacitance increases was not impaired in *Sox4*mt β-cells; if anything, responses in the mutant cells were slightly larger than in the WT (Figure 13). Thus, the cellular defect underlying the impairment of insulin secretion remains an enigma.

This surprising lack of any deleterious phenotype detected at the level of $[Ca^{2+}]_i$ homeostasis or exocytosis is reminiscent of observations made in *ZnT8*KO mice, which become diabetic when challenged with a high-fat diet (Lemaire et al., 2009). In the latter model, the insulin secretion defect was eventually attributed to the impaired insulin crystallisation due to the ablation of the Zn^{2+} transporter mediating Zn^{2+} uptake into the granules. Whilst granules remained functional and the β-cell metabolism was intact, insulin was incorrectly packaged in LDCVs. However, in *Sox4*mt β-cells, insulin granules displayed a normal core (Supplementary figure 2 in (Goldsworthy et al., 2008)), a characteristic of mature granules.

Thus, our initial characterisation failed to identify any obvious defect. Yet, insulin secretion was reduced by ~ 50% (Figure S1), similar to the reduction of insulin secretion in the islets from organ donors with T2D (Rosengren et al., 2012). Although our capacitance data showed a normal exocytosis in *Sox4*mt β-cells (Figure 13), a limitation of the technique is that it only reports changes in the cell surface area, and possibly, the exit of insulin following the fusion of release competent granules with the plasma membrane is somehow impeded.

When a granule fuses with the plasma membrane, a fusion pore may form and connect the granule lumen and the extracellular space. We obtained a value for the fusion pore diameter of ~1.7 nm, in reasonable agreement with previous estimates (Takahashi et al., 2002, MacDonald et al., 2006) but considerably smaller than the ~3-4 nm width of a monomeric insulin. It may thus be predicted that the presence of a 'persistent' fusion pore would impair insulin release by steric hindrance (Figure 18). Indeed, it has previously been demonstrated that exocytosis cannot be equated to cargo release (Barg et al., 2002b, Tsuboi et al., 2004). In the CNS, synaptic vesicles are partially emptied during the transient opening and closing of the fusion pore in a process referred to as 'kiss-and-run' exocytosis (Harata et al., 2006, Balaji and Ryan, 2007). Partially emptied synaptic vesicles can subsequently

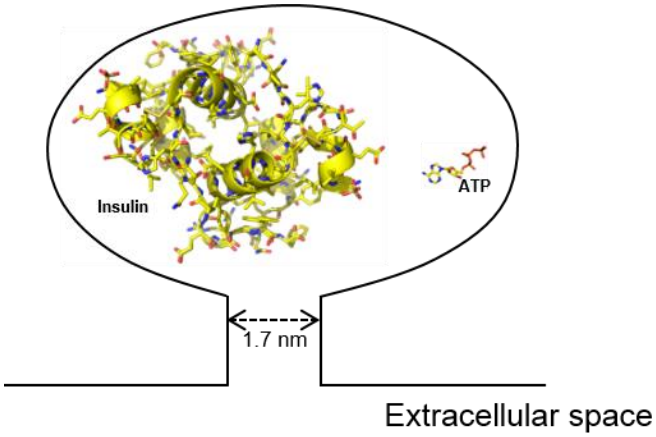


Figure 18. The narrow fusion pore that is formed during kiss-and-run exocytosis hinders the release of insulin, but not ATP.

be refilled and potentially undergo several rounds of exocytosis/endocytosis. It is important to note that such re-filling process does not exist in pancreatic β-cells (Schnell and Borg, 1985, MacDonald and Rorsman, 2007).

We hypothesised that in *Sox4*mt mice, insulin secretion may be reduced because of impaired expansion of the fusion pore. We tested this through a combination of high-resolution biophysical and optical techniques. Using on-cell capacitance measurements, which allow the detection of single-granule exocytosis and measurements of the (persistent) fusion pore, we found that kiss-and-run exocytosis only rarely (~20%) occurred in control β-cells, but the fraction increased to ~50% in *Sox4*mt β-cells (Figure 14C).

We also monitored ATP release in WT and *Sox4*mt β-cells infected with the ATP-sensing $P2X_2Rs$. We found that following exocytosis, the exit of ATP from the granule lumen was a 2.5-fold slower in *Sox4*mt β-cells (Figure 17D). If this effect is already detectable for a relatively small molecule like ATP (MW ~500 Da), it should expect to be more dramatic for a larger and bulkier molecule like insulin (MW ~5000 Da in its monomeric form). Indeed, the distribution of the fusion pore diameters indicate that 40% of them are <1.1nm, similar to the size of ATP (shortest diameter 0.5*1.1 nm). This likely explains why the release of ATP is slower in *Sox4*mt β-cells.

Finally, we combined optical imaging of exocytosis using extracellular SRB (MW 559 Da; to mainly detect full fusion events) and granular VAMP-pHluorin (to detect granule fusion). The VAMP-pHluorin imaging suggests that the total number of release events was similar between WT and *Sox4*mt β-cells, but the number of full fusion events (SRB) was reduced by ~50% (Figure 16D).

Collectively, these observations argue that in *Sox4*mt β-cells, fusion pore expansion is impaired and that many release events are 'aborted' when the fusion pore has only dilated to ~1.7 nm (Figure 14C). The observed increase in the fraction of kiss-and-run exocytosis (not associated with insulin secretion) went from a 13% in WT to a 60% in *Sox4*mt β-cells (Figure 16D). This increase in kiss-and-run exocytosis would predict a 47% decrease in insulin secretion; in surprisingly good agreement with the diminution of glucose- and glucose + tolbutamide-stimulated insulin secretion (Figure S1).

These data also raise the important cell biological question of the physiological role of kiss-and-run exocytosis in a peptide-secreting cell like the pancreatic β-cell. Many endocrine cells contain two types of secretory vesicles: large dense core vesicles (LDCVs) containing peptide hormones, and small synaptic-like micro-vesicles (SLMVs) believed to contain small neurotransmitters (Kasai, 1999). The significance of SLMV exocytosis in islets remains obscure given the observation that GABA (contrary to earlier suggestions: (Reetz et al., 1991)) is principally released by exocytosis of insulin-containing LDCVs (Braun et al., 2007). Indeed, it was concluded that non-LDCV granules contribute marginally (if at all) to the exocytotic responses in rat β-cells (Karanauskaite et al., 2009). It has been speculated that kiss-and-run exocytosis of insulin granules may be used to regulate the release of small transmitters such as ATP (dimensions: 1.6 x 1.1 x 0.5 nm) and GABA (0.75 x 0.3 x 0.2 nm) (Gammelsaeter et al., 2004, Braun et al., 2007) without necessarily resulting in the release of the peptide cargo. Thus, the fusion pore may function as a 'molecular sieve'. As mentioned previously, if granules can be refilled, they may undergo several cycles of kiss-and-run exocytosis. This is significant because insulin granules are otherwise destined for lysosomal degradation

and cannot be refilled with insulin once the peptide hormone has been released (Schnell and Borg, 1985, MacDonald and Rorsman, 2007).

CHAPTER 4

Molecular mechanism of *Sox4* in defective exocytosis

4.1 Introduction

SOX4 was first recognised as a transcription factor in 1993 by Clever and colleagues. They reported that *SOX4* exhibits a distinct high mobility group (HMG)-box (DNA-binding domain) and a trans-activation domain, and that it has the capacity to initiate transcription in lymphocyte (van de Wetering et al., 1993).

SOX4 partially controls the expression of target genes by inducing DNA bending. It preferentially binds to the target sequence AACAAAG in the minor groove of the DNA helix. This action leads to the modification of the chromatin structure, thereby assisting the formation of transcriptional enhancer complexes (Weiss, 2001).

Previous studies have reported a wide range of *SOX4* target genes despite its preferential AACAAAG binding motif (Vervoort et al., 2013). For example, *Sox4* controls the development of pancreatic β-cells. It binds to CTTTG and CTTTGT motifs in the promoter region of neurogenin 3, a transcription factor that is expressed in endocrine progenitor cells (Xu et al., 2015). Furthermore, the *SOX4* HMG domain has been shown to interact with other transcription factors to control target gene expression. For instance, *SOX4*, in cooperation with *SOX11* and *SOX12*, influences the differentiation of neural and mesenchymal cells (Liao et al., 2008, Bhattaram et al., 2010).

Dysregulated *SOX4* expression has been shown to affect the transcription of its target genes, which plays a role in the pathophysiology of several diseases. Indeed, overexpression of *SOX4*, also known as a *signature* oncogene, has been implicated in a wide range of cancers (Vervoort et al., 2013). It works in concert with many downstream target genes, thereby mediating tumourigenesis. For example, an analysis of *SOX4*-

related target genes in prostate cancer revealed changes in the expression of important cancer-related genes such as *IGF2R* (insulin-like growth factor 2 receptor) and *NKX3-1*, a tumour suppressor gene (Scharer et al., 2009). However, the role of *SOX4* in cancer will not be discussed in depth here as this is beyond the scope of the thesis.

The modulation of target genes is a common feature of all *SOX4*-mediated processes. Therefore, it is possible that the synergistic action of *Sox4* in our *Sox4*mt mouse alters the expression of downstream genes. This, in turn, may contribute to the insulin secretory defect.

We examined potential transcriptional partners of *Sox4* that may be implicated in vesicle fusion processes, as well as the changes in their expression due to the point mutation Y123C. The proposed transcriptional target was tested for its 'rescue' ability.

4.2 Results

4.2.1 Identification of a candidate gene(s) mediating the effect of *Sox4*

Sox4, being a transcription factor, influences the expression of a number of genes in β-cells (Penzo-Mendez, 2010), and, thus, it is unlikely that the effects we observed on both exocytosis and insulin secretion are mediated by *Sox4* itself.

To identify the proteins affected by changes in *Sox4* functionality, microarray studies were conducted using pancreatic islet RNA extracted from WT and *Sox4*mt mice to detect differences in the expression of whole genome transcripts. We found that a total of 116 genes were up- (between 1.5- and 2.9-fold; the list of the genes above the blue line) or down-regulated (between 1.5- and 3.3-fold; the list of the genes below the blue line) in *Sox4*mt islets (Table S1). Therefore, it is not immediately evident which one of them is responsible for the effect on insulin secretion. However, we can use our detailed knowledge about the biophysical nature of the secretion defect to narrow the list of candidates. The functional data implicating defective fusion pore expansion allowed us to propose a shortlist of only a couple of genes as candidates. They were *Stxbp6* (upregulated 2.1-fold) and *Doc2b* (downregulated 1.8-fold) (highlighted in red in Table S1). The increased expression of *Stxbp6* (also known as amisyn) is of particular interest. In adrenal chromaffin cells, overexpression of *Stxbp6* (amisyn) was found to inhibit fusion pore expansion as detected by carbon fibre amperometry (Constable et al., 2005). Thus, the cells overexpressing 'pedestals' (representing release of catecholamines via the fusion pore; (Chow et al., 1992)) was increased.

4.2.2 Optimisation of the triple-transfection to assess the effect of *Stxbp6* (amisyn)

Based on the observations from our biophysical and microarray data, we hypothesised that reduced GSIS in *Sox4*mt β-cells is mainly mediated by the increased expression of *Stxbp6*. Additionally, silencing *Stxbp6* expression may increase GSIS as previously reported (Castermans et al., 2010). To validate this, we manipulated the expression of WT *Sox4*, *Sox4*mt (the *Sox4* plasmid containing the Y123C mutation) and *Stxbp6* in clonal rat INS-1 832/13 cells. This is a widely used cell line with good glucose responsiveness (Hohmeier et al., 2000). We co-transfected a siRNA and hGH with our gene of interests to measure hGH release only from successfully transfected cells. Previous work has established that hGH when expressed in insulin-secreting cells is targeted to the insulin granules, and that it is released by Ca^{2+}- and SNARE-dependent exocytosis (Khvotchev et al., 2003, Ohara-Imaizumi et al., 2009).

For triple-transfections (siRNA + gene of interest + hGH), toxicity is a potential concern and the choice of transfection reagents is therefore essential. Indeed, we initially experienced severe cell deaths using the lipid-based Lipofectamine 2000 reagent. To overcome the cytotoxicity, we chose GeneJuice which consists of non-toxic protein components. High toxicity was avoided while maintaining good transfection efficiency.

The knockdown effect of the siRNA targeting *Stxbp6* expression (*si-Stxbp6*) on hGH secretion was assessed at three different incubation times (60, 85, and 110 h post-transfection of the siRNA) for the triple transfection (*si-Stxbp6* + DsRed [a red fluorescent protein] + hGH). It was clear that measuring the secretion 85 h post-transfection yielded the strongest stimulatory effect of silencing *Stxbp6* on hGH secretion

evoked by a combination of 20 mmol/l glucose and 70 mmol/k $[K^+]_o$ (Figure 19A; black bars in 85-h incubation); hGH release at 1 mmol/l was not affected.

A scrambled siRNA was tested for potential off-target effects on *Sox4* and *Stxbp6* expression. No significant differences were observed between non-transfected and scrambled siRNA (+ DsRed + hGH)-transfected cells (Figure 19B). The optimised transfection strategy is summarised diagrammatically in Figure 20.

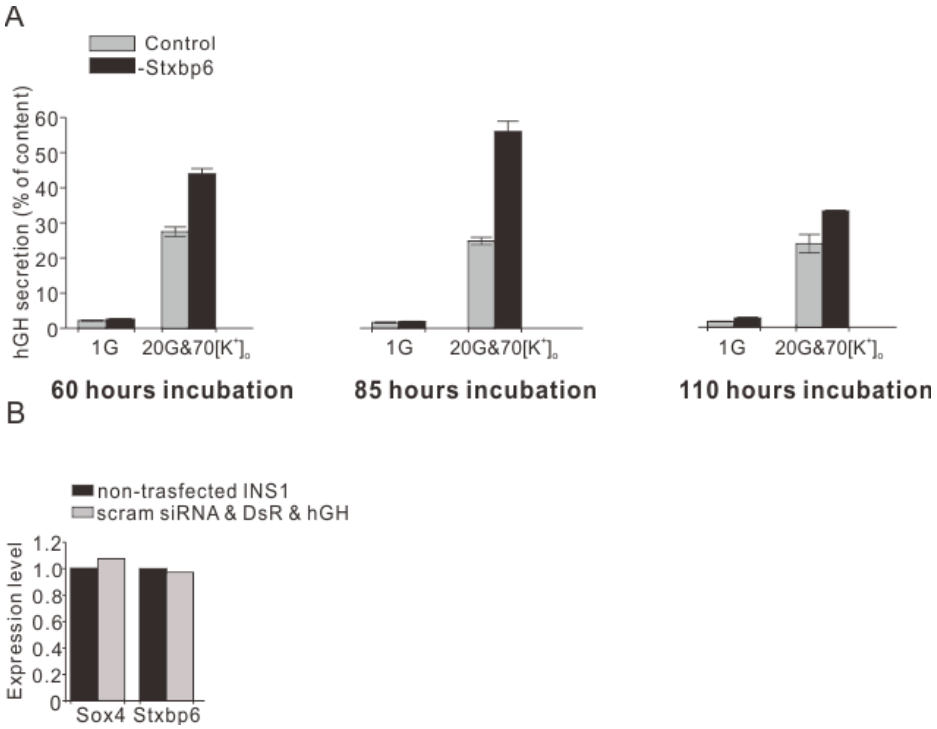


Figure 19. Optimal post-transfection time for maximum *Stxbp6* siRNA efficiency. (A) hGH release in INS-1 832/13 cells transfected with DsRed + hGH + scrambled siRNA (control; grey bars) and DsRed + hGH + *si-Stxbp6* ('-Stxbp6'; black bars) were measured in the presence of 1 mmol/l glucose (1G) and 20 mmol/l glucose (20G) + 70 mmol/l $[K^+]_o$. The post-siRNA transfection time is indicated below the x-axis. hGH secretion is expressed as % of the total hGH content. Data are presented with mean values ± SEM of 3 experiments. (B) The off-target effect of scrambled siRNA on *Sox4* and *Stxbp6* expression was assessed in untransfected INS-1 832/13 cells as compared to scrambled siRNA + hGH + DsRed-transfected cells.

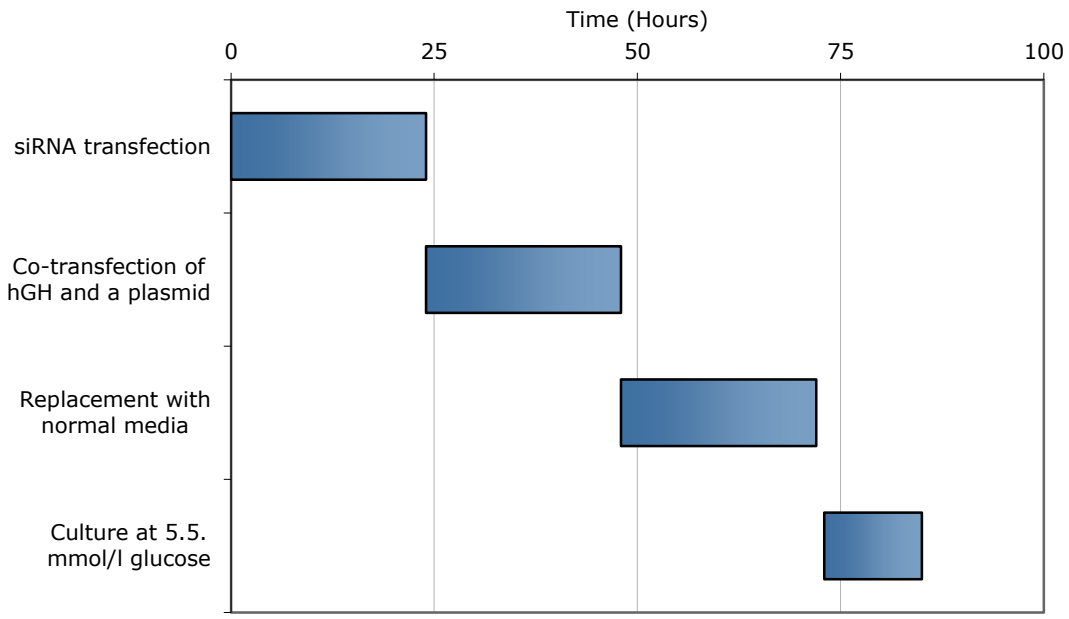


Figure 20. Timeline for triple-transfection for INS-1 832/13 cells. INS-1 832/13 cells were transfected with siRNA for 24 h. The medium in each well was then replaced with fresh culture medium, and hGH and a gene of interest were added immediately. After 24 h, to reduce cytotoxicity, the medium in each well was replaced with fresh culture medium. Prior to the hGH secretion studies, the cells were incubated in a medium containing 5.5 mmol/l instead of 11 mmol/l for 12–15 h. For more details of the procedure, please refer to Materials and Methods section 2.10.5.

4.2.3 *Sox4* mutation impairs insulin secretion via increased *Stxbp6*

We assessed the effect of overexpressing WT *Sox4*, *Sox4*mt (the WT *Sox4* plasmid containing the Y123C mutation) or amisyn on hGH secretion in INS-1 832/13 cells. In addition, the effect of silencing amisyn on its own was tested to elucidate its precise impact on insulin secretion.

Under basal conditions (1 mmol/l glucose exposure), 2.5-3.5% of the total cellular hGH was recovered in the medium (Figure 21 A-B). Upon stimulation with 20 mmol/l glucose alone or in combination with 70 mmol/l $[K^+]_o$, hGH increased an ~3.5- and a >10-fold relative to the basal secretion in control cells (co-transfected with DsRed, serving as plasmid control, hGH and scrambled siRNA) (Figure 21A; black bars).

In the presence of 20 mmol/l glucose, increasing amisyn expression decreased hGH secretion by 40% compared with that of the control (Figure 21A; grey bars). In contrast, silencing amisyn increased hGH secretion by 35% (Figure 21A; white bars). Further stimulation by a combination of 70 mmol/l $[K^+]_o$ and 20 mmol/l glucose resulted in substantially greater hGH secretion (Figure 21A). Under this condition, essentially the same pattern was observed; overexpression and knockdown of amisyn decreased (26 ± 2%) and increased (48 ± 3%) hGH secretion, respectively.

In INS-1 832/13 cells overexpressing WT *Sox4*, hGH secretion was reduced by 20% in the presence of 20 mmol/l glucose (Figure 21B; grey bars). This effect was reversed by the knockdown of amisyn expression, in which the stimulation index returned to that of the control (Figure 21B; light grey bars). A stronger inhibitory effect of 40% was attained with *Sox4*mt (Figure 21B; light blue bars). However, only a partial recovery (but

statistically significant) occurred when amisyn expression was silenced (Figure 21B; blue bars).

A similar trend was observed when a high glucose was supplemented with 70 mmol/l $[K^+]_o$. Increased expression of *Sox4* (Figure 21B; grey bars) or *Sox4*mt (Figure 21B; light blue bars) decreased hGH secretion by 40% and 50%, respectively. The inhibitory effects caused by WT *Sox4* were almost completely reversed by the knockdown of amisyn expression (light grey bars) whereas a partial (but significant) recovery was observed in *Sox4*mt-expressing cells (blue bars) (Figure 21B). It should be noted that all data reported in Figure 21 were obtained in parallel using the same preparation of cells.

To illustrate the usefulness of measuring hGH for assessing secretion in transfected cells, we also tested the effects of WT *Sox4* on insulin secretion. Here, we tested the specificity of hGH secretion in INS-1 832/13 cells overexpressing WT *Sox4*. The direct measurement of insulin masked the inhibitory effect of *Sox4* that we observed via the hGH measurement (Figure 21C). It can be noted that the fraction of insulin released is approximately half that of hGH secreted (15% vs 40%). This may be a consequence of the youngest granules undergoing exocytosis first (Duncan et al., 2003).

We extended the microarray data suggesting that *Sox4*mt leads to increased expression of amisyn (Table S1) by qRT PCR on INS-1 832/13 cells. Overexpression of *Sox4* (+ hGH + scrambled siRNA) and *Sox4*mt (+ hGH + scrambled siRNA) increased amisyn expression by 70% and 170%, respectively (Figure 21D). This suggests that the mutation, contrary to what initially assumed, is a gain-of-function rather than loss-of-function mutation. Notably, transfection of *Sox4* and *Sox4*mt similarly increased WT *Sox4*

expression (Figure 21E).

Next, we assessed the protein expression of Sox4 and Stxbp6 after transfection (Figure 22). While there are a number of commercially available antibodies for both Sox4 and Stxbp6, none of them yielded reliable results in our hands (refer to Materials and Methods section 2.13 for the list of antibodies). To overcome this problem, we used antibodies against green fluorescent protein (GFP), as our plasmids were tagged with GFP. The Sox4 protein has a molecular weight of 45 kDa, and when fused to GFP (27 kDa), the fusion protein migrated at about 72kDa (Figure 22 A-B). The Stxbp6 fusion protein migrated at about 51kDa (24 + 27 kDa) (Figure 22C). Thus, we are confident that transfection of INS-1 832/13 cells with *Sox4* and *Stxbp6* leads to increased expression of the proteins.

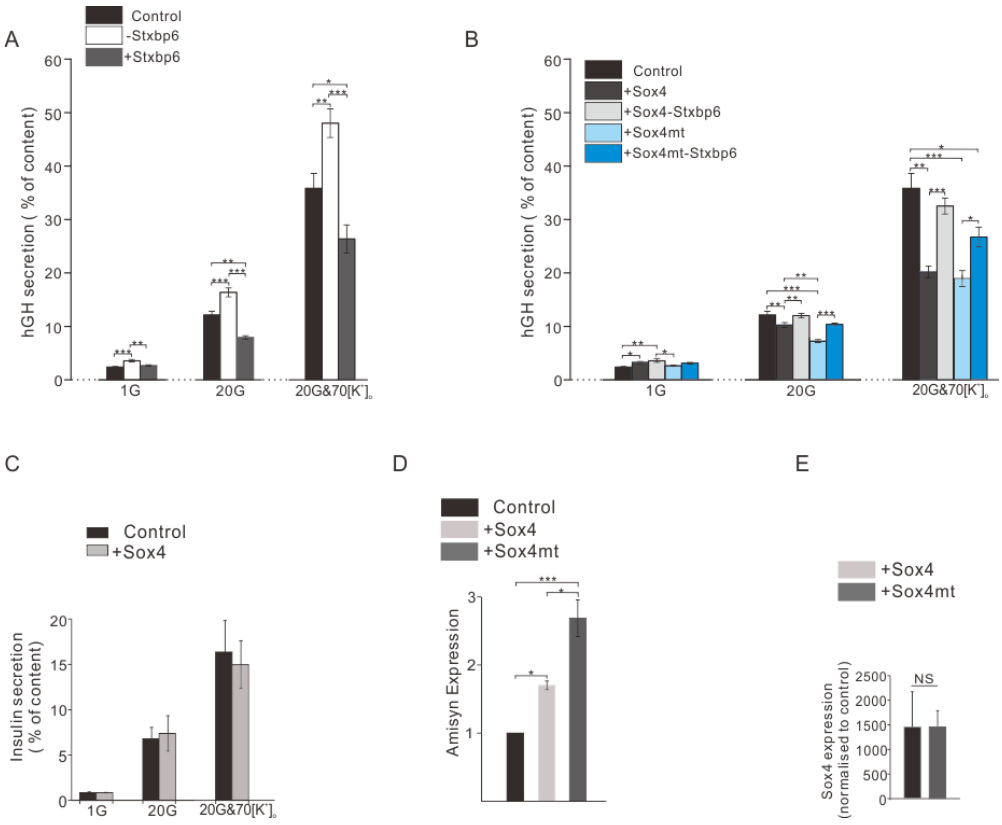


Figure 21. Mutant *Sox4* mediates its effects on insulin secretion via *Stxbp6*. (A) hGH release from INS-1 832/13 cells transfected with scrambled siRNA + DsRed + hGH (control; black bars), *si-Stxbp6* + DsRed + hGH ('-Stxbp6'; white bars) and scrambled siRNA + *Stxbp6* + hGH scrambled siRNA ('+Stxbp6'; grey bars) at 1 mmol/l glucose, 20 mmol/l glucose and 20 mmol/l glucose + 70 mmol/l $[K^+]_o$. (B) hGH release from INS-1 832/13 cells transfected with scrambled siRNA + DsRed + hGH (control; black bars), scrambled siRNA + WT *Sox4* + hGH ('+Sox4'; grey bars), *si-Stxbp6* + WT *Sox4* + hGH ('+Sox4-Stxbp6'; light grey bars), scrambled siRNA + *Sox4*mt + hGH ('+Sox4mt'; light blue bars) and *si-Stxbp6* + *Sox4*mt + hGH ('+Sox4mt-Stxbp6'; blue bars) at 1 mmol/l glucose, 20 mmol/l glucose and 20 mmol/l glucose + 70 mmol/l $[K^+]_o$. Note: (A) and (B) were performed simultaneously but for comparison purposes, they are divided to show the effect of *Stxbp6* and *Sox4*/*Sox4*mt, separately. Both data (A-B) are presented as mean values ± SEM of 4 experiments, each with 3 replicates. **P*<0.05; ***P*<0.01; and ****P*<0.001 for the indicated comparisons according to analysis of variance (ANOVA) and Tukey's tests. (C) Insulin release from INS-1 832/13 cells transfected with scrambled siRNA + DsRed + hGH (control) and scrambled siRNA + *Sox4* + hGH ('+Sox4'). Data

are presented as mean values ± SEM of 3 experiments. (D) qRT PCR analysis of *Stxbp6* expression in INS-1 832/13 cells transfected with scrambled siRNA + DsRed + scrambled siRNA (control), scrambled siRNA + WT *Sox4* + hGH ('+Sox4') or scrambled siRNA + *Sox4*mt + hGH ('+Sox4mt'). Data are presented as mean values ± SEM of 4 experiments, each with 3 replicates. **P*<0.05 and ****P*<0.001 for the indicated comparisons as determined by ANOVA and Tukey's tests. (E) *Sox4* expression was assessed in INS-1 832/13 cells transfected with scrambled siRNA + WT *Sox4* + hGH ('+Sox4') or scrambled siRNA + *Sox4*mt + hGH ('+Sox4mt'). Expression was normalised to that of the control (scrambled siRNA + DsRed + hGH). NS indicates no significant difference (Student's *t*-test).

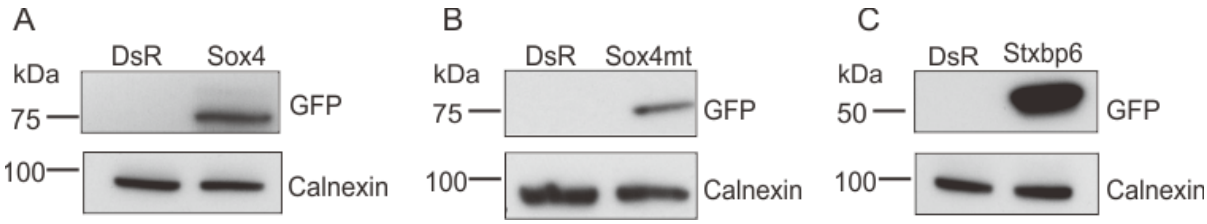


Figure 22. Western blot analysis of GFP expression level. The upper panels show the expression of either WT Sox4 (A), Sox4mt (B) or Stxbp6 (C) fusion proteins with respect to the DsRed (control), as detected using an antibody directed against the GFP tag. Transfection conditions remain same as in Figure 21. The lower panel shows equal protein loading using an antibody directed against calnexin.

4.3 Discussion

Our heterozygous *Sox4*mt mice exhibited inadequate insulin secretion, which is attributable to the inappropriate increase of kiss-and-run exocytosis at the expense of full fusion. The point mutation in the HMG-box domain of *Sox4* (T**A**C->T**G**C) is believed to be responsible for the defective phenotype. Interestingly, this point mutation in *Sox4*mt mice resulted in a 2-fold increase in the WT *Sox4* mRNA level (Goldsworthy et al., 2008). The functional consequences of the mRNA increase, in addition to the point mutation, require functional characterisations. Given that *Sox4* is a transcription factor that interacts with numerous downstream genes, dissection of its transcriptional partners with regards to the malfunctioning phenotype (stabilisation of fusion pores) is essential. At present, knowledge of putative complex partners and genes under the control of *Sox4* in pancreatic β-cells is still limited.

To address the genetic interaction underlying the *Sox4*mt phenotype, we investigated a subset of genes that was potentially implicated in the granule fusion process. These were identified by the combined use of a precise mechanistic data on the functional consequences of the *Sox4*mt and an unbiased genome-wide approach.

S*txbp6* represents a good candidate gene. It encodes the protein amisyn, also known as syntaxin-binding protein 6 (Stxbp6), which exhibits a VAMP-like coiled domain in its C-terminal domain. Given that it interacts with the SNARE complex through its binding partner syntaxin-1, it is implicated as a regulator of the formation of the SNARE complex (Scales et al., 2002), and may therefore interfere with insulin exocytosis. However, the precise role of the protein remains to be elucidated. In previous studies, overexpression and inhibition of *Stxbp6* resulted in a decrease and increase of insulin release, respectively,

in the mouse β-cell line β-TC3 (Castermans et al., 2010). Furthermore, a prolonged 'pre-spike foot' was observed in amperometric recordings of catecholamine release in adrenal chromaffin cells, a finding that is consistent with the idea that amisyn increases the stability of the fusion pore, thereby inhibiting granule release (Constable et al., 2005). This is strikingly similar to the phenotype of the *Sox4*mt β-cells. It is also notable that the expression of the gene encoding the SNARE-related protein *Doc2b* was reduced by 1.8-fold. However, in MIN6 cells, silencing *Doc2b* gene expression had no effect on GSIS in the presence of 30 mmol/l KCl (Miyazaki et al., 2009). An additional complication is that a complete KO of *Doc2b* resulted in normal GSIS and plasma insulin level (Li et al., 2014a), which is insufficient to account for the 50% reduction of GSIS that we observed in *Sox4*mt islets. Furthermore, *DOC2B* is expressed at very low levels in human β-cells (~2% of *SOX4* expression and 8% of *STXBP6* expression) (Nica et al., 2013). Collectively, these considerations make amisyn a strong candidate as the mediator of *Sox4*.

These findings prompted us to analyse the functional effects of *Sox4 in vitro* by transient transfection of WT *Sox4*, *Sox4*mt and *Stxbp6* into INS-1 832/13 cells. In agreement with the previous evidence, we observed that the overexpression of amisyn in INS-1 832/13 cells resulted in an ~30% decrease in both glucose– or high potassium and glucose–stimulated insulin secretions as compared with the controls (Figure 21A). The inhibitory role of amisyn in insulin secretion was further supported by the fact that the knockdown of amisyn expression increased hGH release (Figure 21A).

Overexpression of *Sox4*/*Sox4*mt also inhibited glucose-induced hGH secretion to a similar extent, regardless of whether the medium was supplemented with K^+. This

suggests that the upregulation of these genes inhibits insulin secretion at a late stage, subsequent to the closure of K_{ATP} channels (Figure 21B). This aligns with our biophysical data (Figure 14 in Chapter 3). The rescue of the defective hGH secretion by the knockdown of amisyn expression implicates *Stxbp6* as the major transcriptional target of *Sox4* and suggests that it plays a role in fusion pore expansion. Whereas silencing amisyn completely reversed the effects of overexpressing WT *Sox4* on hGH secretion, the effect was only partial for *Sox4*mt (Figure 21B). It is possible that this is a consequence of higher expression of amisyn expression induced by *Sox4*mt (Figure 21D). The point mutation certainly exacerbates the increase in amisyn expression, which is independent of WT *Sox4* expression (Figure 21E). Finally, we acknowledge that other target genes may have contributed to the inhibition. For example, our microarray data showed that the expression of *Slc39a8* is reduced by 1.6-fold (Table S1). This gene encodes a zinc transporter, ZnT8, in pancreatic β-cells (Chimienti et al., 2004). Insulin secretion is reduced in some ZnT8 KO mice (Pound et al., 2009, Hardy et al., 2012).

It is worth pointing out that it was initially assumed that mutation in *Sox4* is a loss-of-function mutation (Goldsworthy et al., 2008). However, it should be noted that islets from *Sox4*mt mice exhibit a 2-fold expression of WT *Sox4* (Supplementary Fig.3 in (Goldsworthy et al., 2008)). Furthermore, our data demonstrate that the amisyn expression was significantly higher in *Sox4*/*Sox4*mt-overexpressed cells (Figure 21D), which is reminiscent of that observed in *Sox4*mt mouse. Therefore, the earlier conclusion that the elevation of *Sox4* was due to a compensatory increase of 'non-functional' proteins may need to be reconsidered.

The inhibitory effect induced by the overexpression of amisyn is a result of the formation of non-functional SNARE complexes via an interaction with syntaxin-1 (Scales et al., 2002) but there is also evidence for a syntaxin-1-independent action (Constable et al., 2005). The precise molecular mechanism of amisyn action therefore remains to be elucidated. Given that amisyn possesses a VAMP-like domain that allows an interaction with syntaxin-1 (Pobbati et al., 2004, Scales et al., 2002), an increased level of *Stxbp6* may hold syntaxin-1 in an 'intermediate' position. Consequently, fewer syntaxin-1 molecules might be in their open conformation, which is needed to mediate the full-zippering process of the 4-helical SNARE complexes. This means that a lower number of functional SNARE complexes are available to overcome the energy barrier that is created by the electrostatic repulsion of the opposing membranes and the hydration repulsion between the hydrophilic surfaces of the phospholipid bilayers (Helm et al., 1989, Helm et al., 1992) to open the fusion pore. Of note, around 70 VAMPs were detected in synaptic vesicles of rat brain, which implies that the fusion process is mediated by the physiological assembly of many SNARE complexes (Takamori et al., 2006). Therefore, a 2–3–fold increase in amisyn expression would not be expected to completely abolish insulin secretion, as illustrated by our secretion data (Figure 10 in Chapter 3).

Table S1. GCRMA (Guanine Cytosine Robust Multi-Array Analysis) normalised differentially expressed genes with p≤0.05 and a fold change increase between WT and *Sox4*mt of ≥1.5. Based on the blue line as a reference, the list of genes above the line is up-regulated as compared to WT and the rest of the genes are down-regulated. Two potential target genes are highlighted in red as shown below. Experiments performed by Dr A Hough.

Fold change	P-value	Gene Title	Gene Symbol
UPREGULATED			
2.9	0.042	Gastrin	Gast
2.8	0.00311	RIKEN cDNA 6430502M16 gene	6430502M16Rik
2.4	0.0142	"deiodinase, iodothyronine, type I"	Dio1
2.4	0.0263	carboxypeptidase B2 (plasma)	Cpb2
2.2	0.0314	cell division cycle associated 8	Cdca8
2.2	0.0292	centromere autoantigen F	Cenpf
2.1	0.0304	topoisomerase (DNA) II alpha	Top2a
2.1	0.0222	apolipoprotein F	Apof
2.1	0.0207	syntaxin binding protein 6 (amisyn)	Stxbp6
2.1	0.00504	RIKEN cDNA4933405I11gene-mucin 4	4933405I11RikMuc4
2.0	0.0014	Expressed sequence BB164513	BB164513
1.9	0.0441	extracellular proteinase inhibitor	Expi
1.9	0.0234	antigen identified by monoclonal antibody Ki 67	Mki67 ///LOC638774
1.9	0.0438	shugoshin-like 1 (S. pombe)	Sgol1
1.9	0.0307	Sterol O-acyltransferase 1	Soat1
1.9	0.0264	cell division cycle associated 8	Cdca8

1.8	0.0212	budding uninhibited by benzimidazoles 1 homolog (S. cerevisiae)	Bub1
1.8	0.0119	regulator of G-protein signaling 16	Rgs16
1.8	0.0382	cyclin A2	Ccna2
1.8	0.0304	melanoma associated antigen (mutated) 1-like 1	Mum1l1
1.8	0.000652	FXYD domain-containing ion transport regulator 3	Fxyd3
1.8	0.0253	kinesin family member 20A	Kif20a
1.8	0.00912	"upstream binding transcription factor, RNA polymerase I"	Ubtf
1.8	0.0422	"Histone 1, H3i"	Hist1h3i
1.8	0.0115	aminoadipate-semialdehyde synthase	Aass
1.8	0.038	regulator of G-protein signaling 16	Rgs16
1.7	0.0169	RNA binding motif protein 14	Rbm14
1.7	0.0256	mucosal vascular addressin cell adhesion molecule 1	Madcam1
1.7	0.0238	RIKEN cDNA 2810417H13 gene	2810417H13Rik
1.7	0.0322	ubiquitin-conjugating enzyme E2C	Ube2c
1.7	0.0489	Shc SH2-domain binding protein 1	Shcbp1
1.7	0.013	"angiotensinogen (serpin peptidase inhibitor, clade A, member 8)"	Agt
1.7	0.0454	thioredoxin interacting protein	Txnip
1.7	0.00135	nitric oxide synthase trafficker	Nostrin
1.7	0.0186	estrogen-related receptor gamma	Esrrg
1.7	0.00517	"malic enzyme 3, NADP(+)-dependent, mitochondrial"	Me3
1.6	0.0256	RIKEN cDNA 1110064P04 gene	1110064P04Rik
1.6	0.011	centromere protein E	Cenpe

1.6	0.0126	zinc finger and BTB domain containing 16	Zbtb16
1.6	0.0136	"DNA segment, Chr 17, human D6S56E 5"	D17H6S56E-5
1.6	0.0107	protein C	Proc
1.6	0.0389	thyroid hormone receptor interactor 13	Trip13
1.6	0.0115	RIKEN cDNA 4632411J06 gene	4632411J06Rik
1.6	0.00872	thioredoxin interacting protein	Txnip
1.6	0.035	CD44 antigen	Cd44
1.6	0.00834	"cysteine and histidine-rich domain (CHORD)-containing, zinc-binding protein 1"	Chordc1
1.6	0.00406	myosin XVB	Myo15b
1.6	0.0332	RAS-related C3 botulinum substrate 2	Rac2
1.6	0.00409	baculoviral IAP repeat-containing 5	Birc5
1.6	0.0449	RIKEN cDNA 1200016G03 gene	1200016G03Rik
1.6	0.0232	fidgetin-like 1	Fignl1
1.6	0.0348	RIKEN cDNA 1700022C02 gene	1700022C02Rik
1.5	0.00722	SMC2 structural maintenance of chromosomes 2-like 1	Smc2l1
1.5	0.00127	mohawk	Mkx
1.5	0.0418	RIKEN cDNA 4632411J06 gene	4632411J06Rik
1.5	0.0373	relaxin/insulin-like family peptide receptor 2	Rxfp2
1.5	0.0194	RNA binding motif protein 14	Rbm14
1.5	0.0116	hemochromatosis	Hfe
1.5	0.00648	nudix(nucleoside diphosphate linked moiety X)type motif4	Nudt4
1.5	0.0243	thrombospondin 1 /// similar to thrombospondin 1	Thbs1 //LOC640441

DOWNREGULATED

3.3	0.00228	RIKEN cDNA 1100001E04 gene	1100001E04Rik
3.0	0.0208	glutamic acid decarboxylase 1	Gad1
2.7	0.0111	par6 partitioning defective 6 homolog γ (C. elegans)	Pard6g
2.7	0.0457	glutamic acid decarboxylase 1	Gad1
2.4	0.0262	cerebellin 4 precursor protein	Cbln4
2.2	0.0162	protocadherin 8	Pcdh8
2.2	0.000536	RIKEN cDNA 2210019I11 gene	2210019I11Rik
2.2	0.0339	aminolevulinic acid synthase 2, erythroid	Alas2
2.2	0.00775	RAB3C, member RAS oncogene family	Rab3c
2.2	0.0322	leucine-rich repeat LGI family, member 1	Lgi1
2.1	0.0177	Transcribed locus	---
2.0	0.000123	RAB3C, member RAS oncogene family	Rab3c
1.9	0.0112	nicotinamide nucleotide adenylyltransferase 2	Nmnat2
1.9	0.0482	hypothetical protein A230106N23	A230106N23
1.8	0.0087	expressed sequence AI428795	AI428795
1.8	0.0185	angiopoietin-like 7	Angptl7
1.8	0.0393	RIKEN cDNA A830010M20 gene	A830010M20Rik
1.8	0.00221	double C2, beta	Doc2b
1.8	7.82E-05	RIKEN cDNA 2300002D11 gene	2300002D11Rik
1.8	0.00523	cDNA sequence AB182283	AB182283

1.8	0.0234	transient receptor potential cation channel, subfamily M, member 5	Trpm5
1.7	0.0054	polo-like kinase 3 (Drosophila)	Plk3
1.7	0.0314	eyes absent 1 homolog (Drosophila)	Eya1
1.7	0.00572	transient receptor potential cation channel, subfamily M, member 5	Trpm5
1.7	0.0383	nuclear transcription factor, X-box binding 1	Nfx1
1.7	0.0395	solute carrier family 29 (nucleoside transporters), 4	Slc29a4
1.7	0.0466	CEA-related cell adhesion molecule 10	Ceacam10
1.7	0.0438	protocadherin alpha 1/ 2/ 3/ 4/ 5/ 6/ 7/ 8/ 9/ 10/ 11/ 12/ subfamily C, 1 / subfamily C, 2	Pcdha4/ 2/ 3/ 4/ 5/ 6/ 7/ 8/ 9/ 10/ 11/ 12// Pcdhac1/ 2
1.7	0.0433	receptor accessory protein 1	Reep1
1.7	0.0359	expressed sequence AW146242	AW146242
1.7	0.00376	RAS protein-specific guanine nucleotide-releasing factor 1	Rasgrf1
1.7	0.000447	glucagon receptor	Gcgr
1.6	0.0391	dual specificity phosphatase 26 (putative)	Dusp26
1.6	0.00487	F-box and leucine-rich repeat protein 10	Fbxl10
1.6	0.0149	RIKEN cDNA 1500005I02 gene	1500005I02Rik
1.6	0.0092	SEC14-like 1 (S. cerevisiae)	Sec14l1
1.6	0.0142	high mobility group box 3	Hmgb3
1.6	0.00899	leucine-rich repeat LGI family, member 1	Lgi1
1.6	0.0291	cDNA sequence BC020077	BC020077
1.6	0.0156	tubulin, beta 3	Tubb3
1.6	0.0191	RAS protein-specific guanine nucleotide-releasing factor 1	Rasgrf1

1.6	0.0338	RIKEN cDNA 2310028N02 gene	2310028N02Rik
1.6	1.31E-05	latrophilin 3	Lphn3
1.6	0.0384	RIKEN cDNA 6330500D04 gene	6330500D04Rik
1.6	0.0443	RIKEN cDNA 6720475J19 gene /// similar to putative retrovirus-related gag protein	6720475J19Rik /// LOC670480
1.6	0.0339	solute carrier family 39 (metal ion transporter), 8	Slc39a8
1.6	0.0226	acyl-CoA thioesterase 7	Acot7
1.6	0.0197	Adult male corpora quadrigemina cDNA, RIKEN full-length enriched library, clone:B230347A18	---
1.6	0.0298	cDNA sequence BC039632	BC039632
1.5	0.00205	Transcribed locus, moderately similar to XP_574723.1 PREDICTED: similar to LRRGT00097	---
1.5	0.0448	Vac14 homolog (S. cerevisiae)	Vac14
1.5	0.0327	expressed sequence AI428795	AI428795
1.5	0.0478	expressed sequence AI428795	AI428795
1.5	0.026	ciliary neurotrophic factor /// zinc finger protein 91	Cntf /// Zfp91
1.5	0.0256	immunoglobulin superfamily, member 4A	Igsf4a
1.5	0.0385	brachyury 2	T2

CHAPTER 5

Role of *SOX4* in human T2D

5.1 Introduction

The genome-wide association studies (GWAS) have revolutionised the genetic basis of type-2 diabetes. To date, more than 90 genes have been shown to be associated with T2D (Bonnefond and Froguel, 2015). However, a great gap remains between discovered single-nucleotide polymorphisms (SNPs) and their physiological role(s) in T2D pathogenesis. We have provided evidence that abnormal activity of *Sox4* (which is in linkage disequilibrium with a GWAS gene, *Cdkal1*) decreases insulin secretion, and this effect is believed to be mediated through via increased *Stxbp6* expression.

Our primary investigations mainly involved a rodent model and the INS-1 832/13 cell line but it is clearly critical to extend this to human β-cells. Indeed, it has been reported that human *SOX4* produces a protein of 474 amino acids with a molecular weight of 47 kDa whereas rodents produce a protein of 440 amino acids with a molecular weight of 45 kDa (Prior and Walter, 1996), and the human and rodent proteins only show 77% homology at the amino acid level (BLAST analysis: https://blast.ncbi.nlm.nih.gov/) (Figure 23A). By contrast, mouse *Stxbp6* and human *STXBP6* show subtle differences in their amino acid sequences (99% identity) (Figure 23B).

Here, we characterised the functional role of *SOX4* and *STXBP6* in EndoC-βH2 cells, a human β-cell line that was generated from the human foetal pancreas (Scharfmann et al., 2014). We have also had the opportunity to correlate *SOX4* expression to plasma glucose, GSIS and *STXBP6* expression in human pancreatic islets.

A

```
HUMAN SOX4  1    MVQQTNNAENTEALLAGESSDSGAGLELGIASSPTPGSTASTGGKADDPSWCKTPSGHIK  60
                 MVQQTNNAENTEALLAGESSDSGAGLELGIASSPTPGSTASTGGKADDPSWCKTPSGHIK
MOUSE Sox4  1    MVQQTNNAENTEALLAGESSDSGAGLELGIASSPTPGSTASTGGKADDPSWCKTPSGHIK  60

HUMAN SOX4  61   RPMNAFMVWSQIERRKIMEQSPDMHNAEISKRLGKRWKLLKDSDKIPFIREAERLRLKHM  120
                 RPMNAFMVWSQIERRKIMEQSPDMHNAEISKRLGKRWKLLKDSDKIPFI+EAERLRLKHM
MOUSE Sox4  61   RPMNAFMVWSQIERRKIMEQSPDMHNAEISKRLGKRWKLLKDSDKIPFIQEAERLRLKHM  120

HUMAN SOX4  121  ADYPDYKYRPRKKVKSGNANSSSSAAASSKPGEKGDKVGGSGGGGHGGGGGGGSSNAGGG  180
                 ADYPDYKYRPRKKVKSGNA + S  AA++KPGEKGDKV              GSS   G
MOUSE Sox4  121  ADYPDYKYRPRKKVKSGNAGAGS--AATAKPGEKGDKV-------------AGSSGHAGS  165

HUMAN SOX4  181  GGGASGGGANSKPAQKKSCGSKVAGGAGGGVSKPHAKLILAGGGGGGKAAAAAAASFAAE  240
                 G G +SKPA KKSCG KVAG +   V KPHAKL+ AGG       + AAASF+ E
MOUSE Sox4  166  SHAGGGAGGSSKPAPKKSCGPKVAGSS---VGKPHAKLVPAGG-------SKAAASFSPE  215

HUMAN SOX4  241  QAGAAALLPLGAAADHHSLYKARTPSASASASSAASASAALAAPGKHLAEKKVKRVYLFG  300
                 Q   AALLPLG      ++YK RT  ++A+ ++++S S+ALA P KH A+KKVKRVYLFG
MOUSE Sox4  216  Q---AALLPLGEPT---AVYKVRT-PSAATPAASSSPSSALATPAKHPADKKVKRVYLFG  268

HUMAN SOX4  301  GLGTSSSPVGGVGAGADPSDPLGLYEEEGAGCSPDAPSLSGRSSAASSPAAGRSPADHRG  360
                  LG S+SPVGG+GA ADPSDPLGLYE+ G GCSPD  SLSGRSSAASSPAA RSPADHRG
MOUSE Sox4  269  SLGASASPVGGLGASADPSDPLGLYEDGGPGCSPDGRSLSGRSSAASSPAASRSPADHRG  328

HUMAN SOX4  361  YASLRAASPAPSSAPSHASSSASSHSSSSSSSGSSSSDDEFEDDLLDLNPSSNFESMSLG  420
                 YASLRAASPAPSSAPSHASSS SS SSSSS S SS  + E +    DLNPSSNFESMSLG
MOUSE Sox4  329  YASLRAASPAPSSAPSHASSSLSSSSSSSSGSSSSDDEFEDDLL--DLNPSSNFESMSLG  386

HUMAN SOX4  421  SFSSSSALDRDLDFNFEPGSGSHFEFPDYCTPEVSEMISGDWLESSISNLVFTY  474
                 SFSSSSALDRDLDFNFEPGSGSHFEFPDYCTPEVSEMISGDWLESSISNLVFTY
MOUSE Sox4  387  SFSSSSALDRDLDFNFEPGSGSHFEFPDYCTPEVSEMISGDWLESSISNLVFTY  440
```

B

```
HUMAN STXBP6 1   MSAKSAISKEIFAPLDERMLGAVQVKRRTKKKIPFLATGGQGEYLTYICLSVTNKKPTQA  60
                 MSAKSAISKEIFAPLDERMLGAVQVKRRTKKKIPFLATGGQGEYLTYICLSVTNKKPTQA
MOUSE Stxbp6 1   MSAKSAISKEIFAPLDERMLGAVQVKRRTKKKIPFLATGGQGEYLTYICLSVTNKKPTQA  60

HUMAN STXBP6 61  SITKVKQFEGSTSFVRRSQWMLEQLRQVNGIDPNGDSAEFDLLFENAFDQWVASTASEKC  120
                 SITKVKQFEGSTSFVRRSQWMLEQLRQVNGIDPN DSAEFDLLFENAFDQWVASTASEKC
MOUSE Stxbp6 61  SITKVKQFEGSTSFVRRSQWMLEQLRQVNGIDPNRDSAEFDLLFENAFDQWVASTASEKC  120

HUMAN STXBP6 121 TFFQILHHTCQRYLTDRKPEFINCQSKIMGGNSILHSAADSVTSAVQKASQALNERGERL  180
                 TFFQILHHTCQRYLTDRKPEFINCQSKIMGGNSILHSAADSVTSAVQKASQALNERGERL
MOUSE Stxbp6 121 TFFQILHHTCQRYLTDRKPEFINCQSKIMGGNSILHSAADSVTSAVQKASQALNERGERL  180

HUMAN STXBP6 181 GRAEEKTEDLKNSAQQFAETAHKLAMKHKC  210
                 GRAEEKTED+KNSAQQFAETAHKLAMKHKC
MOUSE Stxbp6 181 GRAEEKTEDMKNSAQQFAETAHKLAMKHKC  210
```

Figure 23. Alignment of human SOX4 (A) and STXBP6 (B) with respective orthologues of mouse. Differences in the amino acid sequences are indicated in the areas that are highlighted by yellow.

5.2 Results

5.2.1 Increased *SOX4* expression reduces GSIS in a human β-cell line

Previously, we have observed a 2-fold increase in *Sox4* expression in islets isolated from *Sox4*mt mice. This led to a reduced GSIS via increased *Stxbp6* expression. Importantly, the effect of the *Sox4* mutation was reproduced by over-expressing WT *Sox4* (Figure 21 in Chapter 4). Here, we have explored the effect of increased *SOX4* expression in a recently developed human β-cell line, EndoC-βH2 (Scharfmann et al., 2014). This cell line proved to be glucose-responsive, and it showed a 2.4-fold increase in insulin secretion in response to 20 mmol/l glucose (Figure 24A). This stimulation is in fact greater than that reported in the original publication. We conclude that EndoC-βH2 cells have the potential of becoming an extremely valuable tool for the exploration of the molecular regulation of GSIS in man.

We conducted a triple-transfection of siRNA, hGH and WT *SOX4* plasmid as described previously (cf. Figure 20 in Chapter 4). A combination of 20 mmol/l glucose and 70 mmol/l $[K^+]_o$ stimulated insulin secretion by 230% above basal (1 mmol/l glucose with normal $[K^+]_o$) (Figure 24B). Overexpression of *SOX4* decreased hGH secretion by 35%. Importantly, and in agreement with the data on the INS-1 832/13 cells, this effect of overexpressing *SOX4* was completely reversed by knockdown of *STXBP6* (Figure 24B).

We tested the effect of overexpressing WT *SOX4* on *STXBP6* expression by qRT PCR. In agreement with our microarray study (Table S1 in Chapter 4) and the INS-1 832/13 qRT PCR data (Figure 21 D-E in Chapter 4), upregulated *SOX4* (+ hGH + scrambled siRNA) increased *STXBP6* expression by 350% (Figure 24C). Although the effect of

SOX4 transfection was subtle (but in fact more comparable to that seen in the *Sox4*mt islets (Goldsworthy et al., 2008)) compared with that observed in INS-1 832/13 cells (Figure 21E in Chapter 4), it still increased *STXBP6* expression by 350% (Figure 24C). Importantly, *si-STXBP6* decreased *STXBP6* expression to levels seen in control cells and this correlated with the recovery of hGH secretion (Figure 24 B-C). In addition, we conducted an off-target analysis of scrambled siRNA on both *SOX4* and *STXBP6* expression. It essentially showed no differences compared with untransfected cells (Figure 24D).

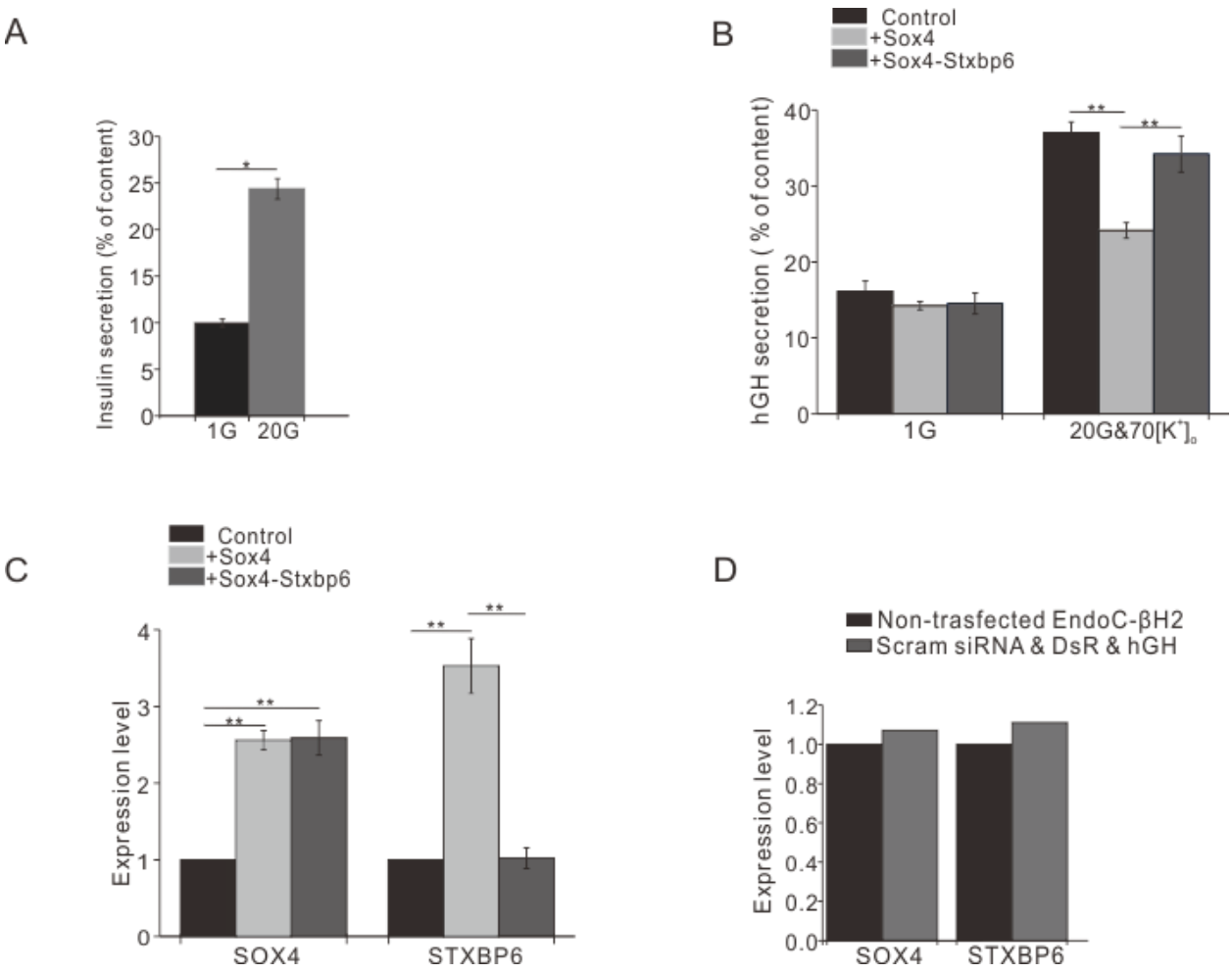


Figure 24. Increased *SOX4* mediates its effects on insulin secretion via *STXBP6*. (A) Insulin secretion by EndoC-βH2 cells in response to 1 and 20 mmol/l glucose. Mean values ± SEM are presented for 3 experiments. **P*<0.05 for the indicated comparison determined by the Student's *t*-test (B) hGH release in EndoC-βH2 cells transfected with scrambled siRNA + DsRed + hGH (control; black bars), scrambled siRNA + WT *SOX4* + hGH ('+SOX4'; light grey bars) and *si-STXBP6* + WT *SOX4* + hGH ('+SOX4-STXBP6'; grey bars) at 1 mmol/l glucose and 20 mmol/l glucose + 70 mmol/l $[K^+]_o$. ***P*<0.01 for the indicated comparisons determined by ANOVA and Tukey's tests (C) qRT PCR analysis of *SOX4* and *STXBP6* expression in human cells transfected with scrambled siRNA + DsRed + hGH (control; black bars), scrambled siRNA + WT *SOX4* + hGH ('+SOX4'; light grey bars) and *si-STXBP6* + WT *SOX4* + hGH ('+SOX4-STXBP6'; grey bars). Data are presented as mean values ± SEM of 3 experiments, each with 3 replicates; ***P*<0.01 for the indicated comparisons by ANOVA and Tukey's tests. (D) The off-target effect of scrambled siRNA on *SOX4* and *STXBP6* expression was

assessed in untransfected EndoC-βH2 cells compared to scrambled siRNA + DsRed + hGH-transfected cells.

5.2.2 Increased *SOX4* expression shows diabetic-like phenotypes in humans

To further evaluate the role of *SOX4* and *STXBP6* in a clinical context, we next correlated the expression of *SOX4* to HbA1C levels (which refers to glycated haemoglobin, a surrogate measure of the long-term blood sugar level) and GSIS in a large number of human islet preparations.

Increased *SOX4* expression showed a positive and a negative correlation with HbA1C levels and GSIS, respectively (Figure 25 A-B). Of note, there was a tendency towards higher *SOX4* expression in samples from T2D donors (HbA1C>6%; Figure 25C), although this was not statistically significant. This is perhaps due to the fact that the measurement was conducted with islets instead of isolated β-cells. 50% of the cells in human islets are non-β-cells (Brissova et al., 2005, Cabrera et al., 2006). It is important to note that HbA1c can be artificially elevated due to the terminal illness of the donors. Therefore, caution would be required to interpret HbA1c data. Our insulin secretion data is clearly reduced by increasing *SOX4* expression, and in the same samples, the HbA1c levels were determined. This may justify that lack of insulin secretion would have caused a higher level of HbA1c so other factors (if any) may have contributed marginally towards the phenotype.

In agreement with our qRT PCR data (Figure 24C), *SOX4* expression correlated positively with *STXBP6* in our human samples (Figure 25D). Increasing *STXBP6* expression correlated with higher HbA1C levels (Figure 25E).

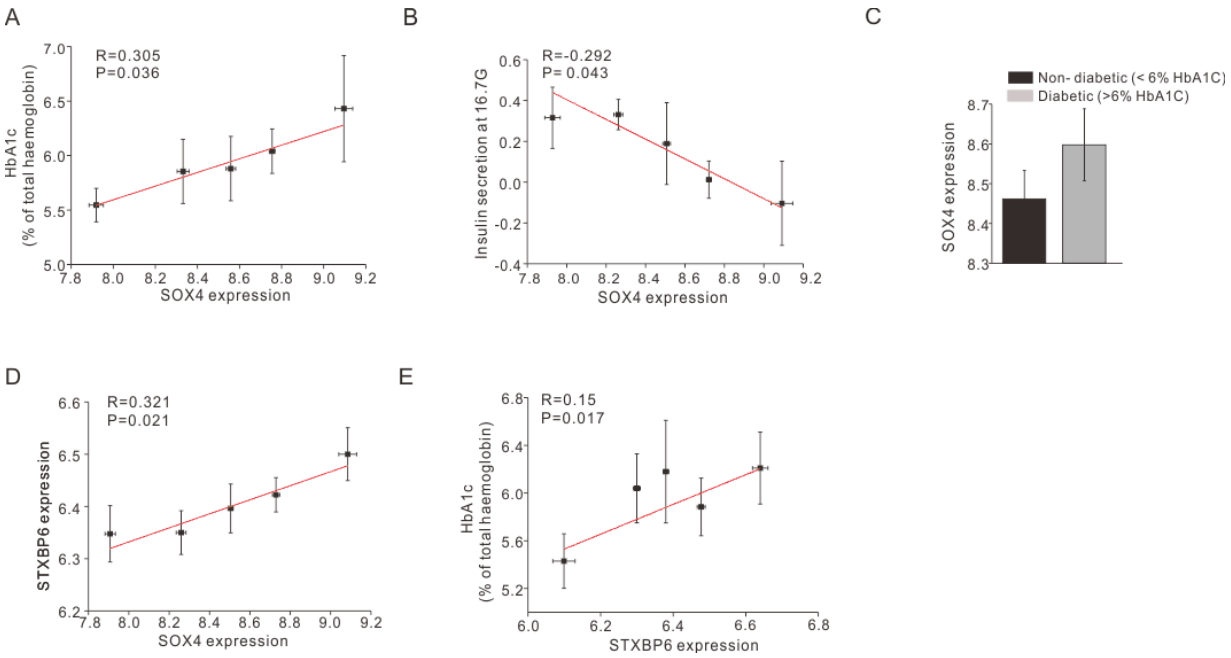


Figure 25. Effects of *SOX4* and *STXBP6* on human β-cell function. (A) Relationship between S*OX4* expression and HbA1C levels. For display purposes, the data have been grouped in quintiles. The red line represents the least-squares fit to all data. R=0.305; P=0.036; n=52. (B) Relationship between *SOX4* expression and GSIS (insulin secretion at 16.7 mmol/l glucose). For display purposes, the data have been grouped in quintiles. The red line represents the least-squares fit to all data. R=-0.292; P=0.043; n=48. (C) *SOX4* expression in islets from non-diabetic (ND) and diabetic (T2D) organ donors. Values are presented as means ± SEM; n=31 for ND donors and n=21 for T2D donors. (D) Relationship between *SOX4* expression and *STXBP6* expression. For display purposes, the data have been grouped in quintiles. The red line represents the least-squares fit to all data. R=0.321; P=0.021; n=63. (E) Relationship between *STXBP6* expression and HbA1C levels. For display purposes, the data have been grouped in quintiles. The red line represents the least-squares fit to all data. R=0.15; P=0.017; n=52.

5.3 Discussion

The GWAS have identified a plethora of T2D susceptibility genes. The majority of them appear to be involved in islet function, specifically in insulin-secreting β-cells (Marullo et al., 2014, Florez, 2008). However, the precise biological role of most of these candidate genes remains to be elucidated. Interpretation of data emanating from the GWAS is also challenging because most of the risk alleles exert mild effects, with odds ratios of < 1.15 (implying that there is less than a 15% increased risk of developing T2D for the risk variant compared to the low-risk variant). Furthermore, the majority of genetic variants (80%) fall into non-coding regions of the locus that are often associated with linkage disequilibrium blocks (intergenic nature) (Bonnefond and Froguel, 2015). These obstacles are exemplified in studies of *CDKAL1*. Individuals in European and Asian populations carrying SNPs in *CDKAL1* show reduced insulin secretion (Steinthorsdottir et al., 2007). However, recent data suggest that *CDKAL1* may not be responsible for the reported association between the lead *CDKAL1* SNP (rs7756992) and T2D susceptibility (Locke et al., 2015). An additional complication is that *CDKAL1* is expressed at very low levels in human β-cells (Nica et al., 2013). Therefore, it is of interest that the *CDKAL1* locus overlaps with the genomic regulatory blocks of *SOX4* in their 200-kb linkage disequilibrium block (Ragvin et al., 2010). Indeed, increased *Sox4* expression is associated with reduced insulin secretion (Figure 10 in Chapter 3). Interestingly, a previous study observed increased *SOX4* expression in human diabetic β-cells ($P<0.05$) (Marselli et al., 2008). These observations indicate that *SOX4*, not *CDKAL1*, may be a causative gene. Here, we showed that increased *SOX4* expression is correlated with reduced insulin secretion and increased plasma glucose levels (which were measured as HbA1C levels).

In the original paper (Scharfmann et al., 2014), EndoC-βH2 showed a poor glucose responsiveness (no increase in insulin secretion at 11 or 15 mmol/l glucose). With our optimised methods (overnight culture at a lower glucose concentration), the human cell line responded to a high glucose level with a 2.4-fold increase in insulin secretion (Figure 24A). For our secretion assay, we supplemented 20 mmol/l glucose with 70 mmol/l $[K^+]_0$ to maximise the hGH secretory response. This facilitated the detection of any inhibitory effect of *SOX4*. In this way, we were able to specifically assess the impact of *SOX4* on granule fusion, given that the secretory defect lies at the exocytosis step (Figure 14 in Chapter 3). In agreement with INS-1 832/13 secretion data (Figure 21 in Chapter 4), we observed a 35% reduction in stimulated hGH release in *SOX4*-overexpressing EndoC-βH2. This effect was completely reversed by the knockdown of *STXBP6* expression. This again demonstrates that *SOX4* regulates fusion pore expansion mainly via *STXBP6*. Such rescue activity correlates with the restoration of a normal *STXBP6* expression level in *SOX4*-overexpressing cells (Figure 24C). Of note, increased *SOX4* expression resulted in a 3.5-fold increase of *STXBP6* (Figure 24C). It is also important to note that the transfection of *SOX4* into EndoC-βH2 cells only produced a 2.5-fold increase in *SOX4* expression. This falls into a more physiological range (as compared to a 1500-fold increase in INS-1 832/13 cells) and compares favourably with the increase that was observed in islets of *Sox4*mt mice (Goldsworthy et al., 2008).

We extended our study to clinical human islet preparations. It is important to validate functional studies in human samples. For example, different investigations of *SLC30A8* have reported conflicting results. Reduced activity of the ZnT8 (encoded by *Slc30a8*), zinc transporter that is mainly expressed in pancreatic β-cells (Chimienti et al., 2004), has been reported to decrease insulin secretion in various *ZnT8* KO mouse models

(Nicolson et al., 2009, Hardy et al., 2012). However, a recent human study demonstrated that protein-truncated variants of *SLC30A8* (less functional ZnT8) actually confer protection against T2D risk (Flannick et al., 2014). Thus, studies on human islets and human whole-body physiology are essential in the exploration of the genetic and molecular causes of T2D.

With regard to the possible relevance to human diabetes, it is of great interest that our human islets analysis showed a negative correlation between *SOX4* expression and GSIS, and a positive correlation between *SOX4* expression and HbA1C levels. In that same material, we detected a positive correlation between *SOX4* and S*TXBP6* expression (Figure 25D). The possible involvement of *STXBP6* was again suggested by the finding that increasing *STXBP6* expression mimicked the effect of upregulating *SOX4* expression; both genes consistently showed a positive association with HbA1C levels (Figure 25 A and E). These expression analyses corroborate the findings made in the *Sox4*mt β-cells, INS-1 832/13 cells and EndoC-βH2 cells. The high degree of reproducibility between different systems justifies the conclusion about the role of *SOX4* in human T2D: Our data suggest that upregulated *SOX4* expression impairs insulin release via the increased *STXBP6* expression and that this impedes the delivery of insulin into the extracellular space by inhibiting adequate fusion pore expansion between the insulin granule and the extracellular space (MacDonald et al., 2006).

How does *SOX4* control *STXBP6* expression? Over-expression of *SOX4* has been implicated in many types of cancers, as it causes upregulated Wnt-signalling (Vervoort et al., 2013). For example, increased levels of SOX4 protein stabilises β-catenin, which leads to the activation of Wnt-target genes. This mechanism is involved in the rapid

proliferation of colon carcinoma cells (Sinner et al., 2007) and endometrial cells (Saegusa et al., 2012). Notably, the expression of various Wnt receptors (also known as Frizzled receptors) have been detected in adult human islets (Heller et al., 2003), which clearly implies a potential physiological role(s) of Wnt-signalling in pancreatic β-cells. Interestingly, one of the Wnt-signalling pathways is Ca^{2+}-dependent and activates protein kinase C (PKC). Previous reports (Chen et al., 2005, Fulop and Smith, 2006) indicate that PKC increases the rate of fusion pore expansion. Therefore, it is an interesting possibility that *STXBP6* expression is under the influence of PKC. This is attractive given the additional biophysical evidence that PKC controls fusion pore expansion (Scepek et al., 1998). Our study finally underscores the importance of a detailed functional characterisation in the exploration of how genetic variability affects T2D risk.

CHAPTER 6

Fh1 plays a key role in insulin secretion by a distal effect on exocytosis: evidence for a mitochondrial signal?

6.1 Introduction

Fumarate hydratase (FH) is a metabolic enzyme catalysing the reversible hydration of fumarate to malate during the Krebs cycle in the mitochondrial matrix (Figure 26). In mammals, FH is encoded from a single mRNA transcript which is then translated into two different proteins: a mitochondrial polypeptide harbouring a mitochondrial targeting sequence (MTS) and a shorter form of cytosolic precursor without MTS (Akiba et al., 1984, Ono et al., 1985, Tuboi et al., 1990) (Figure 27). This process of sorting a single protein into different subcellular compartments, either mitochondria or cytosol, is called dual targeting (or dual location), another example of which is the glutathione S-transferase (Raza, 2011, Yogev et al., 2011). Mitochondrial FH is one of the Krebs cycle enzymes, while cytosolic FH plays a key role in the metabolism of amino acids and the production of urea (Ratner et al., 1953, Yogev et al., 2011).

FH has long been implicated as a tumour suppressor gene. Mutations in the gene have been shown to increase the susceptibility to hereditary leiomyomatosis and renal cell cancer (HLRCC) which causes the development of benign tumours affecting smooth muscle (leiomyomas) in the skin and the uterus. (Kiuru et al., 2001, Tomlinson et al., 2002). One of the key consequences of the mutations is 'succination' of multiple proteins. Accumulated fumarate (which act as electrophiles) react with cysteine residues of multiple proteins to form *S*-(2-succinyl) cysteine (2SC) (Alderson et al., 2006). Interestingly, under hyperglycaemia, fumarate-mediated succination increases in adipocytes of diabetic mouse models, which leads to an impaired release of adiponectin (Nagai et al., 2007, Frizzell et al., 2009). However, to date, no information on the impact of protein succination in pancreatic β-cells is available.

In this chapter, we explore the potential role of the Krebs cycle enzyme, FH, in GSIS using a β-cell specific *Fh1* knockout (*Fh1*KO) mouse (Pollard et al., 2007).

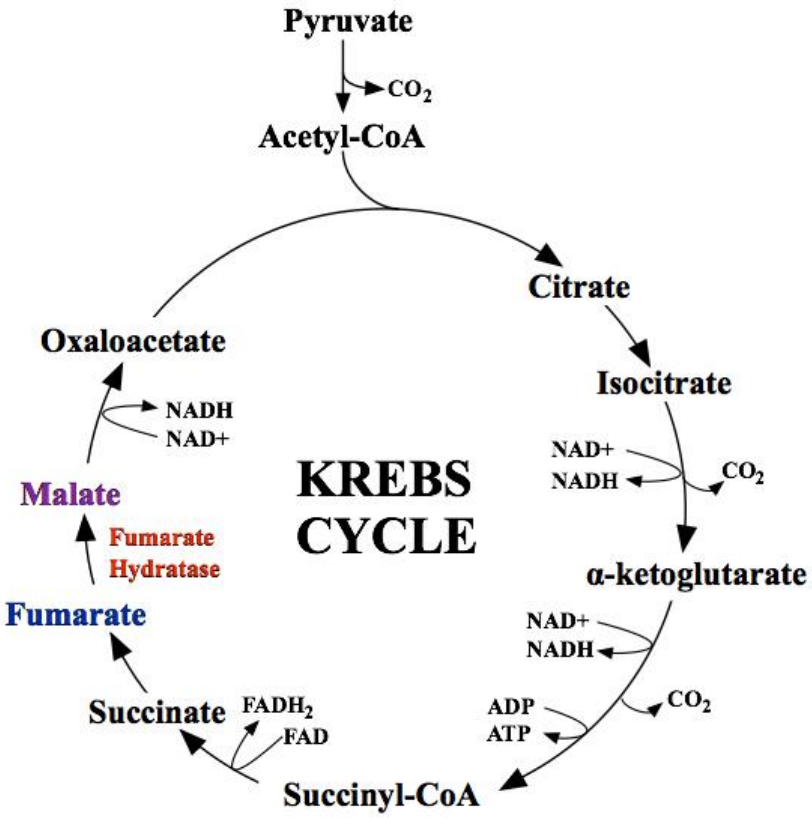


Figure 26. Overview of the Krebs cycle. The intermediate steps of oxidative respiration take place in the mitochondrial matrix, and generate chemical energy in the form of NADH and $FADH_2$ through a series of oxidative decarboxylations that use acetyl-CoA as starting material. Fumarate hydratase (red) catalyses the conversion of fumarate (blue) to malate (purple).

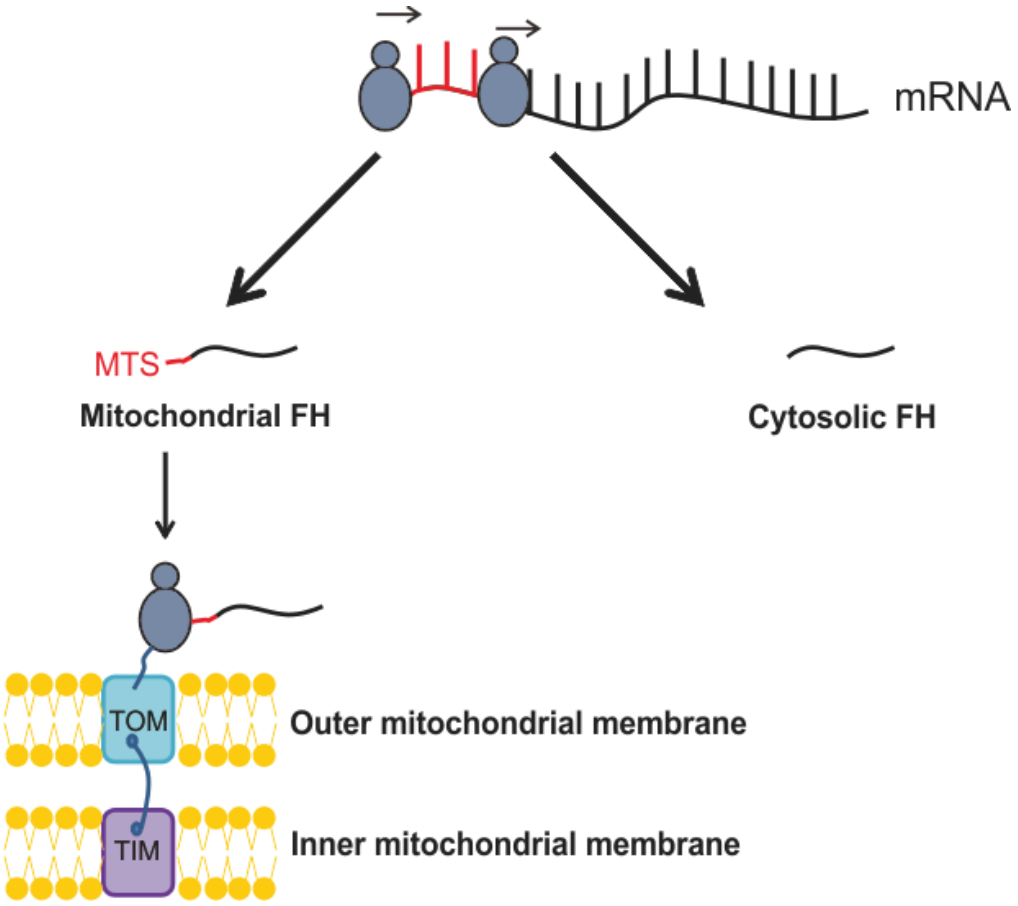


Figure 27. Potential mechanism of the dual targeting of mammalian fumarate hydratase (FH). Two of the same ribosomes initiate translation on different start codons of the mRNA to encode two distinct FH: mitochondrial FH with mitochondrial targeting sequence (MTS; indicated by red) and cytosolic FH without MTS. Import of the former protein into mitochondria is suggested to be coupled with a translation process. The nascent mitochondrial FH precursors enter the mitochondria through the assistance of translocase situated in the outer membrane (TOM) complex and the translocase of the inner membrane (TIM) complex. Import process is mediated by the MTS which interacts with the mitochondrial import receptors on the membranes. MTS is removed after the import by a protease in the mitochondrial matrix (Modified from (Yogev and Pines, 2011)).

6.2 Results

6.2.1 *Fh1* mediates an active role in GSIS

To assess the role of *Fh1* in dynamic insulin secretion, we first performed *in situ* pancreatic perfusion. Pancreatic perfusion does not involve islet isolation, and allows monitoring of both the 1st and 2nd phase of insulin secretion. We compared insulin secretion in control (WT littermates) and *Fh1*KO mice at 1, 6 and 20 mmol/l glucose. We also tested the effects of the incretin hormone GLP-1 at a concentration of 10 pmol/l in the presence of 20 mmol/l glucose.

At basal glucose (1 mmol/l), insulin release in *Fh1*KO mice was reduced by 80% relative to control animals ($P<0.005$) (Figure S2). When glucose was raised to 6 mmol/l, a prominent 1st phase response was seen in control mice reaching a peak ~15-fold higher than basal. By contrast, only a 3-fold increase was seen in *Fh1*KO mice. Subsequent to the elevation of glucose to 20 mmol/l, insulin secretion in control mice was increased to 5.09 ± 1.16 pg/min and, at this glucose concentration, insulin secretion was stimulated 14-fold over basal in *Fh1*KO mice, but still averaged only 15% of that seen in control mice. The suppression of GSIS in *Fh1*KO mice could not be rescued by GLP-1, while the introduction of GLP-1 evoked a strong stimulation of insulin secretion in control mice (Figure S2).

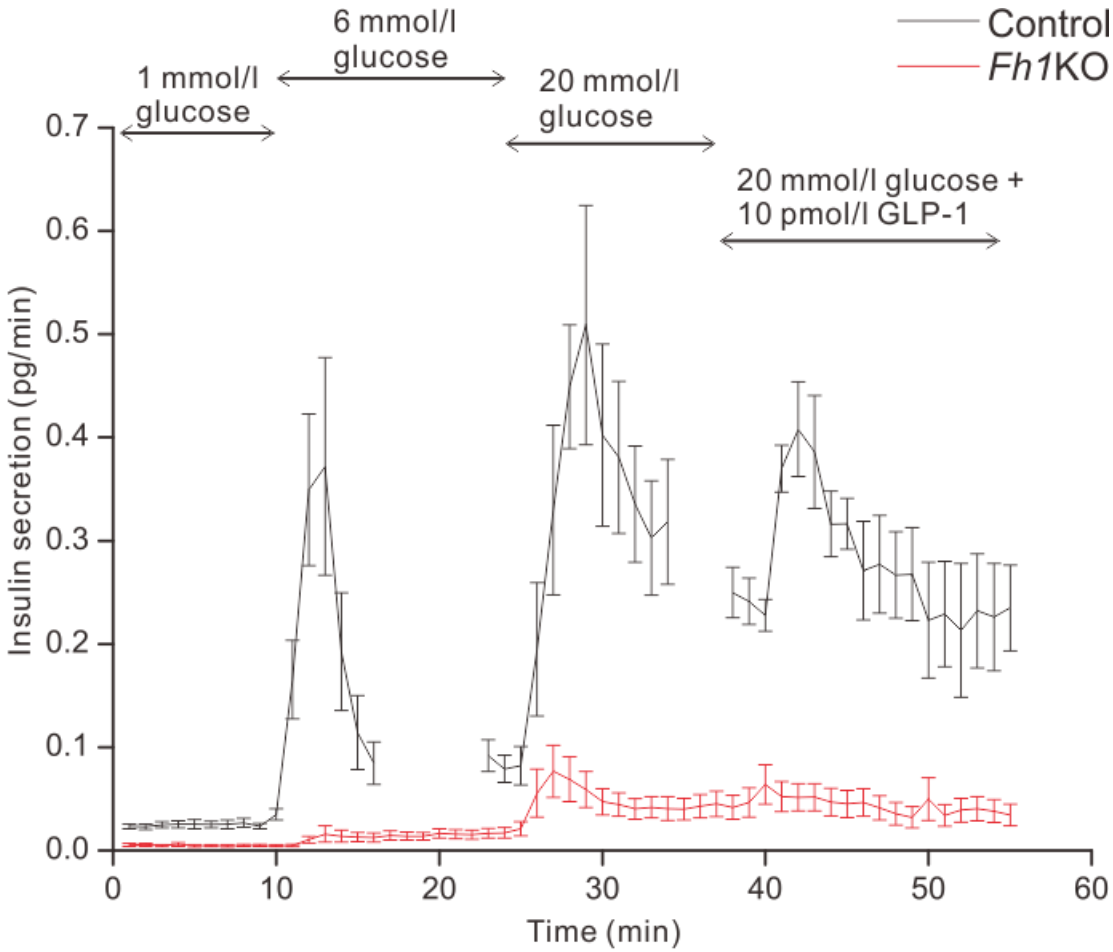


Figure S2. Insulin release measured by *in situ* pancreatic perfusion. Mouse pancreases were perfused *in situ* in the presence of 1, 6, 20 mmol/l glucose (as indicated), and finally at 20 mmol/l glucose + 10 pmol/l GLP-1. Data are presented as mean values ± SEM, and the experiments were repeated with n=5 mice (18 weeks old) per genotype. The difference at all points are significantly different ($P<0.05$; Student's *t*-test), except at 26 and 52 min. In the control mice, glucose (6 and 20 mmol/l) was applied for 15 min instead of 25 min (as in *Fh1*KO mice) and thus responses to 20 mmol/l glucose and 20 mmol/l glucose + 10 pmol/l glucose have been shifted for the different conditions to be aligned. Experiments performed by Mr NJG Rorsman.

6.2.2 Both control and *Fh1*$^{-/-}$ islets show normal increases in ATP content upon glucose exposure

The Krebs cycle plays a key role in oxidative phosphorylation and ATP production. It is therefore conceivable that ablation of *Fh1* interferes with the ability of glucose to increase ATP and that this in turn leads to less efficient closure of the K_{ATP} channels, ultimately resulting in loss of the triggering effect of glucose. However, basal ATP levels were not different between control and *Fh1*$^{-/-}$ islets. Surprisingly, glucose (20 mmol/l) remained as capable of increasing ATP in *Fh1*$^{-/-}$ islets as in WT islets (Figure S3). In both types of islets, the stimulatory effect of glucose was prevented by the ATP synthase blocker oligomycin. We acknowledge that it is only in β-cells that *Fh1* has been knocked down, but given that only ~20% of the islet volume in mice consists of non-β-cells, it seems safe to conclude that most of the increase in ATP in *Fh1*$^{-/-}$ islets reflects enhanced ATP production in β-cells.

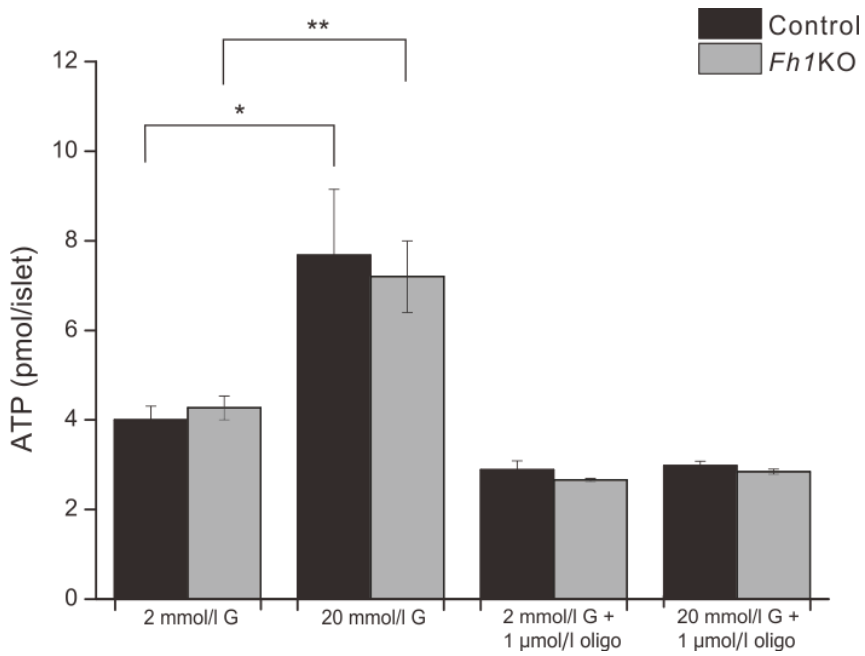


Figure S3. Ablation of *Fh1* does not interfere with ATP production. Islet ATP levels were measured at 2 and 20 mmol/l glucose (G) in the absence and presence of 1 µmol/l oligomycin (oligo) as indicated above. Data are presented as mean values ± SEM (*P<0.05, **P<0.005; Student's *t*-test) (9-14 islets from n=5 mice per genotype). Experiments performed by Dr K Shimomura.

6.2.3 *Fh1*-induced secretory defects is not due to either impaired $[Ca^{2+}]_i$ or reduced exocytosis

Insulin granule exocytosis is highly dependent on an elevation of $[Ca^{2+}]_i$. We therefore hypothesised that the severe impairment of GSIS was due to the failure of glucose to elevate $[Ca^{2+}]_i$ (reported as F_{340}/F_{380} –ratio). We tested this using the ratiometric calcium indicator fura-2 AM (intracellular esteras removes the acetoxymethyl [AM] groups from the molecule thus liberating the indicator in the cytosol).

At 1 mmol/l glucose, there was no significant difference in the F_{340}/F_{380} in both types of islets (Figure 28 A-B). Increasing glucose concentration to 12 mmol/l increased $[Ca^{2+}]_i$ to roughly the same extent in both control and *Fh1*$^{-/-}$ islets. Notably, the initial peak occurred with a longer delay in *Fh1*$^{-/-}$ islets (2.67 ± 0.24 and 7.65 ± 1.63 min after elevation of glucose in control and *Fh1*$^{-/-}$ islets, respectively; $P<0.05$). In both control and *Fh1*$^{-/-}$ islets, the elevation was preceded by a transient reduction of $[Ca^{2+}]_i$ ('phase 0') with a similar minimum F_{340}/F_{380} value. Following the initial peak, $[Ca^{2+}]_i$ oscillations ('phase 2') were seen in both control and *Fh1*$^{-/-}$ islets, respectively, but the F_{340}/F_{380} value was somewhat reduced in the *Fh1*$^{-/-}$ islets ($P<0.05$). This was also the case when glucose was increased to 20 mmol/l glucose, a condition which was associated with a further elevation of $[Ca^{2+}]_i$.

We finally compared the effects of the K_{ATP} channel blocker tolbutamide (0.2 mmol/l) on $[Ca^{2+}]_i$. When applied at 1 mmol/l glucose, tolbutamide similarly increased $[Ca^{2+}]_i$ in both *Fh1*$^{-/-}$ and control islets (Figure 28C).

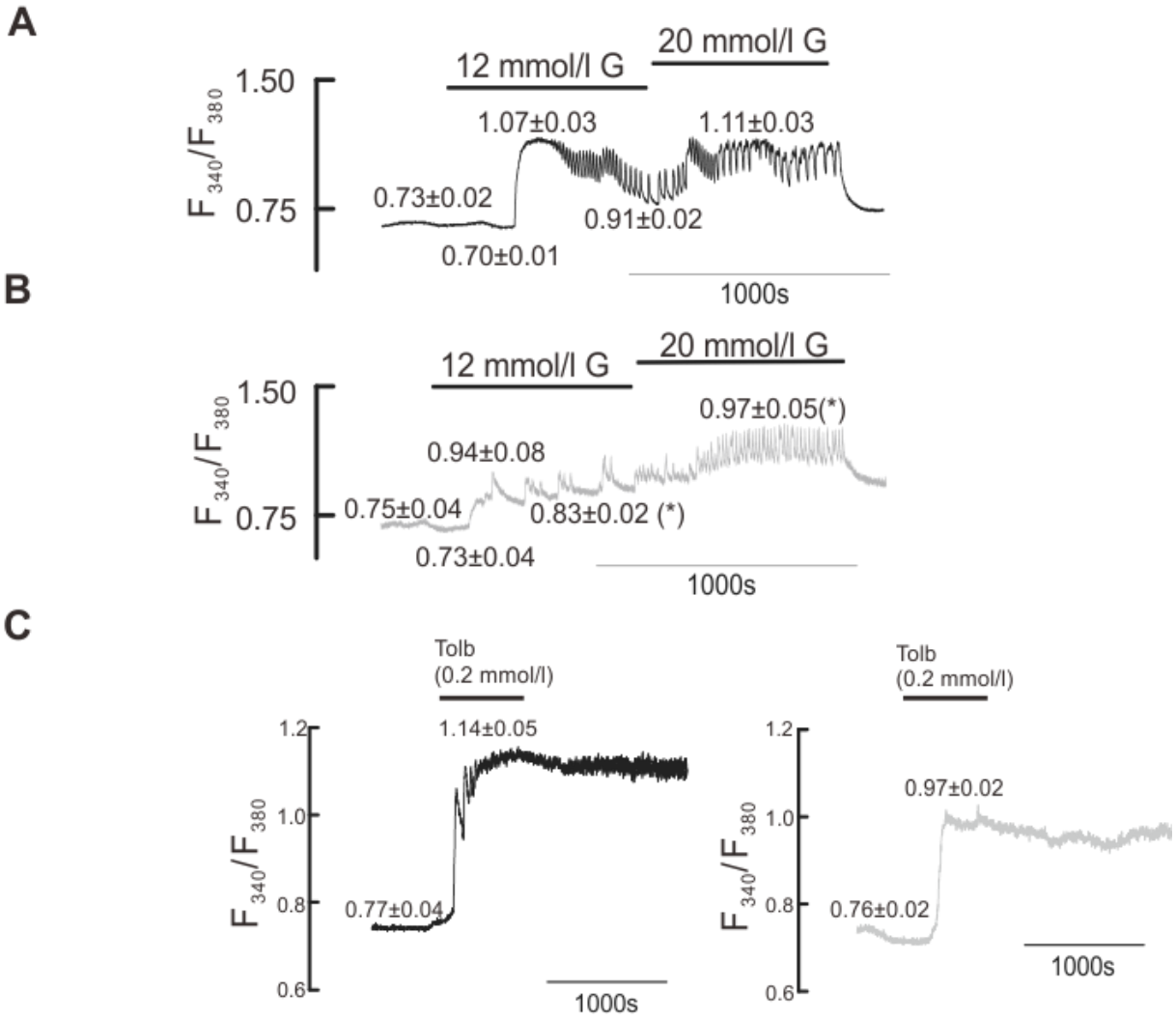


Figure 28. Representative traces of intracellular $[Ca^{2+}]_i$ in control (A) and *Fh1*$^{-/-}$ islets (B). Glucose (G) was increased from 1 to 12, and 20 mmol/l as indicated. $[Ca^{2+}]_i$ is reported as F_{340}/F_{380}-ratios. Values above the traces are means ± SEM under each different experimental condition. Asterisks in brackets indicate statistical significances between *Fh1*$^{-/-}$ and control islets (*$p<0.05$; Student's *t*-test). Recordings are representatives of 17 control islets and 12 *Fh1*$^{-/-}$ islets (from n=3 mice for each genotype). (C) As in (A) and (B), but comparing the effects of tolbutamide (Tolb) in control (left; black) and *Fh1*$^{-/-}$ (right; grey) islets (5 islets in control and *Fh1*KO from n=2 mice per genotype).

The slight reduction of $[Ca^{2+}]_i$ in *Fh1*$^{-/-}$ islets in responses to both glucose and tolbutamide may be accounted for by a reduced Ca^{2+} entry via voltage-gated Ca^{2+} channels. To evaluate this possibility, we performed whole-cell voltage-clamp measurements of the Ca^{2+} current in individual β-cells. However, both the peak amplitude and voltage dependence of the Ca^{2+}-currents were superimposable in β-cells isolated from control and *Fh1*KO mice (Figure 29).

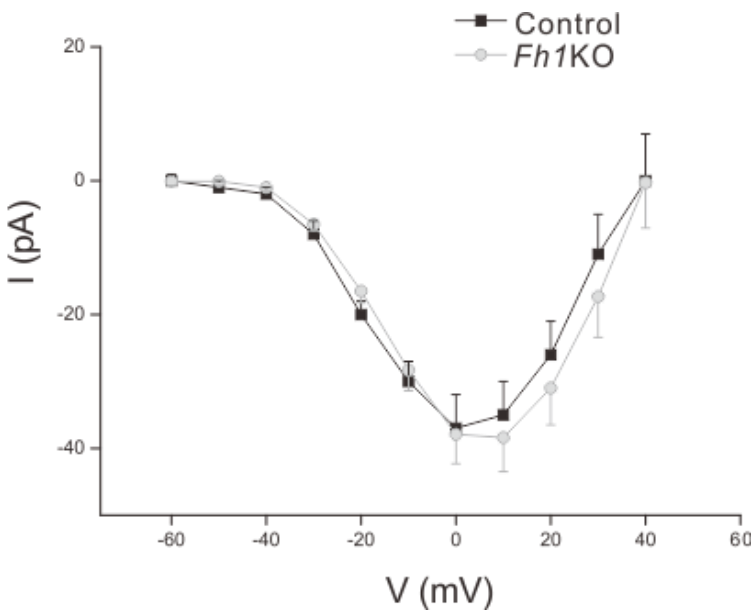


Figure 29. Current (I) - Voltage (V) relationship for Ca^{2+} currents recorded from dispersed β-cells isolated from control (black squares) and *Fh1*KO mice (grey circles). Data are mean values ± SEM of peak currents evoked by 500 ms voltage-clamp depolarisations from -60 mV to +40 mV (42 and 39 cells in control and KO, respectively, from n=6 mice per genotype).

A simple explanation for the severe impairment of insulin secretion in the face of normal $[Ca^{2+}]_i$ and Ca^{2+}-entry is that the exocytotic machinery is defective in *Fh1*$^{-/-}$ β-cells. We tested this aspect by high-resolution capacitance measurements of exocytosis in individual control and *Fh1*$^{-/-}$ β-cells. A train of ten 500 ms depolarising pulses from -70 to 0 mV increased cell capacitance by 116 ± 12 and 115 ± 13 fF in control and *Fh1*KO, respectively (Figure 30). Thus, the exocytotic machinery appears to be intact in *Fh1*$^{-/-}$ β-cells, and we conclude that genetic ablation of *Fh1* interferes with insulin secretion somewhere between the elevations of $[Ca^{2+}]_i$ and the initiation of exocytosis.

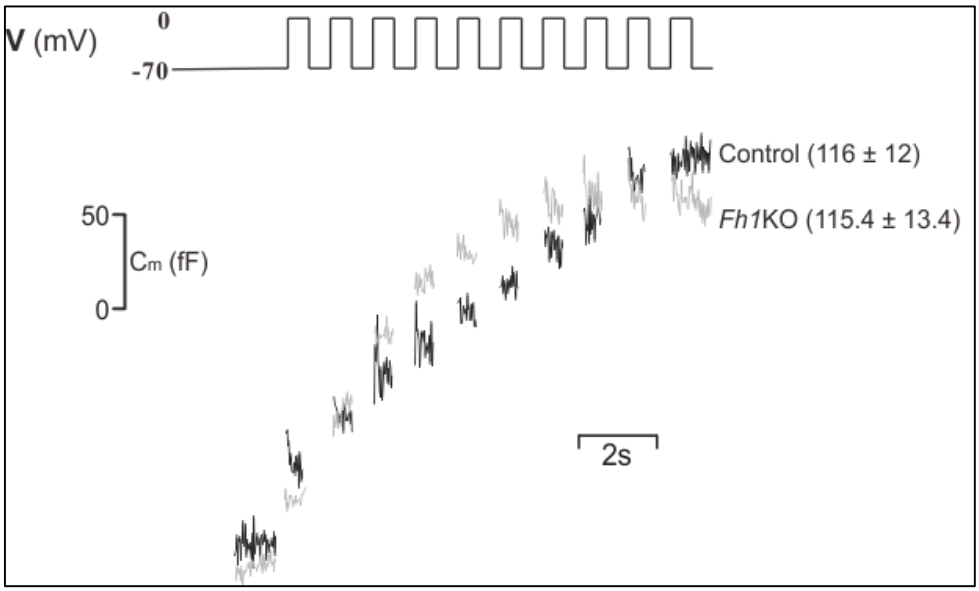


Figure 30. Standard whole-cell capacitance measurements in control and *Fh1*$^{-/-}$ β-cells. Exocytosis was evoked by a train of ten 500 ms depolarisations from -70 to 0 mV applied at a frequency of 1 Hz. Values show mean ± SEM (50 and 47 cells in control and KO, respectively, from n=6 mice per genotype).

6.2.4 Electron microscopy (EM) reveals morphological defects in mitochondria

EM studies revealed the presence of numerous fragmented and a few extremely large mitochondria in *Fh1*$^{-/-}$ β-cells (Figure 31A). In control β-cells, the size of the mitochondria ranged between 0.04 and 0.9 μm^2 with a mean of 0.21 ± 0.01 μm^2. In *Fh1*$^{-/-}$ islets, the size of the mitochondria was much more variable: some were very small (0.005 μm^2), whereas others were exceptionally large (1.9 μm^2) (Figure 31 B-C). Notably, the area density (average mitochondria per 100 μm^2 of cytoplasm) was significantly higher in *Fh1*$^{-/-}$ cells than in control β-cells: 36 ± 3 vs. 25 ± 2, respectively; $P<0.05$ (Figure 31D). The higher density is a result of the fragmentation of many mitochondria due to the disruption of *Fh1*, resulting in an increase of the total number.

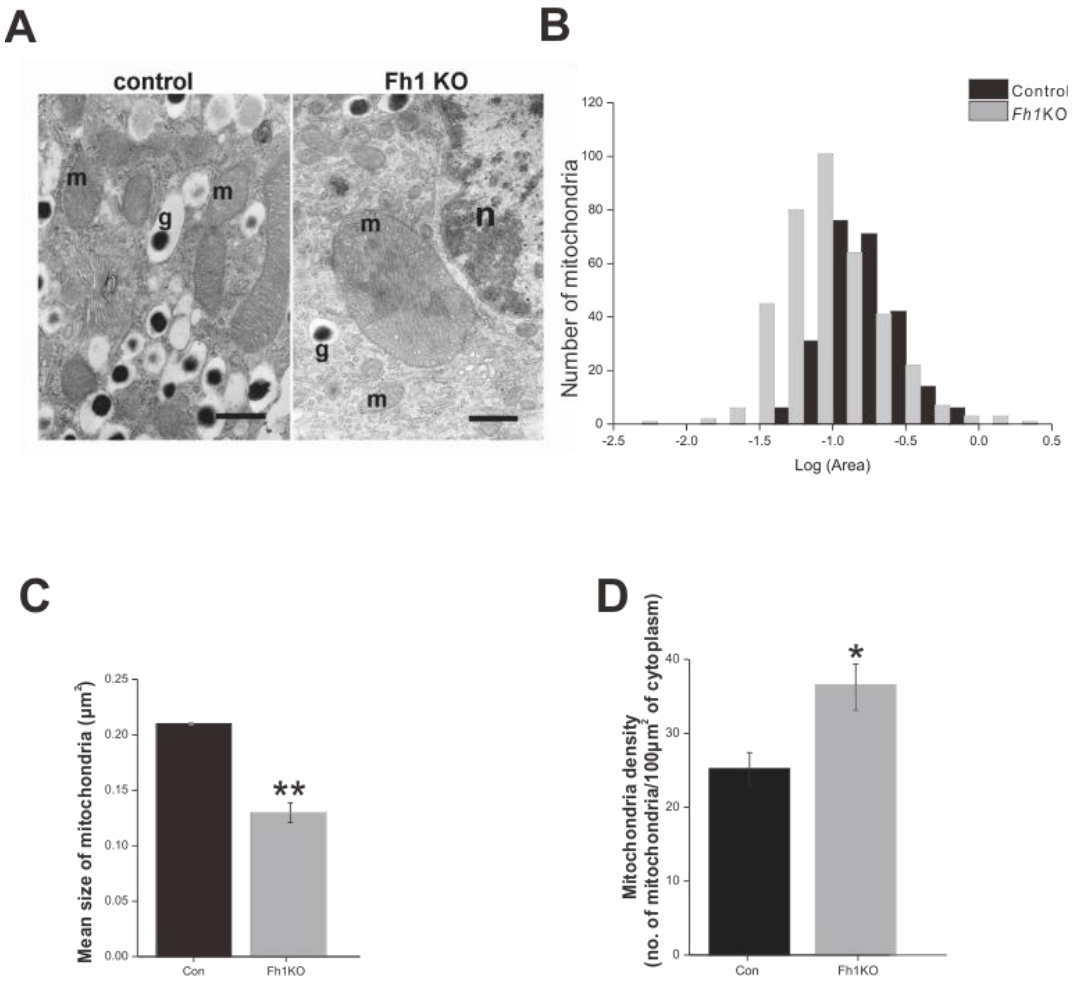


Figure 31. Ablation of *Fh1* alters the size distribution of mitochondria. (A) Representative EM pictures are shown to demonstrate the presence of abnormally large and small mitochondria in *Fh1*$^{-/-}$ β-cells. Abbreviations used: m, mitochondria; g, granules; n, nucleus. Scale bar: 500 nm. Experiments were guided by Dr A Clark. (B) The size distribution of mitochondria in control (black) and *Fh1*KO (grey) is presented on a logarithmic scale. The size distribution is significantly different ($p<0.005$; Kolmogorov–Smirnov test). (C) *Fh1*$^{-/-}$ β-cells exhibit lower average size of mitochondria, but (D) higher density of mitochondria per 100 μm^2 of cytoplasm. Values are means ± SEM (* $P<0.05$, ** $P<0.005$; Student's *t*-test). Data was analysed from 17 and 18 cells from 5 islets of control and *Fh1* KO, respectively.

6.2.5 GSIS in *Fh1*$^{-/-}$ islets is rescued by re-expression of *FH*

The human orthologue *FH* gene was introduced into both cytoplasm and mitochondria of *Fh1*KO mice (full-length rescue mice). These rescue mice were, unlike *Fh1*KO mice, normoglycaemic during an intraperitoneal glucose tolerance test (IPGTT), while *Fh1*KO mice exhibited a 3-fold increase in glycaemia as compared to the control (Figure S4). Control transgenic mice (normal littermate with *FH* cDNA) were also tested to demonstrate no side effect of *FH* cDNA insertion in terms of glucose regulation.

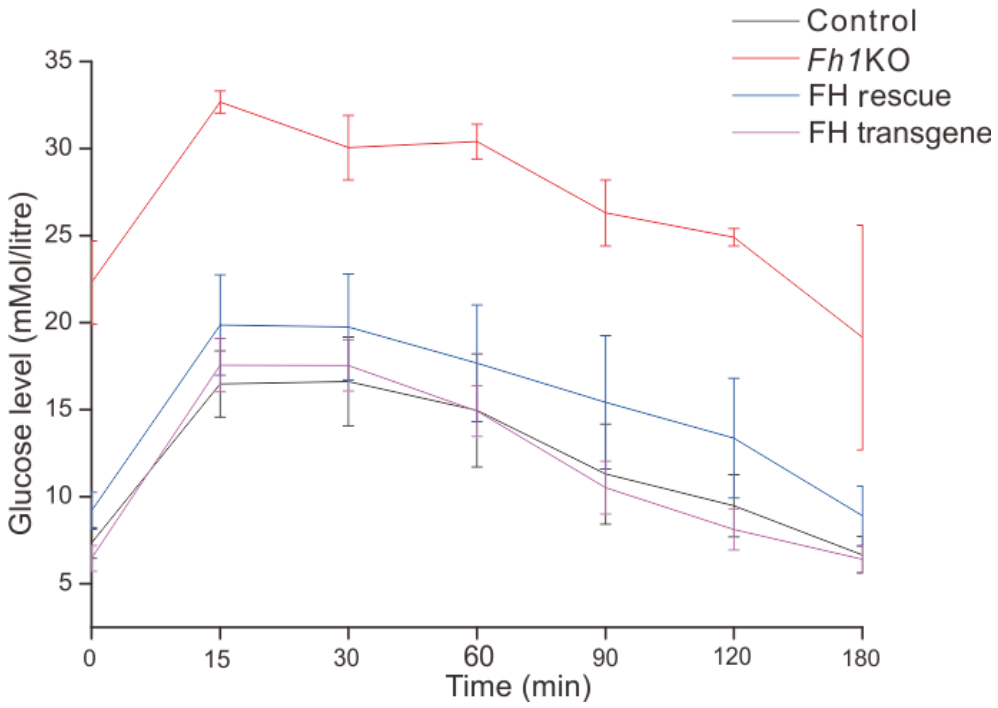


Figure S4. Rescue of *Fh1*KO by human *FH*. IPGTT (2.0 g of glucose/kg bodyweight) were performed in littermate control mice *Fh1*$^{+/+}$ (Control; black), *Fh1*$^{-/-}$ mice (*Fh1*KO; red), *Fh1*$^{-/-}$ X *FH*$^{+/+}$ mice (FH rescue; blue) and *Fh1*$^{+/+}$ X *FH*$^{+/+}$ (FH transgene; purple) mice aged between 18-27 weeks (n=5 for control and FH transgene, n=3 for *Fh1*KO, and n=6 for FH rescue). The difference at all points are significantly between control and *Fh1*KO ($P<0.05$ at 0, 30, 60, 90 min and $P<0.005$ at 15 and 120 min; Student's *t*-test), except at 180 min. For FH rescue vs *Fh1*KO, all points are significantly different ($P<0.05$),

except at 180 min. Values at each time point are means ± SEM. Experiments performed by Dr J Adam.

Our analysis of the effects of ablating *Fh1* on $[Ca^{2+}]_i$ indicated subtle – but statistically significant – effects (Figure 28B). As shown in Figure 32, the introduction of the human *FH* gene into *Fh1*$^{-/-}$ pancreatic islets led to a complete normalisation of the $[Ca^{2+}]_i$ responses to glucose (12 and 20 mmol/l) and tolbutamide (0.2 mmol/l).

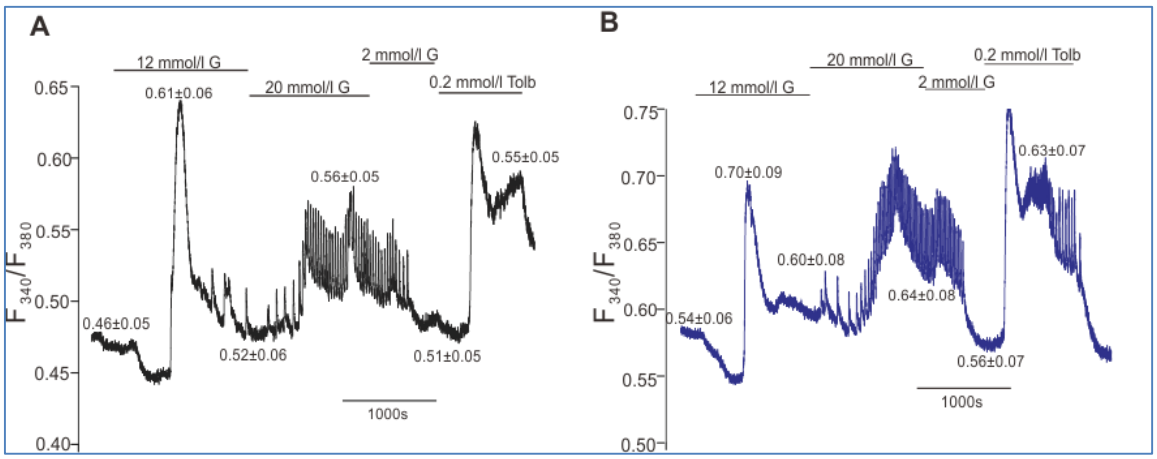


Figure 32. No difference in intracellular β-cell $[Ca^{2+}]_i$ between control (black; left) and rescue (blue; right) islets. Glucose (G) (12 and 20 mmol/l) and tolbutamide (Tolb) (0.2 mmol/l) were introduced as indicated (top). The basal glucose concentration was 2 mmol/l. Experiments were performed in isolated islets from control (*Fh1*$^{+/+}$; A) and rescue (*Fh1*$^{-/-}$ X *FH*$^{+/+}$; B) mice. Representative traces are shown for each group. $[Ca^{2+}]_i$ is expressed as the F_{340}/F_{380}-ratio and values given above the traces are mean ± SEM (8 islets isolated from n=3 mice for both genotypes).

6.2.6 Exogenous glutamate improves insulin secretion in *Fh1*$^{-/-}$ islets

A detailed metabolomics analysis revealed severe abnormalities of amino acid metabolism in *Fh1*$^{-/-}$ islets. Whereas glucose increased the content of all except one of 16 amino acids analysed. For example, the islet content of glutamate increased by ~100%. By contrast, in *Fh1*$^{-/-}$ islets, glucose had much smaller effects on islet amino acid levels: some amino acids did not increase at all or even decreased upon glucose stimulation. For example, the islet levels of asparate were reduced by 50% and glutamate did not change. Glutamate has been suggested to be a mitochondrial messenger that mediates the amplifying effect of glucose on insulin secretion (Maechler and Wollheim, 1999).

Insulin release from pancreatic islets of control and *Fh1*KO mice was measured in static incubation. In control islets, the elevation of glucose from 2 to 20 mmol/l resulted in an 8-fold stimulation of insulin secretion, but this effect was limited to a 3-fold stimulation in *Fh1*$^{-/-}$ islets (in agreement with the perfusion data discussed above). Supplementing the extracellular medium containing 20 mmol/l glucose with 5 mmo/l of the cell permeable dimethyl L-glutamate completely restored insulin secretion in *Fh1*$^{-/-}$ β-cells (Figure S5). No significant effect of glutamate was observed in the control islets.

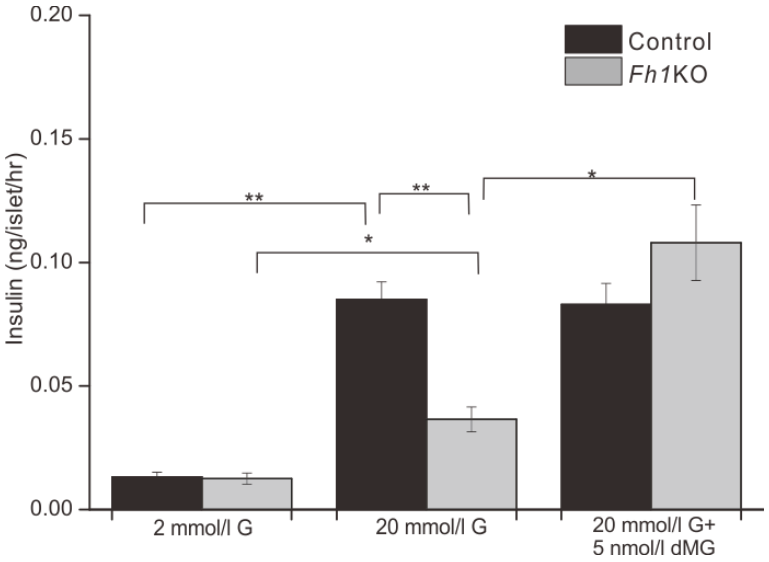


Figure S5. Improvement of impaired GSIS in *Fh1*$^{-/-}$ islets by membrane-permeable L-glutamate. Insulin secretion measured during static incubations performed at 2 and 20 mmol/l glucose (G) in the absence or presence of 5 mmol/l of dimethyl L-glutamate (dMG) in control (black) and *Fh1*$^{-/-}$ islets (grey). Data are mean values ± SEM of 12 experiments across n=4 mice per genotype (**P<0.005, *P<0.05; Student's t-test). Experiments performed by Dr R Ramracheya.

6.3 Discussion

Certain metabolites have been implicated in facilitating transformation of cells to malignancy (Thompson, 2009, Schulze and Harris, 2012). For example, somatic mutations in a metabolic enzyme isocitrate dehydrogenase (which catalyses the conversion of isocitrate to α-ketoglutarate) (Dang et al., 2009) makes cells more vulnerable to transformation by disruption of epigenetic regulation (Xu et al., 2011) and suppression of astrocytes differentiation (Lu et al., 2012), resulting in human brain cancers. Here we demonstrate that *Fh1*, in addition to being an oncogene (Yang et al., 2013) that can trigger HLRCC, also plays a key regulatory role in GSIS.

Genetic deletion of *Fh1* resulted in severe hyperglycaemia (Figure S4), which was correlated with a dramatic reduction of GSIS (Figure S2 and Figure S5). Since the incretin hormone GLP-1 is currently being used to treat T2D (Todd and Bloom, 2007, Gejl et al., 2012), it was interest of us to test the rescue potential of the drug. However, the secretory defect could not be corrected by GLP-1.

Given the important role of FH in glucose metabolism and mitochondrial ATP production, ultimately affecting GSIS, we anticipated that it would be fairly straightforward to explain the diabetic phenotype of *Fh1*KO mice: ablation of *Fh1* would be expected to impede the Krebs cycle, resulting in lowered ATP production, reduced K_{ATP} channel closure, and subsequent decrease of $[Ca^{2+}]_i$ leading to disrupted exocytosis. It was therefore unexpected to find that, despite the strong reduction of GSIS, the glucose-induced increases of $[Ca^{2+}]_i$ in *Fh1*$^{-/-}$ islets were nearly as large as in control islets (Figure 28). This suggests that *Fh1* is not required for glucose sensing in β-cells, but acts rather as an amplifying factor. Moreover, glucose increased islet ATP content in *Fh1*KO mice

to essentially the same amount as compared to the control (Figure S3) and, glucose metabolism (measured both as glucose utilisation and glucose oxidation (Malaisse and Sener, 1988, Vanhoutte et al., 1995)) was normal in *Fh1*$^{-/-}$ islets (E Rebelato, personal communication). We also considered whether ablation of *Fh1* might somehow interfere with the exocytotic machinery, but again the data were negative; Ca^{2+}-entry (Figure 29) as well as depolarisation-evoked exocytosis remained fully operational in *Fh1*$^{-/-}$ cells (Figure 30).

It should be kept in mind that *Fh1* is a tumour suppressor gene. Cancer cells undergo reprogramming of their normal cellular metabolism to switch to an anabolic metabolism in order to support the growth and proliferation of their daughter cells. ATP production through cellular respiration therefore becomes secondary to the synthesis of macromolecules (proteins, lipids and nucleic acids), but this does not mean that ATP production is impaired. Indeed, most cancer cells do not exhibit impaired ATP production (Vander Heiden et al., 2009, Schulze and Harris, 2012). This may explain why *Fh1*$^{-/-}$ β-cells ensure normal ATP production without a fully functional Krebs cycle.

The modest increase of glucose utilisation in *Fh1*$^{-/-}$ islets excludes the possibility that strong stimulation of glycolysis compensates for the loss of ATP production during the Krebs cycle. However, majority of mitochondrial ATP production occurs proximal to fumarate. Given that fumarate can leave the mitochondria, the Krebs cycle may continue to operate at sufficient speed to account for the nearly normal rates of glucose oxidation and ATP production. The exit of fumarate out of the mitochondria is likely mediated by the mitochondrial dicarboxylate carrier (also known as *Slc25a10*). This may be functionally significant because it predicts that there will be a loss of the Krebs cycle

reactants for every pyruvate entering (unless cytosolic metabolites derived from fumarate can re-enter the mitochondria) and the loss must be replenished by anaplerosis. This is brought about by deamination of amino acids, many of which contain the carbon backbone of the Krebs cycle reactants. For example, the oncogenic transcription factor *Myc* is activated to promote the expression of glutaminase to catalyse the deamination of glutamine. This would ensure the steady supply of NH_4^+ for nucleotide synthesis and α-ketoglutarate to fuel the Krebs cycle to maintain the supply of reduced energy that is later converted for ATP production (Figure 33) (DeBerardinis et al., 2007, Gao et al., 2009, Mullen et al., 2012).

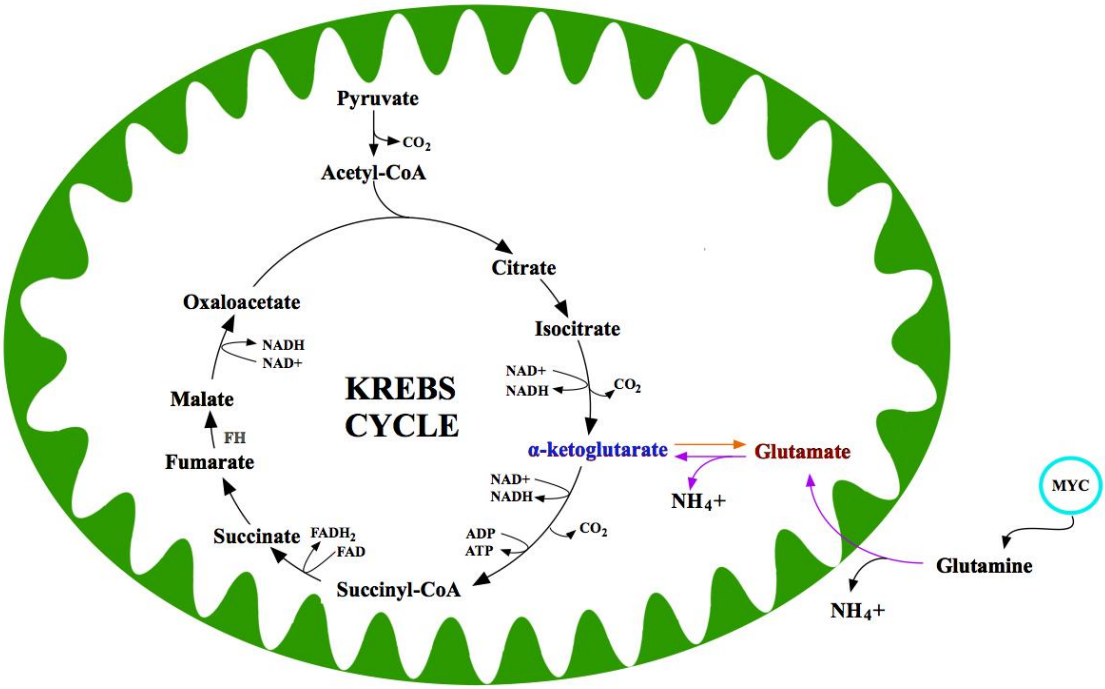


Figure 33. Glutamate involvements in both anaplerosis and cataplerosis during the Krebs cycle. The Krebs cycle intermediate α-ketoglutarate (blue) is used for biosynthesis of glutamate (orange arrows). This prevents the accumulation of the intermediates in the mitochondrial matrix which is called cataplerosis. The level of extracted α-ketoglutarate is maintained constant by glutamine catabolism (purple arrows) as part of anaplerosis to ensure a fully functional Krebs cycle. *MYC* plays a regulatory role in glutamine catabolism which provides nitrogen for the α-ketoglutarate biosynthesis (Modified from (Owen et al., 2002, Finley et al., 2013)).

It is therefore pertinent that in *Fh1*$^{-/-}$ islets, the amounts of all amino acids including glutamate are reduced as compared to WT islets (J Adam, personal communication). In control islets, some of the glucose-derived carbons are funnelled into the production of amino acids as part of cataplerosis. For example, alpha-ketoglutarate leads to the

production of the amino acid glutamate (Figure 33), which was previously postulated to mediate the amplifying effect of glucose on insulin secretion (Maechler and Wollheim, 1999, Gheni et al., 2014). In *Fh1*$^{-/-}$ β-cell, the entire amino acid metabolism is instead geared towards anaplerosis, and glucose therefore fails to increase intracellular glutamate levels with resultant loss of the amplifying action of glucose. Indeed, we found that the insulin secretion defect seen in *Fh1*$^{-/-}$ islets was corrected by supplementing the extracellular medium with membrane-permeable dimethyl L-glutamate whilst having no effect in control islets (Figure S5). The latter observation argues that the effect of dimethyl L-glutamate is not an unspecific one. This scenario explains how glucose metabolism, ATP production and $[Ca^{2+}]_i$ homeostasis all remain essentially normal in *Fh1*$^{-/-}$ islets and yet GSIS is severely impaired.

Fragmentation of mitochondria can occur as a consequence of chronic hyperglycaemic conditions (Yu et al., 2006). It is considered to be a way to deal with the overflowing metabolites such as pyruvate, by increasing their total surface area and thus allowing easy access. This is reminiscent of the preponderance of small mitochondria in *Fh1*$^{-/-}$ β-cells (Figure 31). Thus, it is an interesting possibility that the 'fragmentation' is an adaptive mechanism to decrease the volume/surface area ratio to facilitate exchange between the mitochondria and the cytosol during hyperglycaemia. Moreover, mitochondrial fragmentation may be due to an imbalance in the redox state. Pancreatic β-cells are particularly suited to use the redox as a signal for insulin secretion (Leloup et al., 2011) but are equally vulnerable to excessive oxidative stress as their antioxidant defences in β-cells are up to 80 times lower than in the liver (Tiedge et al., 1998). When mouse islets are exposed to dangerous levels of glucose and fatty acids (Molina et al., 2009), this production of mROS can lead to oxidative stress, a feature associated with disruptions in

the mitochondrial network and insulin secretion (Leloup et al., 2009). It has recently been shown that *Fh1*$^{-/-}$ human cancer cells lose antioxidant properties. When *Fh1* is deleted, accumulated fumarate form a succinated glutathione which competes with glutathione dimers for NADPH, thereby lowering the capability of reduced glutathione to maintain the cellular redox state (Sullivan et al., 2013).

In agreement with the previous *Fh1*$^{-/-}$ phenotype (Pollard et al., 2005, Adam et al., 2011, DeNicola et al., 2011), ablation of β-cell specific *Fh1* has resulted in a 60-fold increase of fumarate (at the whole-islet level) (J Adam, personal communication). As a consequence, succinated glycolytic enzyme GAPDH was observed (J Adam, personal communication), which closely resembles the demonstrated inactivation of *Gapdh* due to fumarate-mediated succination in the muscle of diabetic rats (Blatnik et al., 2008a). It is important to note that a cross-talk has been observed in *Fh1*$^{-/-}$ cancer cells between the cytosolic urea cycle and mitochondria. The accumulated fumarate leaves the mitochondria and participates in the production of the urea cycle metabolites argininosuccinate (potential urine biomarker for HLRCC) (Zheng et al., 2013). This implies that the excessive fumarate in β-cell specific *Fh1*$^{-/-}$ islets may similarly shuttle via mitochondrial transporters into other cytosolic compartments, exposing many proteins for succination. Further investigation in succinated proteins is therefore required to evaluate their functional consequence(s).

CHAPTER 7

Age-dependent alterations of insulin and glucagon secretion in mouse and human pancreatic islets

7.1 Introduction

Ageing is an important risk factor for T2D. There is a strong correlation between age and the prevalence of T2D (Figure 34)(International Diabetes Federation, 2013, Diabetes UK, 2014).

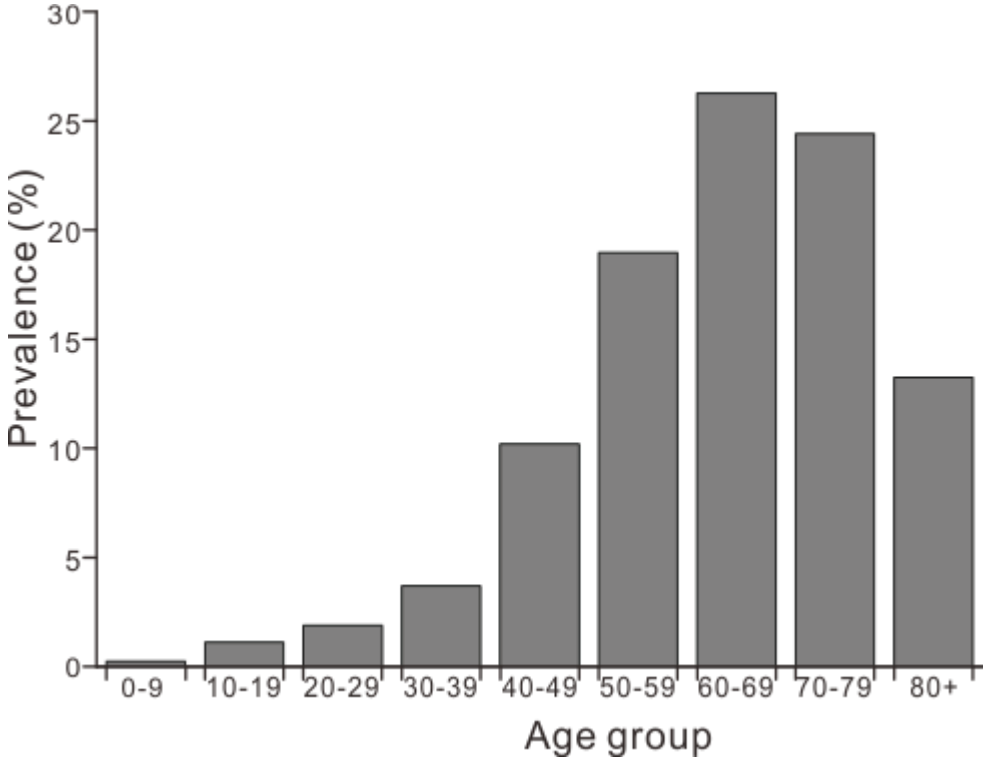


Figure 34. Prevalence of T2D in the UK. A positive correlation between age and the incidence of T2D is observed up to the age of 69.- Modified from (Diabetes UK, 2014).

There are variable reports on the impact of age in β-cell function (Montanya et al., 2000, Wang et al., 1988) and insulin action (Basu et al., 2006). Therefore, the causal mechanism linking age to increased T2D risk remains unclear. Here, some of these divergent findings will be reviewed.

Glucose uptake in mouse pancreatic β-cell is mainly mediated by Glut2. Hyperglycaemia has shown an association with a reduced expression of the gene, *SLC2A2* (which encodes Glut2). This ultimately diminishes GSIS (Thorens et al., 1990, Ohtsubo et al., 2005). One study similarly reported an age-dependent decrease in Glut2 expression in isolated islets from 22-month-old C57BL/6N mice. The mice were associated with defective insulin secretion (Ihm et al., 2007). However, human β-cells utilise GLUT1 for glucose uptake (McCulloch et al., 2011)

Mitochondria play a central role in coupling β-cell glucose metabolism and insulin secretion. Once glucose enters pancreatic β-cells, it undergoes a series of chemical reactions to produce ATP in mitochondria (Figure 26 in Chapter 6). Mitochondrially-derived ATP closes K_{ATP} channels and causes depolarisation, which then leads to the exocytosis of insulin secretory granules (Figure 3 in Chapter 1). In diabetic rodents, abnormal mitochondrial morphology, mitochondrial membrane potential (Lu et al., 2010, Maechler et al., 2010) and increased numbers of mitochondrial DNA (mtDNA) mutations (Kadowaki et al., 1994) have been reported. T2D patients also exhibit impaired ATP production (Anello et al., 2005). An age-dependent decline of mitochondrial function may account for the early observation that the decrease of GSIS in 24-months-old rats correlated with inadequate membrane depolarisation of the β-cells (Ammon et al., 1987), possibly via impaired closure of the K_{ATP} channels. Indeed, a reduced capacity of glucose to inhibit ^{86}Rb efflux (a proxy for K^+ efflux) was observed. There is also a negative correlation between the quantity of mtDNA and age in human islets during senescence (Cree et al., 2008). Berggren and colleagues recently reported a defective mitochondrial function in aged mice, although only a mildly reduced $[Ca^{2+}]_i$ handling was observed (Li et al., 2014b). However, in a paper published during the same month by the same team

of investigators, the increased diabetes risk was instead attributed to reduced insulin permeability of the islet capillaries, and the insulin secretory capacity was in fact greater in islets isolated from 17 months old mice relative to the younger animals (2 months old) (Almaca et al., 2014).

Divergent results have also been reported in human studies. One study reported an inhibitory effect of ageing on insulin secretion (Ihm et al., 2006), while a contradictory study failed to demonstrate such an effect, and actually demonstrated that the insulin secretory capacity increased with age (Almaca et al., 2014).

Previous studies clearly have highlighted the complexity of the interaction between ageing and β-cell functions. Therefore, the cellular mechanisms underlying the impact of ageing on GSIS requires further validation. Here, we re-examined the effect of ageing on GSIS in both mice and humans. An additional aim was to determine the impact of age on glucagon secretion, which provides a new insight about the age-dependent alterations in pancreatic α-cell function.

7.2 Results

7.2.1 No effect of ageing on GSIS in mouse islets

The amount of insulin was measured in isolated islets from mice aged 3, 11 and 24 months. Upon stimulation with 6 mmol/l glucose, only the youngest mice responded with increased GSIS (+60%). However, a sharp increase in insulin secretion was observed when islets were stimulated with 20 mmol/l glucose (Figure 35A). In fact, a positive correlation between the age of mice and the amount of insulin secreted was found; in the youngest mice, we observed a 12-fold increase compared with basal secretion, whereas a higher stimulatory effect (>15-fold increase) was shown in the oldest mice (Figure 35A). A similar trend was shown when insulin secretion is expressed as a percentage of the total insulin content (Figure 35B). When compensated for insulin content, a decrease in insulin secretion at 6 mmol/l glucose was observed between 3 and 11 months (Figure 35C). Furthermore, there was a tendency towards increased basal secretion (at 1 mmol/l glucose) between 11 and 24 months ($P<0.051$). The islet content was essentially the same between the youngest and the oldest mice (49 vs. 42 ng/islet, respectively), but a 25% increase was observed between 3 and 11 months that was followed by a corresponding decrease between 11 and 24 months (Figure 35C).

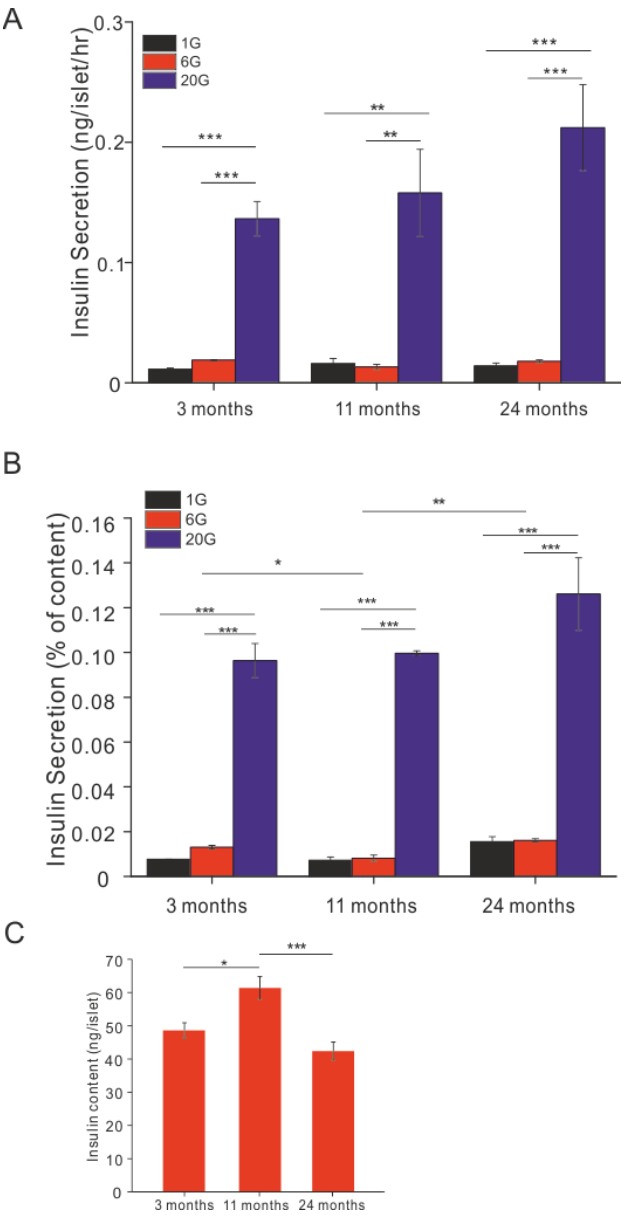


Figure 35. Impact of age on GSIS in mouse pancreatic islets. (A) Insulin secretion is expressed as ng insulin released per islet per hour in isolated islets at 1 (black bars), 6 (red bars) and 20 (blue bars) mmol/l glucose in mice aged 3, 11 and 24 months. Data are mean values ± SEM of 9-15 experiments using islets from n=3 mice. *p<0.05, **p<0.01 and ***p<0.001 for the indicated comparisons as determined by ANOVA and Tukey's tests. (B) As in (A), but secretion is expressed as a percentage of the islet insulin content. (C) Islet insulin content at 3, 11 and 24 months of age. Data are mean values ± SEM of 9-15 experiments using islets from n=3 mice. *p<0.05 and ***p<0.001 for the indicated comparisons as determined by ANOVA and Tukey's tests.

7.2.2 Normal calcium homeostasis in old mice

Activation of L-type Ca^{2+} channels is a pre-requisite for GSIS in mouse β-cells, which subsequently increases $[Ca^{2+}]_i$. Therefore, we examined the effect of age on $[Ca^{2+}]_i$ by ratiometric calcium fluorimetry using fura-2 AM. Islets isolated from 3- and 24-months-old mice were exposed to 1 and 20 mmol/l glucose. Basal, the initial glucose-induced peak and steady-state $[Ca^{2+}]_i$ at high glucose were similar in young and old mice (Figure 36 A-C). In the presence of the high glucose concentration, $[Ca^{2+}]_i$ increased to a plateau, on which the level of $[Ca^{2+}]_i$ oscillated with a periodicity that was ~10s in islets from both young and old mice (Figure 36 A-B insets and D; statistically not significant). The effects of high glucose were reversed promptly when the glucose level was lowered to 1 mmol/l.

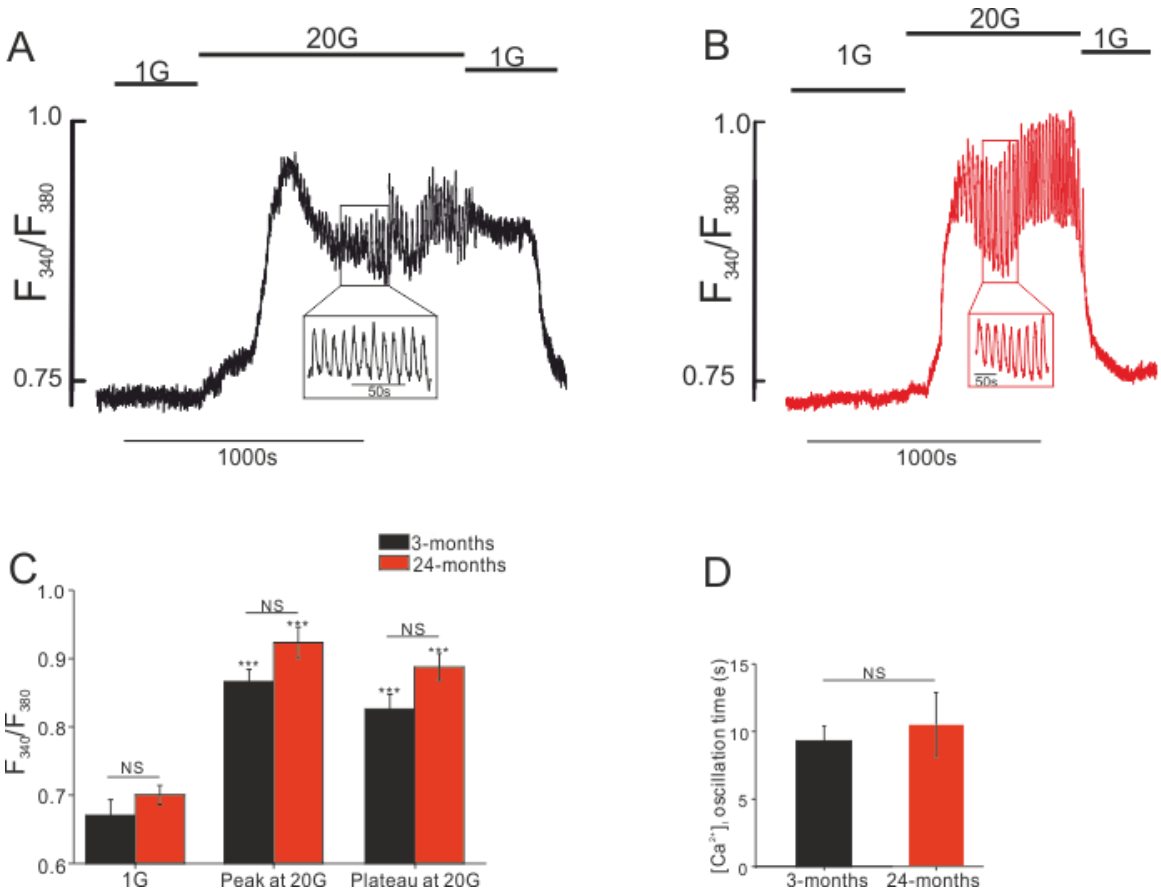


Figure 36. Impact of age on glucose-stimulated increases in cytoplasmic $[Ca^{2+}]_i$ in mouse β-cells. (A - B) Representative traces of ratiometric measurements of cytosolic calcium in β-cells/islets from young (3-months-old; black) and old (24-months-old; red) mice. Glucose (G) was increased from 1 to 20 mmol/l glucose and then reduced to 1 mmol/l glucose. Insets show oscillations superimposed on a plateau at an increased time scale. $[Ca^{2+}]_i$ is reported as the F_{340}/F_{380} ratio (R). (C) Histograms comparing R at 1 mmol/l glucose and the peak, as well as sustained R, in the presence of 20 mmol/l glucose. ***p<0.001 for comparisons to their respective basal R (Student's *t*-test). NS implies no significance for the indicated comparisons. (D) Histogram comparing $[Ca^{2+}]_i$ oscillation speed triggered by 20 mmol/l glucose. NS implies no significance for the indicated comparisons (Student's *t*-test). Data are mean values ± SEM of 10 islets from n=3 young and 9 islets from n=2 old mice.

7.2.3 GSIS increases with age in human islets

Human islets from non-diabetic donors were assessed for GSIS in response to 1, 6 and 20 mmol/l glucose. We grouped the data according to 4 age groups: ≤39 (20-39), 40-49, 50-59, and 60-69 years of age. It is important note that median BMIs of each age group are 28 (20-39 range), 28 (23-36 range), 30 (22-39 range) and 28 (22-34 range), respectively.

Unlike mouse islets, human islets demonstrated clear increases in insulin secretion in the presence of 6 mmol/l glucose. There was a tendency towards increased insulin secretion in response to 6 mmol/l glucose with age (Figure 37 A-C). In the presence of 20 mmol/l glucose, a similar positive impact on insulin secretion was observed with age ($P<0.05$). There was also a significant age-dependent increase in basal secretion: moderate at <60 years but more pronounced in the highest age group ($P<0.05$).

We also analysed the data with respect to the insulin content (% of the total insulin content). An age-dependent increase in insulin secretion was again observed (Figure 37 D-F). There were no significant differences in the insulin contents between different age groups (Figure 37G).

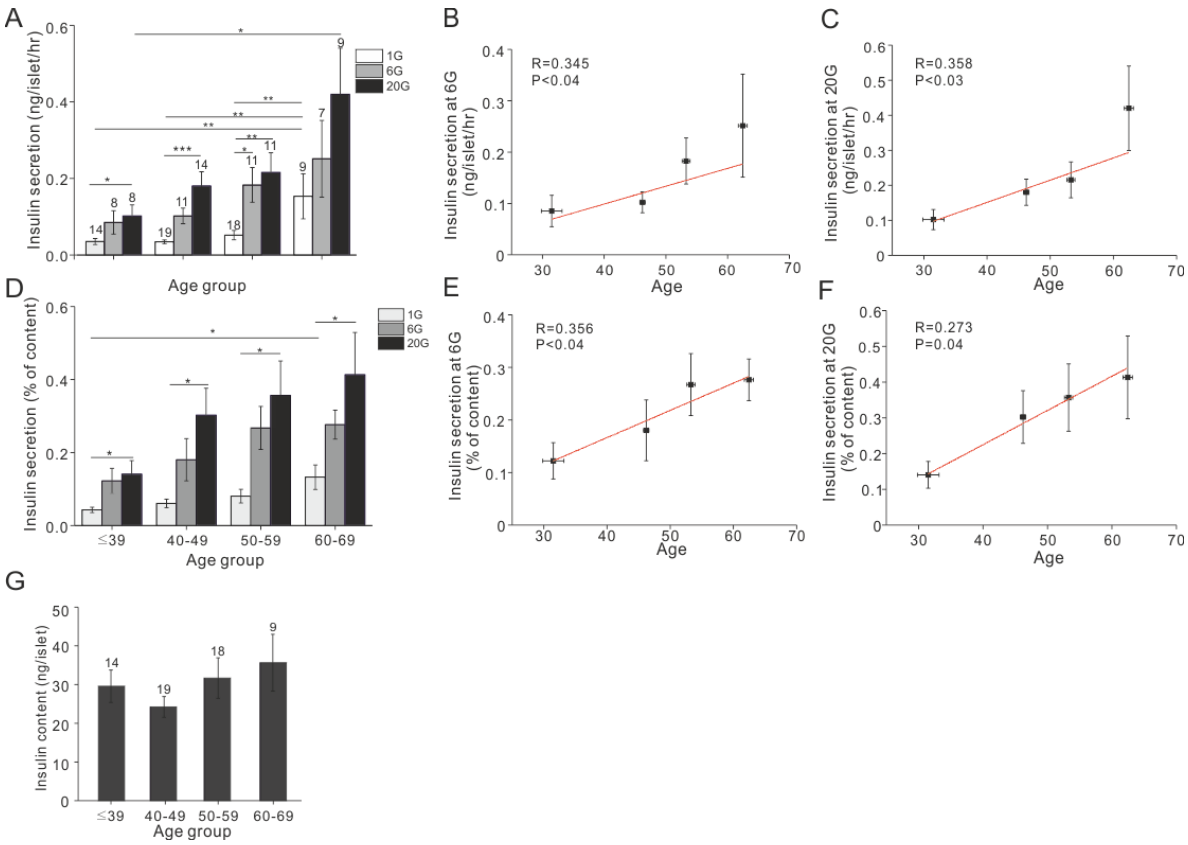


Figure 37. Impact of age on GSIS in human pancreatic islets. (A) Insulin secretion at 1 (white), 6 (grey) and 20 (black) mmol/l glucose in human islets obtained from organ donors aged ≤39 (20-39), 40-49, 50-59 and 60-69 years of age. Data are expressed as ng insulin released per islet per h and are mean values ± SEM using islets from the indicated number of donors (numbers above bars). *p<0.05, **p<0.01 and ***p<0.001 for the indicated comparisons as demonstrated by ANOVA and Tukey's tests. (B - C) The relationship between the amount of insulin released in response to 6 (B) and 20 (C) mmol/l glucose and the age of the donors. Pearson's correlation coefficient (R) and P values assessing the significance of the relationship are indicated in the diagrams. The statistical analysis was conducted based on the individual data. For display purposes, the data have been grouped in quintiles. The red line represents the least-squares fit to all data. (D) As in (A), but secretion is expressed as % of the total islet insulin content. (E - F) As in (B - C), but the comparison was performed using secretion values expressed as a % of the total islet insulin content. (G) Islet insulin content in the indicated age groups. Data are mean values ± SEM of 2-3 experiments using islets from the indicated number

of donors (numbers above bars); the results for the different age groups were not statistically different according to ANOVA and Tukey's tests.

7.2.4 Age-dependent decrease in the inhibitory effect of glucose on glucagon secretion in human islets

Age-dependent glucagon secretion was examined in the same sets of human islets. Glucagon secretion was measured at 1, 6 and 20 mmol/l glucose. Increasing glucose concentrations exerted an inhibitory effect on glucagon secretion across the age groups (Figure 38A). Glucagon secretion in the presence of 6 and 20 mmol/l glucose was lower than that at 1 mmol/l glucose. Of note, in agreement with previous reports (Ramracheya et al., 2010, Salehi et al., 2006), 6 mmol/l glucose, at which the paracrine effects of insulin are limited, induced a stronger glucagon inhibition than 20 mmol/l glucose. However, we did not find any statistically significant differences in the presence of 6 mmol/l glucose compared with basal secretion levels, except in the ≤39 and 50-59-year-old groups (Figure 38A).

The rate of glucagon secretion showed a wide range from a limited number of samples. For example, in the 40-49-year-old group, the responses in the presence of 6 mmol/l glucose ranged from 0.6 to 8.5 pg/islet/h.

To compensate for this variability, we normalised the glucagon secretion to the respective basal responses. We then found a significant inhibitory effect of both 6 and 20 mmol/l glucose, except in the 60-69-year-old group (Figure 38B). Stronger inhibition by 6 mmol/l glucose was again observed, which was statistically significant compared with 20 mmol/l glucose. The relative inhibitory effect of 6 and 20 mmol/l glucose declined with age (Figure 38B). Thus, glucagon secretion in islets from the youngest donors was reduced by 60% and 30% at 6 and 20 mmol/l glucose, respectively. In the oldest age group, glucose showed very limited inhibitory capacities (20 and 0% at 6 and 20 mmol/l

glucose, respectively). To analyse this further, we plotted the ‘glucagon release index’ (glucagon secretion at 1 mmol/l glucose divided by that at 6 mmol/l) in all 45 human islet preparations (Figure 38C). It is important to note that 3 out of 45 human preparations exhibited an inversed response with a glucagon secretion index <1 (indicating that 6 mmol/l glucose stimulated rather than inhibited glucagon secretion). The glucagon contents of the human islets remained more or less constant across the age groups ranging from 600–850 pg/islet (Figure 38D).

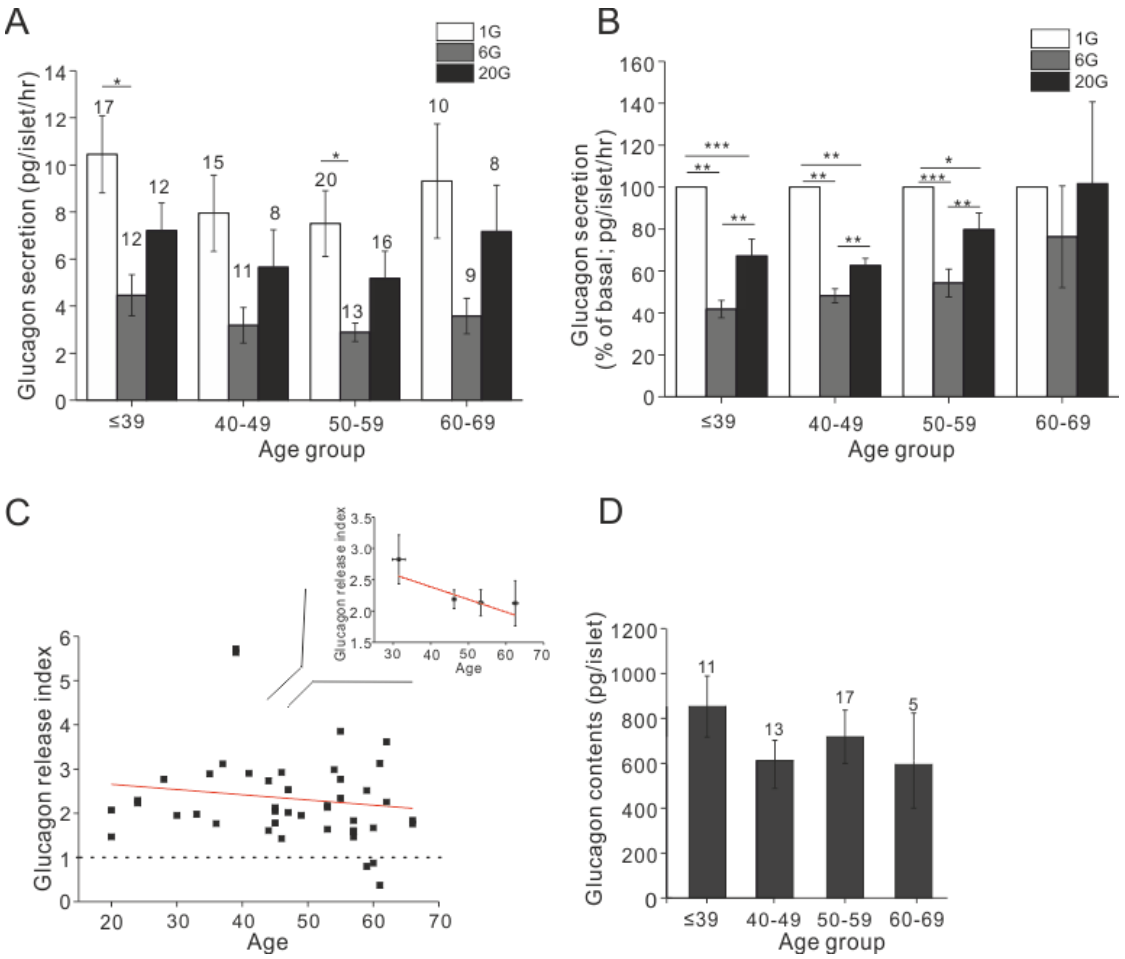


Figure 38. Impact of age on glucose-induced suppression of glucagon secretion in human pancreatic islets. (A) Glucagon secretion at 1 (white), 6 (grey) and 20 (black) mmol/l glucose in human islets obtained from organ donors aged ≤39 (20-39), 40-49, 50-59 and 60-69 years of age. Data are expressed as pg glucagon released per islet per h and are mean values ± SEM of 2-3 experiments using islets from the indicated number of donors (numbers above bars); *P<0.05 as determined by ANOVA and Tukey's tests. (B) As in (A) but glucagon secretion at 6 and 20 mmol/l glucose was normalised to the respective basal secretion (1 mmol/l glucose); statistically significant differences, as determined by ANOVA and Tukey's tests, are indicated (*p<0.05, **p<0.01 and ***p<0.001). (C) The relationship between donor age and the glucagon release index (glucagon secretion at 1 mmol/l glucose/glucagon secretion at 6 mmol/l glucose). The dotted horizontal line indicates a stimulation index of 1. Of note, 3 of the 45 preparations have a stimulation index of <1, indicating that glucagon secretion is inappropriately reduced by increasing glucose concentrations. The inset shows a summary of the relationship. Pearson's

correlation coefficient was -0.141 ($p<0.34$). (D) Islet glucagon content in the indicated age groups. Data are mean values ± SEM of 2–3 experiments using islets from the indicated number of donors (numbers above bars); no statistically significant differences were found using ANOVA and Tukey's tests.

7.3 Discussion

Ageing in T2D pathogenesis is generally known to cause two main defects (Evans and Farrell, 2011): impairment of insulin secretion from pancreatic β-cells and/or insulin resistance in the target organs. Indeed, the elderly are insulin resistant, which undoubtedly contributes to the aetiology of T2D (Petersen et al., 2003, Imamura et al., 2013). However, with regards to the impact of ageing on the capacity of the β-cells to secrete insulin, widely discrepant data have been reported.

We first measured GSIS in three groups of mice: young (3-months-old), middle-aged (11-months-old) and old (24-months-old). The mice described herein were C57BL/6J, which were obtained from the Jackson Laboratory. The average life-span of this particular strain is around 22-25 months (The Jackson Laboratory, 2015). Thus, the mice we used are clearly of advanced age, which should enable detection of any age-dependent decline in islet function.

Previous reports variably suggest either a negative (Li et al., 2014b, Ihm et al., 2007) or positive (Almaca et al., 2014, Gumbiner et al., 1989) impact of ageing on GSIS in mice. We observed no deteriorating effect of ageing on GSIS. In fact, the amount of inulin release increased with age in response to high glucose levels (Figure 35A).

We observed an increase and then a decrease in insulin content between 3-months-old and 11-months-old mice (Figure 35C). Such an increase was also observed in rodent models where the β-cell mass continuously increased until full maturity, which is estimated to be around 12-months of age (Montanya et al., 2000). The decline that occurred between 11 and 24 months may be explained by a reduced rate of β-cell

proliferation after 12 months (Teta et al., 2005), an effect that would be compounded by the relative hyper-secretion of insulin in the older mice. However, it is important to note that there was no statistically difference between the insulin contents of islets isolated from young and old mice.

$[Ca^{2+}]_i$ plays a prominent role in regulating β-cell stimulus-secretion coupling. For our assessment in 24-months-old mice, there were no age-related changes in $[Ca^{2+}]_i$ compared to young mice (Figure 36C). Berggren and colleagues recently reported an age-induced attenuation in $[Ca^{2+}]_i$ as a reason for the reduced GSIS (Li et al., 2014b). However, their own data are contradictory. The initial peak of $[Ca^{2+}]_i$ upon high glucose exposure actually appeared to be ~10 % higher in 20-months-old C57BL/6J mice than in young mice. During the plateau phase after the initial peak, the amplitude of the oscillation again appeared to be higher in the old mice. In both cases, these differences would account for an increased GSIS. They also measured the kinetics of $[Ca^{2+}]_i$ oscillations in the presence of 11 mmol/l glucose and showed very subtle difference in the aged mice. We similarly observed a slightly prolonged $[Ca^{2+}]_i$ oscillatory period in our old mice (Figure 36 A-B; insets), but this did not lead to a dramatically reduction of GSIS.

We were able to extend the rodent data to man by analysing a database that contains secretion data from a large number of human islet preparations. These analyses suggest that the pancreatic β-cells remain fully functional even at an advanced age (Figure 37). In fact, there is a trend towards increased insulin secretion with age. It is important to highlight that there is a marked increase in basal insulin secretion as the donors' age increases, implying insulin resistance. Unlike mouse islets, human islets responded to 6 mmol/l glucose with increased insulin secretion. Such a difference is due to the fact that

the threshold for insulin release in humans is 3 mmol/l (Henquin et al., 2006a, Braun et al., 2010) compared with a threshold of 6 mmol/l in mice (Hedeskov, 1980). In agreement with our own finding, one study found no negative impact on insulin secretion and, if anything, GSIS was enhanced. They examined GSIS in 82 human islet preparations, with donor ages ranging from 17 to 65 years (Almaca et al., 2014). In contrast, another study (Ihm et al., 2006) reported an age-dependent reduction in insulin secretion using a large cohort of 110 human islets. However, they used the glucose-stimulated insulin release (GSIR) index (the fraction of insulin secretion at 16.7 mmol/l glucose over insulin secretion at 1.7 mmol/l glucose), which was reduced due to a 2.6-fold increase in basal secretion. The insulin secretion in response to 16.7 mmol/l glucose was in fact ~15% higher in the elderly group. Thus, there appears to have been a strong bias to present the data in a way that would support the initial premise of the study that there is an age-dependent reduction of insulin secretion. This conclusion does not seem warranted from the authors' own data. In fact, a 'meta-analysis' of secretion studies by three independent groups (including our own) using a total of 255 human islet preparations indicates that there is no such effect.

Previous efforts almost exclusively focused on establishing the impact of ageing on insulin secretion and the effect on glucagon secretion (the second principal gluco-regulatory hormone of the body) has not attracted nearly as much attention. The data we present here suggest that an unexpected age-dependent decline in the capacity of glucose to suppress glucagon secretion (Figure 38). Impaired glucagon regulation is recognised as a main pathology of T2D and it exacerbates the hyperglycaemia resulting from insufficient insulin secretion (Cryer, 2002, Dunning et al., 2005). Up to the age of 50 years, glucose (6 mmol/l) inhibited glucagon secretion by ~60% relative that observed at

1 mmol/l glucose. The inhibitory action increasingly diminished to 50% in the 50-59-year-old group and to 20% in the oldest group (Figure 38B). A similar pattern was observed upon 20 mmol/l glucose exposure. In agreement with our study, Davidovic and colleagues reported ~20% higher glucagon secretion during an oral glucose tolerance test in the elderly, implying a lack of suppression by glucose. The elderly also exhibited higher basal glucagon secretion (Stevic et al., 2007).

The lack of inhibition is attributable to an inverted glucose response in some of the preparations. A similar phenomenon has been observed in 50% of the islets obtained from donors with T2D (Zhang et al., 2013). Importantly, an inverted response to glucose was only observed in the donors aged 59, 60 or 61, which accounted for 30% of the islet preparations from 'our' donors aged 59 or more (Figure 38C). This agrees well with the expected prevalence of T2D observed in the 60-69-year-old age group (Figure 34) (Diabetes UK, 2014) and it is possible that these islets were obtained from undiagnosed T2D individuals. In pancreatic α-cells, K_{ATP} channel activity tightly regulates glucagon secretion (Walker et al., 2011b, Rorsman et al., 2008). It is now known that T2D is associated with increased K_{ATP} channel activity, which can be corrected by low concentrations of sulphonylureas such as tolbutamide (Zhang et al., 2013, Rorsman et al., 2014). Furthermore, insulin resistance in the elderly was shown to be associated with a reduced resting mitochondrial oxidative capacity (Petersen et al., 2003, Szendroedi et al., 2007, Del Guerra et al., 2005). Therefore, we speculate that individuals with an inverted response to glucose have impaired mitochondrial function which culminates in a reduced ATP/ADP ratio and a slight increase in K_{ATP} channel activity, sufficient to induce β-cell-like response to glucose.

CHAPTER 8

Conclusion

8.1 Concluding remarks

T2D is a complex disease involving numerous pathways and genes. The work presented in this thesis dissects the pathophysiological basis of the diabetic phenotypes occurring in three novel T2D animal models, and it has demonstrated the central importance of mouse models in diabetes research.

This is the first time that the pathophysiological mechanism underlying defective insulin secretion in a genetic model of T2D has been associated with 'kiss-and-run' exocytosis. During kiss-and-run exocytosis, the granule lumen becomes (transiently) connected to the exterior via a narrow fusion pore. Using on-cell, single-vesicle capacitance measurements, we estimated the diameter of the fusion pore to be <2 nm. However, Tsuboi *et al.*, using fluorescently-tagged cargo proteins, reported the diameter of the fusion pore to be between 5 and 10 nm. Such an inconsistency arises because their protocol involved the use of fluorescent vesicle cargoes, such as monomeric red fluorescent protein (mRFP) (which has a diameter of ~4 nm) (Tsuboi et al., 2004). Thus, it could be argued that these authors were unable to resolve the opening of narrower fusion pores, and they underestimated the frequency of kiss-and-run events. This highlights the importance of validating a functional study measuring kiss-and-run exocytosis with an alternative technique(s). Thus, our studies integrated two different approaches to address possible discrepancies in kiss-and-run measurements: cell-attached patch clamp and optical techniques. As these two studies concur with one another, our kiss-and-run measurements were shown to be sufficiently accurate enough to draw the conclusion that disproportionate kiss-and-run exocytosis impairs granule fusions in *Sox4*mt β-cells, thereby inhibiting insulin release.

Interestingly, we observed in our preliminary analysis that prolonged exposure of free fatty acid (FFA) increased the rate of kiss-and-run exocytosis; fewer events (mainly full fusion) were detected by SRB, whilst there was no significant difference in VAMP-pHluorin (all exocytotic events) recordings in palmitate-treated islets. Notably, lipotoxicity reduces the exposure of the exocytotic machinery to $[Ca^{2+}]_i$ by disrupting the tight association between VGCCs and the Ca^{2+} sensor (Hoppa et al., 2009). This is sufficient to disrupt fusion events and reduce the magnitude of the capacitance increases triggered by physiological depolarisations. It may also provide a potential explanation of how lipids promote kiss-and-run exocytosis given its negative correlation with $[Ca^{2+}]_i$ (Leitz and Kavalali, 2011).

We showed that the *Sox4* mutation leads to a 3-fold increase in the frequency of kiss-and-run exocytosis and that 50-60% of the release events are aborted before full expansion of the fusion pore. We cannot entirely exclude that this is a consequence of the islets/β-cells being exposed to the diabetic milieu of the mutant mice (with a resultant elevation of plasma FFA levels). However, we think that it is likely to be secondary to the altered expression of key exocytotic protein resulting from the increased expression of *Sox4*. This raises the exciting possibility that stabilisation of the fusion pore represents a common pathophysiological mechanism of T2D that can be triggered by both genetic and environmental factors. It will be interesting to explore whether there is an increased expression of *Sox4* and *Stxbp6* under diabetogenic conditions such as hyperglycaemia and chronic elevation of plasma FFA levels.

Our SOX4 study illustrates that a battery of advanced cell physiological techniques combined with appropriate mouse models is essential to establish the link between genetics and β-cell dysfunction. Our study provides an example of how to proceed from a susceptibility gene to a diabetic phenotype, and eventually to the identification of the actual causal gene. Our findings reported here provide the first example in which impaired fusion pore expansion may be linked to a human morbidity. It is an exciting possibility that restoring full fusion is implicated as a potential therapy for T2D. The activation of PKC, which was initially implicated in long-term potentiation (Malinow et al., 1989), increases the rate of fusion pore openings in rodent adrenal chromaffin cells (Chen et al., 2005, Fulop and Smith, 2006). Interestingly, GLP-1, which is increasingly used in diabetes therapy and partially acts by a PKC-dependent mechanism (Shigeto et al., 2008) and it is therefore possible that part of its therapeutic action is mediated by an effect exerted at the level of the fusion pore.

In the second part of the thesis, the characterisation of the *Fh1*KO mouse phenotype (originally implicated as a cancer model) reveals the complex interplay between altered cellular metabolism and the disruption of GSIS. Our study has demonstrated the importance of glutamate as an elusive factor in the amplification of insulin signalling, and as a potential link between diabetes and cancer.

Many epidemiological studies have speculated on a possible link between diabetes and cancer (Huxley et al., 2005, El-Serag et al., 2006, Giovannucci et al., 2010). These studies indicate that diabetic patients have a higher risk of developing certain types of cancers, including cancers of the liver (Wang et al., 2012), kidney (Larsson and Wolk, 2011), and the pancreas (Ben et al., 2011) as well as the colon and rectum (Larsson et al., 2005).

It is important to note that these epidemiological studies cannot account for causation. On the basis of the Warburg effect, hyperglycaemia was presumed to support the propagation of cancer cells, as they require extra glucose to take the anaerobic respirational route, rather than the conventional aerobic pathway (Vander Heiden et al., 2009). In support of this hypothesis, the restriction of food and a lack of glucose have been shown to have an anti-neoplastic effect in rodent models (Patel et al., 2004). Interestingly, in clinical studies, the use of the anti-diabetic drug metformin, which suppresses hepatic glycogenolysis and increases glucose uptake by muscle, is beneficial in cancer treatment (Evans et al., 2005). However, this hypothesis is still unclear, as the biological basis of the data was not fully elucidated. Moreover, a clear correlation between the level of glucose and cancer initiation still needs to be determined. Given that β-cell-specific *Fh1*KO mice exhibit cancerous characteristics, such as metabolic reprogramming via anaplerosis (Owen et al., 2002, Vander Heiden et al., 2009) that is now identified as a hallmark of cancer (Hanahan and Weinberg, 2011), this novel mouse model may be used to study the precise pathophysiological mechanism linking the two diseases.

Using of a combination of electrophysiological and biochemical techniques, our investigation revealed *Fh1* KO mice to be a novel T2D model. However, it is important to carefully interpret the data by taking into consideration the limitations of the various techniques used in the investigation. In our study, the addition of exogenous glutamate was shown to rescue the insulin secretory defect in *Fh1*KO mice.

We ascertained that depolarisation-evoked exocytosis remained operational in *Fh1*$^{-/-}$ β-cells. Paradoxically, glutamate was found to work by enhancing insulin secretion, in general support of the role of glutamate as an amplifying signal (Maechler and Wollheim, 1999, Gheni et al., 2014). To understand these seemingly discrepant data, we need to carefully consider the difference(s) in the methods used in studying secretion. Whole-cell capacitance was used to assess exocytotic performance in *Fh1*$^{-/-}$ β-cells. Using this approach, the cytoplasm is replaced by the pipette solution, essentially dialysing the cell interior. Of note, whole-cell capacitance measurements are normally performed using high intracellular glutamate levels. This process may mask mitochondrial defects and still trigger exocytosis when β-cells are electrically stimulated because the pipette solution is also normally supplemented with ATP and cAMP to maximise exocytotic responses. We need to take this into consideration in any future work to elucidate the precise mechanism of glutamate in exocytosis. It will also be interesting to explore the relevance of the *Fh1*KO mice to human diabetes. Intriguing observations suggest that succination of islet cells, whilst occurring only rarely in the pancreases from non-diabetic subjects, is a common feature of pancreases from patients with T2D (J Adam, personal communication). This is exactly what is observed in *Fh1*$^{-/-}$ pancreases, raising the interesting possibility that T2D is associated with reduced β-cell expression of *FH*.

It is important to recognise that inappropriate glucagon secretion equally contributes to the pathophysiology of T2D as insulin. Particularly, the role of glucagon in the systemic glucose tolerance has been emphasised by the spectacular observation that a complete chemical destruction of β-cells (using streptozotocin) fails to trigger hyperglycaemia in glucagon receptor KO mice (Lee et al., 2011). We report an age-dependent disruption in glucagon suppression by glucose. This may further exacerbate the progressive insulin

resistance. Therefore, it is important to address the mechanism of age-dependent alterations of glucagon secretion in α-cells and its counter-interaction in β-cells. Based on the previous observation that tolbutamide restores the glucose regulation of glucagon secretion (Zhang et al., 2013), a low dose of sulphonylurea (without triggering further insulin secretion) may be added to current diabetes medication for the elderly.

Overall, all our research efforts should be translated to the clinic, especially for a global health issue such as diabetes (Ashcroft and Rorsman, 2012). Given that diabetes still lacks effective medication, mouse models will be continually developed for T2D research to characterise the specific phenotype resembling human traits. Although diabetic mouse models are not the complete representation of the human aetiology (due to, for examples, structural differences in glucose transporter and calcium channels of pancreatic β-cell), they will still provide significant insights into the physiology of diabetes and contribute to the discovery of novel targets for drug discovery.

8.2 Future work

Based on the findings in the *Sox4*mt mouse model, we have confirmed, in a human study, that the aberrant expression of *SOX4* leads to a diabetic phenotype that is mediated via *STXBP6*. Therefore, it will be interesting to extend our study to a large population of T2D to confirm any variability in *SOX4* and *STXBP6* expression. This may potentially confirm the gene(s) as a novel gene that is common in T2D. Furthermore, any pharmacological intervention targeting either *SOX4* or the downstream mediator, *STXBP6* (or both), should be investigated. This will provide further insights into the maintenance and restoration of the diabetic phenotype, and it will, in turn, lead to the development of new therapeutic strategies for T2D.

Mitochondrial dysfunction was implicated as the main cause behind the insulin secretory defect in *Fh1*KO mice, which was corrected by the addition of exogenous glutamate. Cellular levels of α-ketoglutarate (the glutamate precursor in the Krebs cycle) should be measured to determine whether glutamate depletion (potentially due to anaplerosis) is the main cause of the insulin secretory defect. Furthermore, exocytotic performance needs to be assessed in the intact milieu of *Fh1*$^{-/-}$ β-cells without the addition of glutamate, as explained above, to elucidate the precise mechanism of action of glutamate. This potential finding may agree with the observations by Maechler and Wollheim, who showed that a permissive concentration of glutamate is required for the full capacity of insulin release in response to glucose via activation of the amplifying pathway of the β-cells (Maechler and Wollheim, 1999). On a different note, the identification of protein targets of fumarate-mediated succination is necessary, as previously observed in *Fh1*-deficient and cancer cells (Bardella et al., 2011, Adam et al., 2013). It is important to understand how changes in these proteins contribute to the defective insulin secretory

phenotype given the potential disruption of proteins mediated by succination, for example, succination-mediated inactivation of *Gapdh* (Blatnik et al., 2008a, Blatnik et al., 2008b). Importantly, these effects need not be restricted to β-cells given their proximity to other non-β-cells in an islet. Preliminary data suggest that hyperglycaemia as such leads to inhibition of fumarase activity (with resultant elevation of fumarate and protein succination) in a number of tissues including the pancreatic α-cells, renal tubular cells, skeletal muscle cells and adipocytes. Succination of key proteins in glucagon-producing α-cells may result in the over-secretion of glucagon, which is one of the hallmarks of poorly controlled diabetes.

Ageing may be associated with increased K_{ATP}-channel activity, thereby disturbing glucagon homeostasis. It would be interesting to investigate the potential of sulphonylureas, such as tolbutamide, to rescue the over-secretion of glucagon.

8.3 Summary

This thesis has dealt with the precise function of two novel genes that were implicated in the pathophysiological mechanism of T2D, specifically in the regulation of insulin release. Additionally, the effect of ageing has been elucidated. Over the course of the study, we have reached the following conclusions:

1. The ENU-induced *Sox4* mutation leads to impairment of glucose-stimulated insulin secretion that is not associated with reduced $[Ca^{2+}]_i$. The *Sox4* mutation increases the proportion of kiss-and-run exocytosis at the expense of full fusion events, thereby preventing the exit of insulin, due to steric hindrance, via the fusion pores.
2. A number of downstream target genes of *Sox4* have been identified. In particular, increased expression of amisyn, which was previously implicated in fusion pore stabilisation, was confirmed to be the main mediator. Over-expression of amisyn *in vitro* inhibits insulin release, closely resembling the phenotype of *Sox4*mt mice.
3. Knockdown of amisyn expression in *Sox4*/*SOX4*-overexpressing cells restores insulin secretion in both INS-1 832/13 and EndoC-βH2 cells.
4. Dysregulated *SOX4* or *STXBP6* expression correlates with defective insulin secretions in humans.
5. The deletion of the *Fh1* gene, which was originally implicated as a tumour suppressor in hereditary leiomyomatosis and renal cell cancer (HLRCC) in pancreatic β-cells, results in a complete loss of glucose-stimulated insulin secretion. Defective insulin secretion is associated with fragmentation of mitochondria, but the ATP levels in *Fh1*$^{-/-}$ β-cells remain normal. The addition of exogenous glutamate rescues defective insulin secretion in *Fh1*KO mice,

suggesting that the glucose-induced production of glutamate mediates the amplification of glucose-stimulated insulin secretion.

6. Ageing has been recognised as an important risk factor of T2D, although the underlying mechanism is unknown. Previously, it was speculated to influence β-cell function. However, normal or increased glucose-stimulated insulin secretion was observed with ageing in both the mouse and human studies. Ageing also correlated with a diminished capacity of glucose to lower glucagon secretion.

References

ACCILI, D., DRAGO, J., LEE, E. J., JOHNSON, M. D., COOL, M. H., SALVATORE, P., ASICO, L. D., JOSE, P. A., TAYLOR, S. I. & WESTPHAL, H. 1996. Early neonatal death in mice homozygous for a null allele of the insulin receptor gene. *Nat Genet,* 12**,** 106-9.

ADAM, J., HATIPOGLU, E., O'FLAHERTY, L., TERNETTE, N., SAHGAL, N., LOCKSTONE, H., BABAN, D., NYE, E., STAMP, G. W., WOLHUTER, K., STEVENS, M., FISCHER, R., CARMELIET, P., MAXWELL, P. H., PUGH, C. W., FRIZZELL, N., SOGA, T., KESSLER, B. M., EL-BAHRAWY, M., RATCLIFFE, P. J. & POLLARD, P. J. 2011. Renal cyst formation in Fh1-deficient mice is independent of the Hif/Phd pathway: roles for fumarate in KEAP1 succination and Nrf2 signaling. *Cancer Cell,* 20**,** 524-37.

ADAM, J., YANG, M., BAUERSCHMIDT, C., KITAGAWA, M., O'FLAHERTY, L., MAHESWARAN, P., OZKAN, G., SAHGAL, N., BABAN, D., KATO, K., SAITO, K., IINO, K., IGARASHI, K., STRATFORD, M., PUGH, C., TENNANT, D. A., LUDWIG, C., DAVIES, B., RATCLIFFE, P. J., EL-BAHRAWY, M., ASHRAFIAN, H., SOGA, T. & POLLARD, P. J. 2013. A role for cytosolic fumarate hydratase in urea cycle metabolism and renal neoplasia. *Cell Rep,* 3**,** 1440-8.

ADAMS, M. J., BLUNDELL, T. L., DODSON, E. J., DODSON, G. G., VIJAYAN, M., BAKER, E. N., HARDING, M. M., HODGKIN, D. C., RIMMER, B. & SHEAT, S. 1969. Structure of Rhombohedral 2 Zinc Insulin Crystals. *Nature,* 224**,** 491-&.

AHREN, B. 2000. Autonomic regulation of islet hormone secretion--implications for health and disease. *Diabetologia,* 43**,** 393-410.

AKAGI, K., SANDIG, V., VOOIJS, M., VAN DER VALK, M., GIOVANNINI, M., STRAUSS, M. & BERNS, A. 1997. Cre-mediated somatic site-specific recombination in mice. *Nucleic Acids Res,* 25**,** 1766-73.

AKIBA, T., HIRAGA, K. & TUBOI, S. 1984. Intracellular distribution of fumarase in various animals. *J Biochem,* 96**,** 189-95.

ALANENTALO, T., ASAYESH, A., MORRISON, H., LOREN, C. E., HOLMBERG, D., SHARPE, J. & AHLGREN, U. 2007. Tomographic molecular imaging and 3D quantification within adult mouse organs. *Nat Methods,* 4**,** 31-3.

ALBILLOS, A., DERNICK, G., HORSTMANN, H., ALMERS, W., ALVAREZ DE TOLEDO, G. & LINDAU, M. 1997. The exocytotic event in chromaffin cells revealed by patch amperometry. *Nature,* 389**,** 509-12.

ALDERSON, N. L., WANG, Y., BLATNIK, M., FRIZZELL, N., WALLA, M. D., LYONS, T. J., ALT, N., CARSON, J. A., NAGAI, R., THORPE, S. R. & BAYNES, J. W. 2006. S-(2-Succinyl)cysteine: a novel chemical modification of tissue proteins by a Krebs cycle intermediate. *Arch Biochem Biophys,* 450**,** 1-8.

ALMACA, J., MOLINA, J., ARROJO, E. D. R., ABDULREDA, M. H., JEON, W. B., BERGGREN, P. O., CAICEDO, A. & NAM, H. G. 2014. Young capillary vessels rejuvenate aged pancreatic islets. *Proc Natl Acad Sci U S A,* 111**,** 17612-7.

AMMALA, C., ELIASSON, L., BOKVIST, K., LARSSON, O., ASHCROFT, F. M. & RORSMAN, P. 1993. Exocytosis elicited by action potentials and voltage-clamp calcium currents in individual mouse pancreatic B-cells. *J Physiol,* 472**,** 665-88.

AMMON, H. P., FAHMY, A., MARK, M., WAHL, M. A. & YOUSSIF, N. 1987. The effect of glucose on insulin release and ion movements in isolated pancreatic islets of rats in old age. *J Physiol,* 384**,** 347-54.

AN, S. J. & ALMERS, W. 2004. Tracking SNARE complex formation in live endocrine cells. *Science,* 306**,** 1042-6.

ANELLO, M., LUPI, R., SPAMPINATO, D., PIRO, S., MASINI, M., BOGGI, U., DEL PRATO, S., RABUAZZO, A. M., PURRELLO, F. & MARCHETTI, P. 2005. Functional and morphological alterations of mitochondria in pancreatic beta cells from type 2 diabetic patients. *Diabetologia,* 48**,** 282-9.

ARTALEJO, C. R., ELHAMDANI, A. & PALFREY, H. C. 2002. Sustained stimulation shifts the mechanism of endocytosis from dynamin-1-dependent rapid endocytosis to clathrin- and dynamin-2-mediated slow endocytosis in chromaffin cells. *Proc Natl Acad Sci U S A,* 99**,** 6358-63.

ASAHARA, S., SHIBUTANI, Y., TERUYAMA, K., INOUE, H. Y., KAWADA, Y., ETOH, H., MATSUDA, T., KIMURA-KOYANAGI, M., HASHIMOTO, N., SAKAHARA, M., FUJIMOTO, W., TAKAHASHI, H., UEDA, S., HOSOOKA, T., SATOH, T., INOUE, H., MATSUMOTO, M., AIBA, A., KASUGA, M. & KIDO, Y. 2013. Ras-related C3 botulinum toxin substrate 1 (RAC1) regulates glucose-stimulated insulin secretion via modulation of F-actin. *Diabetologia,* 56**,** 1088-97.

ASHCROFT, F. M. & RORSMAN, P. 2012. Diabetes mellitus and the beta cell: the last ten years. *Cell,* 148**,** 1160-71.

ASHCROFT, F. M. & RORSMAN, P. 2013. K(ATP) channels and islet hormone secretion: new insights and controversies. *Nat Rev Endocrinol,* 9**,** 660-9.

ATANUR, S. S., DIAZ, A. G., MARATOU, K., SARKIS, A., ROTIVAL, M., GAME, L., TSCHANNEN, M. R., KAISAKI, P. J., OTTO, G. W., MA, M. C., KEANE, T. M., HUMMEL, O., SAAR, K., CHEN, W., GURYEV, V., GOPALAKRISHNAN, K., GARRETT, M. R., JOE, B., CITTERIO, L., BIANCHI, G., MCBRIDE, M., DOMINICZAK, A., ADAMS, D. J., SERIKAWA, T., FLICEK, P., CUPPEN, E., HUBNER, N., PETRETTO, E., GAUGUIER, D., KWITEK, A., JACOB, H. & AITMAN, T. J. 2013. Genome Sequencing Reveals Loci under Artificial Selection that Underlie Disease Phenotypes in the Laboratory Rat. *Cell,* 154**,** 691-703.

BALAJI, J. & RYAN, T. A. 2007. Single-vesicle imaging reveals that synaptic vesicle exocytosis and endocytosis are coupled by a single stochastic mode. *Proc Natl Acad Sci U S A,* 104**,** 20576-81.

BALCH, W. E., GLICK, B. S. & ROTHMAN, J. E. 1984. Sequential intermediates in the pathway of intercompartmental transport in a cell-free system. *Cell,* 39**,** 525-36.

BANARER, S., MCGREGOR, V. P. & CRYER, P. E. 2002. Intraislet hyperinsulinemia prevents the glucagon response to hypoglycemia despite an intact autonomic response. *Diabetes,* 51**,** 958-65.

BANTING, F. G., BEST, C. H., COLLIP, J. B., CAMPBELL, W. R. & FLETCHER, A. A. 1922. Pancreatic Extracts in the Treatment of Diabetes Mellitus. *Can Med Assoc J,* 12**,** 141-6.

BARDELLA, C., EL-BAHRAWY, M., FRIZZELL, N., ADAM, J., TERNETTE, N., HATIPOGLU, E., HOWARTH, K., O'FLAHERTY, L., ROBERTS, I., TURNER, G., TAYLOR, J., GIASLAKIOTIS, K., MACAULAY, V. M., HARRIS, A. L., CHANDRA, A., LEHTONEN, H. J., LAUNONEN, V., AALTONEN, L. A., PUGH, C. W., MIHAI, R., TRUDGIAN, D., KESSLER, B., BAYNES, J. W., RATCLIFFE, P. J., TOMLINSON, I. P. & POLLARD, P. J. 2011. Aberrant

succination of proteins in fumarate hydratase-deficient mice and HLRCC patients is a robust biomarker of mutation status. *J Pathol,* 225**,** 4-11.
BARG, S., ELIASSON, L., RENSTROM, E. & RORSMAN, P. 2002a. A subset of 50 secretory granules in close contact with L-type Ca2+ channels accounts for first-phase insulin secretion in mouse beta-cells. *Diabetes,* 51 Suppl 1**,** S74-82.
BARG, S., GALVANOVSKIS, J., GOPEL, S. O., RORSMAN, P. & ELIASSON, L. 2000. Tight coupling between electrical activity and exocytosis in mouse glucagon-secreting alpha-cells. *Diabetes,* 49**,** 1500-10.
BARG, S., MA, X., ELIASSON, L., GALVANOVSKIS, J., GOPEL, S. O., OBERMULLER, S., PLATZER, J., RENSTROM, E., TRUS, M., ATLAS, D., STRIESSNIG, J. & RORSMAN, P. 2001. Fast exocytosis with few Ca(2+) channels in insulin-secreting mouse pancreatic B cells. *Biophys J,* 81**,** 3308-23.
BARG, S., OLOFSSON, C. S., SCHRIEVER-ABELN, J., WENDT, A., GEBRE-MEDHIN, S., RENSTROM, E. & RORSMAN, P. 2002b. Delay between fusion pore opening and peptide release from large dense-core vesicles in neuroendocrine cells. *Neuron,* 33**,** 287-99.
BARRETO, S. G., CARATI, C. J., TOOULI, J. & SACCONE, G. T. 2010. The islet-acinar axis of the pancreas: more than just insulin. *Am J Physiol Gastrointest Liver Physiol,* 299**,** G10-22.
BASU, R., DALLA MAN, C., CAMPIONI, M., BASU, A., KLEE, G., TOFFOLO, G., COBELLI, C. & RIZZA, R. A. 2006. Effects of age and sex on postprandial glucose metabolism: differences in glucose turnover, insulin secretion, insulin action, and hepatic insulin extraction. *Diabetes,* 55**,** 2001-14.
BELL, G. I., PICTET, R. L., RUTTER, W. J., CORDELL, B., TISCHER, E. & GOODMAN, H. M. 1980. Sequence of the human insulin gene. *Nature,* 284**,** 26-32.
BEN, Q., XU, M., NING, X., LIU, J., HONG, S., HUANG, W., ZHANG, H. & LI, Z. 2011. Diabetes mellitus and risk of pancreatic cancer: A meta-analysis of cohort studies. *Eur J Cancer,* 47**,** 1928-37.
BERNARD, C. 1876. Lecons sur la chaleur animale, sur les effets de la chaleur, et sur la fie`vre. *Paris: JB Baillie`re*.
BERNARD, P. & HARLEY, V. R. 2010. Acquisition of SOX transcription factor specificity through protein-protein interaction, modulation of Wnt signalling and post-translational modification. *International Journal of Biochemistry & Cell Biology,* 42**,** 400-410.
BERTHOUD, H. R. & POWLEY, T. L. 1990. Identification of vagal preganglionics that mediate cephalic phase insulin response. *Am J Physiol,* 258**,** R523-30.
BERTRAND, G., ISHIYAMA, N., NENQUIN, M., RAVIER, M. A. & HENQUIN, J. C. 2002. The elevation of glutamate content and the amplification of insulin secretion in glucose-stimulated pancreatic islets are not causally related. *J Biol Chem,* 277**,** 32883-91.
BEST, C. 1972. Letter to PP Foa cited in Changing concepts of glucagon: fifty years of research. In: Lefebvre PJ, Unger RH, eds. Glucagon: molecular physiology, clinical and therapeutic implications. Oxford, UK: Pergamon; 1.
BEST, L., YATES, A. P. & TOMLINSON, S. 1992. Stimulation of insulin secretion by glucose in the absence of diminished potassium (86Rb+) permeability. *Biochem Pharmacol,* 43**,** 2483-5.
BHATTARAM, P., PENZO-MENDEZ, A., SOCK, E., COLMENARES, C., KANEKO, K. J., VASSILEV, A., DEPAMPHILIS, M. L., WEGNER, M. & LEFEBVRE, V.

2010. Organogenesis relies on SoxC transcription factors for the survival of neural and mesenchymal progenitors. *Nat Commun,* 1**,** 9.

BITTNER, G. D. & KENNEDY, D. 1970. Quantitative aspects of transmitter release. *J Cell Biol,* 47**,** 585-92.

BLASI, J., CHAPMAN, E. R., LINK, E., BINZ, T., YAMASAKI, S., DE CAMILLI, P., SUDHOF, T. C., NIEMANN, H. & JAHN, R. 1993. Botulinum neurotoxin A selectively cleaves the synaptic protein SNAP-25. *Nature,* 365**,** 160-3.

BLATNIK, M., FRIZZELL, N., THORPE, S. R. & BAYNES, J. W. 2008a. Inactivation of glyceraldehyde-3-phosphate dehydrogenase by fumarate in diabetes: formation of S-(2-succinyl)cysteine, a novel chemical modification of protein and possible biomarker of mitochondrial stress. *Diabetes,* 57**,** 41-9.

BLATNIK, M., THORPE, S. R. & BAYNES, J. W. 2008b. Succination of proteins by fumarate: mechanism of inactivation of glyceraldehyde-3-phosphate dehydrogenase in diabetes. *Ann N Y Acad Sci,* 1126**,** 272-5.

BLOCK, M. R., GLICK, B. S., WILCOX, C. A., WIELAND, F. T. & ROTHMAN, J. E. 1988. Purification of an N-ethylmaleimide-sensitive protein catalyzing vesicular transport. *Proc Natl Acad Sci U S A,* 85**,** 7852-6.

BLOOM, S. R. & EDWARDS, A. V. 1980. Pancreatic endocrine responses to stimulation of the peripheral ends of the splanchnic nerves in the conscious adrenalectomized calf. *J Physiol,* 308**,** 39-48.

BOKVIST, K., ELIASSON, L., AMMALA, C., RENSTROM, E. & RORSMAN, P. 1995. Co-localization of L-type Ca2+ channels and insulin-containing secretory granules and its significance for the initiation of exocytosis in mouse pancreatic B-cells. *Embo J,* 14**,** 50-7.

BONNEFOND, A. & FROGUEL, P. 2015. Rare and Common Genetic Events in Type 2 Diabetes: What Should Biologists Know? *Cell Metab,* 21**,** 357-368.

BRANDOLIN, G., DUPONT, Y. & VIGNAIS, P. V. 1985. Substrate-induced modifications of the intrinsic fluorescence of the isolated adenine nucleotide carrier protein: demonstration of distinct conformational states. *Biochemistry,* 24**,** 1991-7.

BRAUN, M., RAMRACHEYA, R., BENGTSSON, M., CLARK, A., WALKER, J. N., JOHNSON, P. R. & RORSMAN, P. 2010. gamma-Aminobutyric Acid (GABA) Is an Autocrine Excitatory Transmitter in Human Pancreatic beta-Cells. *Diabetes,* 59**,** 1694-1701.

BRAUN, M., RAMRACHEYA, R., BENGTSSON, M., ZHANG, Q., KARANAUSKAITE, J., PARTRIDGE, C., JOHNSON, P. R. & RORSMAN, P. 2008. Voltage-gated ion channels in human pancreatic beta-cells: electrophysiological characterization and role in insulin secretion. *Diabetes,* 57**,** 1618-28.

BRAUN, M., WENDT, A., KARANAUSKAITE, J., GALVANOVSKIS, J., CLARK, A., MACDONALD, P. E. & RORSMAN, P. 2007. Corelease and differential exit via the fusion pore of GABA, serotonin, and ATP from LDCV in rat pancreatic beta cells. *J Gen Physiol,* 129**,** 221-31.

BRISSOVA, M., FOWLER, M. J., NICHOLSON, W. E., CHU, A., HIRSHBERG, B., HARLAN, D. M. & POWERS, A. C. 2005. Assessment of human pancreatic islet architecture and composition by laser scanning confocal microscopy. *J Histochem Cytochem,* 53**,** 1087-97.

BROWN, H., SANGER, F. & KITAI, R. 1955. The structure of pig and sheep insulins. *Biochem J,* 60**,** 556-65.

BROWN, R. J., SINAII, N. & ROTHER, K. I. 2008. Too much glucagon, too little insulin: time course of pancreatic islet dysfunction in new-onset type 1 diabetes. *Diabetes Care,* 31**,** 1403-4.

BROWN, S. D. & BALLING, R. 2001. Systematic approaches to mouse mutagenesis. *Curr Opin Genet Dev,* 11**,** 268-73.

BROWNLEE, M. 2001. Biochemistry and molecular cell biology of diabetic complications. *Nature,* 414**,** 813-20.

BRUNING, J. C., GAUTAM, D., BURKS, D. J., GILLETTE, J., SCHUBERT, M., ORBAN, P. C., KLEIN, R., KRONE, W., MULLER-WIELAND, D. & KAHN, C. R. 2000. Role of brain insulin receptor in control of body weight and reproduction. *Science,* 289**,** 2122-5.

BRUNING, J. C., MICHAEL, M. D., WINNAY, J. N., HAYASHI, T., HORSCH, D., ACCILI, D., GOODYEAR, L. J. & KAHN, C. R. 1998. A muscle-specific insulin receptor knockout exhibits features of the metabolic syndrome of NIDDM without altering glucose tolerance. *Mol Cell,* 2**,** 559-69.

C CABDERRAHMANI, A., NIEDERHAUSER, G., PLAISANCE, V., ROEHRICH, M. E., LENAIN, V., COPPOLA, T., REGAZZI, R. & WAEBER, G. 2004. Complexin I regulates glucose-induced secretion in pancreatic beta-cells. *J Cell Sci,* 117**,** 2239-47.

CABRERA, O., BERMAN, D. M., KENYON, N. S., RICORDI, C., BERGGREN, P. O. & CAICEDO, A. 2006. The unique cytoarchitecture of human pancreatic islets has implications for islet cell function. *Proc Natl Acad Sci U S A,* 103**,** 2334-9.

CANNON, W. B. 1932. *The wisdom of the Body,* New York: Norton.

CASTERMANS, D., VOLDERS, K., CREPEL, A., BACKX, L., DE VOS, R., FRESON, K., MEULEMANS, S., VERMEESCH, J. R., SCHRANDER-STUMPEL, C. T., DE RIJK, P., DEL-FAVERO, J., VAN GEET, C., VAN DE VEN, W. J., STEYAERT, J. G., DEVRIENDT, K. & CREEMERS, J. W. 2010. SCAMP5, NBEA and AMISYN: three candidate genes for autism involved in secretion of large dense-core vesicles. *Hum Mol Genet,* 19**,** 1368-78.

CECCARELLI, B., GROHOVAZ, F. & HURLBUT, W. P. 1979. Freeze-fracture studies of frog neuromuscular junctions during intense release of neurotransmitter. I. Effects of black widow spider venom and Ca2+-free solutions on the structure of the active zone. *J Cell Biol,* 81**,** 163-77.

CECCARELLI, B., HURLBUT, W. P. & MAURO, A. 1972. Depletion of vesicles from frog neuromuscular junctions by prolonged tetanic stimulation. *J Cell Biol,* 54**,** 30-8.

CECCARELLI, B., HURLBUT, W. P. & MAURO, A. 1973. Turnover of transmitter and synaptic vesicles at the frog neuromuscular junction. *J Cell Biol,* 57**,** 499-524.

CERF, M. E. 2013. Beta cell dysfunction and insulin resistance. *Front Endocrinol (Lausanne),* 4**,** 37.

CHAPMAN, E. R. & JAHN, R. 1994. Calcium-dependent interaction of the cytoplasmic region of synaptotagmin with membranes. Autonomous function of a single C2-homologous domain. *J Biol Chem,* 269**,** 5735-41.

CHASSEROT-GOLAZ, S., VITALE, N., UMBRECHT-JENCK, E., KNIGHT, D., GERKE, V. & BADER, M. F. 2005. Annexin 2 promotes the formation of lipid microdomains required for calcium-regulated exocytosis of dense-core vesicles. *Molecular Biology of the Cell,* 16**,** 1108-1119.

CHEN, X., TOMCHICK, D. R., KOVRIGIN, E., ARAC, D., MACHIUS, M., SUDHOF, T. C. & RIZO, J. 2002. Three-dimensional structure of the complexin/SNARE complex. *Neuron,* 33**,** 397-409.

CHEN, X. K., WANG, L. C., ZHOU, Y., CAI, Q., PRAKRIYA, M., DUAN, K. L., SHENG, Z. H., LINGLE, C. & ZHOU, Z. 2005. Activation of GPCRs modulates quantal size in chromaffin cells through G(betagamma) and PKC. *Nat Neurosci,* 8**,** 1160-8.

CHEN, Y. A. & SCHELLER, R. H. 2001. SNARE-mediated membrane fusion. *Nat Rev Mol Cell Biol,* 2**,** 98-106.

CHENG-XUE, R., GOMEZ-RUIZ, A., ANTOINE, N., NOEL, L. A., CHAE, H. Y., RAVIER, M. A., CHIMIENTI, F., SCHUIT, F. C. & GILON, P. 2013. Tolbutamide controls glucagon release from mouse islets differently than glucose: involvement of K(ATP) channels from both alpha-cells and delta-cells. *Diabetes,* 62**,** 1612-22.

CHIMIENTI, F., DEVERGNAS, S., FAVIER, A. & SEVE, M. 2004. Identification and cloning of a beta-cell-specific zinc transporter, ZnT-8, localized into insulin secretory granules. *Diabetes,* 53**,** 2330-7.

CHOW, R. H., VON RUDEN, L. & NEHER, E. 1992. Delay in vesicle fusion revealed by electrochemical monitoring of single secretory events in adrenal chromaffin cells. *Nature,* 356**,** 60-3.

CLARY, D. O., GRIFF, I. C. & ROTHMAN, J. E. 1990. SNAPs, a family of NSF attachment proteins involved in intracellular membrane fusion in animals and yeast. *Cell,* 61**,** 709-21.

COGHILL, E. L., HUGILL, A., PARKINSON, N., DAVISON, C., GLENISTER, P., CLEMENTS, S., HUNTER, J., COX, R. D. & BROWN, S. D. 2002. A gene-driven approach to the identification of ENU mutants in the mouse. *Nat Genet,* 30**,** 255-6.

CONSTABLE, J. R., GRAHAM, M. E., MORGAN, A. & BURGOYNE, R. D. 2005. Amisyn regulates exocytosis and fusion pore stability by both syntaxin-dependent and syntaxin-independent mechanisms. *J Biol Chem,* 280**,** 31615-23.

CREE, L. M., PATEL, S. K., PYLE, A., LYNN, S., TURNBULL, D. M., CHINNERY, P. F. & WALKER, M. 2008. Age-related decline in mitochondrial DNA copy number in isolated human pancreatic islets. *Diabetologia,* 51**,** 1440-3.

CRYER, P. E. 2002. Hypoglycaemia: the limiting factor in the glycaemic management of Type I and Type II diabetes. *Diabetologia,* 45**,** 937-48.

CUDWORTH, A. G. & WOODROW, J. C. 1974. Letter: HL-A antigens and diabetes mellitus. *Lancet,* 2**,** 1153.

DANG, L., WHITE, D. W., GROSS, S., BENNETT, B. D., BITTINGER, M. A., DRIGGERS, E. M., FANTIN, V. R., JANG, H. G., JIN, S., KEENAN, M. C., MARKS, K. M., PRINS, R. M., WARD, P. S., YEN, K. E., LIAU, L. M., RABINOWITZ, J. D., CANTLEY, L. C., THOMPSON, C. B., VANDER HEIDEN, M. G. & SU, S. M. 2009. Cancer-associated IDH1 mutations produce 2-hydroxyglutarate. *Nature,* 462**,** 739-44.

DANIEL, S., NODA, M., STRAUB, S. G. & SHARP, G. W. 1999. Identification of the docked granule pool responsible for the first phase of glucose-stimulated insulin secretion. *Diabetes,* 48**,** 1686-90.

DE MEYER, J. 1909. Action de la se´cre´tion interne du pancre´as sur diffe´rents organes et en particulier sur la se´cre´tion re´nale. *Arch Fisiol,* 7**,** 96-99.

DEBERARDINIS, R. J., MANCUSO, A., DAIKHIN, E., NISSIM, I., YUDKOFF, M., WEHRLI, S. & THOMPSON, C. B. 2007. Beyond aerobic glycolysis: transformed cells can engage in glutamine metabolism that exceeds the requirement for protein and nucleotide synthesis. *Proc Natl Acad Sci U S A,* 104**,** 19345-50.

DEBUS, K. & LINDAU, M. 2000. Resolution of patch capacitance recordings and of fusion pore conductances in small vesicles. *Biophys J,* 78**,** 2983-97.

DEFRONZO, R. A. 2010. Insulin resistance, lipotoxicity, type 2 diabetes and atherosclerosis: the missing links. The Claude Bernard Lecture 2009. *Diabetologia,* 53**,** 1270-87.

DEL GUERRA, S., LUPI, R., MARSELLI, L., MASINI, M., BUGLIANI, M., SBRANA, S., TORRI, S., POLLERA, M., BOGGI, U., MOSCA, F., DEL PRATO, S. & MARCHETTI, P. 2005. Functional and molecular defects of pancreatic islets in human type 2 diabetes. *Diabetes,* 54**,** 727-35.

DENICOLA, G. M., KARRETH, F. A., HUMPTON, T. J., GOPINATHAN, A., WEI, C., FRESE, K., MANGAL, D., YU, K. H., YEO, C. J., CALHOUN, E. S., SCRIMIERI, F., WINTER, J. M., HRUBAN, R. H., IACOBUZIO-DONAHUE, C., KERN, S. E., BLAIR, I. A. & TUVESON, D. A. 2011. Oncogene-induced Nrf2 transcription promotes ROS detoxification and tumorigenesis. *Nature,* 475**,** 106-9.

DERNICK, G., ALVAREZ DE TOLEDO, G. & LINDAU, M. 2003. Exocytosis of single chromaffin granules in cell-free inside-out membrane patches. *Nat Cell Biol,* 5**,** 358-62.

DERNICK, G., GONG, L. W., TABARES, L., ALVAREZ DE TOLEDO, G. & LINDAU, M. 2005. Patch amperometry: high-resolution measurements of single-vesicle fusion and release. *Nat Methods,* 2**,** 699-708.

DETIMARY, P., DEJONGHE, S., LING, Z., PIPELEERS, D., SCHUIT, F. & HENQUIN, J. C. 1998. The changes in adenine nucleotides measured in glucose-stimulated rodent islets occur in beta cells but not in alpha cells and are also observed in human islets. *J Biol Chem,* 273**,** 33905-8.

DIABETES UK. 2014. DIABETES UK: FACTS AND STATS Available: http://www.diabetes.org.uk/Documents/About%20Us/Statistics/Diabetes-key-stats-guidelines-April2014.pdf.

DIABETES UK. 2015. Available: http://www.diabetes.org.uk/Guide-to-diabetes/Monitoring/Testing/ [Accessed 24/02 2015].

DOBSON, M. 1776. Nature of urine in diabetes. *Medical observations and inquiries,* 5**,** 298-310.

DUBOIS, M., VACHER, P., ROGER, B., HUYGHE, D., VANDEWALLE, B., KERR-CONTE, J., PATTOU, F., MOUSTAID-MOUSSA, N. & LANG, J. 2007. Glucotoxicity inhibits late steps of insulin exocytosis. *Endocrinology,* 148**,** 1605-14.

DULUBOVA, I., KHVOTCHEV, M., LIU, S., HURYEVA, I., SUDHOF, T. C. & RIZO, J. 2007. Munc18-1 binds directly to the neuronal SNARE complex. *Proc Natl Acad Sci U S A,* 104**,** 2697-702.

DUNCAN, R. R., GREAVES, J., WIEGAND, U. K., MATSKEVICH, I., BODAMMER, G., APPS, D. K., SHIPSTON, M. J. & CHOW, R. H. 2003. Functional and spatial segregation of secretory vesicle pools according to vesicle age. *Nature,* 422**,** 176-80.

DUNNING, B. E., FOLEY, J. E. & AHREN, B. 2005. Alpha cell function in health and disease: influence of glucagon-like peptide-1. *Diabetologia,* 48**,** 1700-13.

EL-SERAG, H. B., HAMPEL, H. & JAVADI, F. 2006. The association between diabetes and hepatocellular carcinoma: a systematic review of epidemiologic evidence. *Clin Gastroenterol Hepatol,* 4**,** 369-80.

ELIASSON, L., RENSTROM, E., DING, W. G., PROKS, P. & RORSMAN, P. 1997. Rapid ATP-dependent priming of secretory granules precedes Ca(2+)-induced exocytosis in mouse pancreatic B-cells. *J Physiol,* 503 (Pt 2)**,** 399-412.

ERLICH, H., VALDES, A. M., NOBLE, J., CARLSON, J. A., VARNEY, M., CONCANNON, P., MYCHALECKYJ, J. C., TODD, J. A., BONELLA, P., FEAR, A. L., LAVANT, E., LOUEY, A., MOONSAMY, P. & TYPE 1 DIABETES GENETICS, C. 2008. HLA DR-DQ haplotypes and genotypes and type 1 diabetes risk: analysis of the type 1 diabetes genetics consortium families. *Diabetes,* 57**,** 1084-92.

EVANS, J. M., DONNELLY, L. A., EMSLIE-SMITH, A. M., ALESSI, D. R. & MORRIS, A. D. 2005. Metformin and reduced risk of cancer in diabetic patients. *BMJ,* 330**,** 1304-5.

EVANS, W. J. & FARRELL, P. A. 2011. The Aging Pancreas: Effects of Aging on Insulin Secretion and Action. *Handbook of Physiology, The Endocrine System, The Endocrine Pancreas and Regulation of Metabolism*.

FASSHAUER, D. & MARGITTAI, M. 2004. A transient N-terminal interaction of SNAP-25 and syntaxin nucleates SNARE assembly. *J Biol Chem,* 279**,** 7613-21.

FASSHAUER, D., SUTTON, R. B., BRUNGER, A. T. & JAHN, R. 1998. Conserved structural features of the synaptic fusion complex: SNARE proteins reclassified as Q- and R-SNAREs. *Proc Natl Acad Sci U S A,* 95**,** 15781-6.

FIEBIG, K. M., RICE, L. M., POLLOCK, E. & BRUNGER, A. T. 1999. Folding intermediates of SNARE complex assembly. *Nat Struct Biol,* 6**,** 117-23.

FINLEY, L. W., ZHANG, J., YE, J., WARD, P. S. & THOMPSON, C. B. 2013. SnapShot: cancer metabolism pathways. *Cell Metab,* 17**,** 466-466 e2.

FLANNICK, J., THORLEIFSSON, G., BEER, N. L., JACOBS, S. B., GRARUP, N., BURTT, N. P., MAHAJAN, A., FUCHSBERGER, C., ATZMON, G., BENEDIKTSSON, R., BLANGERO, J., BOWDEN, D. W., BRANDSLUND, I., BROSNAN, J., BURSLEM, F., CHAMBERS, J., CHO, Y. S., CHRISTENSEN, C., DOUGLAS, D. A., DUGGIRALA, R., DYMEK, Z., FARJOUN, Y., FENNELL, T., FONTANILLAS, P., FORSEN, T., GABRIEL, S., GLASER, B., GUDBJARTSSON, D. F., HANIS, C., HANSEN, T., HREIDARSSON, A. B., HVEEM, K., INGELSSON, E., ISOMAA, B., JOHANSSON, S., JORGENSEN, T., JORGENSEN, M. E., KATHIRESAN, S., KONG, A., KOONER, J., KRAVIC, J., LAAKSO, M., LEE, J. Y., LIND, L., LINDGREN, C. M., LINNEBERG, A., MASSON, G., MEITINGER, T., MOHLKE, K. L., MOLVEN, A., MORRIS, A. P., POTLURI, S., RAURAMAA, R., RIBEL-MADSEN, R., RICHARD, A. M., ROLPH, T., SALOMAA, V., SEGRE, A. V., SKARSTRAND, H., STEINTHORSDOTTIR, V., STRINGHAM, H. M., SULEM, P., TAI, E. S., TEO, Y. Y., TESLOVICH, T., THORSTEINSDOTTIR, U., TRIMMER, J. K., TUOMI, T., TUOMILEHTO, J., VAZIRI-SANI, F., VOIGHT, B. F., WILSON, J. G., BOEHNKE, M., MCCARTHY, M. I., NJOLSTAD, P. R., PEDERSEN, O., GO, T. D. C., CONSORTIUM, T. D. G., GROOP, L., COX, D. R., STEFANSSON, K. & ALTSHULER, D. 2014. Loss-of-function mutations in SLC30A8 protect against type 2 diabetes. *Nat Genet,* 46**,** 357-63.

FLOREZ, J. C. 2008. Newly identified loci highlight beta cell dysfunction as a key cause of type 2 diabetes: where are the insulin resistance genes? *Diabetologia,* 51**,** 1100-10.

FRANKLIN, I., GROMADA, J., GJINOVCI, A., THEANDER, S. & WOLLHEIM, C. B. 2005. Beta-cell secretory products activate alpha-cell ATP-dependent potassium channels to inhibit glucagon release. *Diabetes,* 54**,** 1808-15.

FRIZZELL, N., RAJESH, M., JEPSON, M. J., NAGAI, R., CARSON, J. A., THORPE, S. R. & BAYNES, J. W. 2009. Succination of thiol groups in adipose tissue proteins in diabetes: succination inhibits polymerization and secretion of adiponectin. *J Biol Chem,* 284**,** 25772-81.

FULOP, T. & SMITH, C. 2006. Physiological stimulation regulates the exocytic mode through calcium activation of protein kinase C in mouse chromaffin cells. *Biochem J,* 399**,** 111-9.

GALVANOVSKIS, J., BRAUN, M. & RORSMAN, P. 2011. Exocytosis from pancreatic beta-cells: mathematical modelling of the exit of low-molecular-weight granule content. *Interface Focus,* 1**,** 143-52.

GAMMELSAETER, R., FROYLAND, M., ARAGON, C., DANBOLT, N. C., FORTIN, D., STORM-MATHISEN, J., DAVANGER, S. & GUNDERSEN, V. 2004. Glycine, GABA and their transporters in pancreatic islets of Langerhans: evidence for a paracrine transmitter interplay. *J Cell Sci,* 117**,** 3749-58.

GAO, P., TCHERNYSHYOV, I., CHANG, T. C., LEE, Y. S., KITA, K., OCHI, T., ZELLER, K. I., DE MARZO, A. M., VAN EYK, J. E., MENDELL, J. T. & DANG, C. V. 2009. c-Myc suppression of miR-23a/b enhances mitochondrial glutaminase expression and glutamine metabolism. *Nature,* 458**,** 762-5.

GAO, Z., REAVEY-CANTWELL, J., YOUNG, R. A., JEGIER, P. & WOLF, B. A. 2000. Synaptotagmin III/VII isoforms mediate Ca2+-induced insulin secretion in pancreatic islet beta -cells. *J Biol Chem,* 275**,** 36079-85.

GAUTAM, D., RUIZ DE AZUA, I., LI, J. H., GUETTIER, J. M., HEARD, T., CUI, Y., LU, H., JOU, W., GAVRILOVA, O., ZAWALICH, W. S. & WESS, J. 2010. Beneficial metabolic effects caused by persistent activation of beta-cell M3 muscarinic acetylcholine receptors in transgenic mice. *Endocrinology,* 151**,** 5185-94.

GAUTHIER, B. R., DUHAMEL, D. L., IEZZI, M., THEANDER, S., SALTEL, F., FUKUDA, M., WEHRLE-HALLER, B. & WOLLHEIM, C. B. 2008. Synaptotagmin VII splice variants alpha, beta, and delta are expressed in pancreatic beta-cells and regulate insulin exocytosis. *FASEB J,* 22**,** 194-206.

GEJL, M., SONDERGAARD, H. M., STECHER, C., BIBBY, B. M., MOLLER, N., BOTKER, H. E., HANSEN, S. B., GJEDDE, A., RUNGBY, J. & BROCK, B. 2012. Exenatide alters myocardial glucose transport and uptake depending on insulin resistance and increases myocardial blood flow in patients with type 2 diabetes. *J Clin Endocrinol Metab,* 97**,** E1165-9.

GEMBAL, M., DETIMARY, P., GILON, P., GAO, Z. Y. & HENQUIN, J. C. 1993. Mechanisms by which glucose can control insulin release independently from its action on adenosine triphosphate-sensitive K+ channels in mouse B cells. *J Clin Invest,* 91**,** 871-80.

GEMBAL, M., GILON, P. & HENQUIN, J. C. 1992. Evidence that glucose can control insulin release independently from its action on ATP-sensitive K+ channels in mouse B cells. *J Clin Invest,* 89**,** 1288-95.

GHENI, G., OGURA, M., IWASAKI, M., YOKOI, N., MINAMI, K., NAKAYAMA, Y., HARADA, K., HASTOY, B., WU, X., TAKAHASHI, H., KIMURA, K., MATSUBARA, T., HOSHIKAWA, R., HATANO, N., SUGAWARA, K., SHIBASAKI, T., INAGAKI, N., BAMBA, T., MIZOGUCHI, A., FUKUSAKI, E., RORSMAN, P. & SEINO, S. 2014. Glutamate acts as a key signal linking glucose metabolism to incretin/cAMP action to amplify insulin secretion. *Cell Rep,* 9**,** 661-73.

GIOVANNUCCI, E., HARLAN, D. M., ARCHER, M. C., BERGENSTAL, R. M., GAPSTUR, S. M., HABEL, L. A., POLLAK, M., REGENSTEINER, J. G. & YEE, D. 2010. Diabetes and cancer: a consensus report. *Diabetes Care,* 33**,** 1674-85.

GOLDSWORTHY, M., HUGILL, A., FREEMAN, H., HORNER, E., SHIMOMURA, K., BOGANI, D., PIELES, G., MIJAT, V., ARKELL, R., BHATTACHARYA, S., ASHCROFT, F. M. & COX, R. D. 2008. Role of the transcription factor sox4 in insulin secretion and impaired glucose tolerance. *Diabetes,* 57**,** 2234-44.

GOPEL, S. O., KANNO, T., BARG, S. & RORSMAN, P. 2000. Patch-clamp characterisation of somatostatin-secreting -cells in intact mouse pancreatic islets. *J Physiol,* 528**,** 497-507.

GRANSETH, B., ODERMATT, B., ROYLE, S. J. & LAGNADO, L. 2006. Clathrin-mediated endocytosis is the dominant mechanism of vesicle retrieval at hippocampal synapses. *Neuron,* 51**,** 773-786.

GRANSETH, B., ODERMATT, B., ROYLE, S. J. & LAGNADO, L. 2009. Comment on "The dynamic control of kiss-and-run and vesicular reuse probed with single nanoparticles". *Science,* 325**,** 1499; author reply 1499.

GRISE, F., TAIB, N., MONTERRAT, C., LAGREE, V. & LANG, J. 2007. Distinct roles of the C2A and the C2B domain of the vesicular Ca2+ sensor synaptotagmin 9 in endocrine beta-cells. *Biochem J,* 403**,** 483-92.

GROENEWOUD, M. J., DEKKER, J. M., FRITSCHE, A., REILING, E., NIJPELS, G., HEINE, R. J., MAASSEN, J. A., MACHICAO, F., SCHAFER, S. A., HARING, H. U., T HART, L. M. & VAN HAEFTEN, T. W. 2008. Variants of CDKAL1 and IGF2BP2 affect first-phase insulin secretion during hyperglycaemic clamps. *Diabetologia,* 51**,** 1659-63.

GROMADA, J., BOKVIST, K., DING, W. G., BARG, S., BUSCHARD, K., RENSTROM, E. & RORSMAN, P. 1997. Adrenaline stimulates glucagon secretion in pancreatic A-cells by increasing the Ca2+ current and the number of granules close to the L-type Ca2+ channels. *J Gen Physiol,* 110**,** 217-28.

GROMADA, J., DUTTAROY, A. & RORSMAN, P. 2009. The insulin receptor talks to glucagon? *Cell Metab,* 9**,** 303-5.

GUILLOD-MAXIMIN, E., LORSIGNOL, A., ALQUIER, T. & PENICAUD, L. 2004. Acute intracarotid glucose injection towards the brain induces specific c-fos activation in hypothalamic nuclei: involvement of astrocytes in cerebral glucose-sensing in rats. *J Neuroendocrinol,* 16**,** 464-71.

GUMBINER, B., POLONSKY, K. S., BELTZ, W. F., WALLACE, P., BRECHTEL, G. & FINK, R. I. 1989. Effects of aging on insulin secretion. *Diabetes,* 38**,** 1549-56.

HANAHAN, D. & WEINBERG, R. A. 2011. Hallmarks of cancer: the next generation. *Cell,* 144**,** 646-74.

HANNA, S. T., PIGEAU, G. M., GALVANOVSKIS, J., CLARK, A., RORSMAN, P. & MACDONALD, P. E. 2009. Kiss-and-run exocytosis and fusion pores of secretory vesicles in human beta-cells. *Pflugers Arch,* 457**,** 1343-50.

HANSON, P. I., ROTH, R., MORISAKI, H., JAHN, R. & HEUSER, J. E. 1997. Structure and conformational changes in NSF and its membrane receptor complexes visualized by quick-freeze/deep-etch electron microscopy. *Cell,* 90**,** 523-35.

HARATA, N. C., CHOI, S., PYLE, J. L., ARAVANIS, A. M. & TSIEN, R. W. 2006. Frequency-dependent kinetics and prevalence of kiss-and-run and reuse at hippocampal synapses studied with novel quenching methods. *Neuron,* 49**,** 243-56.

HARDY, A. B., WIJESEKARA, N., GENKIN, I., PRENTICE, K. J., BHATTACHARJEE, A., KONG, D., CHIMIENTI, F. & WHEELER, M. B. 2012. Effects of high-fat diet feeding on Znt8-null mice: differences between beta-cell and global knockout of Znt8. *Am J Physiol Endocrinol Metab,* 302**,** E1084-96.

HATAKEYAMA, H., TAKAHASHI, N., KISHIMOTO, T., NEMOTO, T. & KASAI, H. 2007. Two cAMP-dependent pathways differentially regulate exocytosis of large dense-core and small vesicles in mouse beta-cells. *J Physiol,* 582**,** 1087-98.

HAUGE-EVANS, A. C., KING, A. J., CARMIGNAC, D., RICHARDSON, C. C., ROBINSON, I. C., LOW, M. J., CHRISTIE, M. R., PERSAUD, S. J. & JONES, P. M. 2009. Somatostatin secreted by islet delta-cells fulfills multiple roles as a paracrine regulator of islet function. *Diabetes,* 58**,** 403-11.

HEDESKOV, C. J. 1980. Mechanism of glucose-induced insulin secretion. *Physiol Rev,* 60**,** 442-509.

HEIMBERG, H., DE VOS, A., PIPELEERS, D., THORENS, B. & SCHUIT, F. 1995. Differences in glucose transporter gene expression between rat pancreatic alpha- and beta-cells are correlated to differences in glucose transport but not in glucose utilization. *J Biol Chem,* 270**,** 8971-5.

HELLER, R. S., KLEIN, T., LING, Z., HEIMBERG, H., KATOH, M., MADSEN, O. D. & SERUP, P. 2003. Expression of Wnt, Frizzled, sFRP, and DKK genes in adult human pancreas. *Gene Expr,* 11**,** 141-7.

HELM, C. A., ISRAELACHVILI, J. N. & MCGUIGGAN, P. M. 1989. Molecular mechanisms and forces involved in the adhesion and fusion of amphiphilic bilayers. *Science,* 246**,** 919-22.

HELM, C. A., ISRAELACHVILI, J. N. & MCGUIGGAN, P. M. 1992. Role of hydrophobic forces in bilayer adhesion and fusion. *Biochemistry,* 31**,** 1794-805.

HENQUIN, J. C. 2000. Triggering and amplifying pathways of regulation of insulin secretion by glucose. *Diabetes,* 49**,** 1751-60.

HENQUIN, J. C., CHARLES, S., NENQUIN, M., MATHOT, F. & TAMAGAWA, T. 1982. Diazoxide and D600 inhibition of insulin release. Distinct mechanisms explain the specificity for different stimuli. *Diabetes,* 31**,** 776-83.

HENQUIN, J. C., DUFRANE, D. & NENQUIN, M. 2006a. Nutrient control of insulin secretion in isolated normal human islets. *Diabetes,* 55**,** 3470-7.

HENQUIN, J. C. & MEISSNER, H. P. 1983. Dibutyryl cyclic AMP triggers Ca2+ influx and Ca2+-dependent electrical activity in pancreatic B cells. *Biochem Biophys Res Commun,* 112**,** 614-20.

HENQUIN, J. C., NENQUIN, M., RAVIER, M. A. & SZOLLOSI, A. 2009. Shortcomings of current models of glucose-induced insulin secretion. *Diabetes Obes Metab,* 11 Suppl 4**,** 168-79.

HENQUIN, J. C., NENQUIN, M., STIERNET, P. & AHREN, B. 2006b. In vivo and in vitro glucose-induced biphasic insulin secretion in the mouse: pattern and role of cytoplasmic Ca2+ and amplification signals in beta-cells. *Diabetes,* 55**,** 441-51.

HESS, D. T., SLATER, T. M., WILSON, M. C. & SKENE, J. H. 1992. The 25 kDa synaptosomal-associated protein SNAP-25 is the major methionine-rich polypeptide in rapid axonal transport and a major substrate for palmitoylation in adult CNS. *J Neurosci,* 12**,** 4634-41.

HEUSER, J. E. 1989. Review of electron microscopic evidence favouring vesicle exocytosis as the structural basis for quantal release during synaptic transmission. *Q J Exp Physiol,* 74**,** 1051-69.

HEUSER, J. E. & REESE, T. S. 1973. Evidence for recycling of synaptic vesicle membrane during transmitter release at the frog neuromuscular junction. *J Cell Biol,* 57**,** 315-44.

HILLE, B. (ed.) 2001. *Ion channels of excitable membranes,* Sunderland, Massachussets: Sinauer Associates, Inc.

HOHMEIER, H. E., MULDER, H., CHEN, G., HENKEL-RIEGER, R., PRENTKI, M. & NEWGARD, C. B. 2000. Isolation of INS-1-derived cell lines with robust ATP-sensitive K+ channel-dependent and -independent glucose-stimulated insulin secretion. *Diabetes,* 49**,** 424-30.

HOLROYD, P., LANG, T., WENZEL, D., DE CAMILLI, P. & JAHN, R. 2002. Imaging direct, dynamin-dependent recapture of fusing secretory granules on plasma membrane lawns from PC12 cells. *Proc Natl Acad Sci U S A,* 99**,** 16806-11.

HOLZ, G. G. 2004. Epac: A new cAMP-binding protein in support of glucagon-like peptide-1 receptor-mediated signal transduction in the pancreatic beta-cell. *Diabetes,* 53**,** 5-13.

HOPPA, M. B., COLLINS, S., RAMRACHEYA, R., HODSON, L., AMISTEN, S., ZHANG, Q., JOHNSON, P., ASHCROFT, F. M. & RORSMAN, P. 2009. Chronic palmitate exposure inhibits insulin secretion by dissociation of Ca(2+) channels from secretory granules. *Cell Metab,* 10**,** 455-65.

HUXLEY, R., ANSARY-MOGHADDAM, A., BERRINGTON DE GONZALEZ, A., BARZI, F. & WOODWARD, M. 2005. Type-II diabetes and pancreatic cancer: a meta-analysis of 36 studies. *Br J Cancer,* 92**,** 2076-83.

IEZZI, M., KOURI, G., FUKUDA, M. & WOLLHEIM, C. B. 2004. Synaptotagmin V and IX isoforms control Ca2+ -dependent insulin exocytosis. *J Cell Sci,* 117**,** 3119-27.

IHM, S. H., MATSUMOTO, I., SAWADA, T., NAKANO, M., ZHANG, H. J., ANSITE, J. D., SUTHERLAND, D. E. & HERING, B. J. 2006. Effect of donor age on function of isolated human islets. *Diabetes,* 55**,** 1361-8.

IHM, S. H., MOON, H. J., KANG, J. G., PARK, C. Y., OH, K. W., JEONG, I. K., OH, Y. S. & PARK, S. W. 2007. Effect of aging on insulin secretory function and expression of beta cell function-related genes of islets. *Diabetes Res Clin Pract,* 77 Suppl 1**,** S150-4.

IMAMURA, F., MUKAMAL, K. J., MEIGS, J. B., LUCHSINGER, J. A., IX, J. H., SISCOVICK, D. S. & MOZAFFARIAN, D. 2013. Risk factors for type 2 diabetes mellitus preceded by beta-cell dysfunction, insulin resistance, or both in older adults: the Cardiovascular Health Study. *Am J Epidemiol,* 177**,** 1418-29.

INAGAKI, N., GONOI, T., CLEMENT, J. P. T., NAMBA, N., INAZAWA, J., GONZALEZ, G., AGUILAR-BRYAN, L., SEINO, S. & BRYAN, J. 1995. Reconstitution of IKATP: an inward rectifier subunit plus the sulfonylurea receptor. *Science,* 270**,** 1166-70.

INTERNATIONAL DIABETES FEDERATION. 2013. Diabetes atlas (6th edition). Available: www.diabetesatlas.org.

INTERNATIONAL MOUSE KNOCKOUT, C., COLLINS, F. S., ROSSANT, J. & WURST, W. 2007. A mouse for all reasons. *Cell,* 128**,** 9-13.
JAHN, R. & FASSHAUER, D. 2012. Molecular machines governing exocytosis of synaptic vesicles. *Nature,* 490**,** 201-207.
JAHN, R., LANG, T. & SUDHOF, T. C. 2003. Membrane fusion. *Cell,* 112**,** 519-33.
JAHN, R. & SCHELLER, R. H. 2006. SNAREs--engines for membrane fusion. *Nat Rev Mol Cell Biol,* 7**,** 631-43.
JEWELL, J. L., LUO, W., OH, E., WANG, Z. & THURMOND, D. C. 2008. Filamentous Actin Regulates Insulin Exocytosis through Direct Interaction with Syntaxin 4. *J Biol Chem,* 283**,** 10716-26.
JEWELL, J. L., RUSSELL, R. C. & GUAN, K. L. 2013. Amino acid signalling upstream of mTOR. *Nat Rev Mol Cell Biol,* 14**,** 133-9.
JING, X., LI, D. Q., OLOFSSON, C. S., SALEHI, A., SURVE, V. V., CABALLERO, J., IVARSSON, R., LUNDQUIST, I., PEREVERZEV, A., SCHNEIDER, T., RORSMAN, P. & RENSTROM, E. 2005. CaV2.3 calcium channels control second-phase insulin release. *J Clin Invest,* 115**,** 146-54.
JITRAPAKDEE, S., WUTTHISATHAPORNCHAI, A., WALLACE, J. C. & MACDONALD, M. J. 2010. Regulation of insulin secretion: role of mitochondrial signalling. *Diabetologia,* 53**,** 1019-32.
JOHNSON, J. H., NEWGARD, C. B., MILBURN, J. L., LODISH, H. F. & THORENS, B. 1990. The high Km glucose transporter of islets of Langerhans is functionally similar to the low affinity transporter of liver and has an identical primary sequence. *J Biol Chem,* 265**,** 6548-51.
JOSHI, R. L., LAMOTHE, B., CORDONNIER, N., MESBAH, K., MONTHIOUX, E., JAMI, J. & BUCCHINI, D. 1996. Targeted disruption of the insulin receptor gene in the mouse results in neonatal lethality. *EMBO J,* 15**,** 1542-7.
JUSTICE, M. J., NOVEROSKE, J. K., WEBER, J. S., ZHENG, B. & BRADLEY, A. 1999. Mouse ENU mutagenesis. *Hum Mol Genet,* 8**,** 1955-63.
KADOWAKI, T., KADOWAKI, H., MORI, Y., TOBE, K., SAKUTA, R., SUZUKI, Y., TANABE, Y., SAKURA, H., AWATA, T., GOTO, Y. & ET AL. 1994. A subtype of diabetes mellitus associated with a mutation of mitochondrial DNA. *N Engl J Med,* 330**,** 962-8.
KAHN, S. E., HULL, R. L. & UTZSCHNEIDER, K. M. 2006. Mechanisms linking obesity to insulin resistance and type 2 diabetes. *Nature,* 444**,** 840-6.
KANG, G., JOSEPH, J. W., CHEPURNY, O. G., MONACO, M., WHEELER, M. B., BOS, J. L., SCHWEDE, F., GENIESER, H. G. & HOLZ, G. G. 2003. Epac-selective cAMP analog 8-pCPT-2'-O-Me-cAMP as a stimulus for Ca2+-induced Ca2+ release and exocytosis in pancreatic beta-cells. *J Biol Chem,* 278**,** 8279-85.
KARANAUSKAITE, J., HOPPA, M. B., BRAUN, M., GALVANOVSKIS, J. & RORSMAN, P. 2009. Quantal ATP release in rat beta-cells by exocytosis of insulin-containing LDCVs. *Pflugers Arch,* 458**,** 389-401.
KARPE, F., DICKMANN, J. R. & FRAYN, K. N. 2011. Fatty acids, obesity, and insulin resistance: time for a reevaluation. *Diabetes,* 60**,** 2441-9.
KASAI, H. 1999. Comparative biology of Ca2+-dependent exocytosis: implications of kinetic diversity for secretory function. *Trends Neurosci,* 22**,** 88-93.
KAWAMORI, D., KURPAD, A. J., HU, J., LIEW, C. W., SHIH, J. L., FORD, E. L., HERRERA, P. L., POLONSKY, K. S., MCGUINNESS, O. P. & KULKARNI, R. N. 2009. Insulin signaling in alpha cells modulates glucagon secretion in vivo. *Cell Metab,* 9**,** 350-61.

KHAKH, B. S., BAO, X. R., LABARCA, C. & LESTER, H. A. 1999. Neuronal P2X transmitter-gated cation channels change their ion selectivity in seconds. *Nat Neurosci,* 2**,** 322-30.

KHVOTCHEV, M. V., REN, M., TAKAMORI, S., JAHN, R. & SUDHOF, T. C. 2003. Divergent functions of neuronal Rab11b in Ca2+-regulated versus constitutive exocytosis. *J Neurosci,* 23**,** 10531-9.

KIM, A., MILLER, K., JO, J., KILIMNIK, G., WOJCIK, P. & HARA, M. 2009. Islet architecture: A comparative study. *Islets,* 1**,** 129-36.

KIM, Y. B., SHULMAN, G. I. & KAHN, B. B. 2002. Fatty acid infusion selectively impairs insulin action on Akt1 and protein kinase C lambda /zeta but not on glycogen synthase kinase-3. *J Biol Chem,* 277**,** 32915-22.

KIURU, M., LAUNONEN, V., HIETALA, M., AITTOMAKI, K., VIERIMAA, O., SALOVAARA, R., AROLA, J., PUKKALA, E., SISTONEN, P., HERVA, R. & AALTONEN, L. A. 2001. Familial cutaneous leiomyomatosis is a two-hit condition associated with renal cell cancer of characteristic histopathology. *Am J Pathol,* 159**,** 825-9.

KOVACS, P. & STUMVOLL, M. 2005. Fatty acids and insulin resistance in muscle and liver. *Best Pract Res Clin Endocrinol Metab,* 19**,** 625-35.

KOWLURU, A., SEAVEY, S. E., LI, G., SORENSON, R. L., WEINHAUS, A. J., NESHER, R., RABAGLIA, M. E., VADAKEKALAM, J. & METZ, S. A. 1996. Glucose- and GTP-dependent stimulation of the carboxyl methylation of CDC42 in rodent and human pancreatic islets and pure beta cells. Evidence for an essential role of GTP-binding proteins in nutrient-induced insulin secretion. *J Clin Invest,* 98**,** 540-55.

KROGVOLD, L., EDWIN, B., BUANES, T., FRISK, G., SKOG, O., ANAGANDULA, M., KORSGREN, O., UNDLIEN, D., EIKE, M. C., RICHARDSON, S. J., LEETE, P., MORGAN, N. G., OIKARINEN, S., OIKARINEN, M., LAIHO, J. E., HYOTY, H., LUDVIGSSON, J., HANSSEN, K. F. & DAHL-JORGENSEN, K. 2015a. Detection of a low-grade enteroviral infection in the islets of langerhans of living patients newly diagnosed with type 1 diabetes. *Diabetes,* 64**,** 1682-7.

KROGVOLD, L., SKOG, O., SUNDSTROM, G., EDWIN, B., BUANES, T., HANSSEN, K. F., LUDVIGSSON, J., GRABHERR, M., KORSGREN, O. & DAHL-JORGENSEN, K. 2015b. Function of Isolated Pancreatic Islets From Patients at Onset of Type 1 Diabetes: Insulin Secretion Can Be Restored After Some Days in a Nondiabetogenic Environment In Vitro: Results From the DiViD Study. *Diabetes,* 64**,** 2506-12.

KULKARNI, R. N., BRUNING, J. C., WINNAY, J. N., POSTIC, C., MAGNUSON, M. A. & KAHN, C. R. 1999. Tissue-specific knockout of the insulin receptor in pancreatic beta cells creates an insulin secretory defect similar to that in type 2 diabetes. *Cell,* 96**,** 329-39.

LACY, P. E., WALKER, M. M. & FINK, C. J. 1972. Perifusion of isolated rat islets in vitro. Participation of the microtubular system in the biphasic release of insulin. *Diabetes,* 21**,** 987-98.

LAKE, S. P., BASSETT, P. D., LARKINS, A., REVELL, J., WALCZAK, K., CHAMBERLAIN, J., RUMFORD, G. M., LONDON, N. J., VEITCH, P. S., BELL, P. R. & ET AL. 1989. Large-scale purification of human islets utilizing discontinuous albumin gradient on IBM 2991 cell separator. *Diabetes,* 38 Suppl 1**,** 143-5.

LAKSO, M., SAUER, B., MOSINGER, B., JR., LEE, E. J., MANNING, R. W., YU, S. H., MULDER, K. L. & WESTPHAL, H. 1992. Targeted oncogene activation by site-specific recombination in transgenic mice. *Proc Natl Acad Sci U S A,* 89**,** 6232-6.

LAM, P. P., OHNO, M., DOLAI, S., HE, Y., QIN, T., LIANG, T., ZHU, D., KANG, Y., LIU, Y., KAUPPI, M., XIE, L., WAN, W. C., BIN, N. R., SUGITA, S., OLKKONEN, V. M., TAKAHASHI, N., KASAI, H. & GAISANO, H. Y. 2013. Munc18b is a major mediator of insulin exocytosis in rat pancreatic beta-cells. *Diabetes,* 62**,** 2416-28.

LANG, J., FUKUDA, M., ZHANG, H., MIKOSHIBA, K. & WOLLHEIM, C. B. 1997. The first C2 domain of synaptotagmin is required for exocytosis of insulin from pancreatic beta-cells: action of synaptotagmin at low micromolar calcium. *EMBO J,* 16**,** 5837-46.

LARSSON, S. C., ORSINI, N. & WOLK, A. 2005. Diabetes mellitus and risk of colorectal cancer: a meta-analysis. *J Natl Cancer Inst,* 97**,** 1679-87.

LARSSON, S. C. & WOLK, A. 2011. Diabetes mellitus and incidence of kidney cancer: a meta-analysis of cohort studies. *Diabetologia,* 54**,** 1013-8.

LEE, A. W. S. & COX, R. D. 2011. Use of mouse models in studying type 2 diabetes mellitus. *Expert Reviews in Molecular Medicine,* 13.

LEE, Y., WANG, M. Y., DU, X. Q., CHARRON, M. J. & UNGER, R. H. 2011. Glucagon receptor knockout prevents insulin-deficient type 1 diabetes in mice. *Diabetes,* 60**,** 391-7.

LEITZ, J. & KAVALALI, E. T. 2011. Ca2+ Influx Slows Single Synaptic Vesicle Endocytosis. *Journal of Neuroscience,* 31**,** 16318-16326.

LELOUP, C., CASTEILLA, L., CARRIERE, A., GALINIER, A., BENANI, A., CARNEIRO, L. & PENICAUD, L. 2011. Balancing mitochondrial redox signaling: a key point in metabolic regulation. *Antioxid Redox Signal,* 14**,** 519-30.

LELOUP, C., TOURREL-CUZIN, C., MAGNAN, C., KARACA, M., CASTEL, J., CARNEIRO, L., COLOMBANI, A. L., KTORZA, A., CASTEILLA, L. & PENICAUD, L. 2009. Mitochondrial reactive oxygen species are obligatory signals for glucose-induced insulin secretion. *Diabetes,* 58**,** 673-81.

LEMAIRE, K., RAVIER, M. A., SCHRAENEN, A., CREEMERS, J. W., VAN DE PLAS, R., GRANVIK, M., VAN LOMMEL, L., WAELKENS, E., CHIMIENTI, F., RUTTER, G. A., GILON, P., IN'T VELD, P. A. & SCHUIT, F. C. 2009. Insulin crystallization depends on zinc transporter ZnT8 expression, but is not required for normal glucose homeostasis in mice. *Proc Natl Acad Sci U S A,* 106**,** 14872-7.

LEUNG, Y. M., AHMED, I., SHEU, L., TSUSHIMA, R. G., DIAMANT, N. E. & GAISANO, H. Y. 2006. Two populations of pancreatic islet alpha-cells displaying distinct Ca2+ channel properties. *Biochem Biophys Res Commun,* 345**,** 340-4.

LI, D., CHEN, S., BELLOMO, E. A., TARASOV, A. I., KAUT, C., RUTTER, G. A. & LI, W. H. 2011. Imaging dynamic insulin release using a fluorescent zinc indicator for monitoring induced exocytotic release (ZIMIR). *Proc Natl Acad Sci U S A,* 108**,** 21063-8.

LI, J., CANTLEY, J., BURCHFIELD, J. G., MEOLI, C. C., STOCKLI, J., WHITWORTH, P. T., PANT, H., CHAUDHURI, R., GROFFEN, A. J., VERHAGE, M. & JAMES, D. E. 2014a. DOC2 isoforms play dual roles in insulin secretion and insulin-stimulated glucose uptake. *Diabetologia,* 57**,** 2173-82.

LI, L., TRIFUNOVIC, A., KOHLER, M., WANG, Y., BERGLUND, J. P., ILLIES, C., JUNTTI-BERGGREN, L., LARSSON, N. G. & BERGGREN, P. O. 2014b. Defects in beta-Cell Ca2+ Dynamics in Age-Induced Diabetes. *Diabetes*.

LI, Z. & MURTHY, V. N. 2001. Visualizing postendocytic traffic of synaptic vesicles at hippocampal synapses. *Neuron,* 31**,** 593-605.

LIAO, Y. L., SUN, Y. M., CHAU, G. Y., CHAU, Y. P., LAI, T. C., WANG, J. L., HORNG, J. T., HSIAO, M. & TSOU, A. P. 2008. Identification of SOX4 target genes using phylogenetic footprinting-based prediction from expression microarrays suggests that overexpression of SOX4 potentiates metastasis in hepatocellular carcinoma. *Oncogene,* 27**,** 5578-89.

LIN, R. C. & SCHELLER, R. H. 1997. Structural organization of the synaptic exocytosis core complex. *Neuron,* 19**,** 1087-94.

LINDAU, M. 2012. High resolution electrophysiological techniques for the study of calcium-activated exocytosis. *Biochim Biophys Acta,* 1820**,** 1234-42.

LIU, Y. J., VIEIRA, E. & GYLFE, E. 2004. A store-operated mechanism determines the activity of the electrically excitable glucagon-secreting pancreatic alpha-cell. *Cell Calcium,* 35**,** 357-65.

LOCKE, J. M., WEI, F. Y., TOMIZAWA, K., WEEDON, M. N. & HARRIES, L. W. 2015. A cautionary tale: the non-causal association between type 2 diabetes risk SNP, rs7756992, and levels of non-coding RNA, CDKAL1-v1. *Diabetologia*.

LOLLIKE, K., BORREGAARD, N. & LINDAU, M. 1995. The exocytotic fusion pore of small granules has a conductance similar to an ion channel. *J Cell Biol,* 129**,** 99-104.

LOLLIKE, K., BORREGAARD, N. & LINDAU, M. 1998. Capacitance flickers and pseudoflickers of small granules, measured in the cell-attached configuration. *Biophys J,* 75**,** 53-9.

LOLLIKE, K. & LINDAU, M. 1999. Membrane capacitance techniques to monitor granule exocytosis in neutrophils. *J Immunol Methods,* 232**,** 111-20.

LU, C., WARD, P. S., KAPOOR, G. S., ROHLE, D., TURCAN, S., ABDEL-WAHAB, O., EDWARDS, C. R., KHANIN, R., FIGUEROA, M. E., MELNICK, A., WELLEN, K. E., O'ROURKE, D. M., BERGER, S. L., CHAN, T. A., LEVINE, R. L., MELLINGHOFF, I. K. & THOMPSON, C. B. 2012. IDH mutation impairs histone demethylation and results in a block to cell differentiation. *Nature,* 483**,** 474-8.

LU, H., KOSHKIN, V., ALLISTER, E. M., GYULKHANDANYAN, A. V. & WHEELER, M. B. 2010. Molecular and metabolic evidence for mitochondrial defects associated with beta-cell dysfunction in a mouse model of type 2 diabetes. *Diabetes,* 59**,** 448-59.

MACDONALD, P. E., BRAUN, M., GALVANOVSKIS, J. & RORSMAN, P. 2006. Release of small transmitters through kiss-and-run fusion pores in rat pancreatic beta cells. *Cell Metab,* 4**,** 283-90.

MACDONALD, P. E. & RORSMAN, P. 2007. The ins and outs of secretion from pancreatic beta-cells: control of single-vesicle exo- and endocytosis. *Physiology (Bethesda),* 22**,** 113-21.

MACLAREN, N. & ATKINSON, M. 1992. Is insulin-dependent diabetes mellitus environmentally induced? *N Engl J Med,* 327**,** 348-9.

MAECHLER, P., LI, N., CASIMIR, M., VETTERLI, L., FRIGERIO, F. & BRUN, T. 2010. Role of mitochondria in beta-cell function and dysfunction. *Adv Exp Med Biol,* 654**,** 193-216.

MAECHLER, P. & WOLLHEIM, C. B. 1999. Mitochondrial glutamate acts as a messenger in glucose-induced insulin exocytosis. *Nature,* 402**,** 685-9.
MAGKOS, F., PATTERSON, B. W., MOHAMMED, B. S., KLEIN, S. & MITTENDORFER, B. 2007. Women produce fewer but triglyceride-richer very low-density lipoproteins than men. *J Clin Endocrinol Metab,* 92**,** 1311-8.
MALAISSE, W. J. & SENER, A. 1988. Hexose metabolism in pancreatic islets. Feedback control of D-glucose oxidation by functional events. *Biochim Biophys Acta,* 971**,** 246-54.
MALINOW, R., SCHULMAN, H. & TSIEN, R. W. 1989. Inhibition of postsynaptic PKC or CaMKII blocks induction but not expression of LTP. *Science,* 245**,** 862-6.
MARIEB, E. N. H., K. 2005. *Human Anatomy & Physiology* San Francisco, USA, Pearson Benjamin Cummings.
MARLISS, E. B., GIRARDIER, L., SEYDOUX, J., WOLLHEIM, C. B., KANAZAWA, Y., ORCI, L., RENOLD, A. E. & PORTE, D., JR. 1973. Glucagon release induced by pancreatic nerve stimulation in the dog. *J Clin Invest,* 52**,** 1246-59.
MARSELLI, L., THORNE, J., AHN, Y. B., OMER, A., SGROI, D. C., LIBERMANN, T., OTU, H. H., SHARMA, A., BONNER-WEIR, S. & WEIR, G. C. 2008. Gene expression of purified beta-cell tissue obtained from human pancreas with laser capture microdissection. *J Clin Endocrinol Metab,* 93**,** 1046-53.
MARULLO, L., EL-SAYED MOUSTAFA, J. S. & PROKOPENKO, I. 2014. Insights into the genetic susceptibility to type 2 diabetes from genome-wide association studies of glycaemic traits. *Curr Diab Rep,* 14**,** 551.
MARZ, K. E., LAUER, J. M. & HANSON, P. I. 2003. Defining the SNARE complex binding surface of alpha-SNAP: implications for SNARE complex disassembly. *J Biol Chem,* 278**,** 27000-8.
MCCARTHY, M. I. 2010. Genomics, type 2 diabetes, and obesity. *N Engl J Med,* 363**,** 2339-50.
MCCULLOCH, L. J., VAN DE BUNT, M., BRAUN, M., FRAYN, K. N., CLARK, A. & GLOYN, A. L. 2011. GLUT2 (SLC2A2) is not the principal glucose transporter in human pancreatic beta cells: implications for understanding genetic association signals at this locus. *Mol Genet Metab,* 104**,** 648-53.
MCNEW, J. A. 2008. Regulation of SNARE-mediated membrane fusion during exocytosis. *Chem Rev,* 108**,** 1669-86.
MEGLASSON, M. D. & MATSCHINSKY, F. M. 1984. New perspectives on pancreatic islet glucokinase. *Am J Physiol,* 246**,** E1-13.
MELLANDER, L. J., TROUILLON, R., SVENSSON, M. I. & EWING, A. G. 2012. Amperometric post spike feet reveal most exocytosis is via extended kiss-and-run fusion. *Sci Rep,* 2**,** 907.
MENTING, J. G., WHITTAKER, J., MARGETTS, M. B., WHITTAKER, L. J., KONG, G. K., SMITH, B. J., WATSON, C. J., ZAKOVA, L., KLETVIKOVA, E., JIRACEK, J., CHAN, S. J., STEINER, D. F., DODSON, G. G., BRZOZOWSKI, A. M., WEISS, M. A., WARD, C. W. & LAWRENCE, M. C. 2013. How insulin engages its primary binding site on the insulin receptor. *Nature,* 493**,** 241-5.
MICHAEL, D. J., RITZEL, R. A., HAATAJA, L. & CHOW, R. H. 2006. Pancreatic beta-cells secrete insulin in fast- and slow-release forms. *Diabetes,* 55**,** 600-7.
MICHAEL, M. D., KULKARNI, R. N., POSTIC, C., PREVIS, S. F., SHULMAN, G. I., MAGNUSON, M. A. & KAHN, C. R. 2000. Loss of insulin signaling in

hepatocytes leads to severe insulin resistance and progressive hepatic dysfunction. *Mol Cell,* 6**,** 87-97.

MIESENBOCK, G., DE ANGELIS, D. A. & ROTHMAN, J. E. 1998. Visualizing secretion and synaptic transmission with pH-sensitive green fluorescent proteins. *Nature,* 394**,** 192-5.

MIYAZAKI, M., EMOTO, M., FUKUDA, N., HATANAKA, M., TAGUCHI, A., MIYAMOTO, S. & TANIZAWA, Y. 2009. DOC2b is a SNARE regulator of glucose-stimulated delayed insulin secretion. *Biochem Biophys Res Commun,* 384**,** 461-5.

MOLINA, A. J., WIKSTROM, J. D., STILES, L., LAS, G., MOHAMED, H., ELORZA, A., WALZER, G., TWIG, G., KATZ, S., CORKEY, B. E. & SHIRIHAI, O. S. 2009. Mitochondrial networking protects beta-cells from nutrient-induced apoptosis. *Diabetes,* 58**,** 2303-15.

MONTAGUE, C. T. & O'RAHILLY, S. 2000. The perils of portliness: causes and consequences of visceral adiposity. *Diabetes,* 49**,** 883-8.

MONTANYA, E., NACHER, V., BIARNES, M. & SOLER, J. 2000. Linear correlation between beta-cell mass and body weight throughout the lifespan in Lewis rats: role of beta-cell hyperplasia and hypertrophy. *Diabetes,* 49**,** 1341-6.

MORGAN, A., DIMALINE, R. & BURGOYNE, R. D. 1994. The ATPase activity of N-ethylmaleimide-sensitive fusion protein (NSF) is regulated by soluble NSF attachment proteins. *J Biol Chem,* 269**,** 29347-50.

MULLEN, A. R., WHEATON, W. W., JIN, E. S., CHEN, P. H., SULLIVAN, L. B., CHENG, T., YANG, Y., LINEHAN, W. M., CHANDEL, N. S. & DEBERARDINIS, R. J. 2012. Reductive carboxylation supports growth in tumour cells with defective mitochondria. *Nature,* 481**,** 385-8.

MURLIN, J., CLUGH, H., GIBBS, C. & STOKES, A. 1923. Aqueous extracts of the pancreas. 1. Influence on the carbohydrate metabolism of depancreatized animals. *J Biol Chem,* 56**,** 253-296.

MUSSIG, K., STAIGER, H., MACHICAO, F., KIRCHHOFF, K., GUTHOFF, M., SCHAFER, S. A., KANTARTZIS, K., SILBERNAGEL, G., STEFAN, N., HOLST, J. J., GALLWITZ, B., HARING, H. U. & FRITSCHE, A. 2009. Association of type 2 diabetes candidate polymorphisms in KCNQ1 with incretin and insulin secretion. *Diabetes,* 58**,** 1715-20.

NAGAI, R., BROCK, J. W., BLATNIK, M., BAATZ, J. E., BETHARD, J., WALLA, M. D., THORPE, S. R., BAYNES, J. W. & FRIZZELL, N. 2007. Succination of protein thiols during adipocyte maturation: a biomarker of mitochondrial stress. *J Biol Chem,* 282**,** 34219-28.

NAGY, A. 2000. Cre recombinase: the universal reagent for genome tailoring. *Genesis,* 26**,** 99-109.

NEEF, A., HEINEMANN, C. & MOSER, T. 2007. Measurements of membrane patch capacitance using a software-based lock-in system. *Pflugers Arch,* 454**,** 335-44.

NEHER, E. 1998. Vesicle pools and Ca2+ microdomains: new tools for understanding their roles in neurotransmitter release. *Neuron,* 20**,** 389-99.

NEPOM, G. T. 1990. A unified hypothesis for the complex genetics of HLA associations with IDDM. *Diabetes,* 39**,** 1153-7.

NICA, A. C., ONGEN, H., IRMINGER, J. C., BOSCO, D., BERNEY, T., ANTONARAKIS, S. E., HALBAN, P. A. & DERMITZAKIS, E. T. 2013. Cell-type, allelic, and genetic signatures in the human pancreatic beta cell transcriptome. *Genome Res,* 23**,** 1554-62.

NICHOLS, C. G. 2006. K-ATP channels as molecular sensors of cellular metabolism. *Nature,* 440**,** 470-476.

NICOLSON, T. J., BELLOMO, E. A., WIJESEKARA, N., LODER, M. K., BALDWIN, J. M., GYULKHANDANYAN, A. V., KOSHKIN, V., TARASOV, A. I., CARZANIGA, R., KRONENBERGER, K., TANEJA, T. K., DA SILVA XAVIER, G., LIBERT, S., FROGUEL, P., SCHARFMANN, R., STETSYUK, V., RAVASSARD, P., PARKER, H., GRIBBLE, F. M., REIMANN, F., SLADEK, R., HUGHES, S. J., JOHNSON, P. R., MASSEBOEUF, M., BURCELIN, R., BALDWIN, S. A., LIU, M., LARA-LEMUS, R., ARVAN, P., SCHUIT, F. C., WHEELER, M. B., CHIMIENTI, F. & RUTTER, G. A. 2009. Insulin storage and glucose homeostasis in mice null for the granule zinc transporter ZnT8 and studies of the type 2 diabetes-associated variants. *Diabetes,* 58**,** 2070-83.

NIGRO, J., OSMAN, N., DART, A. M. & LITTLE, P. J. 2006. Insulin resistance and atherosclerosis. *Endocr Rev,* 27**,** 242-59.

NISHI, T. & FORGAC, M. 2002. The vacuolar (H+)-atpases - Nature's most versatile proton pumps. *Nature Reviews Molecular Cell Biology,* 3**,** 94-103.

NISHIMORI, I., FUJIKAWAADACHI, K., ONISHI, S. & HOLLINGSWORTH, M. A. 1999. Carbonic anhydrase in human pancreas: hypotheses for the pathophysiological roles of CA isozymes. *Ann N Y Acad Sci,* 880**,** 5-16.

NISHIMORI, I. & ONISHI, S. 2001. Carbonic anhydrase isozymes in the human pancreas. *Dig Liver Dis,* 33**,** 68-74.

NOVEROSKE, J. K., WEBER, J. S. & JUSTICE, M. J. 2000. The mutagenic action of N-ethyl-N-nitrosourea in the mouse. *Mamm Genome,* 11**,** 478-83.

OBERMULLER, S., LINDQVIST, A., KARANAUSKAITE, J., GALVANOVSKIS, J., RORSMAN, P. & BARG, S. 2005. Selective nucleotide-release from dense-core granules in insulin-secreting cells. *J Cell Sci,* 118**,** 4271-82.

OHARA-IMAIZUMI, M., AOYAGI, K., AKIMOTO, Y., NAKAMICHI, Y., NISHIWAKI, C., KAWAKAMI, H. & NAGAMATSU, S. 2009. Imaging exocytosis of single glucagon-like peptide-1 containing granules in a murine enteroendocrine cell line with total internal reflection fluorescent microscopy. *Biochem Biophys Res Commun,* 390**,** 16-20.

OHARA-IMAIZUMI, M., FUJIWARA, T., NAKAMICHI, Y., OKAMURA, T., AKIMOTO, Y., KAWAI, J., MATSUSHIMA, S., KAWAKAMI, H., WATANABE, T., AKAGAWA, K. & NAGAMATSU, S. 2007. Imaging analysis reveals mechanistic differences between first- and second-phase insulin exocytosis. *J Cell Biol,* 177**,** 695-705.

OHARA-IMAIZUMI, M., YOSHIDA, M., AOYAGI, K., SAITO, T., OKAMURA, T., TAKENAKA, H., AKIMOTO, Y., NAKAMICHI, Y., TAKANASHI-YANOBU, R., NISHIWAKI, C., KAWAKAMI, H., KATO, N., HISANAGA, S., KAKEI, M. & NAGAMATSU, S. 2010. Deletion of CDKAL1 affects mitochondrial ATP generation and first-phase insulin exocytosis. *PLoS One,* 5**,** e15553.

OHTSUBO, K., TAKAMATSU, S., MINOWA, M. T., YOSHIDA, A., TAKEUCHI, M. & MARTH, J. D. 2005. Dietary and genetic control of glucose transporter 2 glycosylation promotes insulin secretion in suppressing diabetes. *Cell,* 123**,** 1307-21.

OLEFSKY, J. M., KOLTERMAN, O. G. & SCARLETT, J. A. 1982. Insulin action and resistance in obesity and noninsulin-dependent type II diabetes mellitus. *Am J Physiol,* 243**,** E15-30.

OLOFSSON, C. S., GOPEL, S. O., BARG, S., GALVANOVSKIS, J., MA, X., SALEHI, A., RORSMAN, P. & ELIASSON, L. 2002. Fast insulin secretion reflects exocytosis of docked granules in mouse pancreatic B-cells. *Pflugers Arch,* 444**,** 43-51.

OLOFSSON, C. S., HAKANSSON, J., SALEHI, A., BENGTSSON, M., GALVANOVSKIS, J., PARTRIDGE, C., SORHEDEWINZELL, M., XIAN, X., ELIASSON, L., LUNDQUIST, I., SEMB, H. & RORSMAN, P. 2009. Impaired insulin exocytosis in neural cell adhesion molecule-/- mice due to defective reorganization of the submembrane F-actin network. *Endocrinology,* 150**,** 3067-75.

ONO, H., YOSHIMURA, N., SATO, M. & TUBOI, S. 1985. Translocation of proteins into rat liver mitochondria. Existence of two different precursor polypeptides of liver fumarase and import of the precursor into mitochondria. *J Biol Chem,* 260**,** 3402-7.

ORCI, L., MALAISSE-LAGAE, F., RAVAZZOLA, M., AMHERDT, M. & RENOLD, A. E. 1973. Exocytosis-endocytosis coupling in the pancreatic beta cell. *Science,* 181**,** 561-2.

OWEN, O. E., KALHAN, S. C. & HANSON, R. W. 2002. The key role of anaplerosis and cataplerosis for citric acid cycle function. *J Biol Chem,* 277**,** 30409-12.

PARLATI, F., MCNEW, J. A., FUKUDA, R., MILLER, R., SOLLNER, T. H. & ROTHMAN, J. E. 2000. Topological restriction of SNARE-dependent membrane fusion. *Nature,* 407**,** 194-8.

PARSONS, T. D., COORSSEN, J. R., HORSTMANN, H. & ALMERS, W. 1995. Docked granules, the exocytic burst, and the need for ATP hydrolysis in endocrine cells. *Neuron,* 15**,** 1085-96.

PASCOE, L., TURA, A., PATEL, S. K., IBRAHIM, I. M., FERRANNINI, E., ZEGGINI, E., WEEDON, M. N., MARI, A., HATTERSLEY, A. T., MCCARTHY, M. I., FRAYLING, T. M., WALKER, M., CONSORTIUM, R. & CONSORTIUM, U. K. T. D. G. 2007. Common variants of the novel type 2 diabetes genes CDKAL1 and HHEX/IDE are associated with decreased pancreatic beta-cell function. *Diabetes,* 56**,** 3101-4.

PATEL, A. C., NUNEZ, N. P., PERKINS, S. N., BARRETT, J. C. & HURSTING, S. D. 2004. Effects of energy balance on cancer in genetically altered mice. *J Nutr,* 134**,** 3394S-3398S.

PEDERSEN, M. G. & SHERMAN, A. 2009. Newcomer insulin secretory granules as a highly calcium-sensitive pool. *Proc Natl Acad Sci U S A,* 106**,** 7432-6.

PENZO-MENDEZ, A. I. 2010. Critical roles for SoxC transcription factors in development and cancer. *Int J Biochem Cell Biol,* 42**,** 425-8.

PETERSEN, K. F., BEFROY, D., DUFOUR, S., DZIURA, J., ARIYAN, C., ROTHMAN, D. L., DIPIETRO, L., CLINE, G. W. & SHULMAN, G. I. 2003. Mitochondrial dysfunction in the elderly: possible role in insulin resistance. *Science,* 300**,** 1140-2.

PFAFFL, M. W. 2001. A new mathematical model for relative quantification in real-time RT-PCR. *Nucleic Acids Res,* 29**,** e45.

POBBATI, A. V., RAZETO, A., BODDENER, M., BECKER, S. & FASSHAUER, D. 2004. Structural basis for the inhibitory role of tomosyn in exocytosis. *J Biol Chem,* 279**,** 47192-200.

POCIOT, F., AKOLKAR, B., CONCANNON, P., ERLICH, H. A., JULIER, C., MORAHAN, G., NIERRAS, C. R., TODD, J. A., RICH, S. S. & NERUP, J. 2010. Genetics of type 1 diabetes: what's next? *Diabetes,* 59**,** 1561-71.

POLLARD, P. J., BRIERE, J. J., ALAM, N. A., BARWELL, J., BARCLAY, E., WORTHAM, N. C., HUNT, T., MITCHELL, M., OLPIN, S., MOAT, S. J., HARGREAVES, I. P., HEALES, S. J., CHUNG, Y. L., GRIFFITHS, J. R., DALGLEISH, A., MCGRATH, J. A., GLEESON, M. J., HODGSON, S. V., POULSOM, R., RUSTIN, P. & TOMLINSON, I. P. 2005. Accumulation of Krebs cycle intermediates and over-expression of HIF1alpha in tumours which result from germline FH and SDH mutations. *Hum Mol Genet,* 14**,** 2231-9.

POLLARD, P. J., SPENCER-DENE, B., SHUKLA, D., HOWARTH, K., NYE, E., EL-BAHRAWY, M., DEHERAGODA, M., JOANNOU, M., MCDONALD, S., MARTIN, A., IGARASHI, P., VARSANI-BROWN, S., ROSEWELL, I., POULSOM, R., MAXWELL, P., STAMP, G. W. & TOMLINSON, I. P. 2007. Targeted inactivation of fh1 causes proliferative renal cyst development and activation of the hypoxia pathway. *Cancer Cell,* 11**,** 311-9.

POSTIC, C., SHIOTA, M., NISWENDER, K. D., JETTON, T. L., CHEN, Y., MOATES, J. M., SHELTON, K. D., LINDNER, J., CHERRINGTON, A. D. & MAGNUSON, M. A. 1999. Dual roles for glucokinase in glucose homeostasis as determined by liver and pancreatic beta cell-specific gene knock-outs using Cre recombinase. *J Biol Chem,* 274**,** 305-15.

POUND, L. D., SARKAR, S. A., BENNINGER, R. K., WANG, Y., SUWANICHKUL, A., SHADOAN, M. K., PRINTZ, R. L., OESER, J. K., LEE, C. E., PISTON, D. W., MCGUINNESS, O. P., HUTTON, J. C., POWELL, D. R. & O'BRIEN, R. M. 2009. Deletion of the mouse Slc30a8 gene encoding zinc transporter-8 results in impaired insulin secretion. *Biochem J,* 421**,** 371-6.

PRIOR, H. M. & WALTER, M. A. 1996. SOX genes: architects of development. *Mol Med,* 2**,** 405-12.

PURI, N. & ROCHE, P. A. 2006. Ternary SNARE complexes are enriched in lipid rafts during mast cell exocytosis. *Traffic,* 7**,** 1482-1494.

QADER, S. S., EKELUND, M., ANDERSSON, R., OBERMULLER, S. & SALEHI, A. 2003. Acute pancreatitis, expression of inducible nitric oxide synthase and defective insulin secretion. *Cell Tissue Res,* 313**,** 271-9.

RADKE, R. & STACH, W. 1986. Are the islets of Langerhans neuro-paraneuronal control centers of the exocrine pancreas? *Arch Histol Jpn,* 49**,** 411-20.

RAGVIN, A., MORO, E., FREDMAN, D., NAVRATILOVA, P., DRIVENES, O., ENGSTROM, P. G., ALONSO, M. E., DE LA CALLE MUSTIENES, E., GOMEZ SKARMETA, J. L., TAVARES, M. J., CASARES, F., MANZANARES, M., VAN HEYNINGEN, V., MOLVEN, A., NJOLSTAD, P. R., ARGENTON, F., LENHARD, B. & BECKER, T. S. 2010. Long-range gene regulation links genomic type 2 diabetes and obesity risk regions to HHEX, SOX4, and IRX3. *Proc Natl Acad Sci U S A,* 107**,** 775-80.

RAMRACHEYA, R., WARD, C., SHIGETO, M., WALKER, J. N., AMISTEN, S., ZHANG, Q., JOHNSON, P. R., RORSMAN, P. & BRAUN, M. 2010. Membrane potential-dependent inactivation of voltage-gated ion channels in alpha-cells inhibits glucagon secretion from human islets. *Diabetes,* 59**,** 2198-208.

RASK-MADSEN, C. & KING, G. L. 2007. Mechanisms of Disease: endothelial dysfunction in insulin resistance and diabetes. *Nat Clin Pract Endocrinol Metab,* 3**,** 46-56.

RATNER, S., ANSLOW, W. P., JR. & PETRACK, B. 1953. Biosynthesis of urea. VI. Enzymatic cleavage of argininosuccinic acid to arginine and fumaric acid. *J Biol Chem,* 204**,** 115-25.

RAVIER, M. A. & RUTTER, G. A. 2005. Glucose or insulin, but not zinc ions, inhibit glucagon secretion from mouse pancreatic alpha-cells. *Diabetes,* 54**,** 1789-97.

RAZA, H. 2011. Dual localization of glutathione S-transferase in the cytosol and mitochondria: implications in oxidative stress, toxicity and disease. *FEBS J,* 278**,** 4243-51.

REETZ, A., SOLIMENA, M., MATTEOLI, M., FOLLI, F., TAKEI, K. & DE CAMILLI, P. 1991. GABA and pancreatic beta-cells: colocalization of glutamic acid decarboxylase (GAD) and GABA with synaptic-like microvesicles suggests their role in GABA storage and secretion. *Embo J,* 10**,** 1275-84.

REGAZZI, R., KIKUCHI, A., TAKAI, Y. & WOLLHEIM, C. B. 1992. The small GTP-binding proteins in the cytosol of insulin-secreting cells are complexed to GDP dissociation inhibitor proteins. *J Biol Chem,* 267**,** 17512-9.

REGAZZI, R., SADOUL, K., MEDA, P., KELLY, R. B., HALBAN, P. A. & WOLLHEIM, C. B. 1996. Mutational analysis of VAMP domains implicated in Ca2+-induced insulin exocytosis. *EMBO J,* 15**,** 6951-9.

REGAZZI, R., WOLLHEIM, C. B., LANG, J., THELER, J. M., ROSSETTO, O., MONTECUCCO, C., SADOUL, K., WELLER, U., PALMER, M. & THORENS, B. 1995. VAMP-2 and cellubrevin are expressed in pancreatic beta-cells and are essential for Ca(2+)-but not for GTP gamma S-induced insulin secretion. *EMBO J,* 14**,** 2723-30.

RENSTROM, E., BARG, S., THEVENOD, F. & RORSMAN, P. 2002. Sulfonylurea-mediated stimulation of insulin exocytosis via an ATP-sensitive K+ channel-independent action. *Diabetes,* 51 Suppl 1**,** S33-6.

RENSTROM, E., ELIASSON, L. & RORSMAN, P. 1997. Protein kinase A-dependent and -independent stimulation of exocytosis by cAMP in mouse pancreatic B-cells. *J Physiol,* 502 (Pt 1)**,** 105-18.

RETTIG, J. & NEHER, E. 2002. Emerging roles of presynaptic proteins in Ca++-triggered exocytosis. *Science,* 298**,** 781-5.

RICHARDS, D. A. 2010. Regulation of exocytic mode in hippocampal neurons by intra-bouton calcium concentration. *J Physiol,* 588**,** 4927-36.

RICORDI, C., LACY, P. E., FINKE, E. H., OLACK, B. J. & SCHARP, D. W. 1988. Automated method for isolation of human pancreatic islets. *Diabetes,* 37**,** 413-20.

RORSMAN, P. & BRAUN, M. 2013. Regulation of insulin secretion in human pancreatic islets. *Annu Rev Physiol,* 75**,** 155-79.

RORSMAN, P., ELIASSON, L., RENSTROM, E., GROMADA, J., BARG, S. & GOPEL, S. 2000. The Cell Physiology of Biphasic Insulin Secretion. *News Physiol Sci,* 15**,** 72-77.

RORSMAN, P. & HELLMAN, B. 1988. Voltage-activated currents in guinea pig pancreatic alpha 2 cells. Evidence for Ca2+-dependent action potentials. *J Gen Physiol,* 91**,** 223-42.

RORSMAN, P., RAMRACHEYA, R., RORSMAN, N. J. & ZHANG, Q. 2014. ATP-regulated potassium channels and voltage-gated calcium channels in pancreatic alpha and beta cells: similar functions but reciprocal effects on secretion. *Diabetologia,* 57**,** 1749-61.

RORSMAN, P. & RENSTROM, E. 2003. Insulin granule dynamics in pancreatic beta cells. *Diabetologia,* 46**,** 1029-45.

RORSMAN, P., SALEHI, S. A., ABDULKADER, F., BRAUN, M. & MACDONALD, P. E. 2008. K(ATP)-channels and glucose-regulated glucagon secretion. *Trends Endocrinol Metab,* 19**,** 277-84.

ROSENGREN, A. H., BRAUN, M., MAHDI, T., ANDERSSON, S. A., TRAVERS, M. E., SHIGETO, M., ZHANG, E., ALMGREN, P., LADENVALL, C., AXELSSON, A. S., EDLUND, A., PEDERSEN, M. G., JONSSON, A., RAMRACHEYA, R., TANG, Y., WALKER, J. N., BARRETT, A., JOHNSON, P. R., LYSSENKO, V., MCCARTHY, M. I., GROOP, L., SALEHI, A., GLOYN, A. L., RENSTROM, E., RORSMAN, P. & ELIASSON, L. 2012. Reduced insulin exocytosis in human pancreatic beta-cells with gene variants linked to type 2 diabetes. *Diabetes,* 61**,** 1726-33.

ROSENGREN, A. H., JOKUBKA, R., TOJJAR, D., GRANHALL, C., HANSSON, O., LI, D. Q., NAGARAJ, V., REINBOTHE, T. M., TUNCEL, J., ELIASSON, L., GROOP, L., RORSMAN, P., SALEHI, A., LYSSENKO, V., LUTHMAN, H. & RENSTROM, E. 2010. Overexpression of alpha2A-adrenergic receptors contributes to type 2 diabetes. *Science,* 327**,** 217-20.

ROUX, A., UYHAZI, K., FROST, A. & DE CAMILLI, P. 2006. GTP-dependent twisting of dynamin implicates constriction and tension in membrane fission. *Nature,* 441**,** 528-31.

SABERI, M., BOHLAND, M. & DONOVAN, C. M. 2008. The locus for hypoglycemic detection shifts with the rate of fall in glycemia: the role of portal-superior mesenteric vein glucose sensing. *Diabetes,* 57**,** 1380-6.

SADOUL, K., BERGER, A., NIEMANN, H., WELLER, U., ROCHE, P. A., KLIP, A., TRIMBLE, W. S., REGAZZI, R., CATSICAS, S. & HALBAN, P. A. 1997. SNAP-23 is not cleaved by botulinum neurotoxin E and can replace SNAP-25 in the process of insulin secretion. *J Biol Chem,* 272**,** 33023-7.

SADOUL, K., LANG, J., MONTECUCCO, C., WELLER, U., REGAZZI, R., CATSICAS, S., WOLLHEIM, C. B. & HALBAN, P. A. 1995. SNAP-25 is expressed in islets of Langerhans and is involved in insulin release. *J Cell Biol,* 128**,** 1019-28.

SAEGUSA, M., HASHIMURA, M. & KUWATA, T. 2012. Sox4 functions as a positive regulator of beta-catenin signaling through upregulation of TCF4 during morular differentiation of endometrial carcinomas. *Lab Invest,* 92**,** 511-21.

SAKURA, H., AMMALA, C., SMITH, P. A., GRIBBLE, F. M. & ASHCROFT, F. M. 1995. Cloning and functional expression of the cDNA encoding a novel ATP-sensitive potassium channel subunit expressed in pancreatic beta-cells, brain, heart and skeletal muscle. *FEBS Lett,* 377**,** 338-44.

SALEHI, A., VIEIRA, E. & GYLFE, E. 2006. Paradoxical stimulation of glucagon secretion by high glucose concentrations. *Diabetes,* 55**,** 2318-23.

SALVIOLI, B., BOVARA, M., BARBARA, G., DE PONTI, F., STANGHELLINI, V., TONINI, M., GUERRINI, S., CREMON, C., DEGLI ESPOSTI, M., KOUMANDOU, M., CORINALDESI, R., STERNINI, C. & DE GIORGIO, R. 2002. Neurology and neuropathology of the pancreatic innervation. *JOP,* 3**,** 26-33.

SAMUEL, V. T., LIU, Z. X., QU, X., ELDER, B. D., BILZ, S., BEFROY, D., ROMANELLI, A. J. & SHULMAN, G. I. 2004. Mechanism of hepatic insulin resistance in non-alcoholic fatty liver disease. *J Biol Chem,* 279**,** 32345-53.

SAMUEL, V. T., PETERSEN, K. F. & SHULMAN, G. I. 2010. Lipid-induced insulin resistance: unravelling the mechanism. *Lancet,* 375**,** 2267-77.

SANKARANARAYANAN, S. & RYAN, T. A. 2000. Real-time measurements of vesicle-SNARE recycling in synapses of the central nervous system. *Nat Cell Biol,* 2**,** 197-204.

SATO, Y., ANELLO, M. & HENQUIN, J. C. 1999. Glucose regulation of insulin secretion independent of the opening or closure of adenosine triphosphate-sensitive K+ channels in beta cells. *Endocrinology,* 140**,** 2252-7.

SCALES, S. J., HESSER, B. A., MASUDA, E. S. & SCHELLER, R. H. 2002. Amisyn, a novel syntaxin-binding protein that may regulate SNARE complex assembly. *J Biol Chem,* 277**,** 28271-9.

SCEPEK, S., COORSSEN, J. R. & LINDAU, M. 1998. Fusion pore expansion in horse eosinophils is modulated by Ca2+ and protein kinase C via distinct mechanisms. *EMBO J,* 17**,** 4340-5.

SCHARER, C. D., MCCABE, C. D., ALI-SEYED, M., BERGER, M. F., BULYK, M. L. & MORENO, C. S. 2009. Genome-wide promoter analysis of the SOX4 transcriptional network in prostate cancer cells. *Cancer Res,* 69**,** 709-17.

SCHARFMANN, R., PECHBERTY, S., HAZHOUZ, Y., VON BULOW, M., BRICOUT-NEVEU, E., GRENIER-GODARD, M., GUEZ, F., RACHDI, L., LOHMANN, M., CZERNICHOW, P. & RAVASSARD, P. 2014. Development of a conditionally immortalized human pancreatic beta cell line. *J Clin Invest,* 124**,** 2087-98.

SCHAUB, J. R., LU, X., DONESKE, B., SHIN, Y. K. & MCNEW, J. A. 2006. Hemifusion arrest by complexin is relieved by Ca2+-synaptotagmin I. *Nat Struct Mol Biol,* 13**,** 748-50.

SCHEPERS, G. E., TEASDALE, R. D. & KOOPMAN, P. 2002. Twenty pairs of Sox: Extent, homology, and nomenclature of the mouse and human sox transcription factor gene families. *Developmental Cell,* 3**,** 167-170.

SCHIAVO, G., BENFENATI, F., POULAIN, B., ROSSETTO, O., POLVERINO DE LAURETO, P., DASGUPTA, B. R. & MONTECUCCO, C. 1992. Tetanus and botulinum-B neurotoxins block neurotransmitter release by proteolytic cleavage of synaptobrevin. *Nature,* 359**,** 832-5.

SCHNELL, A. H. & BORG, L. A. 1985. Lysosomes and pancreatic islet function. Glucose-dependent alterations of lysosomal morphology. *Cell Tissue Res,* 239**,** 537-45.

SCHUIT, F., MOENS, K., HEIMBERG, H. & PIPELEERS, D. 1999. Cellular origin of hexokinase in pancreatic islets. *J Biol Chem,* 274**,** 32803-9.

SCHULLA, V., RENSTROM, E., FEIL, R., FEIL, S., FRANKLIN, I., GJINOVCI, A., JING, X. J., LAUX, D., LUNDQUIST, I., MAGNUSON, M. A., OBERMULLER, S., OLOFSSON, C. S., SALEHI, A., WENDT, A., KLUGBAUER, N., WOLLHEIM, C. B., RORSMAN, P. & HOFMANN, F. 2003. Impaired insulin secretion and glucose tolerance in beta cell-selective Ca(v)1.2 Ca2+ channel null mice. *Embo J,* 22**,** 3844-54.

SCHULZE, A. & HARRIS, A. L. 2012. How cancer metabolism is tuned for proliferation and vulnerable to disruption. *Nature,* 491**,** 364-73.

SHAH, P., VELLA, A., BASU, A., BASU, R., SCHWENK, W. F. & RIZZA, R. A. 2000. Lack of suppression of glucagon contributes to postprandial hyperglycemia in subjects with type 2 diabetes mellitus. *J Clin Endocrinol Metab,* 85**,** 4053-9.

SHI, L., SHEN, Q. T., KIEL, A., WANG, J., WANG, H. W., MELIA, T. J., ROTHMAN, J. E. & PINCET, F. 2012. SNARE proteins: one to fuse and three to keep the nascent fusion pore open. *Science,* 335**,** 1355-9.

SHIBASAKI, T., TAKAHASHI, H., MIKI, T., SUNAGA, Y., MATSUMURA, K., YAMANAKA, M., ZHANG, C., TAMAMOTO, A., SATOH, T., MIYAZAKI, J. & SEINO, S. 2007. Essential role of Epac2/Rap1 signaling in regulation of insulin granule dynamics by cAMP. *Proc Natl Acad Sci U S A,* 104**,** 19333-8.

SHIGETO, M., KATSURA, M., MATSUDA, M., OHKUMA, S. & KAKU, K. 2008. Low, but physiological, concentration of GLP-1 stimulates insulin secretion independent of the cAMP-dependent protein kinase pathway. *J Pharmacol Sci,* 108**,** 274-9.

SINGAL, D. P. & BLAJCHMAN, M. A. 1973. Histocompatibility (HL-A) antigens, lymphocytotoxic antibodies and tissue antibodies in patients with diabetes mellitus. *Diabetes,* 22**,** 429-32.

SINNER, D., KORDICH, J. J., SPENCE, J. R., OPOKA, R., RANKIN, S., LIN, S. C., JONATAN, D., ZORN, A. M. & WELLS, J. M. 2007. Sox17 and Sox4 differentially regulate beta-catenin/T-cell factor activity and proliferation of colon carcinoma cells. *Mol Cell Biol,* 27**,** 7802-15.

SKARNES, W. C., ROSEN, B., WEST, A. P., KOUTSOURAKIS, M., BUSHELL, W., IYER, V., MUJICA, A. O., THOMAS, M., HARROW, J., COX, T., JACKSON, D., SEVERIN, J., BIGGS, P., FU, J., NEFEDOV, M., DE JONG, P. J., STEWART, A. F. & BRADLEY, A. 2011. A conditional knockout resource for the genome-wide study of mouse gene function. *Nature,* 474**,** 337-U361.

SOLLNER, T., BENNETT, M. K., WHITEHEART, S. W., SCHELLER, R. H. & ROTHMAN, J. E. 1993a. A protein assembly-disassembly pathway in vitro that may correspond to sequential steps of synaptic vesicle docking, activation, and fusion. *Cell,* 75**,** 409-18.

SOLLNER, T., WHITEHEART, S. W., BRUNNER, M., ERDJUMENT-BROMAGE, H., GEROMANOS, S., TEMPST, P. & ROTHMAN, J. E. 1993b. SNAP receptors implicated in vesicle targeting and fusion. *Nature,* 362**,** 318-24.

STAAL, R. G., MOSHAROV, E. V. & SULZER, D. 2004. Dopamine neurons release transmitter via a flickering fusion pore. *Nat Neurosci,* 7**,** 341-6.

STAIGER, H., STANCAKOVA, A., ZILINSKAITE, J., VANTTINEN, M., HANSEN, T., MARINI, M. A., HAMMARSTEDT, A., JANSSON, P. A., SESTI, G., SMITH, U., PEDERSEN, O., LAAKSO, M., STEFAN, N., FRITSCHE, A. & HARING, H. U. 2008. A candidate type 2 diabetes polymorphism near the HHEX locus affects acute glucose-stimulated insulin release in European populations: results from the EUGENE2 study. *Diabetes,* 57**,** 514-7.

STEFAN, N., KANTARTZIS, K., CELEBI, N., STAIGER, H., MACHANN, J., SCHICK, F., CEGAN, A., ELCNEROVA, M., SCHLEICHER, E., FRITSCHE, A. & HARING, H. U. 2010. Circulating palmitoleate strongly and independently predicts insulin sensitivity in humans. *Diabetes Care,* 33**,** 405-7.

STEINTHORSDOTTIR, V., THORLEIFSSON, G., REYNISDOTTIR, I., BENEDIKTSSON, R., JONSDOTTIR, T., WALTERS, G. B., STYRKARSDOTTIR, U., GRETARSDOTTIR, S., EMILSSON, V., GHOSH, S., BAKER, A., SNORRADOTTIR, S., BJARNASON, H., NG, M. C., HANSEN, T., BAGGER, Y., WILENSKY, R. L., REILLY, M. P., ADEYEMO, A., CHEN, Y., ZHOU, J., GUDNASON, V., CHEN, G., HUANG, H., LASHLEY, K., DOUMATEY, A., SO, W. Y., MA, R. C., ANDERSEN, G., BORCH-JOHNSEN, K., JORGENSEN, T., VAN VLIET-OSTAPTCHOUK, J. V., HOFKER, M. H., WIJMENGA, C., CHRISTIANSEN, C., RADER, D. J., ROTIMI, C., GURNEY, M., CHAN, J. C., PEDERSEN, O., SIGURDSSON, G., GULCHER, J. R.,

THORSTEINSDOTTIR, U., KONG, A. & STEFANSSON, K. 2007. A variant in CDKAL1 influences insulin response and risk of type 2 diabetes. *Nat Genet,* 39**,** 770-5.

STEVIC, R., ZIVKOVIC, T. B., ERCEG, P., MILOSEVIC, D., DESPOTOVIC, N. & DAVIDOVIC, M. 2007. Oral glucose tolerance test in the assessment of glucose-tolerance in the elderly people. *Age Ageing,* 36**,** 459-62.

STEWARD, M. C., ISHIGURO, H. & CASE, R. M. 2005. Mechanisms of bicarbonate secretion in the pancreatic duct. *Annu Rev Physiol,* 67**,** 377-409.

STRAUB, S. G. & SHARP, G. W. 2004. Hypothesis: one rate-limiting step controls the magnitude of both phases of glucose-stimulated insulin secretion. *Am J Physiol Cell Physiol,* 287**,** C565-71.

SUDHOF, T. C. 2004. The synaptic vesicle cycle. *Annu Rev Neurosci,* 27**,** 509-47.

SUDHOF, T. C. & RIZO, J. 2011. Synaptic Vesicle Exocytosis. *Cold Spring Harbor Perspectives in Biology,* 3.

SUGITA, S., HAN, W., BUTZ, S., LIU, X., FERNANDEZ-CHACON, R., LAO, Y. & SUDHOF, T. C. 2001. Synaptotagmin VII as a plasma membrane Ca(2+) sensor in exocytosis. *Neuron,* 30**,** 459-73.

SULLIVAN, L. B., MARTINEZ-GARCIA, E., NGUYEN, H., MULLEN, A. R., DUFOUR, E., SUDARSHAN, S., LICHT, J. D., DEBERARDINIS, R. J. & CHANDEL, N. S. 2013. The Proto-oncometabolite Fumarate Binds Glutathione to Amplify ROS-Dependent Signaling. *Mol Cell,* 51**,** 236-48.

SUTHERLAND, E. W. & DE DUVE, C. 1948. Origin and distribution of the hyperglycemic-glycogenolytic factor of the pancreas. *J Biol Chem,* 175**,** 663-74.

SUTTON, R. B., FASSHAUER, D., JAHN, R. & BRUNGER, A. T. 1998. Crystal structure of a SNARE complex involved in synaptic exocytosis at 2.4 A resolution. *Nature,* 395**,** 347-53.

SZENDROEDI, J., SCHMID, A. I., CHMELIK, M., TOTH, C., BREHM, A., KRSSAK, M., NOWOTNY, P., WOLZT, M., WALDHAUSL, W. & RODEN, M. 2007. Muscle mitochondrial ATP synthesis and glucose transport/phosphorylation in type 2 diabetes. *PLoS Med,* 4**,** e154.

TAKAHASHI, N., KISHIMOTO, T., NEMOTO, T., KADOWAKI, T. & KASAI, H. 2002. Fusion pore dynamics and insulin granule exocytosis in the pancreatic islet. *Science,* 297**,** 1349-52.

TAKAMORI, S., HOLT, M., STENIUS, K., LEMKE, E. A., GRONBORG, M., RIEDEL, D., URLAUB, H., SCHENCK, S., BRUGGER, B., RINGLER, P., MULLER, S. A., RAMMNER, B., GRATER, F., HUB, J. S., DE GROOT, B. L., MIESKES, G., MORIYAMA, Y., KLINGAUF, J., GRUBMULLER, H., HEUSER, J., WIELAND, F. & JAHN, R. 2006. Molecular anatomy of a trafficking organelle. *Cell,* 127**,** 831-46.

TANG, J., MAXIMOV, A., SHIN, O. H., DAI, H., RIZO, J. & SUDHOF, T. C. 2006. A complexin/synaptotagmin 1 switch controls fast synaptic vesicle exocytosis. *Cell,* 126**,** 1175-87.

TARASKA, J. W., PERRAIS, D., OHARA-IMAIZUMI, M., NAGAMATSU, S. & ALMERS, W. 2003. Secretory granules are recaptured largely intact after stimulated exocytosis in cultured endocrine cells. *Proc Natl Acad Sci U S A,* 100**,** 2070-5.

TARASOV, A., DUSONCHET, J. & ASHCROFT, F. 2004. Metabolic regulation of the pancreatic beta-cell ATP-sensitive K+ channel: a pas de deux. *Diabetes,* 53 Suppl 3**,** S113-22.

TERAUCHI, Y., IWAMOTO, K., TAMEMOTO, H., KOMEDA, K., ISHII, C., KANAZAWA, Y., ASANUMA, N., AIZAWA, T., AKANUMA, Y., YASUDA, K., KODAMA, T., TOBE, K., YAZAKI, Y. & KADOWAKI, T. 1997. Development of non-insulin-dependent diabetes mellitus in the double knockout mice with disruption of insulin receptor substrate-1 and beta cell glucokinase genes. Genetic reconstitution of diabetes as a polygenic disease. *J Clin Invest,* 99**,** 861-6.

TETA, M., LONG, S. Y., WARTSCHOW, L. M., RANKIN, M. M. & KUSHNER, J. A. 2005. Very slow turnover of beta-cells in aged adult mice. *Diabetes,* 54**,** 2557-67.

THE JACKSON LABORATORY. 2015. *Lifespan data for inbred laboratory mice* [Online]. Available: http://research.jax.org/faculty/harrison/ger1vi_LifeStudy1.html [Accessed 5th Febuary 2015.

THIM, L., HANSEN, M. T., NORRIS, K., HOEGH, I., BOEL, E., FORSTROM, J., AMMERER, G. & FIIL, N. P. 1986. Secretion and processing of insulin precursors in yeast. *Proc Natl Acad Sci U S A,* 83**,** 6766-70.

THOMPSON, C. B. 2009. Metabolic Enzymes as Oncogenes or Tumor Suppressors. *New England Journal of Medicine,* 360**,** 813-815.

THORENS, B., WEIR, G. C., LEAHY, J. L., LODISH, H. F. & BONNER-WEIR, S. 1990. Reduced expression of the liver/beta-cell glucose transporter isoform in glucose-insensitive pancreatic beta cells of diabetic rats. *Proc Natl Acad Sci U S A,* 87**,** 6492-6.

THURMOND, D. C., GONELLE-GISPERT, C., FURUKAWA, M., HALBAN, P. A. & PESSIN, J. E. 2003. Glucose-stimulated insulin secretion is coupled to the interaction of actin with the t-SNARE (target membrane soluble N-ethylmaleimide-sensitive factor attachment protein receptor protein) complex. *Mol Endocrinol,* 17**,** 732-42.

TIEDGE, M., LORTZ, S., MUNDAY, R. & LENZEN, S. 1998. Complementary action of antioxidant enzymes in the protection of bioengineered insulin-producing RINm5F cells against the toxicity of reactive oxygen species. *Diabetes,* 47**,** 1578-85.

TODD, J. F. & BLOOM, S. R. 2007. Incretins and other peptides in the treatment of diabetes. *Diabet Med,* 24**,** 223-32.

TOLL, L., GUNDERSEN, C. B., JR. & HOWARD, B. D. 1977. Energy utilization in the uptake of catecholamines by synaptic vesicles and adrenal chromaffin granules. *Brain Res,* 136**,** 59-66.

TOMLINSON, I. P., ALAM, N. A., ROWAN, A. J., BARCLAY, E., JAEGER, E. E., KELSELL, D., LEIGH, I., GORMAN, P., LAMLUM, H., RAHMAN, S., ROYLANCE, R. R., OLPIN, S., BEVAN, S., BARKER, K., HEARLE, N., HOULSTON, R. S., KIURU, M., LEHTONEN, R., KARHU, A., VILKKI, S., LAIHO, P., EKLUND, C., VIERIMAA, O., AITTOMAKI, K., HIETALA, M., SISTONEN, P., PAETAU, A., SALOVAARA, R., HERVA, R., LAUNONEN, V., AALTONEN, L. A. & MULTIPLE LEIOMYOMA, C. 2002. Germline mutations in FH predispose to dominantly inherited uterine fibroids, skin leiomyomata and papillary renal cell cancer. *Nat Genet,* 30**,** 406-10.

TORREJON-ESCRIBANO, B., ESCORIZA, J., MONTANYA, E. & BLASI, J. 2011. Glucose-dependent changes in SNARE protein levels in pancreatic beta-cells. *Endocrinology,* 152**,** 1290-9.

TRUBE, G., RORSMAN, P. & OHNO-SHOSAKU, T. 1986. Opposite effects of tolbutamide and diazoxide on the ATP-dependent K+ channel in mouse pancreatic beta-cells. *Pflugers Arch,* 407**,** 493-9.

TSUBOI, T., MCMAHON, H. T. & RUTTER, G. A. 2004. Mechanisms of dense core vesicle recapture following "kiss and run" ("cavicapture") exocytosis in insulin-secreting cells. *J Biol Chem,* 279**,** 47115-24.

TUBOI, S., SUZUKI, T., SATO, M. & YOSHIDA, T. 1990. Rat liver mitochondrial and cytosolic fumarases with identical amino acid sequences are encoded from a single mRNA with two alternative in-phase AUG initiation sites. *Adv Enzyme Regul,* 30**,** 289-304.

ULLRICH, A., SHINE, J., CHIRGWIN, J., PICTET, R., TISCHER, E., RUTTER, W. J. & GOODMAN, H. M. 1977. Rat insulin genes: construction of plasmids containing the coding sequences. *Science,* 196**,** 1313-9.

UMBRECHT-JENCK, E., DEMAIS, V., CALCO, V., BAILLY, Y., BADER, M. F. & CHASSEROT-GOLAZ, S. 2010. S100A10-Mediated Translocation of Annexin-A2 to SNARE Proteins in Adrenergic Chromaffin Cells Undergoing Exocytosis. *Traffic,* 11**,** 958-971.

UNGER, R. H. 1976. The Banting Memorial Lecture 1975. Diabetes and the alpha cell. *Diabetes,* 25**,** 136-51.

UNGER, R. H., EISENTRAUT, A. M., MC, C. M., KELLER, S., LANZ, H. C. & MADISON, L. L. 1959. Glucagon antibodies and their use for immunoassay for glucagon. *Proc Soc Exp Biol Med,* 102**,** 621-3.

UNGER, R. H., EISENTRAUT, A. M., MC, C. M. & MADISON, L. L. 1961. Glucagon antibodies and an immunoassay for glucagon. *J Clin Invest,* 40**,** 1280-9.

UNGER, R. H., EISENTRAUT, A. M., MC, C. M. & MADISON, L. L. 1962. Measurements of endogenous glucagon in plasma and the influence of blood glucose concentration upon its secretion. *J Clin Invest,* 41**,** 682-9.

UNGER, R. H. & ORCI, L. 1977. Role of glucagon in diabetes. *Arch Intern Med,* 137**,** 482-91.

VAN DE WETERING, M., OOSTERWEGEL, M., VAN NORREN, K. & CLEVERS, H. 1993. Sox-4, an Sry-like HMG box protein, is a transcriptional activator in lymphocytes. *EMBO J,* 12**,** 3847-54.

VAN SCHAFTINGEN, E. 1994. Short-term regulation of glucokinase. *Diabetologia,* 37 Suppl 2**,** S43-7.

VANDER HEIDEN, M. G., CANTLEY, L. C. & THOMPSON, C. B. 2009. Understanding the Warburg effect: the metabolic requirements of cell proliferation. *Science,* 324**,** 1029-33.

VANHOUTTE, C., MALAISSE-LAGAE, F. & MALAISSE, W. J. 1995. D-glucose metabolism in cross-linked pancreatic islets. *Biochem Biophys Res Commun,* 217**,** 561-5.

VELUTHAKAL, R., MADATHILPARAMBIL, S. V., MCDONALD, P., OLSON, L. K. & KOWLURU, A. 2009. Regulatory roles for Tiam1, a guanine nucleotide exchange factor for Rac1, in glucose-stimulated insulin secretion in pancreatic beta-cells. *Biochem Pharmacol,* 77**,** 101-13.

VERVOORT, S. J., VAN BOXTEL, R. & COFFER, P. J. 2013. The role of SRY-related HMG box transcription factor 4 (SOX4) in tumorigenesis and metastasis: friend or foe? *Oncogene,* 32**,** 3397-409.

VETTERLI, L., CAROBBIO, S., POURNOURMOHAMMADI, S., MARTIN-DEL-RIO, R., SKYTT, D. M., WAAGEPETERSEN, H. S., TAMARIT-RODRIGUEZ,

J. & MAECHLER, P. 2012. Delineation of glutamate pathways and secretory responses in pancreatic islets with beta-cell-specific abrogation of the glutamate dehydrogenase. *Molecular Biology of the Cell,* 23**,** 3851-3862.

VIGNALI, S., LEISS, V., KARL, R., HOFMANN, F. & WELLING, A. 2006. Characterization of voltage-dependent sodium and calcium channels in mouse pancreatic A- and B-cells. *J Physiol,* 572**,** 691-706.

VIKMAN, J., MA, X., HOCKERMAN, G. H., RORSMAN, P. & ELIASSON, L. 2006. Antibody inhibition of synaptosomal protein of 25 kDa (SNAP-25) and syntaxin 1 reduces rapid exocytosis in insulin-secreting cells. *J Mol Endocrinol,* 36**,** 503-15.

VISSCHER, P. M., BROWN, M. A., MCCARTHY, M. I. & YANG, J. 2012. Five years of GWAS discovery. *Am J Hum Genet,* 90**,** 7-24.

VOIGHT, B. F., SCOTT, L. J., STEINTHORSDOTTIR, V., MORRIS, A. P., DINA, C., WELCH, R. P., ZEGGINI, E., HUTH, C., AULCHENKO, Y. S., THORLEIFSSON, G., MCCULLOCH, L. J., FERREIRA, T., GRALLERT, H., AMIN, N., WU, G., WILLER, C. J., RAYCHAUDHURI, S., MCCARROLL, S. A., LANGENBERG, C., HOFMANN, O. M., DUPUIS, J., QI, L., SEGRE, A. V., VAN HOEK, M., NAVARRO, P., ARDLIE, K., BALKAU, B., BENEDIKTSSON, R., BENNETT, A. J., BLAGIEVA, R., BOERWINKLE, E., BONNYCASTLE, L. L., BENGTSSON BOSTROM, K., BRAVENBOER, B., BUMPSTEAD, S., BURTT, N. P., CHARPENTIER, G., CHINES, P. S., CORNELIS, M., COUPER, D. J., CRAWFORD, G., DONEY, A. S., ELLIOTT, K. S., ELLIOTT, A. L., ERDOS, M. R., FOX, C. S., FRANKLIN, C. S., GANSER, M., GIEGER, C., GRARUP, N., GREEN, T., GRIFFIN, S., GROVES, C. J., GUIDUCCI, C., HADJADJ, S., HASSANALI, N., HERDER, C., ISOMAA, B., JACKSON, A. U., JOHNSON, P. R., JORGENSEN, T., KAO, W. H., KLOPP, N., KONG, A., KRAFT, P., KUUSISTO, J., LAURITZEN, T., LI, M., LIEVERSE, A., LINDGREN, C. M., LYSSENKO, V., MARRE, M., MEITINGER, T., MIDTHJELL, K., MORKEN, M. A., NARISU, N., NILSSON, P., OWEN, K. R., PAYNE, F., PERRY, J. R., PETERSEN, A. K., PLATOU, C., PROENCA, C., PROKOPENKO, I., RATHMANN, W., RAYNER, N. W., ROBERTSON, N. R., ROCHELEAU, G., RODEN, M., SAMPSON, M. J., SAXENA, R., SHIELDS, B. M., SHRADER, P., SIGURDSSON, G., SPARSO, T., STRASSBURGER, K., STRINGHAM, H. M., SUN, Q., SWIFT, A. J., THORAND, B., et al. 2010. Twelve type 2 diabetes susceptibility loci identified through large-scale association analysis. *Nat Genet,* 42**,** 579-89.

VON MERING, J. M., O. 1890. Diabetes mellitus nach Pankreasexstirpation. . *Archiv fu¨r experimentelle Pathologie und Pharmakologie* 26**,** 371–387.

WALKER, J. N., JOHNSON, P. R., SHIGETO, M., HUGHES, S. J., CLARK, A. & RORSMAN, P. 2011a. Glucose-responsive beta cells in islets isolated from a patient with long-standing type 1 diabetes mellitus. *Diabetologia,* 54**,** 200-2.

WALKER, J. N., RAMRACHEYA, R., ZHANG, Q., JOHNSON, P. R., BRAUN, M. & RORSMAN, P. 2011b. Regulation of glucagon secretion by glucose: paracrine, intrinsic or both? *Diabetes Obes Metab,* 13 Suppl 1**,** 95-105.

WANG, C., WANG, X., GONG, G., BEN, Q., QIU, W., CHEN, Y., LI, G. & WANG, L. 2012. Increased risk of hepatocellular carcinoma in patients with diabetes mellitus: a systematic review and meta-analysis of cohort studies. *Int J Cancer,* 130**,** 1639-48.

WANG, S. Y., HALBAN, P. A. & ROWE, J. W. 1988. Effects of aging on insulin synthesis and secretion. Differential effects on preproinsulin messenger RNA levels, proinsulin biosynthesis, and secretion of newly made and preformed insulin in the rat. *J Clin Invest,* 81**,** 176-84.

WANG, Z., OH, E. & THURMOND, D. C. 2007. Glucose-stimulated Cdc42 signaling is essential for the second phase of insulin secretion. *J Biol Chem,* 282**,** 9536-46.

WANG, Z. & THURMOND, D. C. 2009. Mechanisms of biphasic insulin-granule exocytosis - roles of the cytoskeleton, small GTPases and SNARE proteins. *J Cell Sci,* 122**,** 893-903.

WEBER, T., ZEMELMAN, B. V., MCNEW, J. A., WESTERMANN, B., GMACHL, M., PARLATI, F., SOLLNER, T. H. & ROTHMAN, J. E. 1998. SNAREpins: minimal machinery for membrane fusion. *Cell,* 92**,** 759-72.

WEGNER, M. 1999. From head to toes: the multiple facets of Sox proteins. *Nucleic Acids Res,* 27**,** 1409-20.

WEIR, G. C. & BONNER-WEIR, S. 2004. Five stages of evolving beta-cell dysfunction during progression to diabetes. *Diabetes,* 53 Suppl 3**,** S16-21.

WEISS, M. A. 2001. Floppy SOX: mutual induced fit in hmg (high-mobility group) box-DNA recognition. *Mol Endocrinol,* 15**,** 353-62.

WHEELER, M. B., SHEU, L., GHAI, M., BOUQUILLON, A., GRONDIN, G., WELLER, U., BEAUDOIN, A. R., BENNETT, M. K., TRIMBLE, W. S. & GAISANO, H. Y. 1996. Characterization of SNARE protein expression in beta cell lines and pancreatic islets. *Endocrinology,* 137**,** 1340-8.

WILSON, D. W., WILCOX, C. A., FLYNN, G. C., CHEN, E., KUANG, W. J., HENZEL, W. J., BLOCK, M. R., ULLRICH, A. & ROTHMAN, J. E. 1989. A fusion protein required for vesicle-mediated transport in both mammalian cells and yeast. *Nature,* 339**,** 355-9.

WILSON, M. E., YANG, K. Y., KALOUSOVA, A., LAU, J., KOSAKA, Y., LYNN, F. C., WANG, J., MREJEN, C., EPISKOPOU, V., CLEVERS, H. C. & GERMAN, M. S. 2005. The HMG box transcription factor Sox4 contributes to the development of the endocrine pancreas. *Diabetes,* 54**,** 3402-9.

XU, E. E., KRENTZ, N. A., TAN, S., CHOW, S. Z., TANG, M., NIAN, C. & LYNN, F. C. 2015. SOX4 cooperates with neurogenin 3 to regulate endocrine pancreas formation in mouse models. *Diabetologia*.

XU, L. Z., HARRISON, R. W., WEBER, I. T. & PILKIS, S. J. 1995. Human beta-cell glucokinase. Dual role of Ser-151 in catalysis and hexose affinity. *J Biol Chem,* 270**,** 9939-46.

XU, W., YANG, H., LIU, Y., YANG, Y., WANG, P., KIM, S. H., ITO, S., YANG, C., WANG, P., XIAO, M. T., LIU, L. X., JIANG, W. Q., LIU, J., ZHANG, J. Y., WANG, B., FRYE, S., ZHANG, Y., XU, Y. H., LEI, Q. Y., GUAN, K. L., ZHAO, S. M. & XIONG, Y. 2011. Oncometabolite 2-hydroxyglutarate is a competitive inhibitor of alpha-ketoglutarate-dependent dioxygenases. *Cancer Cell,* 19**,** 17-30.

YANG, B., STEEGMAIER, M., GONZALEZ, L. C., JR. & SCHELLER, R. H. 2000. nSec1 binds a closed conformation of syntaxin1A. *J Cell Biol,* 148**,** 247-52.

YANG, M., SOGA, T. & POLLARD, P. J. 2013. Oncometabolites: linking altered metabolism with cancer. *J Clin Invest,* 123**,** 3652-8.

YANG, Y. & GILLIS, K. D. 2004. A highly Ca2+-sensitive pool of granules is regulated by glucose and protein kinases in insulin-secreting INS-1 cells. *J Gen Physiol,* 124**,** 641-51.

YASUDA, K., MIYAKE, K., HORIKAWA, Y., HARA, K., OSAWA, H., FURUTA, H., HIROTA, Y., MORI, H., JONSSON, A., SATO, Y., YAMAGATA, K., HINOKIO, Y., WANG, H. Y., TANAHASHI, T., NAKAMURA, N., OKA, Y., IWASAKI, N., IWAMOTO, Y., YAMADA, Y., SEINO, Y., MAEGAWA, H., KASHIWAGI, A., TAKEDA, J., MAEDA, E., SHIN, H. D., CHO, Y. M., PARK, K. S., LEE, H. K., NG, M. C., MA, R. C., SO, W. Y., CHAN, J. C., LYSSENKO, V., TUOMI, T., NILSSON, P., GROOP, L., KAMATANI, N., SEKINE, A., NAKAMURA, Y., YAMAMOTO, K., YOSHIDA, T., TOKUNAGA, K., ITAKURA, M., MAKINO, H., NANJO, K., KADOWAKI, T. & KASUGA, M. 2008. Variants in KCNQ1 are associated with susceptibility to type 2 diabetes mellitus. *Nat Genet,* 40**,** 1092-7.

YOGEV, O., NAAMATI, A. & PINES, O. 2011. Fumarase: a paradigm of dual targeting and dual localized functions. *FEBS J,* 278**,** 4230-42.

YOGEV, O. & PINES, O. 2011. Dual targeting of mitochondrial proteins: mechanism, regulation and function. *Biochim Biophys Acta,* 1808**,** 1012-20.

YU, T., ROBOTHAM, J. L. & YOON, Y. 2006. Increased production of reactive oxygen species in hyperglycemic conditions requires dynamic change of mitochondrial morphology. *Proc Natl Acad Sci U S A,* 103**,** 2653-8.

ZHANG, Q., LI, Y. & TSIEN, R. W. 2009. The dynamic control of kiss-and-run and vesicular reuse probed with single nanoparticles. *Science,* 323**,** 1448-53.

ZHANG, Q., RAMRACHEYA, R., LAHMANN, C., TARASOV, A., BENGTSSON, M., BRAHA, O., BRAUN, M., BRERETON, M., COLLINS, S., GALVANOVSKIS, J., GONZALEZ, A., GROSCHNER, L. N., RORSMAN, N. J., SALEHI, A., TRAVERS, M. E., WALKER, J. N., GLOYN, A. L., GRIBBLE, F., JOHNSON, P. R., REIMANN, F., ASHCROFT, F. M. & RORSMAN, P. 2013. Role of KATP channels in glucose-regulated glucagon secretion and impaired counterregulation in type 2 diabetes. *Cell Metab,* 18**,** 871-82.

ZHENG, L., MACKENZIE, E. D., KARIM, S. A., HEDLEY, A., BLYTH, K., KALNA, G., WATSON, D. G., SZLOSAREK, P., FREZZA, C. & GOTTLIEB, E. 2013. Reversed argininosuccinate lyase activity in fumarate hydratase-deficient cancer cells. *Cancer Metab,* 1**,** 12.

ZHOU, P., BACAJ, T., YANG, X., PANG, Z. P. & SUDHOF, T. C. 2013. Lipid-anchored SNAREs lacking transmembrane regions fully support membrane fusion during neurotransmitter release. *Neuron,* 80**,** 470-83.

ZHU, D., ZHANG, Y., LAM, P. P., DOLAI, S., LIU, Y., CAI, E. P., CHOI, D., SCHROER, S. A., KANG, Y., ALLISTER, E. M., QIN, T., WHEELER, M. B., WANG, C. C., HONG, W. J., WOO, M. & GAISANO, H. Y. 2012. Dual role of VAMP8 in regulating insulin exocytosis and islet beta cell growth. *Cell Metab,* 16**,** 238-49.

ZHU, Y. L., XU, J. & HEINEMANN, S. F. 2009. Two Pathways of Synaptic Vesicle Retrieval Revealed by Single-Vesicle Imaging. *Neuron,* 61**,** 397-411.